TESE DE DOUTORAMENTO

Aerobic granular sludge technology for fish-canning wastewater treatment: optimisation and scale up

Paula Carrera Fernández

ESCOLA DE DOUTORAMENTO INTERNACIONAL

PROGRAMA DE DOUTORAMENTO EN ENXEÑARÍA QUÍMICA E AMBIENTAL

SANTIAGO DE COMPOSTELA

ANO 2020

USC
UNIVERSIDADE
DE SANTIAGO
DE COMPOSTELA

DECLARACIÓN DO AUTOR/A DA TESE

Aerobic granular sludge technology for fish-canning wastewater treatment: optimisation and scale up

Dna. Paula Carrera Fernández

Presento a miña tese, seguindo o procedemento axeitado ao Regulamento, e declaro que:

1) A tese abarca os resultados da elaboración do meu traballo.
2) De selo caso, na tese faise referencia ás colaboracións que tivo este traballo.
3) A tese é a versión definitiva presentada para a súa defensa e coincide coa versión enviada en formato electrónico.
4) Confirmo que a tese non incorre en ningún tipo de plaxio doutros autores nin de traballos presentados por min para a obtención doutros títulos.

En Santiago de Compostela, 16 de Abril de 2020

Asdo: Paula Carrera Fernández

AUTORIZACIÓN DO DIRECTOR / TITOR DA TESE

Aerobic granular sludge technology for fish-canning wastewater treatment: optimisation and scale up

Dna. Anuska Mosquera Corral, Profesora Titular en Enxeñaría Química
Dna. Ángeles Val del Río, Profesora Axudante Doutor en Enxeñaría Química

INFORMA/N:

Que a presente tese, correspóndese co traballo realizado por Dna. ***Paula Carrera Fernández****, baixo a miña dirección, e autorizo a súa presentación, considerando que reúne os requisitos esixidos no Regulamento de Estudos de Doutoramento da USC, e que como director desta non incorre nas causas de abstención establecidas na Lei 40/2015.*

En Santiago de Compostela, 16 de Abril de 2020

Anuska Mosquera Corral

Firmado digitalmente por Anuska Mosquera Corral
Nombre de reconocimiento (DN): cn=Anuska Mosquera Corral, o=Universidade de Santiago de Compostela, ou=Departamento de Ingeniería Química, email=anuska.mosquera@usc.es, c=ES
Fecha: 2020.04.16 11:55:45 +02'00'

Asdo: Anuska Mosquera Corral

VAL DEL RIO MARIA ANGELES - 44825284D

Firmado digitalmente por VAL DEL RIO MARIA ANGELES - 44825284D
Nombre de reconocimiento (DN): c=ES, serialNumber=IDCES-44825284D, givenName=MARIA ANGELES, sn=VAL DEL RIO, cn=VAL DEL RIO MARIA ANGELES - 44825284D
Fecha: 2020.04.16 07:17:53 +02'00'

Asdo: Ángeles Val del Río

Acknowledgements

En primeiro lugar, grazas ás miñas directoras de tese Ángeles e Anuska, por darme a oportunidade de entrar no mundo da investigación e aprender tanto nestes últimos anos.

Grazas a todos os colegas do laboratorio que me axudastes/aturastes durante todo este tempo no grupo: Andrés, Chechu, Riccardino, Miguel, Antonio, Luchi, Kennes, Xela, Nieves, Isa, Elisa, Noelia, Clovia, Ricky, Alba Roibás… Foi un pracer enorme compartir con vós este tempo entre zombies, tartas, voley, singstar, cafés, ceas, concertos, noticias de actualidade, petiscos, IPIES… Grazas tamén a Celia e Tamara, compañeiras do piloto e da cultura gorrilla, por toda a vosa axuda e por facer máis amenas as innumerables viaxes ao Grove. I would also like to thank all my colleages of Bioco for making me feel like home during my research stay.

Grazas tamén a todos os colegas externos ao Biogroup, que me tivestes que aturar falando da tese horas e horas: os colegas enxeñeiros Zasiño, Nati, Pili, Iago e Romaní e as ourensanas mochileras Miri e Paula Can.

Grazas tamén á miña familia, con especial mención a miña nai, meu pai, Uxi e miña avoa Pepita por escoitarme e apoiarme todo este tempo. Grazas tamén a Ourego por alegrarme as voltas a casa con eses 5 kg de adorabilidade.

E por último, pero non menos importante, grazas a David, polo asesoramento científico-filosófico e o teu gran e incondicional apoio, como persoa e como investigador, durante todos estes anos.

Se non fose por todos vós completar este traballo tería sido moito máis difícil. Esta tese leva un gran *et al.* do que todos formades parte.

皆さん, どうも有難うございました!

USC
UNIVERSIDADE
DE SANTIAGO
DE COMPOSTELA

There is no such thing as the unknown.

Only things temporarily hidden, temporarily not understood.

- Captain Kirk, Star Trek

USC
UNIVERSIDADE
DE SANTIAGO
DE COMPOSTELA

USC
UNIVERSIDADE
DE SANTIAGO
DE COMPOSTELA

Outline of the thesis

Resumo i

List of acronyms ix

List of symbols x

Chapter 1 1

1.1. CONVENTIONAL AEROBIC BIOLOGICAL PROCESSES 3

1.2. AEROBIC GRANULAR SLUDGE 4

1.2.1. Processes inside the aerobic granules 5

1.2.2. Operational conditions to produce AGS 7

1.2.3. Parameters influencing aerobic granules performance 9

1.2.4. Advantages of the AGS technology 11

1.2.5. Main bottlenecks of AGS 12

1.3. AGS TECHNOLOGY FOR THE TREATMENT OF INDUSTRIAL WASTEWATER 12

1.4. SCALE UP OF THE AGS TECHNOLOGY 20

1.4.1. Pilot-scale studies 20

1.4.2. Full-scale studies 24

1.5. BIOLOGICAL MODELLING 24

1.6. SCOPE OF THE THESIS 25

1.7. REFERENCES 26

Chapter 2 35

2.1. ANALYSIS OF THE LIQUID PHASE 38

2.1.1. Chemical Oxygen Demand (COD) 38

2.1.2. Total Organic Carbon (TOC) 39

2.1.3. Volatile Fatty Acids (VFAs) 40

2.1.4. Nitrogen compounds 40

2.1.5. Orthophosphate (PO_4^{3-}-P) 44

2.1.6. Inorganic ions 45

2.1.7. Proteins 46
2.1.8. Carbohydrates 47
2.1.9. Fats 48
2.1.10. Biological Oxygen Demand (BOD) 49
2.1.11. COD fractionation 50
2.1.12. Other parameters 52
2.2. BIOMASS CHARACTERISATION 52
2.2.1. Solids concentration 52
2.2.2. Sludge Volume Index (SVI) 53
2.2.3. Granule density 53
2.2.4. Average diameter of the granules 54
2.2.5. Extracellular Polymeric Substances (EPS) 55
2.3. IDENTIFICATION OF BACTERIAL POPULATIONS BY FLUORESCENT *in situ* HYBRIDISATION 55
2.3.1. Identification of bacterial populations 55
2.3.2. Quantification of bacterial populations 58
2.4. CALCULATIONS 58
2.4.1. Hydraulic and sludge retention time (HRT and SRT) 59
2.4.1. Carbon 59
2.4.2. Nitrogen 60
2.4.3. Phosphorus 61
2.4.4. Biomass growth 62
2.4.5. Consumption and production rates of the nitrogen compounds 63
2.4.7. Salinity (g NaCl/L) 64
2.5. REFERENCES 65
Chapter 3 67
3.1. INTRODUCTION 69
3.2. OBJECTIVES 70
3.3. MATERIALS AND METHODS 70
3.3.1. Experimental set-up 70
3.3.2. Operational conditions 72
3.3.3. Analytical and microbiological methods 73
3.4. RESULTS AND DISCUSSION 74
3.4.1. Pulsed vs continuous aeration 74

3.4.2. Evaluation of the minimum air consumption 82
3.4.3. Reactivation of the granules 85
3.5. CONCLUSIONS 87
3.6. REFERENCES 88
Chapter 4 91
4.1. INTRODUCTION 93
4.2. OBJECTIVES 94
4.3. MATERIALS AND METHODS 94
4.3.1. Experimental set-up 94
4.3.2. Operational periods 95
4.3.3. Analytical methods 95
4.4. RESULTS AND DISCUSSION 96
4.4.1. Pulsed vs continuous aeration 96
4.4.2. Evaluation of the decrease of the air pulses frequency 101
4.4.3. Evaluation of the pulsed aeration with different feeding strategies 103
4.5. CONCLUSIONS 105
4.6. REFERENCES 106
Chapter 5 109
5.1. INTRODUCTION 111
5.2. OBJECTIVES 112
5.3. MATERIALS AND METHODS 112
5.3.1. Experimental set-up 112
5.3.2. Operational conditions 113
5.3.3. Analytical and microbiological methods 114
5.4. RESULTS AND DISCUSSION 115
5.4.1. Operation of the reactor 115
5.4.2. Evaluation of different feeding strategies to treat fish-canning wastewater 123
5.5. CONCLUSIONS 126
5.6. REFERENCES 127
Chapter 6 131
6.1. INTRODUCTION 133
6.2. OBJECTIVES 134
6.3. MATERIALS AND METHODS 134

6.4. INDUSTRIAL WASTEWATER CHARACTERISATION 134
6.4.1. Low-strength wastewater (LS-WW) 135
6.4.2. High-strength wastewater (HS-WW) 136
6.4.3. Current wastewater treatment of the factory 137
6.5. AGS PILOT PLANT DESCRIPTION 137
6.5.1. Pilot AGS reactor pre-treatments 138
6.5.2. Pilot plant reactor 141
6.5.3. Pilot AGS reactor post-treatment 143
6.5.4. Control system 143
6.6. OPERATIONAL STRATEGY 144
6.7. CONCLUSIONS 146
6.8. REFERENCES 147
APPENDIX A: Scheme of the wastewater treatment plant of the fish-canning factory 148
APPENDIX B: Scheme of the AGS pilot plant 149
APPENDIX C: Dimensions of the units of the pilot plant 150
Chapter 7 151
7.1. INTRODUCTION 153
7.2. OBJECTIVES 154
7.3. MATERIALS AND METHODS 154
7.3.1. Experimental set-up 154
7.3.2. Operational conditions 154
7.3.3. Analytical methods 156
7.4. RESULTS AND DISCUSSION 156
7.4.1. Low-strength wastewater treatment. Stages I and II 156
7.4.2. High-strength wastewater treatment. Stage III 167
7.4.3. AGS effluent post-treatment 169
7.4.4. Effluent quality 170
7.5. CONCLUSIONS 171
7.6. REFERENCES 172
Chapter 8 175
8.1. INTRODUCTION 177
8.2. OBJECTIVES 178
8.3. MATERIALS AND METHODS 178

8.3.1. Experimental data 178
8.3.2. Simulation set-up 179
8.4. GRANULAR SLUDGE REACTOR MODEL 179
8.4.1. Biological processes 179
8.4.2. Granule characteristics 180
8.4.3. SBR operation 181
8.4.4. Inclusion of salinity effect in the model 181
8.5. RESULTS AND DISCUSSION 183
8.5.1. Calibration of the model 183
8.5.1. Validation of the model 187
8.6. CONCLUSIONS 189
8.7. REFERENCES 190
APPENDIX A: reference case 194
APPENDIX B: bioconversion reactions 196
APPENDIX C: Stoichiometric matrix 198
APPENDIX D: kinetic and stoichiometric parameters 200
APPENDIX E: estimation of the inhibition constants 202
General conclusions 205
Publications & Conferences 209

USC
UNIVERSIDADE
DE SANTIAGO
DE COMPOSTELA

Resumo

O tratamento de augas residuais mediante procesos aerobios adoita ser realizado en sistemas de lamas activas. A pesar de ser a tecnoloxía máis implantada, presenta unha serie de desvantaxes, como a baixa capacidade de tratamento, a necesidade de amplos espazos de implantación ou a alta demanda enerxética asociada. A crecente xeración de augas residuais, así como as esixencias de efluentes de cada vez maior calidade, motivaron a busca de tecnoloxías alternativas para facer fronte ao tratamento de augas. Dentro das tecnoloxías aerobias, amosouse un especial interese nas tecnoloxías de biopelícula. Nelas, a biomasa crece adherida sobre soportes dentro do reactor, en vez de estar en suspensión como nos sistemas de lamas activas. Isto permite aumentar a capacidade de tratamento do sistema, así como reducir o espazo de implantación necesario.

Dentro dos sistemas aerobios de biopelícula, a biomasa granular aerobia é un caso especial, xa que a biomasa é capaz de agregarse e formar gránulos sen necesidade de ningún tipo de soporte. A estrutura destes agregados permite a formación de capas aerobias, anóxicas e anaerobias en función da penetración do osíxeno no gránulo, favorecendo a coexistencia de distintos tipos de bacterias. Deste xeito, nunha única unidade é posible a eliminación de materia orgánica e nutrientes, mentres que nos sistemas convencionais de lamas activas son necesarios varios tanques con distintas condicións. Porén, esta tecnoloxía aínda presenta algunhas limitacións que impiden a súa extensión no tratamento de augas, como son os longos tempos de granulación, a inestabilidade a longo prazo dos agregados biolóxicos ou o elevado consumo enerxético asociado á aeración.

A viabilidade da tecnoloxía granular aerobia para o tratamento de augas industriais foi amplamente demostrada a escala laboratorio. Obtivéronse resultados satisfactorios, que inclúen biomasa granular estable e altas eficacias de eliminación, ao tratar augas residuais procedentes de diversas industrias, como procesado de produtos lácteos, mariños, soia ou azucre, matadoiros, industria cervexeira, gandeira, papeleira ou petroquímica. Porén, os traballos con biomasa granular aerobia a escala piloto son máis escasos, e gran parte deles se centran no tratamento de augas residuais urbanas, mentres que só uns poucos tratan augas industriais. A escala industrial, a día de hoxe só existe unha tecnoloxía patentada, que está orientada fundamentalmente ao tratamento de augas urbanas.

Tendo en conta este contexto, a presente tese de doutoramento ten como obxectivo a avaliación, optimización e escalado da tecnoloxía baseada en biomasa granular aerobia para o tratamento de efluentes industriais procedentes da industria conserveira. Os principais obxectivos a partir do desenvolvemento desta tese relaciónanse con:

- Estudo da implantación dun novo sistema de aeración en reactores granulares aerobios para a redución do coste enerxético asociado, así como avaliación do impacto deste novo sistema nas propiedades da biomasa granular e na capacidade de tratamento.

- Comparación de diferentes estratexias de alimentación en termos de estabilidade, propiedades de gránulos e calidade de efluente, con variacións de carga e salinidade.

- Avaliación da tecnoloxía de biomasa granular aerobia para o tratamento de augas residuais procedentes da industria conserveira, incluíndo o seu estudo a escala laboratorio así como o escalado da tecnoloxía e implantación nunha planta conserveira.

- Elaboración dun modelo matemático dos procesos biolóxicos que teñen lugar nestes sistemas a partir dos datos obtidos experimentalmente.

Deste xeito, nos capítulos con resultados experimentais abórdase a implantación dun novo sistema de aeración, a comparativa de distintas estratexias de alimentación, e o escalado e modelado da tecnoloxía aplicada no tratamento de auga residual procedente da industria conserveira. Os contidos principais e obxectivos específicos correspondentes a cada capítulo da presente tese descríbense máis detalladamente a continuación.

No **Capítulo 1** preséntase un resumo actualizado do contexto referente ao tratamento de augas industriais, así como o estado de implantación da tecnoloxía de biomasa granular aerobia. Préstase especial atención ás condicións de operación necesarias para obter biomasa granular aerobia, as diferentes configuracións dos reactores, así como a outros parámetros que poden afectar á estabilidade do sistema. Ademais, resúmense os traballos de investigación publicados sobre a aplicación desta tecnoloxía para o tratamento de augas industriais, así como o escalado e implantación a escala industrial. Por último, introdúcense as bases sobre os modelos matemáticos que poden ser empregados para describir os procesos biolóxicos asociados á biomasa granular aerobia.

No **Capítulo 2**, proporciónase unha descrición dos métodos analíticos empregados para determinar os parámetros convencionais na caracterización das augas residuais e da biomasa granular. Os parámetros máis convencionais como o pH, a demanda química de osíxeno (DQO), a concentración de especies nitroxenadas (amonio, nitrito e nitrato), fosfatos, graxas ou a concentración de sólidos, medíronse seguindo as instrucións do "Standard Methods". Ademais, inclúense outros parámetros como a concentración de ións inorgánicos, proteínas, carbohidratos, condutividade ou fraccionamento de DQO.

No referente á caracterización da biomasa granular aerobia, detállanse os protocolos das técnicas analíticas empregadas para determinar a sedimentabilidade (Índice Volumétrico de Lodos), densidade ou morfoloxía e tamaño de partícula dos gránulos aerobios. Ademais, descríbese a técnica microbiolóxica de Hibridación *in situ* con Fluorescencia (FISH) para a identificación de distintas poboacións microbianas. A maiores, preséntanse tamén neste capítulo

os cálculos empregados para determinar os parámetros que permiten analizar os resultados obtidos ao longo da tese.

Unha das limitacións que presenta a tecnoloxía baseada en biomasa granular aerobia é o alto consumo enerxético asociado á etapa de aeración. Para a obtención de gránulos estables é necesario o aporte de grandes caudais de aire, para así crear un alto estrés hidrodinámico e favorecer a granulación. Porén, isto implica un alto coste enerxético asociado. Por este motivo, diferentes estratexias foron estudadas para tratar de reducir os requirimentos de aire, incluíndo etapas anóxicas, redución do caudal de aire, mantemento da concentración de osíxeno en valores baixos no reactor ou alimentacións en condicións anaerobias. Non obstante, isto adoita implicar tempos de granulación máis longos así como a obtención de gránulos menos robustos debido á redución do estrés hidrodinámico aplicado. Así, nos **Capítulos 3 e 4**, estudiouse unha nova estratexia de aeración, baseada no aporte de aire de forma pulsante, en vez de continua, co obxectivo de reducir o volume de aire necesario sen comprometer a estabilidade dos agregados biolóxicos.

No **Capítulo 3** esta estratexia avaliouse nun reactor SBR (en inglés Sequencing Batch Reactor) a escala laboratorio cun volume de 1.7 L e alimentación anaerobia, co obxectivo de favorecer o crecemento de organismos acumuladores de fósforo (en inglés Phosphate Accumulating Organisms, PAOs). O aporte de aire realizouse mediante un réxime pulsante (R1), mentres que en outro reactor idéntico que serviu de control (R2) a aeración foi continua. Así, para un mesmo volume de aire aportado, o caudal e a velocidade ascensional de aire foron maiores no caso da aeración pulsante. Ambos reactores foron alimentados con auga sintética, cunha carga aplicada de 0.8 kg $DQO_S/(m^3 \cdot d)$. O obxectivo deste traballo foi a comparación do tempo de granulación, o desenvolvemento das PAOs, a estabilidade de gránulos e a capacidade de eliminación de ambos reactores. Tamén se compararon ambas estratexias de aeración a través de ensaios de reactivación de gránulos almacenados. Ademais, realizáronse reducións do caudal de aire de ambos reactores, co obxectivo de determinar o caudal mínimo necesario en cada caso para manter a estabilidade do sistema.

A estratexia de aeración pulsante permitiu unha redución do tempo de granulación do 21 %. Ademais, o crecemento das PAOs foi máis rápido e os gránulos formados foron máis densos, levando a unha maior retención de biomasa en R1. As eficacias de eliminacións globais foron similares en ambos reactores, sendo do 85 %, 95 % e 30 % para DQO, nitróxeno e fósforo, respectivamente. As subsecuentes reducións do caudal de aire aportado amosaron que é posible manter a integridade dos gránulos con velocidades ascensionais de gas iguais ou inferiores ás mínimas recomendadas para obter gránulos estables (1.2 cm/s). A menor velocidade ascensional que permitiu manter a estabilidade no sistema foi de 1.2 cm/s en R1 e 0.7 cm/s en R2, supoñendo un aforro con respecto ao caudal inicial aportado do 67 e 60 % para R1 e R2, respectivamente. Os resultados dos ensaios de reactivación dos gránulos non amosaron grandes diferenzas no referente á estratexia de aeración empregada. No tempo de duración dos ensaios, aínda que non se restableceu a actividade das PAOs, si o fixo a actividade heterótrofa. En canto ás bacterias nitrificantes, unicamente se recuperou a actividade AOB (en inglés Ammonia Oxidising Bacteria), indicando a maior resistencia a longos tempos de almacenaxe destas bacterias con respecto ás NOBs (en inglés Nitrite Oxidising Bacteria).

Existen fundamentalmente dúas estratexias de alimentación que favorecen a formación da biomasa granular aerobia: unha fase de alimentación anaerobia seguida dunha etapa de aeración, na que se establece o réxime de saciedade anaerobia/fame aerobia (**Capítulos 3 e 5**) ou ben unha alimentación curta seguida dun longo período de aeración (saciedade aerobia/fame aerobia, **Capítulos 4, 5, 6 e 7**). Os reactores operados seguindo esta última estratexia son máis doados de controlar, e adoitan presentar operacións máis estables. En cambio, o consumo enerxético é maior, dado que a aeración supón unha maior porcentaxe do tempo total do ciclo. Por este motivo, a redución do aporte de aire necesario é aínda máis importante que no caso dos sistemas con alimentación anaerobia.

Así, no **Capítulo 4**, implantouse a estratexia de aeración pulsante empregada no Capítulo 3 nun reactor completamente aerobio a escala laboratorio cun volume de 1.7 L (R1). Á súa vez, operouse un reactor co mesmo volume e estratexia de alimentación, pero aerado de forma continua en vez de pulsante (R2, serviu de control). Para un mesmo volume de aire aportado, o caudal e a velocidade ascensional foron maiores no caso da aeración pulsante. Ambos reactores foron alimentados con auga sintética, cunha carga aplicada de 1.8 – 2.3 kg $DQO_S/(m^3 \cdot d)$. O obxectivo deste traballo foi a comparación do tempo de granulación, estabilidade de gránulos e capacidade de eliminación de ambos reactores. Ademais, estudáronse distintas frecuencias dos pulsos de aire para determinar a configuración que leva a un maior aforro enerxético sen comprometer a estabilidade do sistema. Por último, realizouse unha comparativa do efecto da aeración pulsante nos reactores completamente aerobios descritos neste capítulo, e os reactores con alimentación anaerobia recollidos no Capítulo 3.

As distintas estratexias de aeración non supuxeron diferenzas en canto ao tempo necesario para a granulación, que foi arredor dun mes en ambos reactores. Non obstante, as diferenzas foron significativas no relativo ás propiedades dos gránulos obtidos. En R1, a aeración pulsante favoreceu a proliferación de gránulos ben formados e con boa sedimentabilidade. En R2, a baixa velocidade ascensional aportada pola aeración continua provocou o crecemento descontrolado de bacterias filamentosas, aínda que a sedimentabilidade dos agregados foi boa. As eficacias de eliminación de ambos reactores foron similares, dun 90 % e 65 % de DQO e nitróxeno, respectivamente. Os resultados da avaliación da redución da frecuencia de pulsos de aire indicaron que a menor frecuencia que permite manter a estabilidade do sistema é de 1 s de aeración e 4 s de tempo de non aeración. Frecuencias menores provocaron a rotura dos gránulos debido á falta de osíxeno suficiente para levar a cabo as reaccións biolóxicas. Os períodos de saciedade incrementáronse demasiado e nos períodos de fame a concentración de osíxeno foi moi baixa (menor de 2 mg O_2/L).

O sector conserveiro ten un gran impacto na economía galega, e xera grandes volumes de augas residuais, que exercen presión sobre os ecosistemas mariños galegos. Estes efluentes caracterízanse por presentar altas concentracións de materia orgánica, nutrientes e sal. Dada a limitación de espazo das industrias conserveiras para a implantación de sistemas de tratamento dos efluentes, a tecnoloxía baseada en biomasa granular aerobia preséntase como unha alternativa atractiva para o tratamento destas correntes, que ademais amosou tratar de forma efectiva outras augas residuais con altas cargas.

No **Capítulo 5**, operouse un SBR a escala laboratorio totalmente aerobio cun volume útil de 1.7 L, para o tratamento de auga residual procedente dunha conserveira galega. A operación do

reactor dividiuse en distintas etapas, dependendo das características de cada lote de auga empregado como alimentación. O obxectivo deste traballo foi a avaliación da tecnoloxía de biomasa granular aerobia para o tratamento deste efluente industrial, incluíndo o estudo do desenvolvemento e estabilidade dos gránulos, así como da capacidade de tratamento e calidade de efluente, ante concentracións variables de sal (4.9 – 13.4 g NaCl/L) e carga orgánica aplicada (1.8 – 6.6 kg $DQO_S/(m^3 \cdot d)$). Ademais, realizouse unha comparativa con outro reactor granular alimentado coa mesma auga e nas mesmas condicións operacionais, pero distinta estratexia de alimentación (anaerobia).

O proceso de granulación completouse tras 90 días, dando lugar a gránulos densos e con boa sedimentabilidade. Ante as flutuacións da alimentación, a biomasa mantívose estable e acadáronse altas concentracións no reactor, con tempos de retención celular de ata 15.2 días. Aos 150 días de operación, observouse actividade de bacterias nitrificantes dentro do reactor, o que causou unha mellora da eficacia de eliminación de nitróxeno, que aumentou dende 30 ata valores do 80 %. En canto á eliminación de DQO soluble, foi alta durante toda a operación (75 – 80 %), con duracións da fase de saciedade de 10 – 40 minutos (nun total de 167 – 227 min de reacción aerobia), dependendo da carga orgánica aplicada. A comparativa da operación deste reactor (totalmente aerobio) cun reactor alimentado de forma anaerobia, amosou que o proceso de granulación foi máis rápido no caso do reactor con alimentación anaerobia, pero a biomasa foi menos estable fronte ás flutuacións da alimentación. Ademais, a retención de biomasa foi maior no caso do sistema totalmente aerobio, e só neste caso se observou o crecemento de bacterias nitrificantes. En canto á calidade do efluente, as eficacias de eliminación de DQO foron un pouco mellores con alimentación anaerobia (80 – 90 %), pero a eliminación de nitróxeno foi moito máis alta no sistema completamente aerobio.

As augas residuais producidas polas empresas conserveiras divídense normalmente en augas de baixa carga con alto volume, e alta carga con baixo volume. A variabilidade da composición das augas depende da materia prima empregada e o procesado específico. O tratamento habitual destas correntes adoita comprender tratamentos primarios para a eliminación de materia insoluble en suspensión (tamizado, sedimentación ou flotación por aire disolto). Ademais, para augas de alta carga, adóitanse empregar sistemas biolóxicos, tanto aerobios como anaerobios.

No **Capítulo 6**, realizouse o deseño dunha planta piloto baseada en biomasa granular aerobia para o tratamento *in situ* de auga residual procedente dunha conserveira. Para isto, realizouse previamente un estudo das correntes de auga residual, así como do tratamento actual da conserveira na que se instalou a planta piloto. O obxectivo deste capítulo foi a definición e dimensionamento das unidades da planta piloto, incluíndo etapas de pre e postratamento, así como da estratexia de operación. Para isto realizáronse caracterizacións dos efluentes da planta e ensaios no laboratorio.

A conserveira na que se situou o piloto producía dúas correntes diferenciadas de auga residual: baixa carga (95 % do volume total de auga residual producida) e alta carga (5 % do volume total de auga residual producida). A auga de baixa carga presentaba baixas concentracións de DQO e nutrientes, alta e variable salinidade e sólidos insolubles. A auga de alta carga caracterizábase por ter un maior contido en DQO, nutrientes, sólidos e graxas, e salinidade máis baixa e estable. Para o pretratamento da auga de baixa carga antes de ser alimentada ao reactor granular, a planta piloto constou dun tambor rotatorio, para eliminar os sólidos presentes. Para o

pretratamento da auga de alta carga seleccionouse un separador de graxa, co obxectivo de eliminar tanto os sólidos como as graxas presentes. A continuación das liñas de pretratamento instalouse un tanque de homoxeneización previo ao reactor. Como postratamento do efluente do reactor granular, instalouse un decantador, co obxectivo de eliminar os sólidos do efluente. O reactor granular deseñouse para tratar unha carga máxima de 6 kg $DQO_S/(m^3 \cdot d)$. A estratexia de operación definiuse tendo en conta a produción da conserveira, é dicir, reaxustando os ciclos operacionais en función das paradas da planta.

Existe unha gran cantidade de estudos a escala laboratorio que teñen como obxectivo o tratamento de augas industriais con biomasa granular aerobia. En cambio, o número de traballos con esta tecnoloxía que afronten o tratamento de augas industriais a maior escala é moi reducido. A escala piloto presenta dificultades asociadas que non existen en reactores a escala laboratorio, como a variabilidade do influente (asociada á variabilidade de produción da industria) ou cambios na hidrodinámica dentro do reactor. Como consecuencia, os maiores colos de botella da tecnoloxía de biomasa granular aerobia a escala piloto foron os longos períodos de granulación, así como a inestabilidade a longo prazo.

No **Capítulo 7**, operouse o reactor SBR deseñado no Capítulo 6, cunha configuración de ciclo totalmente aerobia e un volume útil de 3 m^3, situado nunha conserveira galega, para o tratamento dos efluentes xerados. O reactor tratou de forma separada as dúas correntes producidas na planta: baixa e alta carga. A operación do reactor dividiuse en varias etapas, dependendo da alimentación empregada. Primeiro tratouse a auga de baixa carga, e despois a auga de alta carga (diluída con auga de baixa carga). O obxectivo deste traballo foi a avaliación da viabilidade da tecnoloxía de biomasa granular aerobia a escala piloto, tratando auga industrial coas flutuacións asociadas ao proceso de produción da planta na que se instalou o reactor. Para iso, realizouse un seguimento das propiedades da biomasa, así como da capacidade de tratamento e calidade de efluente. Ademais, prestouse atención ao efecto das paradas de produción da planta na operación do reactor.

Os resultados da operación amosaron que o uso de distintos efluentes como alimentación do reactor favoreceron o crecemento de biomasa con distintas propiedades. Polo tanto, a formación de biomasa granular dependeu das características da auga empregada. Ao tratar auga de baixa carga, os primeiros agregados observáronse tras un mes de operación. En cambio, o baixo contido de materia orgánica e nutrientes da auga residual provocaron o crecemento descontrolado de bacterias filamentosas e un empeoramento da sedimentabilidade da biomasa. A pesar diso, o sistema foi capaz de eliminar DQO e nitróxeno con eficacias do 70 – 80 %. Ao tratar auga de alta carga, observouse a formación de pequenos agregados con boa sedimentabilidade, pero o tempo de operación non foi suficiente para completar o proceso de granulación e obter gránulos maduros. Porén, a proliferación de bacterias filamentosas non tivo lugar, debido ás maiores concentracións de DQO e nitróxeno do influente. As eficacias de eliminación acadadas foron do 80 – 90 % para DQO e 30 % para nitróxeno. A pesar da redución da concentración dos distintos contaminantes, a calidade do efluente da planta piloto de ambos tipos de augas residuais non foi o suficientemente boa como para cumprir os límites de vertido establecidos. No caso da auga de baixa carga, o principal problema foi un mal pretratamento da auga, no cal non se eliminaron correctamente as graxas. No caso da auga de alta carga, a pesar do bo funcionamento da planta as

concentracións de materia orgánica e nutrientes foron altos debido as elevadas concentracións do influente. Neste escenario sería necesario un postratamento do efluente.

As altas concentracións de sal, características dos efluentes da industria conserveira, causan impacto tanto nas propiedades físicas dos gránulos aerobios como na actividade biolóxica dos distintos tipos de bacteria que os conforman. Unha forma de describir o impacto desta variable na biomasa granular aerobia é a través de modelos matemáticos. Existen diferentes modelos cinéticos que describen os procesos de eliminación de materia orgánica e nutrientes, que poden ser adaptados para modelar as reaccións de bioconversión que teñen lugar na biomasa granular aerobia.

No **Capítulo 8**, desenvolveuse un modelo matemático para describir a operación dun reactor granular aerobio alimentado con efluentes da industria conserveira. Para a calibración e validación do modelo empregáronse os resultados experimentais do Capítulo 5. Para a elaboración do modelo, seleccionáronse os compostos de interese e todas as reaccións de bioconversión que tiveron lugar no sistema, elaborouse a matriz estequiométrica e definíronse os parámetros cinéticos e estequiométricos do modelo. Ademais, considerouse a inclusión dun termo de inhibición non competitiva para expresar o efecto da sal nos parámetros cinéticos. A calibración realizouse con datos dunha etapa experimental na que a concentración de sal foi de 13 g NaCl/L, mentres que a validación foi feita con datos dunha etapa operacional con 5 g NaCl/L.

Os resultados do modelo amosaron que, tras a calibración do mesmo, os parámetros cinéticos das bacterias heterótrofas foron similares aos valores habituais obtidos en outros traballos. En cambio, os parámetros cinéticos das bacterias nitrificantes foron considerablemente menores. A causa destas diferenzas posiblemente foi unha combinación de varios factores, como a presenza de sal ou a complexidade da auga residual tratada. Os resultados da validación amosaron que o modelo foi capaz de predicir correctamente as concentracións de efluente dos distintos contaminantes. O termo de inhibición asociado á presenza de sal, amosou reducións das taxas de crecemento máximo de todas as poboacións bacterianas, sendo maiores na operación con 13 g NaCl/L. Non obstante, o modelo foi avaliado con salinidades baixas-moderadas, polo que sería desexable a avaliación do termo de inhibición con concentracións de sal maiores.

USC
UNIVERSIDADE
DE SANTIAGO
DE COMPOSTELA

List of acronyms

AGS	Aerobic Granular Sludge
AND	Alternating Nitrification Denitrification
AOB	Ammonia Oxidising Bacteria
ASM	Activated Sludge Model
CAS	Conventional Activated Sludge
CFR	Continuous Flow Reactor
DAF	Dissolved Air Flotation
EBPR	Enhanced Biological Phosphorus Removal
EPS	Extracellular Polymeric Substances
FISH	Fluorescence *in Situ* Hybridisation
GAO	Glycogen Accumulating Organism
HB	Heterotrophic Bacteria
HS-WW	High-Strength Wastewater
IFAS	Integrated Fixed Film Activated Sludge
LS-WW	Low-Strength Wastewater
MBBR	Moving Bed Biofilm Reactor
MBR	Membrane Bioreactor
NOB	Nitrite Oxidising Bacteria
PAO	Phosphate Accumulating Organism
PHA	Poly-Hydroxyalkanoate
PN	Protein content of EPS
PS	Carbohydrate content of EPS
PLC	Programmable Logic Controller
SBR	Sequencing Batch Reactor
SND	Simultaneous Nitrification Denitrification
UASB	Upflow Anaerobic Sludge Blanket
UAF	Upflow Anaerobic Filter
WW	Wastewater
WWTP	Wastewater Treatment Plant

List of symbols

BOD	Biological Oxygen Demand	mg L^{-1}
COD	Chemical Oxygen Demand	mg L^{-1}
COD_b	Biodegradable COD	mg L^{-1}
COD_I	Inert COD	mg L^{-1}
COD_S	Soluble COD	mg L^{-1}
COD_T	Total COD	mg L^{-1}
DO	Dissolved Oxygen	mg L^{-1}
FA	Free Ammonia	mg NH_3-N L^{-1}
FNA	Free Nitrous Acid	mg HNO_2-N L^{-1}
HRT	Hydraulic Retention Time	d
ISS	Inorganic Suspended Solids	mg L^{-1}
NLR	Nitrogen Loading Rate	kg N m^{-3} d^{-1}
OLR	Organic Loading Rate	kg COD m^{-3} d^{-1}
PLR	Phosphorus Loading Rate	g P m^{-3} d^{-1}
SGV	Superficial Gas Velocity	cm s^{-1}
S_I	Inert soluble COD	mg L^{-1}
S_S	Easily biodegradable soluble COD	mg L^{-1}
SRT	Sludge Retention Time	d
SVI	Sludge Volume Index	mL g^{-1}
TN	Total Nitrogen	mg L^{-1}
TOC	Total Organic Carbon	mg L^{-1}
TSS	Total Suspended Solids	mg L^{-1}
TP	Total Phosphorus	mg L^{-1}
VER	Volume Exchange Ratio	%
VFAs	Volatile Fatty Acids	mg L^{-1}
VSS	Volatile Suspended Solids	mg L^{-1}
X_I	Inert particulate COD	mg L^{-1}
X_S	Slowly biodegradable particulate COD	mg L^{-1}
Y	Growth yield	g VSS·g COD^{-1}

The symbols used in the biological model are detailed in the appendixes of Chapter 8.

Chapter 1

Introduction

Summary

In this chapter, the current context for the industrial wastewater treatment by aerobic technologies was briefly described. The stricter regulations regarding the effluent quality requirements as well as the increase of the population are pushing the evolution of the conventional aerobic systems to more compact and efficient technologies.

The present thesis addressed the application of the Aerobic Granular Sludge (AGS) technology with two main focus: 1) the configuration of the operational cycles and the aeration strategy and 2) the treatment of industrial saline effluents, from the fish-canning industry.

AGS is a type of aerobic biofilm constituted by self-aggregated bacteria which can be developed if some triggering conditions are imposed in the reactor. AGS technology presents some advantages compared to conventional aerobic processes, like the compactness or the high treatment capacity. Although it is a promising alternative for organic matter and nutrients removal, AGS technology still presents some drawbacks, like the instability at long term-operation or the high energy requirements. Therefore, further research is needed to overcome these limitations and ensure a good performance of the system.

The AGS technology has been widely applied at laboratory-scale, but not so much for larger scales. The application of AGS technology for the treatment of industrial effluents, as well as the scale-up of the process to pilot and full scale, are also reviewed in this Chapter.

OUTLINE

Chapter 1 1

1.1. CONVENTIONAL AEROBIC BIOLOGICAL PROCESSES 3

1.2. AEROBIC GRANULAR SLUDGE 4

1.2.1. Processes inside the aerobic granules 5

1.2.2. Operational conditions to produce AGS 7

1.2.3. Parameters influencing aerobic granules performance 9

1.2.4. Advantages of the AGS technology 11

1.2.5. Main bottlenecks of AGS 12

1.3. AGS TECHNOLOGY FOR THE TREATMENT OF INDUSTRIAL WASTEWATER 12

1.4. SCALE UP OF THE AGS TECHNOLOGY 20

1.4.1. Pilot-scale studies 20

1.4.2. Full-scale studies 24

1.5. BIOLOGICAL MODELLING 24

1.6. SCOPE OF THE THESIS 25

1.7. REFERENCES 26

1.1. CONVENTIONAL AEROBIC BIOLOGICAL PROCESSES

The biological reactors used for the wastewater treatment are based on the use of microorganisms which aim to remove the dissolved and particulate biodegradable compounds and/or nutrients, such as nitrogen or phosphorus, and capture colloidal solids into the biological flocs (Tchobanoglous et al., 2014). The aerobic biological treatment of wastewater is often accomplished through the application of Conventional Activated Sludge (CAS) systems (Figure 1.1). These systems comprise aerated and mixed tanks, where the wastewater gets in contact with a suspension of microorganisms and pollutants are removed. Then, treated wastewater is separated from the microorganisms in secondary settlers. A fraction of the settled biological sludge is recirculated to the aeration tank, to maintain a stable concentration, whereas the rest of the sludge is purged (Tchobanoglous et al., 2014).

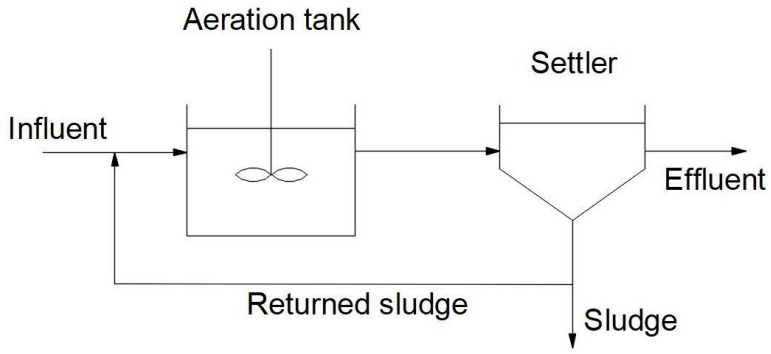

Figure 1.1: Scheme of the CAS process (adapted from Tchobanoglous et al. (2014)).

The CAS process has evolved since it was developed in the early 1900s, in response to the requirements of high-quality effluents, the need of nutrient removal, the reduction of capital and operating costs, the technological advances and the understanding of microbial processes. Initially, CAS systems were conceived to only remove organic matter and suspended solids. Later, the nitrification process gained attention and was included in the conception of the Wastewater Treatment Plants (WWTPs). Over time, due to the adverse effects on the water bodies, the removal of nitrite, nitrate and phosphorus was also considered (Dezotti et al., 2018). Currently, CAS systems are constituted by reactors placed in series, operated under aerobic, anoxic and/or anaerobic conditions, to enable organic matter, nitrogen and phosphorus removal (Tchobanoglous et al., 2014).

The increase in the number of inhabitants, as well as the stricter regulations regarding effluent quality, made necessary the upgrade of already existing WWTPs or building of new ones to cope with the increase of the generated wastewater. However, the available space for the implementation of new WWTPs is generally limited (Campos et al., 2009). Although CAS systems are widely implemented, they require large areas for their installation, mainly due to the need for large settlers and the low concentration of solids in the aeration tanks, which leads to relatively low treating capacities (0.5–2.0 kg/(m^3·day) of Chemical Oxygen Demand (COD)). Thus, the construction of compact treatment plants which manage to maintain stable operation with reduced environmental impact is necessary.

To overcome the limitations of CAS, in recent years the interest in biofilm processes for the treatment of municipal and industrial wastewater has increased (Dezotti et al., 2018). These systems are based on the use of biomass attached to different carrier elements. They allow the retention of higher concentrations of biomass inside the reactor, and thus, increase the treatment capacity. At the same time, they are more compact than CAS and present lower surface requirements. The most common used biofilm reactors include Integrated Fixed Film Activated Sludge (IFAS), Membrane Bioreactors (MBRs) or Moving Bed Biofilm Reactors (MBBRs) (Wilén et al., 2018). Although these technologies present several advantages compared to CAS, they have the drawback of high operational and maintenance costs. MBR reactors are energy-intensive mainly because they require pumping for sludge return and high aeration to minimise fouling on the membranes (Nancharaiah et al., 2019). MBBR and IFAS systems also require high energy demand associated with the mixing of the carriers and pumping for sludge recirculation (Bengtsson et al., 2019).

1.2. AEROBIC GRANULAR SLUDGE

Aerobic Granular Sludge (AGS) is a special type of self-immobilised biofilm. It consists of dense and compact aggregates (Figure 1.2.b), formed by different bacterial groups with a specific function in the removal of the pollutants present in the wastewater (Liu and Tay, 2004). Aerobic granules were defined in the Aerobic Granular Sludge Workshop (Munich, Germany, 2004) as microbial aggregates formed without the addition of carrier materials, which settle significantly faster compared to activated sludge, and do not coagulate under reduced hydrodynamic shear (De Kreuk et al., 2005). Granules have a structure where the relative position of the bacterial populations does not rapidly change, as in the case of CAS systems. In general, these aggregates present low values of the Sludge Volume Index (SVI) of 30 – 60 mL/g TSS, SVI_{30}/SVI_{10} ratios above 0.80 and minimum average particle sizes of 0.2 mm. A system can be considered granular when granules correspond to at least 80 % of the total solids present in the reactor (De Kreuk et al., 2005).

a) b)

Figure 1.2: Picture of (a) activated sludge and (b) aerobic granules.

The first studies about AGS were performed in the 1990s. Mishima and Nakamura (1991) were the first ones reporting the cultivation of granules in aerobic conditions. They observed the formation of aerobic aggregates in a continuous anaerobic upflow sludge blanket reactor to remove the organic matter of previously aerated wastewater. Morgenroth et al. (1997) were the first to use a Sequencing Batch Reactor (SBR) for AGS cultivation. Since then, AGS technology has been widely studied at laboratory-scale to treat municipal and industrial wastewater. Furthermore, experiences with pilot plants are available. Besides, nowadays there are several full-scale plants in operation in different countries based on the Nereda® technology developed by DHV (The Netherlands), which apply the AGS for the treatment of municipal wastewater (https://www.royalhaskoningdhv.com/nereda).

1.2.1. Processes inside the aerobic granules

The biological processes that take place in AGS reactors are the same as in CAS systems, and similar microbial populations are involved (Bengtsson et al., 2018). Whereas in CAS reactors, different stages or tanks are needed to create different conditions (aerobic, anoxic or anaerobic), in AGS systems all the processes occur in a single unit. This is because the morphology of the granules creates concentration gradients inside of them, leading to zones with different environmental conditions (Figure 1.3). Depending on the oxygen penetration depth, the granules present outer aerobic layers, and anoxic and/or anaerobic cores, which promote the coexistence of different bacteria populations. Nitrifying and heterotrophic bacteria are usually located in the outer layers, whereas Phosphate Accumulating Organisms (PAOs) and denitrifiers are located in the inner parts (Guimarães et al., 2017; Winkler et al., 2013). Due to the bacteria diversity in aerobic granules, several metabolic pathways for the removal of organic matter and nutrients can occur.

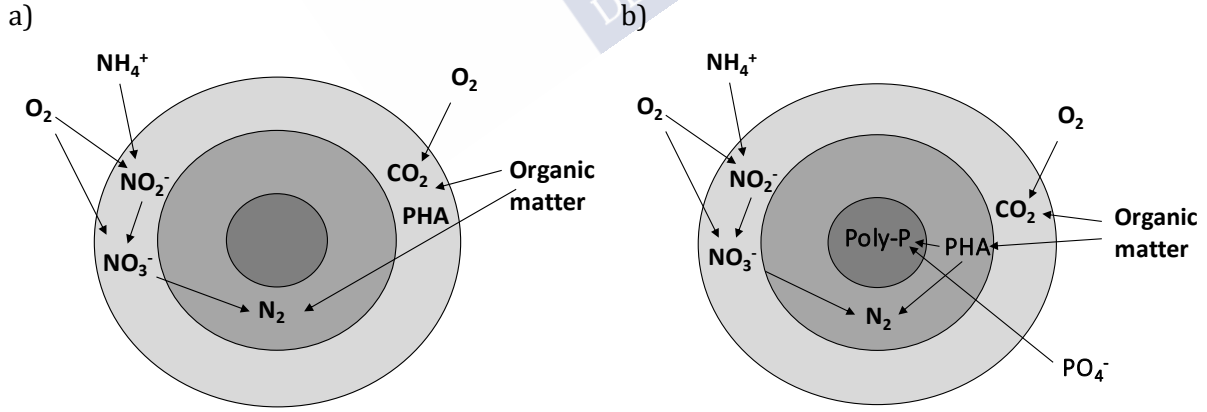

Figure 1.3: Biological processes that may take place inside a granule for (a) organic matter and nitrogen removal and (b) organic matter, nitrogen and phosphorus removal. (Adapted from Campos et al. (2009)).

Organic matter removal

The easily biodegradable organic matter can be removed under aerobic conditions either by biological oxidation, by fast-growing heterotrophic bacteria or intracellular storage, in form of biopolymers (Poly-Hydroxyalkanoates, PHA), by slow-growing heterotrophic bacteria. If the

operation of the AGS reactor includes an anaerobic stage, a specific type of slow-growing organisms is selected: PAOs or Glycogen Accumulating Organisms (GAOs). These organisms are also able to intracellularly store the organic matter as PHA (Bengtsson et al., 2018).

The particulate organic matter needs to be hydrolysed into dissolved compounds before being consumed by bacteria. In aerobic granules, particulate compounds are adsorbed and hydrolysed on the surface (de Kreuk et al., 2010). Then, the hydrolysis products are consumed at the same place, which creates substrate diffusion limitation gradients. This behaviour can provoke the development of irregular surfaces on the granules and the growth of filamentous bacteria, leading to the instability of the system (Wagner et al., 2015).

Nitrogen removal

Nitrogen, usually present in the wastewater in the form of ammonium, can be removed by biomass assimilation for growth or the nitrification – denitrification biological pathway (Wagner et al., 2015). When nitrification occurs, ammonia is oxidised through a two-step process in aerobic conditions. Firstly, the ammonium is oxidised to nitrite (nitritation) by Ammonia Oxidising Bacteria (AOB). Then, nitrite is oxidised to nitrate (nitratation) by Nitrite Oxidising Bacteria (NOB). This process requires relatively high oxygen concentrations. There is usually a competition between heterotrophic and autotrophic organisms for oxygen and space in the outer layers of the granule (Bengtsson et al., 2018).

At optimal operational conditions, the produced nitrite or nitrate can be immediately consumed by heterotrophic denitrifying bacteria in the inner layers of the granule, where dissolved oxygen is not present, carrying out the Simultaneous Nitrification – Denitrification (SND) process in the same unit. If there are anoxic phases for denitrification in-between aerobic phases for nitrification, the Alternating Nitrification – Denitrification (AND) process occurs (Bengtsson et al., 2018). Although both processes do not take place simultaneously, high removal efficiencies can be also achieved (Lochmatter et al., 2013). The denitrification process needs a carbon source, which can come from the wastewater, from the biomass itself or external carbon sources (Ni et al., 2017), for the reduction of the nitrogen oxide to nitrogen gas.

Phosphorus removal

If the growth of PAOs is promoted, it is possible to remove phosphorus coupled to organic matter by the Enhanced Biological Phosphorus Removal (EBPR) process. To do that, the operational cycle of the AGS reactor needs include an anaerobic stage, followed by an aerobic stage. Under anaerobic conditions, PAOs release phosphorus, intracellularly stored as polyphosphate, to get energy for the biotransformations involved in the uptake and storage of organic matter in the form of PHAs. At the same time, the glycolysis of internally stored glycogen occurs to provide reducing power for PHA formation (Mino et al., 1998). Then, under aerobic conditions, PAOs use their stored PHA as energy source for biomass growth, glycogen replenishment, phosphorus uptake and polyphosphate storage (Oehmen et al., 2007). Like PAOs, GAOs are able to proliferate under alternating anaerobic and aerobic conditions. However, they do not perform phosphorus release and uptake, so they do not contribute to phosphorus removal.

1.2.2. Operational conditions to produce AGS

1.2.2.1. Triggering forces

Granules can be formed when specific operational conditions are established in the reactor, independently of which types of microorganisms and metabolic activities are involved (Bengtsson et al., 2018). The main important triggering forces for successful AGS cultivation under aerobic conditions are a high substrate concentration to create a feast-famine regime, high hydrodynamic shear stress and short settling time (Nancharaiah and Reddy, 2018).

Feast – famine regime

The high gradient of substrate (organic matter and nutrients) concentrations between the bulk liquid and the biomass facilitates its diffusion into the inner layers of the granules. In addition, it exposes the biomass to alternating periods of high and low availability of substrate, establishing a feast – famine regime. Under feast conditions, storage of organic matter dominates over biomass growth. During the famine phase, the biomass grows on the internally stored polymers (Bengtsson et al., 2018). With this regime, the bacterial cell surface hydrophobicity increases, the growth of slow-growing over fast-growing organisms is promoted and the microbial aggregation is accelerated (Adav et al., 2008). To create the high gradient of substrate inside the reactor, the most common strategies are a short feeding, followed by aeration or mixing, and a plug-flow regime from the bottom of the reactor under anaerobic conditions.

Shear stress

Hydrodynamic shear stress promotes the production of Extracellular Polymeric Substances (EPS), increases the cell surface hydrophobicity and triggers cell-cell interactions, which contribute to initiate the granulation process (Nancharaiah and Reddy, 2018). Aerobic granules become more stable and compact if they are exposed to high shear stress (Wilén et al., 2018), which means a high aeration inside the reactor or intense mixing. Aeration is the main parameter used to control the applied shear force, which is usually expressed in terms of Superficial Gas Velocity (SGV). This parameter is calculated as the ratio between the airflow and the cross-sectional area of the reactor. The airflow, as well as the height/diameter ratio of the reactor, are directly related to the shear stress imposed in the system. Previous studies indicate that a minimum value of 1.2 cm/s is necessary for the granulation process (Tay et al., 2001). Lower values lead to unstable and breakable aggregates, whereas values between 2.4 and 3.2 cm/s are optimal to maintain stable granules and achieve good removal performances at long-term operation (Chen et al., 2007). Besides, air is necessary to supply the oxygen required for the biological reactions, which should not be limited (Mosquera-Corral et al., 2005a). For this reason, fixed SGV values should comply with both purposes. However, these optimal values of SGV usually imply high energy consumption, one of the drawbacks of the AGS technology.

Settling time

The selection pressure for rapidly settling aggregates is a key factor for AGS formation. To select dense microbial aggregates and washout light microbial flocs from the reactor, short settling times must be selected (Rollemberg et al., 2018). With this strategy, a minimum settling velocity is imposed to the biomass to remain inside the reactor by fixing a short settling period. Aerobic granules can be formed when the minimum imposed settling velocity is above 1 m/h, and

become dominant when it is higher than 4 m/h (Nancharaiah and Reddy, 2018). To define the minimum settling velocity, the settling time, the volume exchange ratio and the discharge time should be considered.

1.2.2.2. Discontinuous vs continuous operation

AGS is usually obtained in SBRs operated in cycles, which comprise different operational periods (commonly feeding, aeration, settling and effluent discharge), and which are repeated throughout time. The discontinuous operation in stages makes easy to impose the abovementioned driving forces to promote the granulation of the biomass. Nevertheless, the cultivation of AGS in continuous-flow reactors (CFRs) is also under research. These reactors are usually constituted by an aeration compartment, a settling tank and a sludge return area. Continuous-flow systems present some advantages in comparison to discontinuous processes: the operational costs are lower, they are easy to manage and the equipment is efficiently used (Zou et al., 2018). However, it is more difficult to impose the conditions to favour the growth of AGS, like the establishment of the feast-famine regime or the hydraulic selection pressure. Thus, the granulation process is not always completed and aerobic granules usually present poor settleability. To overcome these drawbacks, some new configurations of the CFRs have been proposed, like two-zone settling tanks (Zou et al., 2018), effluent recirculation (Ahmad et al., 2019), intraclarifiers in the aeration tank (Li et al., 2014a) or one tank for feeding followed by an aerated tank (Cofré et al., 2018). Although progress has been made in understanding how granulation occurs and how to promote it, further research is needed to establish the comprehensive mechanisms and optimise the CFR design (Zou et al., 2018).

1.2.2.3. Fully aerobic vs anaerobic-fed configuration

Two main ways have been reported in literature to favour the granulation of the biomass based on the establishment of the feast – famine regime. The first option is the feeding supply in a short time at the beginning of the cycle, to create aerobic feast – aerobic famine conditions (fully aerobic system) (Beun et al., 1999; Ni et al., 2009). In this configuration, the shear stress and the geometry of the reactor, as well as the settling time, have a big importance to select dense aggregates and favour the granulation of the biomass (Liu and Tay, 2004). This configuration enables organic matter removal by slow-growing heterotrophic bacteria and nitrogen removal by autotrophic nitrifying and heterotrophic denitrifying bacteria.

The other option is an anaerobic feeding followed by an aerobic reaction, to create an anaerobic feast – aerobic famine and select specific microorganisms able to anaerobically store COD and grow forming stable granules, like PAOs and/or GAOs (De Kreuk et al., 2005). This feeding is commonly done under non-mixed conditions from the bottom of the reactor. The influent wastewater is fed in a plug-flow mode through the settled bed of granules, which are exposed to relatively high concentrations of organic matter and nutrients (Bengtsson et al., 2018). In this case, it is important a correct management of the anaerobic stage to maximise the COD uptake and reduce its presence during the aerobic stage to avoid the growth of filamentous bacteria (Devlin et al., 2017). This configuration allows the removal of organic matter and phosphorus if PAOs are selected, as well as nitrogen removal by autotrophic nitrification and heterotrophic denitrification (which can be also done by denitrifying PAOs).

1.2.3. Parameters influencing aerobic granules performance

In addition to the key cultivation parameters (shear stress, settling time, feast-famine regime), there are additional factors directly related to the stability and good performance of the granules.

Organic Loading Rate (OLR)

AGS has been successfully cultivated with applied Organic Loading Rates (OLRs) of 1 – 10 kg COD/(m^3·d) (Li et al., 2008; Szabó et al., 2017; Tay et al., 2004). In general, high OLRs promote the faster formation of larger granules, while low OLRs enhance the slower formation of smaller granules (Li et al., 2008). With OLRs below 1 kg COD/(m^3·d), difficulties have been found to achieve a stable granular system. Long start-up periods, the overgrowth of filamentous bacteria or the achievement of a mixture of flocs/filamentous aggregates with aerobic granules have been reported (Ji et al., 2010; Li et al., 2011; Ni et al., 2009; Wang et al., 2009). In addition, high OLRs (above 10 – 20 kg COD/(m^3·d)), lead to the breakage and loss of granule stability. For example, Long et al. (2015) observed that at OLRs of 18 kg COD/(m^3·d), the granule size increased, caused the formation of massive dead cells in the core and provoked the disintegration of granules. Adav et al. (2010) also reported the loss of AGS stability operating at an OLR of 21.3 kg COD/(m^3·d). In both research works the reactor was fed with synthetic wastewater. When using industrial wastewater as feeding, lower values of OLR have been reported to provoke the instability of the granular system. Nguyen et al. (2016) observed the presence of dark cores and the breakage of granules with an applied OLR of 10 kg COD/(m^3·d) treating tapioca wastewater. Val Del Río et al. (2013) reported the loss of stability of the granules due to an excessive growth in size when the applied OLR was of 4.4 – 9 kg COD/(m^3·d).

COD/N ratio

The influent COD/N ratio adjustments may lead to the establishment of a microbial selection pressure to enrich either heterotrophic bacteria (aerobic or anaerobic) or nitrifying species, contributing to granulation, thus, affecting the treatment performance of AGS (Wu et al., 2012). Aerobic granulation is favoured with COD/N ratios of 1 – 20 g COD/g N (Kocaturk and Erguder, 2016; Yang et al., 2005). Kocaturk and Erguder (2016) found that the optimum ratio was of 7.5. g COD/g N. Ratios of 7.5 – 30 g COD/g N favoured the growth of heterotrophic over nitrifying bacteria, leading to fluffy flocs and large granules with high COD removal but low N removal efficiencies. COD/N ratios of 2 – 5 g COD/g N promoted the growth of slow-growing nitrifiers forming small and dense granules with high N removal capacity but relatively low COD removal efficiencies. COD/N ratios lower than 2 g COD/g N were reported to provoke disintegration of granules (previously formed under COD/N ratios of 4 g COD/g N) (Luo et al., 2014).

Dissolved Oxygen (DO) concentration

To achieve optimum nitrogen removals, the Dissolved Oxygen (DO) concentration is very important. It must be high enough to assure full nitrification, but low enough to prevent the absence of anoxic layers inside the granules (Beun et al., 2001). AGS can be formed in a wide range of DO concentrations, from 0.7 – 1.0 up to 2 – 7 mg O_2/L. Authors like de Kreuk and van Loosdrecht (2004) reported the operation with stable granules enriched in PAOs and GAOs with DO concentrations of 20 – 100 % of the saturation level. At DO concentrations of 20 %, the nitrogen

removal efficiencies were of 90 %. However, in a fully aerobic configuration, the stability of the aerobic granules was lost when the DO was reduced to the 40 % of the saturation concentration (Mosquera-Corral et al., 2005a).

Granule size

Granules seem to reach a certain more or less stable granule size determined by the balance between granule growth, attrition and breakage (Wilén et al., 2018). Small granule diameters lead to deep penetration of oxygen and fast oxidation of ammonia. However, when ammonia and phosphate are removed from the system, oxygen will diffuse through the entire granule and denitrification will be inhibited (De Kreuk et al., 2007). Nevertheless, with large granule diameters, the surface area for substrate exchange becomes limiting for oxygen transport and conversion processes. Liu et al. (2016) found that particle diameters of 0.6 – 1.2 mm were preferred for AOB development, whereas NOB grow preferably in large granules of 1.2 – 1.8 mm. Large granules are not desired since they lead to instability and small surface area, which reduces the substrate removal and growth rates. De Kreuk et al. (2007) reported that the optimal diameter to achieve 100 % of nitrogen and phosphorus removal was between 1.2 – 1.4 mm.

Sludge Retention Time (SRT)

This parameter is not a decisive factor for aerobic granulation in SBR, but it is important for the stabilisation of the granules and the achievement of nitrogen removal by nitrifying bacteria (Rollemberg et al., 2018). It was reported that the growth of nitrifying bacteria was favoured when SRTs above 5 – 7 days are reached (Wagner et al., 2015; Winkler et al., 2012). However, long and uncontrolled SRTs can provoke the deterioration of the aerobic granules and the growth of filamentous bacteria. Some research works have applied the strategy of SRT control (between 10 – 30 days), by periodical purges of biomass to avoid the worsening of aerobic granules (Caluwé et al., 2017a; Kishida et al., 2009; Moura et al., 2018).

Salinity

One of the inhibitory compounds that affect AGS performance is sodium chloride. The impact of this compound in AGS has been widely studied. Moderate concentrations of salt (below 15 g NaCl/L) can speed up the granulation process and promote the growth of dense granules. Nevertheless, wastewater types characterised by high salt concentrations (above 20 g NaCl/L) have a negative effect on biological systems. Organic matter and nutrients removal is affected, as well as the structure and settling properties of the biological aggregates (Bassin et al., 2011). NOB have been reported as the most sensitive bacteria to salt, with complete inhibition at salt concentrations of 15 – 20 g NaCl/L (Li et al., 2018; Pronk et al., 2014). AOB are more resistant, maintaining their activity with salt concentrations up to 30 – 50 g NaCl/L (Bassin et al., 2011; Wan et al., 2014). Heterotrophs can withstand the highest salinity, and in general, a complete inhibition has not been reported even with salt concentrations of 75 – 80 g NaCl/L (Corsino et al., 2016; Wang et al., 2015).

Saline wastewater usually presents other ions in addition to sodium and chloride, like sulphate, magnesium or calcium. However, the studies addressing the treatment of saline wastewater have focused only on the effect of sodium chloride on the biological activity of bacterial populations (Thwaites et al., 2018; van den Akker et al., 2015). Divalent ions like magnesium or calcium have been proved to play an important role in the granulation process, by

promoting self-aggregation of bacteria (Liu et al., 2010). However, their impact on biological activity has not been studied yet. Further research is needed to clarify if ions different from sodium and chloride can also affect the performance of the AGS reactors.

1.2.4. Advantages of the AGS technology

CAS process requires large areas for their installation, which is mainly due to the need for large settlers and the low concentration of solids in the aeration tanks. Considerable excess sludge production, high sensitivity to fluctuations in the applied load, and relatively low volumetric conversion capacities are some disadvantages of these conventional process.

The use of AGS reactors instead of CAS reactors, presents some advantages. AGS has a denser and stronger microbial structure with better settling properties. The settling velocities of CAS are lower than 10 m/h, whereas in AGS they are in the range of 10 – 90 m/h (Rollemberg et al., 2019). This promotes a better biomass retention, leading to average biomass concentrations of 7 – 9 g TSS/L, whereas in CAS the average value is of 1.4 g TSS/L (Sarma and Tay, 2018). Consequently, AGS reactors are able to treat higher organic loadings (Adav et al., 2008). The higher SRTs compared to CAS systems enable the development of slow-growing microorganisms and lead to a lower sludge production (Franca et al., 2018). The strong, compact and layered structure of granules provides a protector environment for the microbial populations, increasing the tolerance to high toxicity levels, as well as the capacity of withstanding load variations (Liu and Tay, 2004). For example, Corsino et al. (2019) compared the tolerance of halophilic granular and flocculent sludge (adapted to 30 g NaCl/L) to short and long-term salinity fluctuations. They observed that granular sludge was more suited to withstand seasonal and weekly salt fluctuations. After salinity shocks (70 g NaCl/L), carbon removal efficiencies were recovered after 18 days in AGS and 27 days in CAS. Besides, autotrophic activity was severely affected during long-term salinity shocks in CAS (nitrogen removal efficiencies below 30 %), whereas in AGS the removal efficiencies were higher (50 – 60 % of nitrogen).

The surface requirements of AGS are smaller compared to CAS, since it is possible to simultaneously remove carbon and nitrogen in a single unit, whereas in CAS reactors, different compartments or units with different oxygen conditions are necessary. Moreover, the easy separation of the treated effluent from the biomass due to its good settling properties, avoids the use of big clarifiers that are necessary in CAS systems. In addition, the energy consumption is lower. Pronk et al. (2015) observed a volume reduction of 30 % of an AGS full-scale plant compared to CAS, since the treatment capacity was higher (1.2 m^3/d for AGS and 0.8 m^3/d for CAS) and the clarifiers were not necessary. Niermans et al. (2014) reported that the full-scale AGS plants allowed for 30 % electricity savings associated to aeration compared to CAS, as well as an overall potential reduction of 50 % due the absence of settling tanks, sludge recirculation pumps and post-filtration units.

1.2.5. Main bottlenecks of AGS

Despite the significant advances in the development of AGS process, there are still challenging issues and relevant limitations to the broader application of this technology. The long start-up periods of 100 – 300 days and the instability of the aerobic granules at long-term operation are considered the main bottlenecks (Franca et al., 2018).

Instability of the system at long-term operation

The stability concept for AGS is regarded as a null variation in the granule performance, in terms of removal efficiency, and size distribution of granules, as well as no occurrence of granule break-up and biomass washout from the reactor (Franca et al., 2018). Several research works have reported the loss of stability of AGS, due to different causes, such as variations in the OLR, feast-famine balance, shear stress, dissolved oxygen concentration, substrate type, absence of nutrients or toxic compounds. As explained in the previous section, when key parameters influencing the features and performance of aerobic granules are far from recommended ranges for stable operation, the growth of filamentous bacteria, breakage of granules or the worsening of the removal efficiencies are observed, which provoke the loss of stability of the AGS system.

Energy consumption associated with aeration

To promote the growth of dense and compact granules, a high aeration intensity is required. However, it results in high energy consumption during wastewater treatment, which might be disadvantageous for the application of AGS technology (Gao et al., 2013). Therefore, different strategies have been tested to reduce the energy costs associated to aeration, including the implementation of an anaerobic feeding strategy, anoxic stages or DO control at low concentrations (Jiang et al., 2016; Lochmatter et al., 2013; Yilmaz et al., 2008). However, these strategies sometimes lead to long start-up periods and the reduction of the shear stress necessary for the formation and long-term maintenance of compact and stable granules.

1.3. AGS TECHNOLOGY FOR THE TREATMENT OF INDUSTRIAL WASTEWATER

AGS has been evaluated for the treatment of various industrial wastewater types, mainly from the food and beverage industry (dairy products, abattoir, fish processing, malting, brewery, palm oil mill, soy, sugar beet), and agricultural sector (livestock, winery) (Table 1.1). In addition, the treatment of the wastewater produced in other industries has been addressed with AGS, like pulp and paper, rubber, petrochemical or textile industry. Most of the studies have been conducted at laboratory-scale, with reactor volumes of 1.5 – 15 L. In general, the cultivation of AGS was successful with all the types of industrial effluents used as feeding.

Table 1.1: Composition of industrial effluents, AGS properties and reactor performance.

Industry	Wastewtater composition (mg/L)	Wastewater pretreatment	AGS properties	Removal efficiency (%)	Ref
Dairy products	COD_S: 300 – 1,600 TN: 50 – 200 TP: 20 – 60	pH adjustment[4]	Particle size: 3.5 mm SVI_{30}: 50 – 100 mL/g TSS MLSS: 5 – 8 g/L	COD: 80 – 95 N: 50 – 95 P: 65 – 90	[1] – [4]
Brewery and malting	COD_S: 470 – 3,670 TN: 50 – 136 TP: 20 – 34	N and P dosage	Particle size: 0.2 – 1.5 mm SVI_{30}: 30 – 70 mL/g TSS MLSS: 2 – 3 g/L	COD: 80– 99 N: 85 P: 89 – 90	[5], [6], [7]
Abattoir	COD_S: 1,250 – 1,360 TN: 120 – 160 TP: 20 – 30	Acetate addition[8]	Particle size: 0.5 – 1.6 mm SVI_{30}: < 100 mL/g TSS MLSS: 5 – 20 g/L	COD: 86 – 80 N: 74 – 86 P: 85 – 97	[8], [9], [10]
Palm oil mill	COD_S: 700 TN: 100	N and P dosage, centrifugation and alkalinity addition	Particle size: 4 – 5 mm SVI_{30}: 20 – 30 mL/g TSS MLSS: 6 – 8 g/L	COD: 86 N: 89 – 98	[11], [12]
Soy processing	COD_S: 54,00 – 21,100 TN: 50 – 200 TP: 20 – 60	P and micronutrients dosage[13], pH adjustment[13]	Particle size: 1 – 1.5 mm SVI_{30}: 25 – 30 mL/g TSS MLSS: 8 – 11 g/L	COD: 82 – 99 N: 73 – 89 P: 77 – 79	[13], [14]
Fish processing	COD_S: 410 – 2800 TN: 45 – 500 TP: 7 – 50 Cl^-: 7,100 – 45,500		Particle size: 2.2 – 9 mm SVI_{30}: 30 – 120 mL/g TSS MLSS: 6 – 18 g/L	COD: 70 – 100 N: 20 – 90	[15], [16], [17]
Livestock	COD_S: 210 – 3,600 TN: 480 – 840 TP: 12 – 380	pH adjustment[18]	Particle size: 0.5 – 3 mm SVI_{30}: 25 – 40 mL/g TSS MLSS: 3.5 – 10 g/L	COD: 51 – 90 N: 50 – 90 P: 59 – 90	[18] – [21]

Table 1.1 (continued).

Industry	Wastewtater composition (mg/L)	Wastewater pretreatment	AGS properties	Removal efficiency (%)	Ref
Pulp and paper	COD_S: 780 – 3,000	N and P dosage	Particle size: 0.5 – 4 mm SVI_{30}: 60 – 100 mL/g TSS MLSS: 2 – 8 g/L	COD: 76 – 88	[22], [23]
Textile	COD_S: 250 – 1,600 TN: 15 – 34 TP: 65 – 87		Particle size: 1 – 10 mm SVI_{30}: < 130 mL/g TSS MLSS: 16 g/L	COD: 60– 90	[24], [25]
Petrochemical	COD_S: 1,350 – 2,230 TN: 3 – 115 TP: 7 – 25 Cl^-: 3,200 – 25,000	N and P dosage	Particle size: 0.3 – 1.9 mm SVI_{30}: 25 – 70 mL/g TSS MLSS: 1.5 – 6.5 g/L	COD: 88– 90 N: 26	[26], [27], [28]
Landfill leachate	COD_S: 700 TN: 100		Particle size: 0.2 – 1 mm MLSS: 5 – 13 g/L	COD: 20– 90 N: 20 – 92	[29], [30]

MLSS: Mixed Liquor Suspended Solids.

References: [1] Arrojo et al. (2004), [2] Bumbac et al. (2015), [3] Meunier et al. (2016), [4] Schwarzenbeck et al. (2005), [5] Corsino et al. (2017), [6] Stes et al. (2019), [7] Schwarzenbeck et al. (2004), [8] Yilmaz et al. (2008), [9] Liu et al. (2015), [10] Dobbeleers et al. (2020), [11] Abdullah et al. (2011), [12] Abdullah et al. (2013), [13] Su and Yu (2005), [14] Harun et al. (2014), [15] Corsino et al. (2016), [16] Figueroa et al. (2008), [17] Val del Río et al. (2013), [18] Kishida et al. (2009), [19] Liu et al. (2017), [20] Othman et al. (2013), [21] Morales et al. (2013), [22] Morais et al. (2016), [23] Farooqi and Basheer (2017), [24] Lotito et al. (2014), [25] Ibrahim et al. (2010), [26] Caluwé et al. (2017a), [27] Caluwé et al. (2017b), [28] Corsino et al. (2015), [29] Wei et al. (2012), [30] Bella and Torregrossa (2014).

Dairy wastewater

Dairy effluents usually present high concentrations of organic carbon, suspended solids and oil-grease, mainly coming from carbohydrates, proteins and fats (Nancharaiah and Reddy, 2018). The presence of particulate compounds can suppose a challenge to maintain the stability of the reactor since it favours the growth of filamentous bacteria.

Arrojo et al. (2004) managed to achieve high removal efficiencies of 85 – 95 % of COD and 80 % of N, operating an AGS treating OLRs of 1 – 7 kg COD/(m^3·d). The biomass became full granular after 3 weeks of operation. Bumbac et al. (2015) obtained aerobic granules after 2 weeks of operation in a continuous-flow AGS reactor with an OLR of 3.8 kg COD/(m^3·d). The system was able to remove COD, N and P, with efficiencies in the ranges of 81 – 93, 52 – 80 and 65 – 90 %, respectively. Meunier et al. (2016) operated an anaerobic-fed AGS reactor, with OLRs of 0.9 – 4.6 kg COD/(m^3·d). They fixed the anaerobic feeding length to maximise the hydrolysis of the particulate substrate, obtaining removal efficiencies up to 94, 95 and 83 % of COD, N and P, respectively. Schwarzenbeck et al. (2005) also operated an anaerobic-fed AGS reactor, with removal efficiencies of 90 % for COD, 80 % for Total Nitrogen (TN) and 67 % for Total Phosphorus (TP). Although initially the growth of filamentous bacteria was observed, the system evolved to stable granules after 15 weeks of operation. They treated an OLR of 2.4 – 2.9 kg COD/(m^3·d).

Brewery and malting wastewater

Brewery and malting effluents are characterised by their high organic matter content, in a range of 2,000 – 6,000 mg/L (Bakare et al., 2017), due to the presence of starch, sugar or yeast. However, the nutrients concentration is usually low, which could hinder biomass growth and limit COD removal. To address the problem of nutrient deficit, all the research studies with AGS treating brewery effluents, added N and P to maintain appropriate ratios of COD:N:P (100:10:1 – 100:2:0.5).

Corsino et al. (2017) obtained stable granules after 4 weeks operating an anaerobic-fed reactor fed with brewery wastewater. They imposed extended famine conditions to be able to remove particulate COD in addition to soluble COD, achieving removal efficiencies of 65 – 87 and 85 %, respectively. Stes et al. (2019) operated two reactors with short filling, followed by an anaerobic phase, to treat malting and brewery effluents. The biomass of the reactor treating brewery wastewater became granular after 80 days, with OLR values of 1.18 – 1.90 kg COD/(m^3·d). It was able to remove almost all the COD (87 – 97 %) during the anaerobic stage, achieving global COD removal efficiencies of 95 – 99 %. The reactor treating malting wastewater reached removal efficiencies of 85 % for COD and N, and 89 % for P, with an average OLR of 0.99 kg COD/(m^3·d). Schwarzenbeck et al. (2004) treated malting wastewater with an anaerobic-fed AGS reactor. They observed a complete granular system after 21 weeks, able to remove COD, with efficiencies of 80 % for soluble COD and 50 % for total COD.

Abattoir wastewater

Abattoir wastewater usually contains considerable concentrations of proteins, lipids, fibres and carbohydrates. Besides, it contains substantial amounts of fat, oil and grease, which can negatively affect sludge settleability. The wastewater is often pre-treated to reduce the fats, oils and greases content (Yilmaz et al., 2008).

Yilmaz et al. (2008) used AGS as inoculum in a reactor with filling + anaerobic mixing. Their strategy consisted of a stepwise increase of the fraction of abattoir effluent fed to the reactor, starting with synthetic wastewater and ending up with 100 % abattoir effluent. The system was able to remove TN, TP and COD with removal efficiencies of 86, 74 and 85 %, respectively. Liu et al. (2015) obtained similar removal efficiencies (85 % COD, 84 % PO_4-P and 97 % NH_4-N), and a fully granular system after 90 days of operation. Dobbeleers et al. (2020) operated a pilot-scale AGS reactor, with anaerobic feeding. The removal efficiencies were of 90, 86 and 84 for COD, N and P, respectively, in a system where granulation took place between days 21 – 142.

Palm oil mill wastewater

Palm oil mill effluents present high COD and BOD_5 concentrations, in the range of 15,000 – 100,000 and 10,300 – 44,000 mg/L, respectively. However, TN and NH_4-N concentrations are low, being of 80 – 1,400 and 4 – 80 mg/L, respectively (Abdullah et al., 2013), which could hinder biomass growth.

Abdullah et al. (2011) and Abdullah et al. (2013) addressed the treatment of palm oil mill effluents. In both studies the addition of nutrients (N and P) was necessary to assure COD:N:P ratios adequate to promote the growth of AGS. Abdullah et al. (2011) operated an AGS reactor with anaerobic feeding, under an OLR of 2.5 kg COD/(m^3·d). They obtained a complete granular system after 8 weeks, and high COD and N removal efficiencies of 86 and 89 – 98 %, respectively. Abdullah et al. (2013) reported the achievement of a full granular system after 60 days, operating at OLRs of 2.5 – 3.5 kg COD/(m^3·d) with a short feeding of 5 min followed by an aeration phase.

Soy-processing wastewater

Soy-processing wastewater is characterised by high COD concentrations (up to 5,400 mg/L), due to the presence of proteins, polypeptides and other organic compounds (Harun et al., 2014). However, the nitrogen concentration is usually low (70 mg TN/L), and biomass growth could be limited.

Su and Yu (2005) treated soybean-processing wastewater with a fully aerobic configuration. Previous to feeding the reactor, the raw wastewater was diluted, and P was dosed to fix a COD:P ratio of 10:1. In addition, microelements were added and the pH was adjusted to 7. The applied OLR was stepwise increased from 1.5 to 6.0 kg COD/(m^3·d). The granulation process was completed after 46 days of operation, and high COD removal efficiencies of 98 – 99 % were reached. Harun et al. (2014) obtained stable granules after 60 days of operation treating soy sauce wastewater. The configuration of the reactor included a short feeding of 5 min followed by

anaerobic recirculation before the aeration step. The removal efficiencies of COD, P and N were in the ranges of 82 – 89, 73 – 89 and 77 – 79, respectively.

Fish-processing wastewater

These effluents present high concentrations of COD (1,300 – 90,000 mg/L) and nutrients (77 – 2,000 mg TN/L), and high salinity (2 – 36 g NaCl/L) (Chowdhury et al., 2010). Their considerable salt content constitutes the main constraint for the optimum performance of the biological processes such as nitrification, denitrification and phosphorus removal.

Corsino et al. (2016) operated an anaerobic-fed reactor using AGS as inoculum. They diluted the raw wastewater to study the performance of the system with salinities of 30 – 75 g NaCl/L and OLRs of 3.2 – 8 kg COD/(m^3·d). The system was able to remove COD and N with efficiencies of 70 – 90 % and 30 – 90 %, respectively. The high salinity of the wastewater inhibited NOB activity, so the nitrogen removal pathway was via biological nitritation – denitritation. Figueroa et al. (2008) obtained stable granules after 75 days in a fully aerobic reactor, with OLRs of 1.46 – 1.72 kg COD/(m^3·d). The removal efficiencies were of 90 – 95 % for COD and 20 – 45 % for TN with 7.1 – 7.5 g Cl^-/L. Val del Río et al. (2013) treated seafood-processing wastewater in a fully aerobic configuration. Full granulation was achieved after 170 days operating under OLRs of 3 – 12 kg COD/(m^3·d). The system was able to remove an 80 – 100 % and 30 % of the incoming COD and N, respectively.

Other food-processing wastewaters

Dobbeleers et al. (2017) treated wastewater from the potato industry in an anaerobic-fed reactor. To have a COD/N ratio of 6.5 g COD/g N, they added acetate, which was after substituted by raw wastewater. They obtained a full granular system between days 127 – 205. The removal efficiencies were of 95 % for N and 66 % for P.

Kocaturk and Erguder (2015) treated sugar beet wastewater, using AGS as inoculum. This effluent presents high concentrations of COD (up to 10,000 mg/L) and suspended solids (up to 5,000 mg/L). The configuration of the reactor operational cycle included a short feeding of 5 min and an anoxic phase before aeration. The start-up strategy consisted of the addition of synthetic feeding, which was changed to the effluent of the anaerobic digester of the sugar beet industry and then to the raw wastewater. The OLR was increased from 0.18 to 6 kg COD/(m^3·d). They obtained a granular system, with a flocculent fraction of 71 – 93 % of the total solid concentration. The removal efficiencies were in the ranges of 72 – 87 % and 57 – 58 % for COD and N, respectively.

Nguyen et al. (2016) treated tapioca wastewater, in a fully aerobic reactor with applied OLRs of 2.5 – 7.5 kg COD/(m^3·d). They added nutrients before feeding the reactor, and adjusted the pH to 6.8 – 7.2. The granulation process was completed after 3 weeks, and the removal efficiencies of COD, N and P were of 92 – 97, 61 – 69 and 80 – 95 %, respectively.

López-Palau et al. (2009) treated winery wastewater in a fully aerobic reactor. This effluent presents most of the organic matter in a soluble and easily biodegradable form. However, there is

usually a lack of nitrogen and phosphorus. Before feeding the reactor, nutrients were added to the wastewater. They obtained a completely granular biomass after 40 days, and COD removal efficiencies of 90 % operating with OLRs of 2.7 – 22.5 kg COD/(m^3·d).

Livestock wastewater

Livestock wastewater presents high COD (up to 6,000 mg/L) and nitrogen (TN of 1,200 mg/L) concentrations (Han et al., 2011). Besides, it usually contains high suspended solids concentrations (Othman et al., 2013).

Kishida et al. (2009) treated the effluent from a pig farm in an anaerobic-fed reactor inoculated with AGS. First, the reactor was fed with synthetic wastewater, and afterwards, it was fed with diluted livestock wastewater. The system was able to achieve removal efficiencies higher than 90 % for Total Organic Carbon (TOC), N and P. Liu et al. (2017) operated a fully aerobic reactor fed with piggery wastewater. They obtained granular biomass after 18 days and removal efficiencies of 51 and 50 % for COD and N, respectively. Othman et al. (2013) treated wastewater from a cattle farm previously passed through a 1 mm mesh sieve. Mature granules were observed after 4 weeks, and the removal efficiencies were in the ranges of 70 – 74, 60 – 73 and 59 – 70 % for COD, N and P, respectively. Morales et al. (2013) operated a pilot-scale reactor to treat swine slurry at OLRs of 1.91 – 4 kg COD/(m^3·d). The granulation process lasted 70 days and the removal efficiencies of COD and N were of 61 – 73 and 56 – 76 %, respectively.

Pulp and paper wastewater

Pulp and paper effluents are rich in organic matter (953 – 38,588 mg COD/L) but present low nitrogen concentrations (0 – 86 mg TN/L). The organic and inorganic pollutants come from tannins, lignins, resins and chlorine compounds (Ashrafi et al., 2015). The low nitrogen concentrations might limit biomass growth, so that nutrient addition is necessary for the biological treatment of this wastewater.

Morais et al. (2016) treated paper mill wastewater, in a fully aerobic reactor. Nutrients (N, P) were added to the wastewater before feeding, to have a COD:N:P ratio of 100:5:1. COD removal efficiencies of 76 % were achieved, and the granulation process was completed after 51 days. Farooqi and Basheer (2017) operated a fully aerobic pilot-scale reactor fed with pulp and paper wastewater. The granulation process was completed after 180 days, with applied OLRs of 0.3 – 4.5 kg COD/(m^3·d), and the COD removal efficiency was of 75 – 88 %.

Textile wastewater

Wastewater from the textile industry contains recalcitrant and toxic pollutants like acids, alkalis, dyes, hydrogen peroxide, starch, surfactants dispersing agents and soaps of metals (Holkar et al., 2016). Besides, it contains organic matter (620 – 49,170 mg COD/L) and nitrogen (30 – 1,700 mg TN/L) (Bisschops and Spanjers, 2003).

Lotito et al. (2014) treated this industrial effluent with a fully aerobic reactor where the biomass grew in the form of biofilm over carriers and in the form of AGS. High removal efficiencies were achieved operating at OLRs of 2.4 – 2.6 kg COD/(m^3·d). Ibrahim et al. (2010) operated a fully aerobic reactor fed with sterilised wastewater. The granulation process lasted 3 weeks and the achieved COD removal efficiencies were of 60 – 90 %.

Petrochemical wastewater

Petrochemical wastewater is characterised by high COD (1,300 – 2,200 mg/L), as well as the presence of chloride (3,200 – 25,000 g Cl^-/L). The low nitrogen content (2.6 – 115 mg TN/L) makes necessary the dosage of N and P to avoid biomass growth limitation (Caluwé et al., 2017a; Corsino et al., 2015).

Caluwé et al. (2017a) operated an anaerobic-fed reactor with OLRs between 0.37 – 1.35 kg COD/(m^3·d). After 80 days, they obtained robust stable flocs, able to remove more than the 90 % of the COD in the feeding. Caluwé et al. (2017b) operated two reactors, one of them with anaerobic feeding, and the other with a fully aerobic cycle configuration. They observed similar results with both configurations: the granulation process was completed after 30 days and the COD removal efficiencies were over 90 %. Corsino et al. (2015) operated a fully aerobic reactor to treat slop. In addition to N dosage, the slop was diluted with synthetic wastewater. Mature granules were obtained after 30 days of operation, and the removal efficiencies of the system were of 88 and 26 % for COD and N, respectively.

Other industrial wastewaters

Rosman et al. (2014) treated rubber wastewater using a fully aerobic AGS reactor, with applied OLRs of 0.9 – 3.6 kg COD/(m^3·d). The obtained granular biomass was able to remove COD and N, with efficiencies of 73 – 95 % for COD and 70 – 80 for TN. Zhang et al. (2013) treated HMX (octahydro – 1, 3, 5, 7 – tetranitro – 1, 3, 5, 7 – tetrazocine), from the industry of explosive production. Before feeding the AGS reactor, the pH was adjusted and P and micronutrients were added to the wastewater. The inoculum of the reactor was AGS. During the start-up, the industrial effluent was diluted with tap water, and the OLR was stepwise increased up to 10.6 kg COD/(m^3·d). The aerobic granules were maintained, and the removal efficiencies of the system were higher than 95 and 80 % for COD and N, respectively. In addition, the HMX was degraded.

Landfill leachate

Landfill leachate presents high concentrations of organic carbon (2,000 – 20,000 mg COD/L), nitrogen compounds (1,000 – 4,000 mg NH_4-N/L), phosphorus and heavy metals.

Wei et al. (2012) operated two reactors to treat this kind of effluent: one was fed with the raw wastewater, whereas in the other magnesium and phosphorus were added to the wastewater to reduce the nitrogen concentration. The COD removal efficiencies of the reactors were similar, being of 82 – 84 %. The N removal efficiencies treating the raw wastewater were of 44 – 62 %,

whereas when using the pre-treated wastewater, they were up to 92 %. Di Bella and Torregrossa (2014) operated two fully aerobic reactors fed at OLRs between 2.4 – 7.2 kg COD/(m^3·d). The COD removal efficiencies oscillated between 20 – 90 %, whereas the N removal efficiencies were of 20 – 60 %. The implementation of a pre-treatment was recommended for decreasing the ammonium concentration of the wastewater.

1.4. SCALE UP OF THE AGS TECHNOLOGY

1.4.1. Pilot-scale studies

In recent years, different studies have been carried out for the development of aerobic granules in pilot scale reactors (60 L – 30 m^3) to treat municipal and industrial wastewater (Table 1.2). The pilot plants treating municipal wastewater were usually operated under low OLRs (0.4 – 2 kg COD/(m^3·d)) due to the low COD concentrations of the influent (35 – 535 mg/L). The cycle configuration of most of them comprised an anaerobic feeding followed by an aeration phase. In general, long granulation periods were reported, being of from 37 to 300 days, and in some cases, there was a fraction of flocculent sludge in steady-state conditions (corresponding to 18 – 30 % of the solid concentration). Granules presented average particle diameters below 1 mm and good settling properties (average SVI_{30} values of 30 – 80 mL/g TSS). COD and P removal efficiencies were high in all the studies (higher than 80 %), whereas N removal efficiencies were more irregular (40 – 98 %).

In the pilot-scale studies addressing the treatment of industrial wastewater, the COD concentrations treated were higher compared to municipal sewage (200 – 3,000 mg/L) and higher OLRs were applied (1.3 – 4.5 kg COD/(m^3·d)). The cycle configuration comprised an anaerobic feeding followed by aeration phase or short feeding and a long aeration period. The granulation time was in the range of 30 – 140 days, being lower than in the case of municipal sewage treatment. The obtained granules were bigger (0.5 – 4.0 mm) due to the higher OLRs and with good settleability (SVI of 30 – 100 mL/g TSS). Most of the research works were focused on the removal of COD and N, achieving efficiencies in the ranges of 75 – 95 % of COD and 76 – 99 % of TN, respectively.

Table 1.2: Performance and operational conditions of pilot-scale AGS reactors.

Reactor volume (L)	Feeding strategy	Type of wastewater	WW composition (mg/L)	OLR (kg COD/(m³·d))	Granulation time (d)	AGS properties	Removal efficiency (%)	Ref
100	Anaerobic	Synthetic	COD_S: 400 NH_4-N: 40 P: 10	-	51	Particle size: 2.4 mm SVI_{30}: 13 – 17 mL/g TSS MLSS: 12 – 17 g/L	COD: 80 – 90 N: 75 – 90 P: 45 – 70	[1]
100	Short aerobic	Synthetic	COD_S: 700 – 1500 NH_4-N: 40 – 120	2.4 – 9.7	36	Particle size: 3.5 mm MLSS: 4 – 8 g/L	COD: 96 N: 53 – 67	[2]
63.9	Anaerobic	Municipal sewage	COD_T: 535 NH_4-N: 35 TN: 56	0.76 – 1.15	37	SVI_{30}: 38 – 58 mL/g TSS MLSS: 5 – 7 g/L	COD: 5 – 50 TN: 16 – 98	[3]
85	Anaerobic	Municipal sewage	COD_T: 200 – 320 TN: 38 – 55 TP: 6 – 13	0.35 – 1.35	45	Particle size: 0.7 – 0.8 mm SVI_{30}: 39 mL/g TSS MLSS: 4 g/L	COD: 92 TN: 81 TP: 85	[4]
118.7	Anaerobic static	Municipal sewage	COD_S: 304 TN: 83 NH_4-N: 82	1	56 (18 % flocculent)	Particle size: 0.47 mm SVI_{30}: 76 mL/g TSS MLSS: 1.8 g/L	COD: 92 TN: 60	[5]
120.5	Anaerobic	Septic tank sewage	COD_S: 535 – 810 TN: 59 – 86 NH_4-N: 49 – 74 TP: 5 – 12	2.69	37	Particle size: 1.5 – 2.4 mm SVI_{30}: 50 – 70 mL/g TSS MLVSS: 4.4 – 5 g/L	COD: > 90 TN: 40 – 50 TP: > 90	[6]
190	Anaerobic	Municipal sewage	COD_S: 304 TN: 32 NH_4-N: 18 TP: 5 PO_4-P: 2	0.4	90 (60 – 70 % granules)	Particle size: 0.25 – 0.63 mm SVI_{30}: 50 mL/g TSS MLSS: 1.2 – 6 g/L	COD: > 80 TN: 28 – 96 TP: 89	[7]

Table 1.2 (continued).

Reactor volume (L)	Feeding strategy	Type of wastewater	WW composition (mg/L)	OLR (kg COD/(m³·d))	Granulation time (d)	AGS properties	Removal efficiency (%)	Ref
1,000	Short	Municipal sewage	COD_S: 35 – 120 TN: 12 – 50 NH_4-N: 10 – 40	-	300 (> 80 % granules)	Particle size: 0.2 – 0.8 mm SVI_{30}: 30 – 40 mL/g TSS MLSS: 8 – 9 g/L	COD: 85 – 95 N: 90 – 99	[8]
1,500	Anaerobic	Municipal sewage	COD_S: 270 – 400	-	180	-	-	[9]
4,000	Short + an. Mixing	Municipal sewage (+ acetate)	COD_T: 287 – 492 NH_4-N: 49 TP: 6.8	0.5 – 2	100	Particle size: 1.1 mm MLSS: 3 – 8 g/L	-	[10]
100	Short	Swine slurry	COD_S: 487 – 1003 NH_4-N: 148 – 249	1.91 – 4	70	Particle size: 1 – 3 mm SVI_{30}: 30 – 40 mL/g TSS MLVSS: 6 – 8 g/L	COD: 61 – 73 TN: 56 – 76	[11]
450	Anaerobic	Abattoir	COD_S: 1223 – 1361 NH_4-N: 143 – 161 TP: 16	-	142	Particle size: 0.5 mm SVI_{30}: < 100 mL/g TSS MLSS: < 3 g/L	COD: 90 TN: 89 P: 84	[12]
1,470	Short + an. mixing	Soy protein	COD_S: 700 – 2400 NH_4-N: 200	1.33	30	Particle size: 1.2 – 2 mm SVI_5: 43 – 55 mL/g TSS MLVSS: 6 – 7 g/L	COD: 80 – 95 TN: 95 – 99	[13]
3,394	Short	Pulp and paper	COD_S: 2000 - 3000	0.3 – 4.5	180	Particle size: 0.5 – 4 mm SVI_{30}: 60 – 110 mL/g TSS MLSS: 5 – 8 g/L	COD: > 80 TN: 28 – 96 TP: 89	[14]

Table 1.2 (continued).

Reactor volume (L)	Feeding strategy	Type of wastewater	WW composition (mg/L)	OLR (kg COD/(m³·d))	Granulation time (d)	AGS properties	Removal efficiency (%)	Ref
31,400 (2 SBR in parallel)	Short	30 % municipal 70 % industrial	COD_S: 500 – 1000 NH_4-N: 30 – 80 TP: 2 – 4	-	50	Particle size: 0.3 mm SVI_{30}: 43 mL/g TSS MLSS: 8 – 9 g/L	COD: 88 N: 100	[15]

[1] Isanta et al. (2012) [2] Jungles et al. (2011) [3] Thwaites et al. (2017) [4] Su et al. (2012) [5] J. Wagner et al. (2015) [6] Long et al. (2019) [7] Derlon et al. (2016) [8] Ni et al. (2009) [9] De Kreuk et al. (2006) [10] Rocktäschel et al. (2015) [11] Morales et al. (2013) [12] Dobbeleers et al. (2020) [13] Wei et al. (2013)[14] Farooqi and Basheer (2017) [15] Li et al. (2014b).

1.4.2. Full-scale studies

At full scale, Nereda® was the first mature technology to be applied. This technology uses an SBR in which fill and draw are combined in a first process step. During this step, the influent is distributed at the bottom of the reactor and the effluent is simultaneously displaced from the reactor at the top. After feeding, the aeration process starts. In the last step of the cycle, the granular biomass is allowed to settle (Giesen et al., 2013).

More than a decade was needed to translate results from laboratory-scale to pilot and full-scale installations (Giesen et al., 2013). It was first adapted for industrial applications and then further scaled-up for domestic sewage treatment (Pronk et al., 2015). The first full-scale Nereda® plant was commissioned in 2006 at a cheese factory in the Netherlands (van der Roest et al., 2011). Subsequently, more treatment plants were started up. Currently, there are 68 Nereda® full-scale projects all over the world (Table 1.3). Most of them are focused on the treatment of municipal sewage, and only 6 of them address the treatment of industrial wastewater (food industry).

Table 1.3: Nereda® full-scale plants in operation.

World region	Number of plants	Peak flow (m^3/h)	Person equivalents (PE)	Wastewater
Africa	3	208 – 600	28,182 – 47,000	Municipal
Asia	1		4,630	Municipal
Europe	45	10 – 50,000	4,167 – 2,400,000	Municipal Industrial
North America	3	961 – 1135	60,717	Municipal
South America	12	1,492 – 10,333	99,500 – 1,057,460	Municipal
Oceania	3	450 – 5,400	10,001 – 147,200	Municipal Industrial

Data from webpage: https://www.royalhaskoningdhv.com/nereda.

Pronk et al. (2015) have demonstrated the full-scale application of Nereda® technology treating municipal wastewater. The plant, with a working capacity of 4,200 m^3/d, produced an effluent with N and P concentrations lower than 7 and 1 mg/L, respectively, fulfilling the imposed discharge requirements. The biomass accumulated in the system contained over 80 % of granular sludge, with good settleability (SVI_5 and SVI_{30} of 45 and 35 mL/g TSS, respectively) and biomass concentrations higher than 8 g TSS/L. van Dijk et al. (2018) reported the operation of another plant of 1,050 m^3 treating municipal wastewater. The effluent generated in the plant presented average concentrations of 41 mg COD/L, 4 mg TN/L, and 0.5 mg TP/L. The biomass consisted of smooth granules bigger than 1 mm, with SVI_5 of 34 – 57 mL/g TSS and concentrations of 8 – 12 g TSS/L.

1.5. BIOLOGICAL MODELLING

Mathematical modelling of wastewater treatment processes has become a widely accepted tool used for different purposes like research, plant design, optimisation, training, model-based development and testing of process control (Corominas et al., 2010).

The first biological model of aerobic processes (Activated Sludge Model 1, ASM1) was introduced by the International Water Association (IWA) in 1987, for the description of the biological COD and nitrogen removal in CAS processes (Henze et al., 2000). This model became a reference for many scientific and practical projects and has been implemented in most of the commercial software for modelling and simulation of WWTPs (Gernaey et al., 2004).

From this first model, others have been developed, introducing modifications to include additional biological processes and describe the removal of other compounds from the wastewater (Henze et al., 2000). ASM1 was primarily created to describe the removal of organic matter and nutrients due to heterotrophic growth and nitrifying activity. Later, ASM2 was developed, to include the biological processes associated with the metabolism of PAOs, thus, including phosphorus as a substrate in the model. Both the biological removal by PAOs and the chemical removal via precipitation were considered. PAOs were modelled with internal cell structure, and the stored organic substrates were used for further growth of the biomass. Then, a modification of ASM2 was made (ASM2d), to add the denitrifying activity of PAOs and provide a better description of the dynamics of phosphate and nitrate. Additionally, the ASM3 model was developed with the same goal as ASM1, to describe the removal of both organic matter and nitrogen. This model took into account the removal of organic matter by internal storage of heterotrophic bacteria, in a similar way as ASM2. It did not consider the heterotrophic growth on external substrate, as described in ASM1, but based on the internal stored compounds (Henze et al., 2000).

In ASM models, biomass is supposed in suspension in the bulk liquid. However, this approach is not suitable when bacteria grow forming aerobic granules, since the biological processes are defined by concentration gradients of oxygen and different substrates inside the aggregates. The concentration profiles are the result of factors like diffusion coefficients, conversion rates, granule size, biomass spatial distribution or density (De Kreuk et al., 2007). For that reason, biofilm models, which consider mass transfer limitations within the biofilm, in addition to the bioconversion rates, have been adapted to describe the biological conversion processes in AGS. They provide information about the most important factors that affect the reactor performance and the distribution of different populations in the microbial aggregates (De Kreuk et al., 2007).

1.6. SCOPE OF THE THESIS

The research work developed during this thesis was divided into two blocks. The first block (Chapters 3 and 4), focused on the implementation of a new aeration strategy to address the issue of high energy costs associated to oxygen supply in AGS reactors. The new strategy, based on the use of pulsed aeration, was evaluated in two different configurations: anaerobic-aerobic and fully aerobic. In addition, the features of the aerobic granules were studied using different feeding strategies. In the second block (Chapters 5 to 8), AGS technology was evaluated for the treatment of industrial saline wastewater, in particular fish-canning wastewater. Firstly, a laboratory-scale reactor was operated. Then, the technology was scaled up and a pilot plant was used for *in situ* treatment of this industrial wastewater. Additionally, a biological model was developed from the obtained experimental data to study the impact of this industrial saline effluent in the conversion rates of the process.

1.7. REFERENCES

Abdullah, N., Ujang, Z., Yahya, A., 2011. Aerobic granular sludge formation for high strength agro-based wastewater treatment. Bioresour. Technol. 102, 6778–6781. https://doi.org/10.1016/j.biortech.2011.04.009

Abdullah, N., Yuzir, A., Curtis, T.P., Yahya, A., Ujang, Z., 2013. Characterization of aerobic granular sludge treating high strength agro-based wastewater at different volumetric loadings. Bioresour. Technol. 127, 181–187. https://doi.org/10.1016/j.biortech.2012.09.047

Adav, S.S., Lee, D.J., Lai, J.Y., 2010. Potential cause of aerobic granular sludge breakdown at high organic loading rates. Appl. Microbiol. Biotechnol. 85, 1601–1610. https://doi.org/10.1007/s00253-009-2317-9

Adav, S.S., Lee, D.J., Show, K.Y., Tay, J.H., 2008. Aerobic granular sludge: Recent advances. Biotechnol. Adv. https://doi.org/10.1016/j.biotechadv.2008.05.002

Ahmad, J.S.M., Zhao, Z., Zhang, Z., Shimizu, K., Utsumi, M., Lei, Z., Lee, D.J., Tay, J.H., 2019. Algal-bacterial aerobic granule based continuous-flow reactor with effluent recirculation instead of air bubbling: Stability and energy consumption analysis. Bioresour. Technol. Reports. https://doi.org/10.1016/j.biteb.2019.100215

Arrojo, B., Mosquera-Corral, A., Garrido, J.M., Méndez, R., 2004. Aerobic granulation with industrial wastewater in sequencing batch reactors. Water Res. 38, 3389–3399. https://doi.org/10.1016/j.watres.2004.05.002

Ashrafi, O., Yerushalmi, L., Haghighat, F., 2015. Wastewater treatment in the pulp-and-paper industry: A review of treatment processes and the associated greenhouse gas emission. J. Environ. Manage. https://doi.org/10.1016/j.jenvman.2015.05.010

Bakare, B.F., Shabangu, K., Chetty, M., 2017. Brewery wastewater treatment using laboratory scale aerobic sequencing batch reactor. South African J. Chem. Eng. https://doi.org/10.1016/j.sajce.2017.08.001

Bassin, J.P., Pronk, M., Muyzer, G., Kleerebezem, R., Dezotti, M., van Loosdrecht, M.C.M., 2011. Effect of elevated salt concentrations on the aerobic granular sludge process: Linking microbial activity with microbial community structure. Appl. Environ. Microbiol. https://doi.org/10.1128/AEM.05016-11

Bella, G. Di, Torregrossa, M., 2014. Aerobic granular sludge for leachate treatment. Chem. Eng. Trans. 38, 493–498. https://doi.org/10.3303/CET1438083

Bengtsson, S., de Blois, M., Wilén, B.M., Gustavsson, D., 2019. A comparison of aerobic granular sludge with conventional and compact biological treatment technologies. Environ. Technol. (United Kingdom). https://doi.org/10.1080/09593330.2018.1452985

Bengtsson, S., de Blois, M., Wilén, B.M., Gustavsson, D., 2018. Treatment of municipal wastewater with aerobic granular sludge. Crit. Rev. Environ. Sci. Technol. 48, 119–166. https://doi.org/10.1080/10643389.2018.1439653

Beun, J.J., Heijnen, J.J., van Loosdrecht, M.C., 2001. N-removal in a granular sludge sequencing batch airlift reactor. Biotechnol. Bioeng.

Beun, J.J., Hendriks, A., Van Loosdrecht, M.C.M., Morgenroth, E., Wilderer, P.A., Heijnen, J.J., 1999. Aerobic granulation in a sequencing batch reactor. Water Res. 33, 2283–2290. https://doi.org/10.1016/S0043-1354(98)00463-1

Bisschops, I., Spanjers, H., 2003. Literature review on textile wastewater characterisation. Environ. Technol. (United Kingdom). https://doi.org/10.1080/09593330309385684

Bumbac, C., Ionescu, I.A., Tiron, O., Badescu, V.R., 2015. Continuous flow aerobic granular sludge reactor for dairy wastewater treatment. Water Sci. Technol. 71, 440–445. https://doi.org/10.2166/wst.2015.007

Caluwé, M., Daens, D., Blust, R., Geuens, L., Dries, J., 2017a. The sequencing batch reactor as an excellent configuration to treat wastewater from the petrochemical industry. Water Sci. Technol. 75, 793–801. https://doi.org/10.2166/wst.2016.562

Caluwé, M., Dobbeleers, T., D'aes, J., Miele, S., Akkermans, V., Daens, D., Geuens, L., Kiekens, F., Blust, R., Dries, J., 2017b. Formation of aerobic granular sludge during the treatment of petrochemical wastewater. Bioresour. Technol. 238, 559–567. https://doi.org/10.1016/j.biortech.2017.04.068

Campos, J.L., Figueroa, M., Corral, A.M., Mendez, R., 2009. Aerobic sludge granulation: state-of-the-art. Int. J. Environ. Eng. 1, 136. https://doi.org/10.1504/IJEE.2009.027311

Chen, Y., Jiang, W., Liang, D.T., Tay, J.H., 2007. Structure and stability of aerobic granules cultivated under different shear force in sequencing batch reactors. Appl. Microbiol. Biotechnol. 76, 1199–1208. https://doi.org/10.1007/s00253-007-1085-7

Chowdhury, P., Viraraghavan, T., Srinivasan, A., 2010. Biological treatment processes for fish processing wastewater - A review. Bioresour. Technol. https://doi.org/10.1016/j.biortech.2009.08.065

Cofré, C., Campos, J.L., Valenzuela-Heredia, D., Pavissich, J.P., Camus, N., Belmonte, M., Pedrouso, A., Carrera, P., Mosquera-Corral, A., Val del Río, A., 2018. Novel system configuration with activated sludge like-geometry to develop aerobic granular biomass under continuous flow. Bioresour. Technol. https://doi.org/10.1016/j.biortech.2018.07.146

Corominas, L., Rieger, L., Takács, I., Ekama, G., Hauduc, H., Vanrolleghem, P.A., Oehmen, A., Gernaey, K. V., Van Loosdrecht, M.C.M., Comeau, Y., 2010. New framework for standardized notation in wastewater treatment modelling. Water Sci. Technol. 61, 841–857. https://doi.org/10.2166/wst.2010.912

Corsino, S.F., Campo, R., Di Bella, G., Torregrossa, M., Viviani, G., 2015. Cultivation of granular sludge with hypersaline oily wastewater. Int. Biodeterior. Biodegrad. 105, 192–202. https://doi.org/10.1016/j.ibiod.2015.09.009

Corsino, S.F., Capodici, M., Di Pippo, F., Tandoi, V., Torregrossa, M., 2019. Comparison between kinetics of autochthonous marine bacteria in activated sludge and granular sludge systems at different salinity and SRTs. Water Res. 148, 425–437. https://doi.org/10.1016/j.watres.2018.10.086

Corsino, S.F., Capodici, M., Morici, C., Torregrossa, M., Viviani, G., 2016. Simultaneous nitritation-denitritation for the treatment of high-strength nitrogen in hypersaline wastewater by aerobic granular sludge. Water Res. 88, 329–336. https://doi.org/10.1016/j.watres.2015.10.041

Corsino, S.F., di Biase, A., Devlin, T.R., Munz, G., Torregrossa, M., Oleszkiewicz, J.A., 2017. Effect of extended famine conditions on aerobic granular sludge stability in the treatment of brewery wastewater. Bioresour. Technol. 226, 150–157. https://doi.org/10.1016/j.biortech.2016.12.026

De Kreuk, M.K., Heijnen, J.J., Van Loosdrecht, M.C.M., 2005. Simultaneous COD, nitrogen, and phosphate removal by aerobic granular sludge. Biotechnol. Bioeng. 90, 761–769. https://doi.org/10.1002/bit.20470

de Kreuk, M.K., Kishida, N., Tsuneda, S., van Loosdrecht, M.C.M., 2010. Behavior of polymeric substrates in an aerobic granular sludge system. Water Res. https://doi.org/10.1016/j.watres.2010.07.033

De Kreuk, M.K., Picioreanu, C., Hosseini, M., Xavier, J.B., Van Loosdrecht, M.C.M., 2007. Kinetic model of a granular sludge SBR: Influences on nutrient removal. Biotechnol. Bioeng. https://doi.org/10.1002/bit.21196

de Kreuk, M.K., van Loosdrecht, M.C.M., 2004. Selection of slow growing organisms as a means for improving aerobic granular sludge stability. Water Sci. Technol. 49, 9–17

De Kreuk, M.K., Van Loosdrecht, M.C.M., Heijnen, J.J., 2006. Aerobic granular sludge : scaling up a new technology, Department of Biochemical Engineering

de Sousa Rollemberg, S.L., Mendes Barros, A.R., Milen Firmino, P.I., Bezerra dos Santos, A., 2018. Aerobic granular sludge: Cultivation parameters and removal mechanisms. Bioresour. Technol. 270, 678–688. https://doi.org/10.1016/j.biortech.2018.08.130

Derlon, N., Wagner, J., da Costa, R.H.R., Morgenroth, E., 2016. Formation of aerobic granules for the treatment of real and low-strength municipal wastewater using a sequencing batch reactor operated at constant volume. Water Res. 105, 341–350. https://doi.org/10.1016/j.watres.2016.09.007

Devlin, T.R., di Biase, A., Kowalski, M., Oleszkiewicz, J.A., 2017. Granulation of activated sludge under low hydrodynamic shear and different wastewater characteristics. Bioresour. Technol. 224, 229–235. https://doi.org/10.1016/j.biortech.2016.11.005

Dezotti, M., Lippel, G., Bassin, J.P., 2018. Advanced Biological Processes for Wastewater Treatment, Advanced Biological Processes for Wastewater Treatment. https://doi.org/10.1007/978-3-319-58835-3

Dobbeleers, T., Caluwé, M., Dockx, L., Daens, D., D'aes, J., Dries, J., 2020. Biological nutrient removal from slaughterhouse wastewater via nitritation/denitritation using granular sludge: an onsite pilot demonstration. J. Chem. Technol. Biotechnol. 95, 111–122. https://doi.org/10.1002/jctb.6212

Dobbeleers, T., Daens, D., Miele, S., D'aes, J., Caluwé, M., Geuens, L., Dries, J., 2017. Performance of aerobic nitrite granules treating an anaerobic pre-treated wastewater originating from the potato industry. Bioresour. Technol. 226, 211–219. https://doi.org/10.1016/j.biortech.2016.11.117

Farooqi, I.H., Basheer, F., 2017. Treatment of Adsorbable Organic Halide (AOX) from pulp and paper industry wastewater using aerobic granules in pilot scale SBR. J. Water Process Eng. 19, 60–66. https://doi.org/10.1016/j.jwpe.2017.07.005

Figueroa, M., Mosquera-Corral, A., Campos, J.L., Méndez, R., 2008. Treatment of saline wastewater in SBR aerobic granular reactors. Water Sci. Technol. https://doi.org/10.2166/wst.2008.406

Franca, R.D.G., Pinheiro, H.M., van Loosdrecht, M.C.M., Lourenço, N.D., 2018. Stability of aerobic granules during long-term bioreactor operation. Biotechnol. Adv. 36, 228–246. https://doi.org/10.1016/j.biotechadv.2017.11.005

Gao, D.W., Liu, L., Liang, H., 2013. Influence of aeration intensity on mature aerobic granules in sequencing batch reactor. Appl. Microbiol. Biotechnol. 97, 4213–4219. https://doi.org/10.1007/s00253-012-4226-6

Gernaey, K. V., Van Loosdrecht, M.C.M., Henze, M., Lind, M., Jørgensen, S.B., 2004. Activated sludge wastewater treatment plant modelling and simulation: State of the art, in: Environmental Modelling and Software. https://doi.org/10.1016/j.envsoft.2003.03.005

Giesen, A., de Bruin, L.M.M., Niermans, R.P., van der Roest, H.F., 2013. Advancements in the application of aerobic granular biomass technology for sustainable treatment of wastewater. Water Pract. Technol. 8, 47–54. https://doi.org/10.2166/wpt.2013.007

Guimarães, L.B., Mezzari, M.P., Daudt, G.C., da Costa, R.H.R., 2017. Microbial pathways of nitrogen removal in aerobic granular sludge treating domestic wastewater. J. Chem. Technol. Biotechnol. 92, 1756–1765. https://doi.org/10.1002/jctb.5176

Han, Z., Zhu, J., Ding, Y., Wu, W., Chen, Y., Zhang, R., Wang, L., 2011. Effect of Feeding Strategy on the Performance of Sequencing Batch Reactor with Dual Anoxic Feedings for Swine Wastewater Treatment. Water Environ. Res. https://doi.org/10.2175/106143010x12851009156880

Harun, H., Anuar, A.N., Ujang, Z., Rosman, N.H., Othman, I., 2014. Performance of aerobic granular sludge at variable circulation rate in anaerobic-aerobic conditions. Water Sci. Technol. 69, 2252–2257. https://doi.org/10.2166/wst.2014.156

Henze, M., Gujer, W., Mino, T., Loosdrecht, M. van, 2000. Activated Sludge Models ASM1, ASM2, ASM2d and ASM3 IWA Scientific and Technical Report No.9, Journal of Chemical Information and Modeling. https://doi.org/10.1017/CBO9781107415324.004

Holkar, C.R., Jadhav, A.J., Pinjari, D. V., Mahamuni, N.M., Pandit, A.B., 2016. A critical review on textile wastewater treatments: Possible approaches. J. Environ. Manage. https://doi.org/10.1016/j.jenvman.2016.07.090

Ibrahim, Z., Amin, M.F.M., Yahya, A., Aris, A., Muda, K., 2010. Characteristics of developed granules containing selected decolourising bacteria for the degradation of textile wastewater. Water Sci. Technol. 61, 1279–1288. https://doi.org/10.2166/wst.2010.021

Isanta, E., Suárez-Ojeda, M.E., Val del Río, Á., Morales, N., Pérez, J., Carrera, J., 2012. Long term operation of a granular sequencing batch reactor at pilot scale treating a low-strength wastewater. Chem. Eng. J. 198–199, 163–170. https://doi.org/10.1016/j.cej.2012.05.066

Ji, G., Zhai, F., Wang, R., Ni, J., 2010. Sludge granulation and performance of a low superficial gas velocity sequencing batch reactor (SBR) in the treatment of prepared sanitary wastewater. Bioresour. Technol. 101, 9058–9064. https://doi.org/10.1016/j.biortech.2010.07.045

Jiang, X., Yuan, Y., Ma, F., Tian, J., Wang, Y., 2016. Enhanced biological phosphorus removal by granular sludge in anaerobic/aerobic/anoxic SBR during start-up period. Desalin. Water Treat. 57, 5760–5771. https://doi.org/10.1080/19443994.2015.1004114

Jungles, M.K., Figueroa, M., Morales, N., Val del Río, Á., da Costa, R.H.R., Campos, J.L., Mosquera-Corral, A., Méndez, R., 2011. Start up of a pilot scale aerobic granular reactor for organic matter and nitrogen removal. J. Chem. Technol. Biotechnol. 86, 763–768. https://doi.org/10.1002/jctb.2589

Kishida, N., Tsuneda, S., Kim, J.H., Sudo, R., 2009. Simultaneous nitrogen and phosphorus removal from high-strength industrial wastewater using aerobic granular sludge. J. Environ. Eng. 135, 153–158. https://doi.org/10.1061/(ASCE)0733-9372(2009)135:3(153)

Kocaturk, I., Erguder, T.H., 2016. Influent COD/TAN ratio affects the carbon and nitrogen removal efficiency and stability of aerobic granules. Ecol. Eng. 90, 12–24. https://doi.org/10.1016/j.ecoleng.2016.01.077

Kocaturk, I., Erguder, T.H., 2015. Investigation of the use of aerobic granules for the treatment of sugar beet processing wastewater. Environ. Technol. (United Kingdom) 36, 2577–2587. https://doi.org/10.1080/09593330.2015.1039070

Li, A.J., Li, X.Y., Yu, H.Q., 2011. Granular activated carbon for aerobic sludge granulation in a bioreactor with a low-strength wastewater influent. Sep. Purif. Technol. 80, 276–283. https://doi.org/10.1016/j.seppur.2011.05.006

Li, A.J., Yang, S.F., Li, X.Y., Gu, J.D., 2008. Microbial population dynamics during aerobic sludge granulation at different organic loading rates. Water Res. https://doi.org/10.1016/j.watres.2008.05.005

Li, J., Cai, A., Wang, M., Ding, L., Ni, Y., 2014a. Aerobic granulation in a modified oxidation ditch with an adjustable volume intraclarifier. Bioresour. Technol. https://doi.org/10.1016/j.biortech.2014.01.130

Li, J., Ding, L. Bin, Cai, A., Huang, G.X., Horn, H., 2014b. Aerobic sludge granulation in a full-scale sequencing batch reactor. Biomed Res. Int. 2014. https://doi.org/10.1155/2014/268789

Li, X., Yuan, Yan, Yuan, Yi, Bi, Z., Liu, X., Huang, Y., Liu, H., Chen, C., Xu, S., 2018. Effects of salinity on the denitrification efficiency and community structure of a combined partial nitritation- anaerobic ammonium oxidation process. Bioresour. Technol. 249, 550–556. https://doi.org/10.1016/j.biortech.2017.10.037

Liu, J., Li, J., Wang, X., Zhang, Q., Littleton, H., 2017. Rapid aerobic granulation in an SBR treating piggery wastewater by seeding sludge from a municipal WWTP. J. Environ. Sci. (China) 51, 332–341. https://doi.org/10.1016/j.jes.2016.06.012

Liu, L., Gao, D.W., Zhang, M., Fu, Y., 2010. Comparison of Ca^{2+} and Mg^{2+} enhancing aerobic granulation in SBR. J. Hazard. Mater. https://doi.org/10.1016/j.jhazmat.2010.05.021

Liu, Y., Kang, X., Li, X., Yuan, Y., 2015. Performance of aerobic granular sludge in a sequencing batch bioreactor for slaughterhouse wastewater treatment. Bioresour. Technol. 190, 487–491. https://doi.org/10.1016/j.biortech.2015.03.008

Liu, Y., Tay, J.H., 2004. State of the art of biogranulation technology for wastewater treatment. Biotechnol. Adv. https://doi.org/10.1016/j.biotechadv.2004.05.001

Liu, Y.Q., Zhang, X., Zhang, R., Liu, W.T., Tay, J.H., 2016. Effects of hydraulic retention time on aerobic granulation and granule growth kinetics at steady state with a fast start-up strategy. Appl. Microbiol. Biotechnol. 100, 469–477. https://doi.org/10.1007/s00253-015-6993-3

Lochmatter, S., Gonzalez-Gil, G., Holliger, C., 2013. Optimized aeration strategies for nitrogen and phosphorus removal with aerobic granular sludge. Water Res. 47, 6187–6197. https://doi.org/10.1016/j.watres.2013.07.030

Long, B., Xuan, X., Yang, C., Zhang, L., Cheng, Y., Wang, J., 2019. Stability of aerobic granular sludge in a pilot scale sequencing batch reactor enhanced by granular particle size control. Chemosphere 225, 460–469. https://doi.org/10.1016/j.chemosphere.2019.03.048

Long, B., Yang, C.Z., Pu, W.H., Yang, J.K., Liu, F.B., Zhang, L., Zhang, J., Cheng, K., 2015. Tolerance to organic loading rate by aerobic granular sludge in a cyclic aerobic granular reactor. Bioresour. Technol. 182, 314–322. https://doi.org/10.1016/j.biortech.2015.02.029

López-Palau, S., Dosta, J., Mata-Álvarez, J., 2009. Start-up of an aerobic granular sequencing batch reactor for the treatment of winery wastewater. Water Sci. Technol. 60, 1049–1054. https://doi.org/10.2166/wst.2009.554

Lotito, A.M., De Sanctis, M., Di Iaconi, C., Bergna, G., 2014. Textile wastewater treatment: Aerobic granular sludge vs activated sludge systems. Water Res. 54, 337–346. https://doi.org/10.1016/j.watres.2014.01.055

Luo, J., Hao, T., Wei, L., Mackey, H.R., Lin, Z., Chen, G.H., 2014. Impact of influent COD/N ratio on disintegration of aerobic granular sludge. Water Res. 62, 127–135. https://doi.org/10.1016/j.watres.2014.05.037

Meunier, C., Henriet, O., Schroonbroodt, B., Boeur, J.M., Mahillon, J., Henry, P., 2016. Influence of feeding pattern and hydraulic selection pressure to control filamentous bulking in biological treatment of dairy wastewaters. Bioresour. Technol. 221, 300–309. https://doi.org/10.1016/j.biortech.2016.09.052

Mino, T., Van Loosdrecht, M.C.M., Heijnen, J.J., 1998. Microbiology and biochemistry of the enhanced biological phosphate removal process. Water Res. 32, 3193–3207. https://doi.org/10.1016/S0043-1354(98)00129-8

Mishima, K., Nakamura, M., 1991. Self-immobilization of aerobic activated sludge - A pilot study of the Aerobic Upflow Sludge Blanket Process in municipal sewage treatment, in: Water Science and Technology. https://doi.org/10.2166/wst.1991.0550

Morais, I.L.H., Silva, C.M., Borges, C.P., 2016. Aerobic granular sludge to treat paper mill effluent: organic matter removal and sludge filterability. Desalin. Water Treat. 57, 8119–8126. https://doi.org/10.1080/19443994.2015.1022803

Morales, N., Figueroa, M., Fra-Vázquez, A., Val Del Río, A., Campos, J.L., Mosquera-Corral, A., Méndez, R., 2013. Operation of an aerobic granular pilot scale SBR plant to treat swine slurry. Process Biochem. 48, 1216–1221. https://doi.org/10.1016/j.procbio.2013.06.004

Morgenroth, E. Sherden, T. Van Loosdrecht, M.C.M. Heijnen, J.J. Wilderer, P.A., 1997. Aerobic Granular Sludge in a Sequencing Batch Reactor. Water Res. 31, 3191–3194

Mosquera-Corral, A., De Kreuk, M.K., Heijnen, J.J., Van Loosdrecht, M.C.M., 2005. Effects of oxygen concentration on N-removal in an aerobic granular sludge reactor. Water Res. 39, 2676–2686. https://doi.org/10.1016/j.watres.2005.04.065

Moura, L.L., Duarte, K.L.S., Santiago, E.P., Mahler, C.F., Bassin, J.P., 2018. Strategies to re-establish stable granulation after filamentous outgrowth: Insights from lab-scale experiments. Process Saf. Environ. Prot. 117, 606–615. https://doi.org/10.1016/j.psep.2018.06.005

Nancharaiah, Y. V., Kiran Kumar Reddy, G., 2018. Aerobic granular sludge technology: Mechanisms of granulation and biotechnological applications. Bioresour. Technol. 247, 1128–1143. https://doi.org/10.1016/j.biortech.2017.09.131

Nancharaiah, Y. V., Sarvajith, M., Krishna Mohan, T. V., 2019. Aerobic granular sludge: The future of wastewater treatment. Curr. Sci. https://doi.org/10.18520/cs/v117/i3/395-404

Nguyen, P.T.T., Van Nguyen, P., Truong, H.T.B., Bui, H.M., 2016. The formation and stabilization of aerobic granular sludge in a sequencing batch airlift reactor for treating tapioca-processing wastewater. Polish J. Environ. Stud. 25, 2077–2084. https://doi.org/10.15244/pjoes/62736

Ni, B.J., Pan, Y., Guo, J., Virdis, B., Hu, S., Chen, X., Yuan, Z., 2017. CHAPTER 16: Denitrification Processes for Wastewater Treatment, in: RSC Metallobiology. https://doi.org/10.1039/9781782623762-00368

Ni, B.J., Xie, W.M., Liu, S.G., Yu, H.Q., Wang, Y.Z., Wang, G., Dai, X.L., 2009. Granulation of activated sludge in a pilot-scale sequencing batch reactor for the treatment of low-strength municipal wastewater. Water Res. 43, 751–761. https://doi.org/10.1016/j.watres.2008.11.009

Niermans, R., Giesen, A., Van Loosdrecht, M., De Buin, B., 2014. Full-scale experiences with aerobic granular biomass technology for treatment of urban and industrial wastewater. 87th Annu. Water Environ. Fed. Tech. Exhib. Conf. WEFTEC 2014 1, 2347–2357

Oehmen, A., Lemos, P.C., Carvalho, G., Yuan, Z., Keller, J., Blackall, L.L., Reis, M.A.M., 2007. Advances in enhanced biological phosphorus removal: From micro to macro scale. Water Res. 41, 2271–2300. https://doi.org/10.1016/j.watres.2007.02.030

Othman, I., Anuar, A.N., Ujang, Z., Rosman, N.H., Harun, H., Chelliapan, S., 2013. Livestock wastewater treatment using aerobic granular sludge. Bioresour. Technol. 133, 630–634. https://doi.org/10.1016/j.biortech.2013.01.149

Pronk, M., Bassin, J.P., De Kreuk, M.K., Kleerebezem, R., Van Loosdrecht, M.C.M., 2014. Evaluating the main and side effects of high salinity on aerobic granular sludge. Appl. Microbiol. Biotechnol. https://doi.org/10.1007/s00253-013-4912-z

Pronk, M., de Kreuk, M.K., de Bruin, B., Kamminga, P., Kleerebezem, R., van Loosdrecht, M.C.M., 2015.

Full scale performance of the aerobic granular sludge process for sewage treatment. Water Res. 84, 207–217. https://doi.org/10.1016/j.watres.2015.07.011

Rocktäschel, T., Klarmann, C., Ochoa, J., Boisson, P., Sørensen, K., Horn, H., 2015. Influence of the granulation grade on the concentration of suspended solids in the effluent of a pilot scale sequencing batch reactor operated with aerobic granular sludge. Sep. Purif. Technol. 142, 234–241. https://doi.org/10.1016/j.seppur.2015.01.013

Rollemberg, S.L. de S., Barros, A.N. de, Lira, V.N.S.A., Firmino, P.I.M., dos Santos, A.B., 2019. Comparison of the dynamics, biokinetics and microbial diversity between activated sludge flocs and aerobic granular sludge. Bioresour. Technol. https://doi.org/10.1016/j.biortech.2019.122106

Rosman, N.H., Nor Anuar, A., Chelliapan, S., Md Din, M.F., Ujang, Z., 2014. Characteristics and performance of aerobic granular sludge treating rubber wastewater at different hydraulic retention time. Bioresour. Technol. 161, 155–161. https://doi.org/10.1016/j.biortech.2014.03.047

Sarma, S.J., Tay, J.H., 2018. Carbon, nitrogen and phosphorus removal mechanisms of aerobic granules. Crit. Rev. Biotechnol. 38, 1077–1088. https://doi.org/10.1080/07388551.2018.1451481

Schwarzenbeck, N., Borges, J.M., Wilderer, P.A., 2005. Treatment of dairy effluents in an aerobic granular sludge sequencing batch reactor. Appl. Microbiol. Biotechnol. 66, 711–718. https://doi.org/10.1007/s00253-004-1748-6

Schwarzenbeck, N., Erley, R., Mc Swain, B.S., Wilderer, P.A., Irvine, R.L., 2004. Treatment of malting wastewater in a granular sludge sequencing batch reactor (SBR). Acta Hydrochim. Hydrobiol. 32, 16–24. https://doi.org/10.1002/aheh.200300517

Stes, H., Aerts, S., Caluwe, M., D'Aes, J., De Vleesschauwer, F., Dobbeleers, T., De Langhe, P., Kiekens, F., Dries, J., 2019. Influence of mixed feeding rate in a conventional SBR on biological P-removal and granule stability while treating different industrial effluents. Water Sci. Technol. 79, 645–655. https://doi.org/10.2166/wst.2019.081

Stes, H., Aerts, S., Caluwé, M., Dobbeleers, T., Wuyts, S., Kiekens, F., D'Aes, J., De Langhe, P., Dries, J., 2018. Formation of aerobic granular sludge and the influence of the pH on sludge characteristics in a SBR fed with brewery/bottling plant wastewater. Water Sci. Technol. 77, 2253–2264. https://doi.org/10.2166/wst.2018.132

Su, B., Cui, X., Zhu, J., 2012. Optimal cultivation and characteristics of aerobic granules with typical domestic sewage in an alternating anaerobic/aerobic sequencing batch reactor. Bioresour. Technol. https://doi.org/10.1016/j.biortech.2012.01.127

Su, K.Z., Yu, H.Q., 2005. Formation and characterization of aerobic granules in a sequencing batch reactor treating soybean-processing wastewater. Environ. Sci. Technol. 39, 2818–2827. https://doi.org/10.1021/es048950y

Szabó, E., Liébana, R., Hermansson, M., Modin, O., Persson, F., Wilén, B.M., 2017. Microbial population dynamics and ecosystem functions of anoxic/aerobic granular sludge in sequencing batch reactors operated at different organic loading rates. Front. Microbiol. 8, 1–14. https://doi.org/10.3389/fmicb.2017.00770

Tay, J.-H., Pan, S., He, Y., Tay, S.T.L., 2004. Effect of Organic Loading Rate on Aerobic Granulation. II: Characteristics of Aerobic Granules. J. Environ. Eng. https://doi.org/10.1061/(asce)0733-9372(2004)130:10(1102)

Tay, J.H., Liu, Q.S., Liu, Y., 2001. The effects of shear force on the formation, structure and metabolism of aerobic granules. Appl. Microbiol. Biotechnol. 57, 227–233. https://doi.org/10.1007/s002530100766

Tchobanoglous, G., Stensel, H.D., Tsuchihashi, R., Burton, F., Abu-Orf, M., Bowden, G., Pfrang, W., 2014. Wastewater Engineering: Treatment and Resource Recovery, Fifth Edition (International Edition), Metcalf & Eddy I AECOM, McGraw-Hill Education

Thwaites, B.J., Reeve, P., Dinesh, N., Short, M.D., van den Akker, B., 2017. Comparison of an anaerobic feed and split anaerobic–aerobic feed on granular sludge development, performance and ecology. Chemosphere 172, 408–417. https://doi.org/10.1016/j.chemosphere.2016.12.133

Thwaites, B.J., Van Den Akker, B., Reeve, P.J., Short, M.D., Dinesh, N., Alvarez-Gaitan, J.P., Stuetz, R., 2018. Ecology and performance of aerobic granular sludge treating high-saline municipal wastewater. Water Sci. Technol. https://doi.org/10.2166/wst.2017.626

Val Del Río, A., Figueroa, M., Mosquera-Corral, A., Campos, J.L., Méndez, R., 2013. Stability of aerobic granular biomass treating the effluent from a seafood industry. Int. J. Environ. Res. 7, 265–276. https://doi.org/10.22059/ijer.2013.606

van den Akker, B., Reid, K., Middlemiss, K., Krampe, J., 2015. Evaluation of granular sludge for secondary treatment of saline municipal sewage. J. Environ. Manage. 157, 139–145. https://doi.org/10.1016/j.jenvman.2015.04.027

van der Roest, H.F., de Bruin, L.M.M., Gademan, G., Coelho, F., 2011. Towards sustainable waste water treatment with Dutch Nereda® technology. Water Pract. Technol. https://doi.org/10.2166/wpt.2011.059

van Dijk, E.J.H., Pronk, M., van Loosdrecht, M.C.M., 2018. Controlling effluent suspended solids in the aerobic granular sludge process. Water Res. 147, 50–59. https://doi.org/10.1016/j.watres.2018.09.052

Wagner, J., Guimarã;es, L.B., Akaboci, T.R.V., Costa, R.H.R., 2015. Aerobic granular sludge technology and nitrogen removal for domestic wastewater treatment. Water Sci. Technol. 71, 1040–1046. https://doi.org/10.2166/wst.2015.064

Wagner, Jamile, Weissbrodt, D.G., Manguin, V., Ribeiro da Costa, R.H., Morgenroth, E., Derlon, N., 2015. Effect of particulate organic substrate on aerobic granulation and operating conditions of sequencing batch reactors. Water Res. https://doi.org/10.1016/j.watres.2015.08.030

Wan, C., Yang, X., Lee, D.J., Liu, X., Sun, S., Chen, C., 2014. Partial nitrification of wastewaters with high NaCl concentrations by aerobic granules in continuous-flow reactor. Bioresour. Technol. 152, 1–6. https://doi.org/10.1016/j.biortech.2013.10.112

Wang, S.G., Gai, L.H., Zhao, L.J., Fan, M.H., Gong, W.X., Gao, B.Y., Ma, Y., 2009. Aerobic granules for low-strength wastewater treatment: Formation, structure, and microbial community. J. Chem. Technol. Biotechnol. 84, 1015–1020. https://doi.org/10.1002/jctb.2127

Wang, Z., Gao, M., She, Z., Wang, S., Jin, C., Zhao, Y., Yang, S., Guo, L., 2015. Effects of salinity on performance, extracellular polymeric substances and microbial community of an aerobic granular sequencing batch reactor. Sep. Purif. Technol. https://doi.org/10.1016/j.seppur.2015.02.042

Wei, D., Qiao, Z., Zhang, Y., Hao, L., Si, W., Du, B., Wei, Q., 2013. Effect of COD/N ratio on cultivation of aerobic granular sludge in a pilot-scale sequencing batch reactor. Appl. Microbiol. Biotechnol. https://doi.org/10.1007/s00253-012-3991-6

Wei, Y., Ji, M., Li, R., Qin, F., 2012. Organic and nitrogen removal from landfill leachate in aerobic granular sludge sequencing batch reactors. Waste Manag. 32, 448–455. https://doi.org/10.1016/j.wasman.2011.10.008

Wilén, B.M., Liébana, R., Persson, F., Modin, O., Hermansson, M., 2018. The mechanisms of granulation of activated sludge in wastewater treatment, its optimization, and impact on effluent quality.

Appl. Microbiol. Biotechnol. https://doi.org/10.1007/s00253-018-8990-9

Winkler, M.K.H., Kleerebezem, R., De Bruin, L.M.M., Verheijen, P.J.T., Abbas, B., Habermacher, J., Van Loosdrecht, M.C.M., 2013. Microbial diversity differences within aerobic granular sludge and activated sludge flocs. Appl. Microbiol. Biotechnol. https://doi.org/10.1007/s00253-012-4472-7

Winkler, M.K.H., Kleerebezem, R., Khunjar, W.O., de Bruin, B., van Loosdrecht, M.C.M., 2012. Evaluating the solid retention time of bacteria in flocculent and granular sludge. Water Res. https://doi.org/10.1016/j.watres.2012.06.027

Wu, L., Peng, C., Peng, Y., Li, L., Wang, S., Ma, Y., 2012. Effect of wastewater COD/N ratio on aerobic nitrifying sludge granulation and microbial population shift. J. Environ. Sci. 24, 234–241. https://doi.org/10.1016/S1001-0742(11)60719-5

Yang, S.F., Tay, J.H., Liu, Y., 2005. Effect of substrate nitrogen/chemical oxygen demand ratio on the formation of aerobic granules. J. Environ. Eng. 131, 86–92. https://doi.org/10.1061/(ASCE)0733-9372(2005)131:1(86)

Yilmaz, G., Lemaire, R., Keller, J., Yuan, Z., 2008. Simultaneous nitrification, denitrification, and phosphorus removal from nutrient-rich industrial wastewater using granular sludge. Biotechnol. Bioeng. 100, 529–541. https://doi.org/10.1002/bit.21774

Zhang, J., Wang, M., Zhu, X., 2013. Treatment of HMX-Production Wastewater in an Aerobic Granular Reactor. Water Environ. Res. 85, 301–307. https://doi.org/10.2175/106143013x13596524516068

Zou, J., Tao, Y., Li, J., Wu, S., Ni, Y., 2018. Cultivating aerobic granular sludge in a developed continuous-flow reactor with two-zone sedimentation tank treating real and low-strength wastewater. Bioresour. Technol. https://doi.org/10.1016/j.biortech.2017.09.088

Chapter 2

Materials and methods

Summary

In this chapter, the analytical methods used during the experimental work performed in this thesis were presented. The methodology applied to measure the conventional parameters used for the liquid and solid phase characterisation was described in detail.

The methods to characterise the liquid phase (wastewater) included organic matter, nitrogenous and phosphorus compounds, greases, proteins, carbohydrates, inorganic ions, pH, conductivity and dissolved oxygen measurements.

The granular sludge was characterised by parameters such as the solids concentration, settleability (sludge volume index), density and average particle diameter. In addition, the Fluorescent *In Situ* Hybridisation (FISH) technique, applied to the identification of the microbial populations involved in the biological processes, is described.

Finally, the descriptions of the general calculations such as mass balances, organic matter, phosphorus and nitrogen removal efficiencies are also presented, as well as the calculations related to specific activity of the biomass populations.

OUTLINE

Chapter 2 35

2.1. ANALYSIS OF THE LIQUID PHASE 38

2.1.1. Chemical Oxygen Demand (COD) 38

2.1.2. Total Organic Carbon (TOC) 39

2.1.3. Volatile Fatty Acids (VFAs) 40

2.1.4. Nitrogen compounds 40

2.1.5. Orthophosphate (PO_4^{3-}-P) 44

2.1.6. Inorganic ions 45

2.1.7. Proteins 46

2.1.8. Carbohydrates 47

2.1.9. Fats 48

2.1.10. Biological Oxygen Demand (BOD) 49

2.1.11. COD fractionation 50

2.1.12. Other parameters 52

2.2. BIOMASS CHARACTERISATION 52

2.2.1. Solids concentration 52

2.2.2. Sludge Volume Index (SVI) 53

2.2.3. Granule density 53

2.2.4. Average diameter of the granules 54

2.2.5. Extracellular Polymeric Substances (EPS) 55

2.3. IDENTIFICATION OF BACTERIAL POPULATIONS BY FLUORESCENT *in situ* HYBRIDISATION 55

2.3.1. Identification of bacterial populations 55

2.3.2. Quantification of bacterial populations 58

2.4. CALCULATIONS 58

2.4.1. Hydraulic and sludge retention time (HRT and SRT) 59

2.4.1. Carbon 59
2.4.2. Nitrogen 60
2.4.3. Phosphorus 61
2.4.4. Biomass growth 62
2.4.5. Consumption and production rates of the nitrogen compounds 63
2.4.7. Salinity (g NaCl/L) 64
2.5. REFERENCES 65

2.1. ANALYSIS OF THE LIQUID PHASE

In this section, the methods used to determine the concentration of the conventional parameters of the wastewater are described. All liquid samples were filtered, through 0.45 μm pore size filter (MF-Millipore, Millipore), to remove the solids as indicated in the Standard and Methods (APHA/AWWA/WEF, 2012).

2.1.1. Chemical Oxygen Demand (COD)

The Chemical Oxygen Demand (COD) is defined as the amount of oxygen required to oxidise the organic matter present in a liquid sample in an acid medium by the use of a strong chemical oxidant (potassium dichromate). A catalyst (silver sulphate) is used to improve the oxidation of some organic compounds. After digestion, the remaining unreduced $K_2Cr_2O_7$ is titrated with ferrous ammonium sulphate to determine the amount of $K_2Cr_2O_7$ consumed. From this value, the amount of oxidised organic matter contained in the sample is calculated in terms of oxygen equivalents. The main reaction follows Eq. 2.1:

$$Cr_2O_7^{2-} + \text{Organic matter} + H^+ \Leftrightarrow Cr_3^+ + CO_2 + H_2O \qquad \text{Eq. 2.1}$$

The total and soluble COD concentrations (COD_T and COD_S, respectively), were measured following the method 5220C (Closed Reflux) of the Standard Methods (APHA/AWWA/WEF, 2012), combined with another method for samples with high concentration of salts previously developed (Soto et al., 1989). The COD_T was determined without filtering the sample, whereas the COD_S was measured by filtering through a 0.45 μm pore size filter (MF-Millipore, Millipore).

Reagents preparation

- Standard potassium dichromate digestion solution: 10.216 g of $K_2Cr_2O_7$ and 33 g of $HgSO_4$ were dissolved in 500 mL of distilled water. Then, 167 mL of concentrated H_2SO_4 was added. This solution was cooled at room temperature and diluted to 1000 mL.
- Sulphuric acid catalytic solution: 10.7 g of Ag_2SO_4 was added to 1 L of concentrated H_2SO_4. The solution needs to stand for 48 hours after preparation previous to its use.
- Ferroin indicator solution: 1.485 g of $C_{18}H_8N_2 \cdot H_2O$ (phenanthroline monohydrate) and 0.695 g of $FeSO_4 \cdot 7\ H_2O$ was dissolved in 100 mL of distilled water.
- Potassium dichromate solution 0.05 N: 1.226 g of $K_2Cr_2O_7$ previously dried at 105 °C for 2 hours, was dissolved in 500 mL of distilled water.
- Ferrous ammonium sulphate titrant (FAS) 0.035 N: 13.72 g of $Fe(NH_4)_2(SO_4)_2 \cdot 6\ H_2O$ was dissolved in distilled water. Then, 20 mL of concentrated H_2SO_4 was added and the solution was cooled and diluted to 1000 mL.

Determination procedure

This procedure was applicable to samples with COD concentrations between 90 and 900 mg/L. Firstly, 2.5 mL of sample was placed in a 10 mL Pyrex® glass tube. 1.5 mL of digestion solution was added, together with 3.5 mL of sulphuric acid reagent. This last reagent must be slowly added on the wall of the tube, which had to be tilt, to avoid the mixing. A blank sample using

distilled water, which acted as "reference" value (the COD was supposed to be negligible), was prepared in the same way.

The Pyrex® glass tubes were tightly sealed with Teflon®, capped and shaken until the complete mixing. Then, they were placed for 2 h in the block thermo-digester (ECO 16, VELP SCIENTIFICA) preheated at 150 °C. After digestion, the Pyrex® tubes were cooled to room temperature. Finally, the content of the tubes was transferred into a stirred beaker, together with 3 drops of ferroin indicator, and titrated with standard FAS. The end-point was visualised by a sharp change of colour from turquoise to reddish-brown.

The FAS solution was standardised daily as follows: 5 mL of distilled water was added into a small beaker together with 3.5 mL of sulphuric acid reagent. The liquid was cooled at room temperature before the addition of 5 mL of the standard potassium dichromate solution (0.05 N). Approximately 1-2 drops of ferroin were added as indicator before titrating with FAS in a similar way as applied to the samples. The molarity of the FAS solution was calculated using Eq. 2.2:

$$M_{FAS} = \frac{5 \cdot 0.05}{V_{FAS}} \qquad \text{Eq. 2.2}$$

Where M_{FAS} is the FAS molarity (mol/L) and V_{FAS} is the volume of FAS consumed in the titration (mL).

The COD was calculated following Eq. 2.3:

$$COD\ [mg/L] = \frac{(A - B) \cdot M_{FAS} \cdot 8000}{V} \qquad \text{Eq. 2.3}$$

Where A is the volume of FAS solution consumed by the blank (mL), B is the volume of FAS solution consumed by the sample (mL), 8000 is the milliequivalent weight of oxygen multiplied by 1000 (mL/L) and V is the volume of sample (mL).

Interferences

The most common interference of this method is the chloride ion at concentrations higher than 2 g/L of Cl^-. Chloride reacts with silver ion to precipitate silver chloride, and thus inhibits the catalytic activity of silver. Bromide and Iodide can interfere similarly.

2.1.2. Total Organic Carbon (TOC)

The Total Organic Carbon (TOC) includes a variety of organic compounds in different oxidation states and does not measure other organically bound elements, such as nitrogen, hydrogen and inorganics that can contribute to the oxygen demand measured by COD (APHA/AWWA/WEF, 2012). To determine the quantity of organically bound carbon, the organic molecules must be broken down and converted to a single carbon molecular form that can be measured quantitatively.

Determination procedure

The TOC concentration was determined by a Shimadzu analyzer (TOC-L_{CSN}) as the difference between the Total Carbon (TC) and the Inorganic Carbon (IC) concentrations of the sample. The instrument was connected to an automated sampler (Shimadzu, ASI-L). The TC concentration was determined from the amount of CO_2 produced during the combustion of the sample at 720 °C, using platinum immobilised over alumina spheres as catalyst. The IC concentration was obtained from the CO_2 produced in the chemical decomposition of the sample with HCl (1 M) at room temperature. The CO_2 produced was optically measured with a non-dispersive infrared analyser (NDIR) after being cooled and dried. High purity air was used as carrier gas with a flow of 150 mL/min. A curve comprising four calibration points in the range of 0.5 to 1,000 mg C/L, using potassium phthalate ($C_8H_5KO_4$) as standard for TC and a mixture of sodium carbonate and bicarbonate (Na_2CO_3/$NaHCO_3$, 3:4 w/w) for IC, was used for quantification.

2.1.3. Volatile Fatty Acids (VFAs)

Volatile Fatty Acids (VFAs) are fatty acids with a carbon chain of six carbons or fewer, such as acetic (HAc), propionic (HPr), i-butyric and n-butyric (Hbu) and valeric (HVa).

Determination procedure

A volume of 1 mL of sample together with 10 µL of H_3PO_4 (85 %), was used to determine VFAs by gas chromatography (GC) (6850 Series II, Agilent Technologies). The instrument was equipped with a flame ionisation detector (FID) and an automatic injector (Hewlett Packard 7673A, USA). The determination was performed using a glass column (3 m long and 2 mm of internal diameter).

N_2 gas was used as carrier gas at a flow of 45 mL/min. The injector and detector temperatures were, respectively, 250 and 300 °C. The oven was programmed to start at a temperature of 70 °C, which increased at a rate of 15 °C/min to 130 °C, 3°C/min to 150 °C, 10 °C/min to 180 °C; then it remained at 180 °C for 1 min, and increased again at a rate of 65 °C/min to 250 °C. This final temperature was held for 5 min. Air and H_2 were used as auxiliary gases with flows of 400 and 40 mL/min, respectively. The sample injection volume was 1 µL, and the VFA were separated in the column according to their molecular weights.

A commercial mixture of VFA in deionised water was used as standard (Supelco, USA). The obtained chromatogram provides information about the area of the obtained peaks corresponding to each analysed VFA. Each VFA was identified by the retention time of its corresponding peak. The quantification of the sample was made with a calibration curve for each acid in the range of concentrations of 0 – 0.6 g/L, which was related to the area of each peak.

2.1.4. Nitrogen compounds

2.1.4.1. Ammonium (NH_4^+)

Ammonium concentration was determined spectrophotometrically by an analytical method based on the production of indophenol blue by the reaction of ammonia with salicylate and hypochlorite, in the presence of sodium nitroprusside (Bower and Holm-Hansen, 1980).

Reagents preparation

- Reagent A: 0.28 g of sodium nitroprusside ($Na_2(Fe(CN)_5NO)$) and 440 g of sodium salicylate ($C_7H_5NaO_3$) was dissolved in 1 L of distilled water.
- Reagent B: 18.5 g of NaOH and 120 g of sodium citrate ($Na_3C_6H_5O_7$) were dissolved in 1 L of distilled water.
- Reagent C: commercial solution of sodium hypochlorite (NaClO), with a 5 % (w/w) concentration.
- Reagent D: mixture of 7 parts of reagent B and 1 part of reagent C. Reagent D was stable for 1 hour after preparation.

Determination procedure

600 µL of reagent A and 1 mL of reagent D were added to 5 mL of filtered sample. Reaction time was fixed between 2 and 3 hours, and the samples must be protected from light during this time. The measurement of coloured sample was done with a spectrophotometer (Shimadzu UV-1800) at a wavelength of 640 nm. The quantification was done with a calibration curve (Figure 2.1).

Calibration curve

From a stock solution of 10 mg NH_4^+/L, more diluted samples were prepared in a range of 0 – 0.9 mg NH_4^+-N/L. The absorbance of each sample was measured with the spectrophotometer and related to the NH_4^+ concentration (in terms of NH_4^+-N/L) by means of the calibration curve (Figure 2.1).

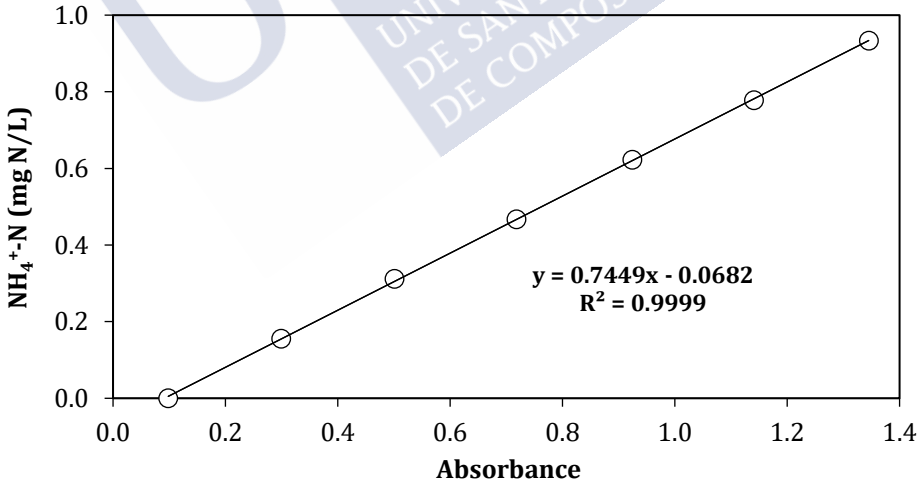

Figure 2.1: Calibration curve for ammonium determination.

Where "x" is the absorbance of the measured sample and "y" the ammonium concentration (mg NH_4^+-N/L).

2.4.1.2. Nitrite (NO_2^-)

Nitrite was determined spectrophotometrically by a method based on the production of a reddish-purple azo dye at pH 2.0 – 2.5 by coupling diazotised sulphanilamide with N-(1-napthyl)-ethylenediamine dihydrochloride (NED dihydrochloride). This procedure corresponds to the method 4500-NO_2^- B (Colorimetric Method) described in the Standard Methods (APHA/AWWA/WEF, 2012).

Reagents preparation

- Sulphanilamide solution: 10 g of sulphanilamide ($C_6H_8N_2O_2S$) was dissolved in 100 mL of concentrated HCl and 600 mL of distilled water. After cooling, the volume was filled up to 1 L with distilled water.
- NED solution: 0.5 g of NED ($C_{10}H_7NHCH_2CH_2NH_2 \cdot 2HCl$) was dissolved in 500 mL of distilled water.

Determination procedure

A volume of 0.1 mL of each reagent was added to 5 mL of sample. The minimum reaction time for colour stabilisation was 20 minutes. The measurement of the coloured sample was done in the spectrophotometer (Shimadzu UV-1800) at a wavelength of 543 nm. The concentration was given by the comparison of the obtained absorbance with the values of the calibration curve (Figure 2.2)

Calibration curve

From a stock solution of 10 mg NO_2^-/L, more diluted samples were prepared in the range of 0 – 0.25 mg NO_2^--N/L. The absorbance of each sample was measured with the spectrophotometer and related to the NO_2^- concentration (in terms of NO_2^--N /L) by means of the calibration curve (Figure 2.2).

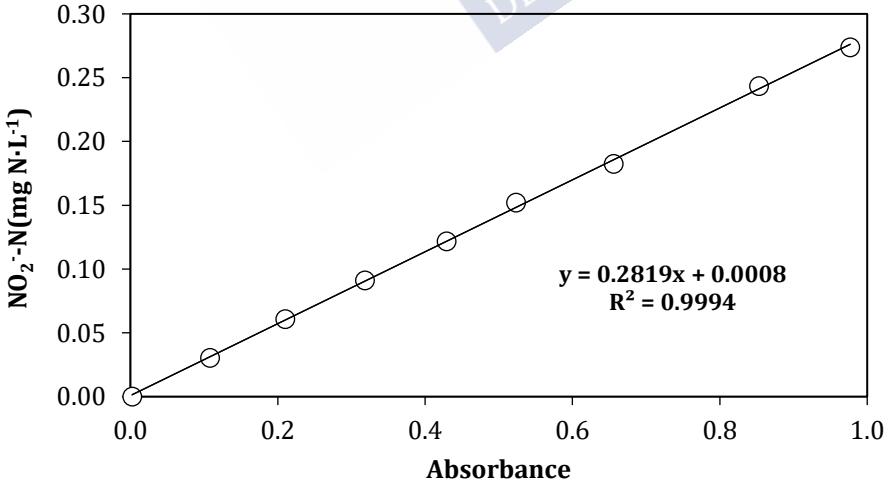

Figure 2.2: Calibration curve for nitrite determination.

Where "x" is the absorbance of the sample measured and "y" the nitrite concentration (mg NO_2^--N/L).

2.4.1.3. Nitrate (NO_3^-)

Nitrate concentration was determined by the measurement of UV absorption at a wavelength of 220 nm. Because dissolved organic matter also may absorb at 220 nm and NO_3^- does not absorb at 275 nm, a second measurement at 275 nm is used to correct the value of NO_3^-. This procedure corresponds to the method 4500- NO_3^- B (Ultraviolet Spectrophotometric Screening Method) described in the Standard Methods (APHA/AWWA/WEF, 2012).

Reagents preparation

- HCl 1 N: 8.3 mL of HCl (37 %, w/v, 1.19 g/L) was dissolved in 100 mL of distilled water.
- Sulfamic acid: commercial chemical reagent (H_3NSO_3).

Determination procedure

A volume of 100 µL of HCl 1N was added to 5 mL of sample. Then, the absorbance of each sample was measured at 220 and 275 nm with the spectrophotometer (Shimadzu UV-1800) and the NO_3^- concentration (in terms of NO_3^--N /L) was calculated by using the calibration curve (Figure 2.3). The absorbance related to nitrate was obtained by subtracting two times the absorbance reading at 275 nm from the reading at 220 nm, following Eq. 2.4:

$$\text{Absorbance } (NO_3^- - N) = Abs_{220} - 2 \cdot Abs_{275} \qquad \text{Eq. 2.4}$$

Calibration curve

From a stock solution of 10 mg NO_3^-/L, more diluted samples were prepared in the range of 0 – 3 mg NO_3^--N/L. Then, the absorbance of each sample was measured with the spectrophotometer and related to the NO_3^- concentration (in terms of NO_3^--N /L) through the calibration curve (Figure 2.3).

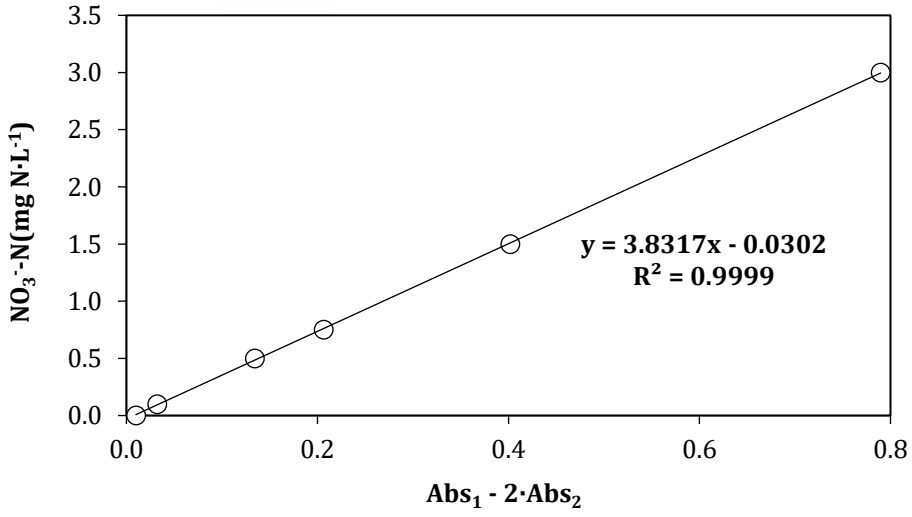

Figure 2.3: Calibration curve for nitrate determination.

Where "x" is the difference between the absorbance at 220 nm and double the absorbance at 275 nm (Eq. 2.4) of the sample, and "y" the nitrate concentration (mg NO_3^--N/L).

Interferences

The known interferences of this method are the organic matter and the nitrite. The interference due to the presence of the organic matter in the sample is resolved by taking into account the absorbance related to nitrate at the second wavelength (275 nm), while the interference by nitrite is avoided by adding a small amount of sulfamic acid before the addition of the HCl 1 N.

2.4.1.4. Total Nitrogen (TN)

The Total Nitrogen (TN) was determined by a Shimadzu analyser (TOC-L_{CSN}) equipped with a quimio-luminescence detector and connected to an automated sampler (Shimadzu, ASI-L). All the nitrogen compounds were converted to N_2O through oxidative pyrolysis at 720 °C with platinum immobilised over alumina spheres as catalyst. The N_2O produced during the combustion was cooled and dried, and then it was optically measured with the quimio-luminescence detector. The calibration was carried out by a standard commercial solution of ammonium (1000 mg/L, Merck) in the range of 0 – 0.7 g NH_4^+/L.

2.1.5. Orthophosphate (PO_4^{3-}-P)

Orthophosphate was measured spectrophotometrically following the method 4500-P E (Ascorbic Acid Method) described in the Standard Methods (APHA/AWWA/WEF, 2012). Ammonium molybdate and antimony potassium tartrate react with orthophosphate in acid medium to form phosphomolybdic heteropolyacid, which is reduced by ascorbic acid into intensely coloured molybdenum blue.

Reagents preparation

- Reagent A: sulphuric acid 5 N.
- Reagent B: 1.3715 g of antimony potassium tartrate ($K(SbO)C_4H_4O_6$-$0.5H_2O$) was dissolved in 500 mL of distilled water. The solution was kept in a bottle with glass top to be preserved.
- Reagent C: 20 g of ammonium molybdate ($(NH_4)_6Mo_7O_{24}\cdot 4H_2O$) was dissolved in 500 mL of distilled water. The solution was kept in a bottle with glass top to be preserved.
- Reagent D: ascorbic acid 0.01 M. This solution was stable for a week.
- Reagent E: to prepare 100 mL of reagent E, the reagents A to D were mixed according to the following volumes: 50 mL of reagent A, 5 mL of reagent B, 15 mL of reagent C and 30 mL of reagent D. The mixture was stirred after the addition of each reagent, following the mentioned order. Reagent E was stable for 4 hours.

Determination procedure

A volume of 5 mL of sample was taken and one drop of phenolphthalein indicator solution (0.5 – 1.0 g phenolphthalein in 1 L of ethanol at 80 % concentration) was added. If red colour appeared, reagent A was added by drops until the red colour disappeared. Then, 0.8 mL of reagent E was added and the mixture was stirred. After 10 minutes, but before 30 minutes, the absorbance of the coloured sample was measured in the spectrophotometer (Shimadzu UV-1800) at a wavelength of 880 nm. The concentration was given by the calibration curve (Figure 2.4).

Calibration curve

From a stock solution of 10 mg PO_4^{-3}/L, more diluted samples were prepared in the range of 0 – 1 mg PO_4^{-3}-P/L. Then, the absorbance of each sample was measured with the spectrophotometer and related to the PO_4^{-3} concentration (in terms of PO_4^{-3}-P/L) by means of the calibration curve (Figure 2.4).

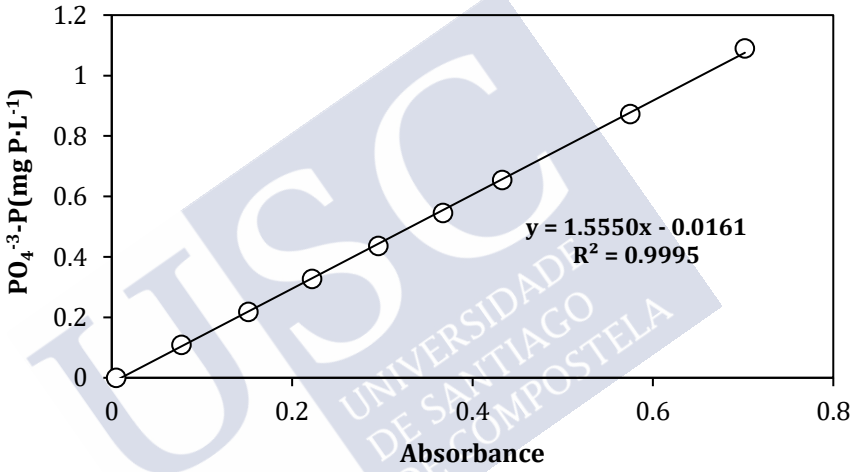

Figure 2.4: Calibration curve of orthophosphate determination.

Where "x" is the absorbance of the sample measured, and "y" the phosphate concentration (mg PO_4^{-3}-P/L).

2.1.6. Inorganic ions

The anions nitrite (NO_2^-), nitrate (NO_3^-), chloride (Cl^-), bromide (Br^-), phosphate (PO_4^{3-}), sulphate (SO_4^{2-}), and the cations lithium (Li^+), sodium (Na^+), ammonium (NH_4^+), potassium (K^+), magnesium (Mg^{2+}) and calcium (Ca^{2+}) were determined by ion chromatography (IC) with an Advanced Compact IC system (861, Metrohm), equipped with a CO_2 suppressor (MCS 853, Metrohm) and a sample processor/injector (838, Metrohm). The injected volume of the sample (20 µL), went through the column and each ion was separated at a different retention time along the resin column. Anions were determined with a Metrosep A column Supp 5 (250 × 4.0 mm) and a mobile phase (buffer) with 3.2 mM Na_2CO_3 and 1.0 mM $NaHCO_3$ at a flow rate of 0.7 mL/min. Cations were determined with a column Metrosep C3, Metrohm (250 × 4.0 mm) and nitric acid 3.5 mM as mobile phase at a flow rate of 1 mL/min. Then, the sample passed through the conductimetric detector after the separation, where the obtained signal of each retention time

was registered. The resulting chromatogram identified each measured ion by its retention time position together with the amount of ion, which was related to the area under the curve described by the chromatogram.

Reagents

- Mobile phase for anions: Na_2CO_3 3.2 mM (339.2 mg Na_2CO_3 in 100 mL of deionised water) and $NaHCO_3$ 1.0 mM (84 mg $NaHCO_3$ in 1000 mL of deionised water).
- Mobile phase for cations: Nitric acid 3.5 mM (0.243 mL of nitric acid 65 % in 1000 mL of deionised water).
- Standard commercial solutions for anions and cations (Fluka).

Determination Procedure

The chromatogram provided information about the different identified ions and their respective quantity in the sample by means of a calibration procedure. The final concentrations of the detected ions were automatically determined by the equipment and its software (IC Net 2.3). Table 2.1 shows the calibration ranges for the different inorganic ion concentrations, which defined the proper dilutions in some samples with distilled water in order to fit these ranges.

Table 2.1: Calibration ranges for the different inorganic ions (mg/L).

Anions	Lower value	Higher value	Cation	Lower value	Higher value
Cl^-	1.0	100	Li^+	0.05	5
NO_2^-	0.05	5	Na^+	1.5	150
NO_3^-	0.5	50	NH_4^+	0.1	10
Br^-	0.2	20	K^+	0.5	50
PO_4^{3-}	0.5	50	Mg^{2+}	0.5	50
SO_4^{2-}	1.5	150	Ca^{2+}	0.5	50

2.1.7. Proteins

Protein determination was done according to the Lowry's method (Lowry et al., 1951). The procedure was based on two chemical reactions, which yield a blue coloured complex: Biuret reaction, in which the alkaline cupric tartrate reagent complexes the peptide bonds of the protein, followed by the reduction of the Folin and Ciocalteu's phenol reagent in alkaline conditions.

Reagents preparation

- Copper sulphate solution (1 %): 1 g of $CuSO_4$ was dissolved in 100 mL of distilled water.
- Sodium tartrate solution (2 %): 2 g of $C_4H_4O_6Na_2$ was dissolved in 100 mL of distilled water.
- NaOH 1 N solution: 4 g of NaOH was dissolved in 1 L of distilled wastewater.
- Reagent A: 2 g of Na_2CO_3 and 1 mL of copper sulphate and sodium tartrate solution were dissolved in 100 mL.
- Reagent B: 1 mL of commercial Folin and Ciocalteu's phenol reagent was dissolved in 10 mL of distilled water.

All the solutions have to be stored at 4 °C. Reagents A and B need to be prepared the same day of the analysis.

Determination procedure

A volume of 0.5 mL of NaOH 1 N solution and 5 mL of reagent A were added to 0.5 mL of sample, and the mixture was left for 10 minutes at room temperature. Then, 0.5 mL of reagent B was added and mixed. The minimum reaction time for colour stabilisation was 30 min. The measurement of the coloured sample was done spectrophotometrically (Shimadzu, UV-1800) at a wavelength of 750 nm. The concentration was determined by comparison of the obtained absorbance with the values of the calibration curve (Figure 2.5).

Calibration curve

Firstly, a stock solution of bovine serum albumin (BSA) of 10 g/L was prepared. Secondly, more diluted samples were prepared, in the range of 0 – 0.5 g BSA/L. Then, the absorbance of each sample was measured with the spectrophotometer and related to the carbohydrate concentration (in terms of mg of equivalent BSA/L) by means of the calibration curve (Figure 2.5).

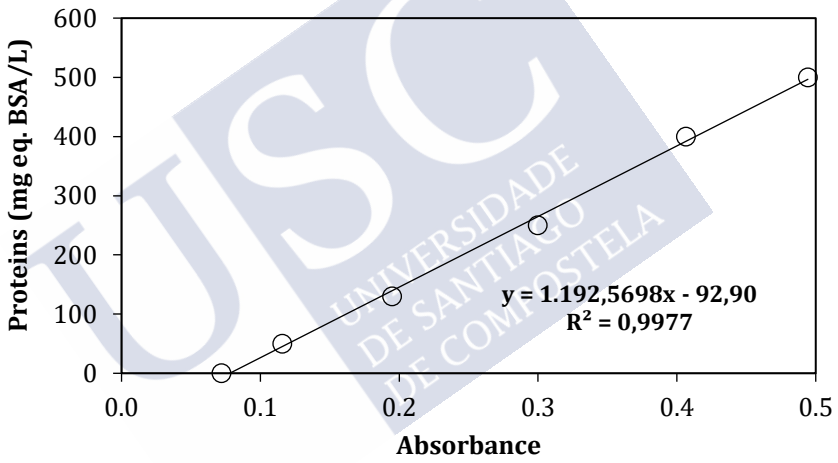

Figure 2.5: Calibration curve for proteins determination.

Where "x" is the absorbance of the sample measured, and "y" the proteins concentration (mg eq. BSA/L).

2.1.8. Carbohydrates

The carbohydrate concentration was measured with the anthrone method (Dreywood, 1946) and expressed in equivalent glucose. The carbohydrates react with the anthrone reagent under acidic conditions to yield a blue-green coloured sample. This method determines both reducing and non-reducing carbohydrates because of the presence of the strongly oxidising sulphuric acid.

Reagents preparation

- Anthrone solution: 200 mg of anthrone was dissolved in 100 mL of sulphuric acid (98 %). This solution was not stable, and it was necessary to prepare it the same day of the analysis.

Determination procedure

A volume of 2 mL of sample was placed in Pyrex® glass tubes and 4 mL of anthrone solution was added. The solution was mixed and the tubes were placed in a thermodigester (ECO 16, VELP SCIENTIFICA) at 100 °C for 10 minutes. To stop the reaction, the tubes were immediately placed in a water bath to be cooled with ice. Then, the absorbance was measured at a wavelength of 625 nm and the carbohydrates concentration was calculated by the calibration curve (Figure 2.6).

Calibration curve

From a stock solution of 250 mg glucose/L, more diluted samples were prepared in the range of 0 – 83 mg glucose/L. Then, the absorbance of each sample was measured with the spectrophotometer and related to the carbohydrates concentration (in terms of mg of equivalent glucose/L) by means of the calibration curve (Figure 2.6).

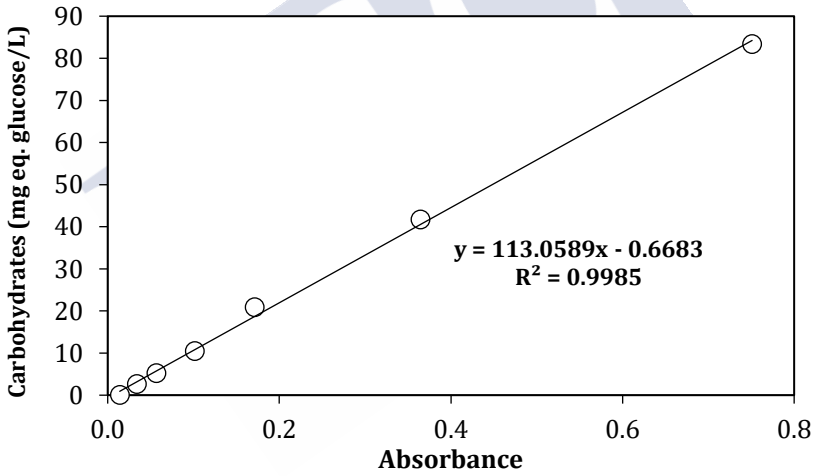

Figure 2.6: Calibration curve for carbohydrates determination.

Where "x" is the absorbance of the sample measured, and "y" the carbohydrate concentration (mg eq. glucose/L).

2.1.9. Fats

Fat concentration was measured from biomass samples submitted to solvent extraction. Fats were determined following the Standard Methods (APHA/AWWA/WEF, 2012). The samples required of acidification to pH < 2 and storage in the fridge if they were not going to be analysed immediately.

Reagents

- Petroleum ether

Determination procedure

The sample was placed in a separatory funnel together with 30 mL of petroleum ether. The mixture was shaken vigorously for a couple of minutes. The narrow part of the funnel was located upwards to open the stopcock and release the produced gases. The volume of sample depended on its fat concentration and several assays were attempted previously to the obtainment of the value of the fat concentration.

After a good mixing of the sample and the petroleum ether, the separatory funnel was located in a stand with a metal ring to allow the separation of the two phases. The organic phase was filtrated through a glass funnel with a Whatman® filter and poured into a distillation flask of known weight. Then, a distillation at 70 °C was performed with a rotary evaporator (Buchi, Switzerland). Finally, the flask was put into an oven at 105 °C for 2 hours and weighed after cooling. The amount of fats in the sample corresponded to the flask weight increase.

Calculations

Samples for the determination of fats need to be weighed accurately in order to calculate the exact percentage present in the sample. The result was expressed in concentration units by using Eq. 2.5:

$$\text{Fats [mg/L]} = \frac{(P_2 - P_1) \cdot 1000}{V} \qquad \text{Eq. 2.5}$$

Where P_1 is the weight of the distillation flask (mg), P_2 is the weight of the distillation flask plus the sample after the evaporation (mg) and V is the volume of sample (mL).

2.1.10. Biological Oxygen Demand (BOD)

The biological oxygen demand (BOD) is a parameter that measures the biodegradability of the organic matter in a liquid sample. It allows the estimation of the dissolved oxygen used by the microorganisms to oxidise the organic matter present in a liquid sample. The reaction can be described according to Eq. 2.6:

$$O_2 + \text{Organic matter} \xrightarrow{\text{microorganisms}} \text{microorganisms} + CO_2 + H_2O \qquad \text{Eq. 2.6}$$

In the present research work, the measurement was done on day 5 of the experiment (BOD_5). The equipment to determine the BOD_5 was an *Oxitop* (WTW, Germany). This system was based on the difference of pressure generated due to the CO_2 production. The measurement was done by determining the pressure with a piezoresistive electronic sensor, which directly gave the BOD_5 measurement in mg/L. This system acquired and saved data during the 5 days of the experiment.

2.1.11. COD fractionation

The total COD of the wastewater (COD_T) was fractionated in the two major divisions: total biodegradable COD (COD_b) and total inert COD (COD_I). The COD_b was further classified into the soluble easily biodegradable COD (S_S) and the particulate slowly biodegradable COD (X_S) fractions, whereas the COD_I was divided into soluble inert COD (S_I) and particulate inert COD (X_I) (Figure 2.7).

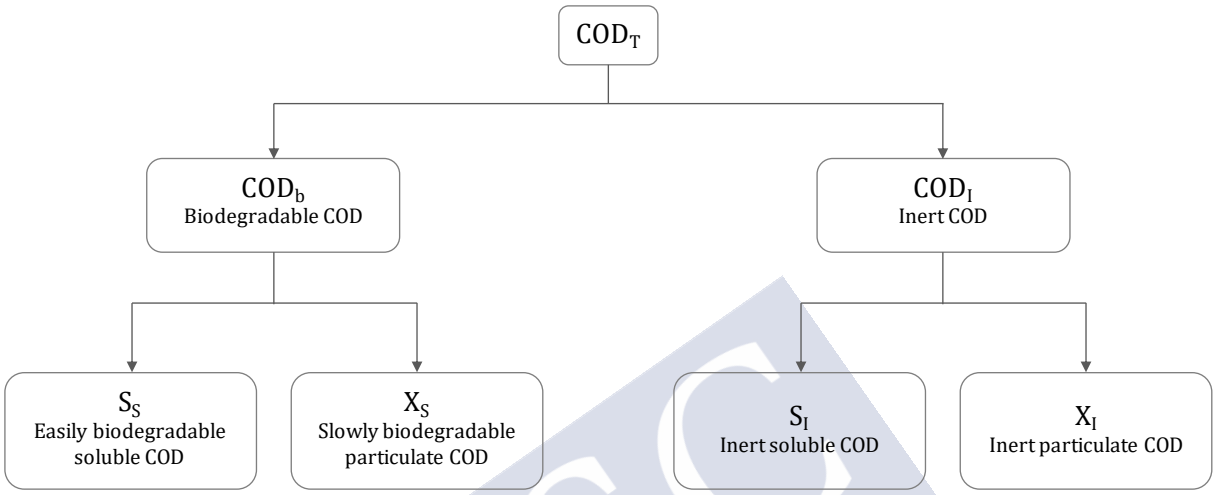

Figure 2.7: COD fractions determined in the experiment of the COD fractionation.

The COD_b and COD_I fractions were experimentally determined through independent respirometric batch assays from the profiles of consumed (dissolved) oxygen in a BM-T + Respirometer (SURCIS L., Spain). The procedure included the determination of the yield of the aerobic sludge, which was used for the fractionation, and the fractionation of the COD. Both were dynamic respiration rate (R) tests. In this type of assays, the software integrated the dynamic respiration rates of the sludge, corresponding to the metabolisation of the organic matter, and calculated the consumed oxygen (CO) in a continuous mode.

The experiments were performed at 25 °C, in a completely mixed system with aeration, recirculation of the liquid medium and continuous dissolved oxygen monitoring. The test was considered finished when all the biodegradable material was completely consumed, and the oxygen consumption rate decreased and remains near zero. All the tests were made in triplicate.

For the estimation of the total fractions (X_S and X_I), the raw wastewater was added as substrate, while for the soluble fractions (S_S and S_I) the samples were filtered through a 0.45 µm pore size filter (MF-Millipore, Millipore).

COD fractionation

The respirometer was loaded with 1 L of activated sludge adapted to treat the wastewater to be fractionated. In order to inhibit the nitrification process, allylthiourea at a concentration of 2 - 3 mg N per gram of VSS was added.

Before the start of the test, the sludge was aerated until reaching the endogenous respiration state, where the DO concentration remained at a constant value. Afterwards, the sample of wastewater to be analysed was added. The volume of sample depended on its COD concentration, according to the manufacturer specifications (Table 2.2).

Table 2.2: Volume of sample to add depending on its COD concentration.

Total COD (mg/L)	Volume of sample (mL)
< 300	80 – 50
300 – 5000	40 – 20
5000 – 10000	20 – 15
10000 – 25000	15 – 10
> 25000	10 – 5

At the end of the assay, the respirometric software gave the biodegradable fraction of the sample (COD_b) based on the total oxygen consumption measured and the normal biomass yield. The different fractions of COD were calculated with Eq. 2.7, Eq. 2.8, Eq. 2.9 and Eq. 2.10:

$$S_S = \frac{CO}{1 - Y_H} \quad \text{Eq. 2.7}$$

$$S_I = COD_S - S_S \quad \text{Eq. 2.8}$$

$$X_S = COD_b - S_S \quad \text{Eq. 2.9}$$

$$X_I = COD_T - COD_b - S_I \quad \text{Eq. 2.10}$$

Where CO is the oxygen consumed during the respirometric test, with the filtered sample of wastewater, COD_S and COD_T are the soluble and total COD of the sample (determined as described in Section 2.1.1) and COD_b is the biodegradable COD of the non-filtered sample (given by the respirometer).

Determination of the yield of the sludge

The heterotrophic growth yield (Y) was determined in the same operational conditions as in the previous batch assays, with sodium acetate (0.4 g/L) as substrate in a 50 mL sample volume. The value was calculated with Eq. 2.11:

$$Y_H = 1 - \frac{CO}{COD_{ac}} \quad \text{Eq. 2.11}$$

Where Y_H is the heterotrophic yield of the biomass (g $VSS_{COD,produced}$/g $COD_{consumed}$), CO is the oxygen consumed during the R test (given by the respirometer) and COD_{ac} is the soluble COD of the sodium acetate solution (determined as described in Section 2.1.1)

2.1.12. Other parameters

All these parameters were measured using different instruments depending on the reactor operation.

pH

Laboratory-scale reactors: electrode (Crison Instruments GLP22, USA) equipped with an automatic compensatory temperature device and connected to a pH-meter (GLP-22, Crison Instruments).

Pilot-scale reactor: probe pHDSc, located in a PVC pole for immersion assembly, connected to a universal multichannel controller SC1000 (HACH Lange, USA).

The electrode of both probes was calibrated at room temperature with two standard buffer solutions of pH 7.02 and 4.00, respectively.

Conductivity

Laboratory-scale reactors: platinum cell electrode (HACH Lange 50 60, Platinum Cell), connected to a portable conductivity meter (HACH Lange sensION + EC5). The electrode was calibrated at room temperature with one of these three standard buffer solutions: 147 µS/cm, 1413 µS/cm and 12.88 mS/cm depending on the concentration to be measured.

Pilot-scale reactor: probe 3798-S sc, located in a PVC pole for immersion assembly, connected to a universal multichannel controller SC1000 (HACH Lange, USA). This probe was calibrated in air.

Dissolved Oxygen (DO)

Laboratory-scale reactors: probe with a membrane-covered galvanic dissolved oxygen sensor (LDO101) connected to a digital multimeter device (HQ40D, HACH Lange, USA).

Pilot-scale reactor: probe LDO sc, located in a PVC pole for immersion assembly, connected to a universal multichannel controller SC1000 (HACH Lange, USA). This probe was calibrated in air.

Temperature

The DO probes mentioned before were equipped with a thermopar that measures the temperature.

2.2. BIOMASS CHARACTERISATION

2.2.1. Solids concentration

Total Suspended Solids (TSS) and Volatile Suspended Solids (VSS) were determined following the methods 2540D and 2540E, respectively, described in Standard Methods (APHA/AWWA/WEF, 2012).

Determination procedure

Total Solids (TS) concentration was determined introducing a selected well-mixed sample volume (in order to yield a residue between 2.5 and 200 mg) in a previously tared (heated to 103 – 105 °C for 2 h) crucible and evaporating it at 103 – 105 °C to reach a constant weight. The increase in weight over that of the empty crucible represented the total solids content in the initial volume of sample. For the determination of TSS, a selected well-mixed sample volume (in order to yield a residue between 2.5 and 200 mg) was filtered through a weighed glass fibre filter (Whatman, GF/C, 4.7 cm of diameter, 1.2 μm of pore size). The residue retained on the filter was dried to a constant weight (approximately 2 h) at 103 – 105 °C until achieving a constant weight. The increase in weight of the filter represented the TSS content of the sample.

To determine the VSS the residues from method 2540D were burnt to constant weight at 550 °C during half an hour. The weight lost during ignition corresponded to the volatile fraction, since only a small amount of inorganic salts was decomposed and volatilised at that temperature. This determination offered a rough approximation of the amount of organic matter present in the solid fraction of the wastewater and the sludge.

2.2.2. Sludge Volume Index (SVI)

The Sludge Volume Index (SVI) was determined according to the procedure specified in the Standard Methods (APHA/AWWA/WEF, 2012). The SVI is the volume in mL occupied by 1 g of a suspension after 30 minutes of settling, determined according to Eq. 2.12.

$$\text{SVI [mL/g TSS]} = \frac{V_{\text{settled sludge}}}{\text{TSS}} \qquad \text{Eq. 2.12}$$

Where $V_{\text{settled sludge}}$ is the volume of the settled bed of sludge after a fixed time of settling (mL/L) and TSS is the Total Suspended Solids concentration of the sludge (g/L). In the case of granular biomass, this parameter was measured after 5 and 30 min of settling.

2.2.3. Granule density

The biomass density (as mass of granules per volume of granules) was determined using the method described by Beun et al. (2002). Firstly, a known amount of a homogenous biomass sample was taken from the reactor and weighed (W_2) in a graduated cylinder previously tared (W_1). Then, a known amount of the supernatant was removed from the sample, and the cylinder was weighed again (W_3). A known volume of dextran blue solution (1 g/L) was added to the cylinder with the sample, in a volume ratio of about 1:1 (W_4). The sample and the dextran blue solution were mixed and subsequently, granules were allowed to settle. A sample of the supernatant (Abs_1) and of the original dextran blue solution (Abs_0) were taken and measured spectrophotometrically at a wavelength of 620 nm. Then, the volume occupied by the biomass in the sample was calculated, since dextran blue only diffused in water and not into the biomass granules (Eq. 2.13).

$$\rho\ [g\ VSS/L_{granule}] = VSS \cdot \frac{W_2 - W_1}{W_4 - W_1 - \left(\frac{Abs_0}{Abs_1} \cdot (W_4 - W_3)\right)} \qquad \text{Eq. 2.13}$$

Where ρ is the density of the granules (g VSS/$L_{granule}$), VSS is the Volatile Suspended Solids concentration of the initial sample (g/L), W_1 is the weight of the empty graduated cylinder (g), W_2 is the weight of the graduated cylinder with sample (g), W_3 is the weight of the graduated cylinder with sample after the removal of the supernatant (g), W_4 is the weight of the graduated cylinder after dextran blue addition (g), Abs_0 is the absorbance of the dextran blue solution and Abs_1 is the absorbance of the mixture between the sample and dextran blue.

2.2.4. Average diameter of the granules

The diameter of the granules was measured using an Image Analysis procedure (Tijhuis et al., 1994). Images of the granular sludge were taken with a digital camera (Coolsnap, Roper Scientific Photometrics) combined with a stereomicroscope (Stemi 2000-C, Zeiss). The digital image analysis was made with the program Image ProPlus®. A caption of the program is represented in (Figure 2.8). The procedure of average diameter determination was as follows:

1. Definition of the range of colours corresponding to the area of interest in the image, i.e. the granules (Manual or Automatic), and delimitation of each aggregate.
2. Selection of the measurements of interest.
3. Exportation of the data of interest selected with the software to a worksheet (Excel). The average diameter obtained from the programme corresponded to the mean feret diameter of the granules. The feret diameter was estimated as an average value from the shortest and the longest measured segments of each granule.

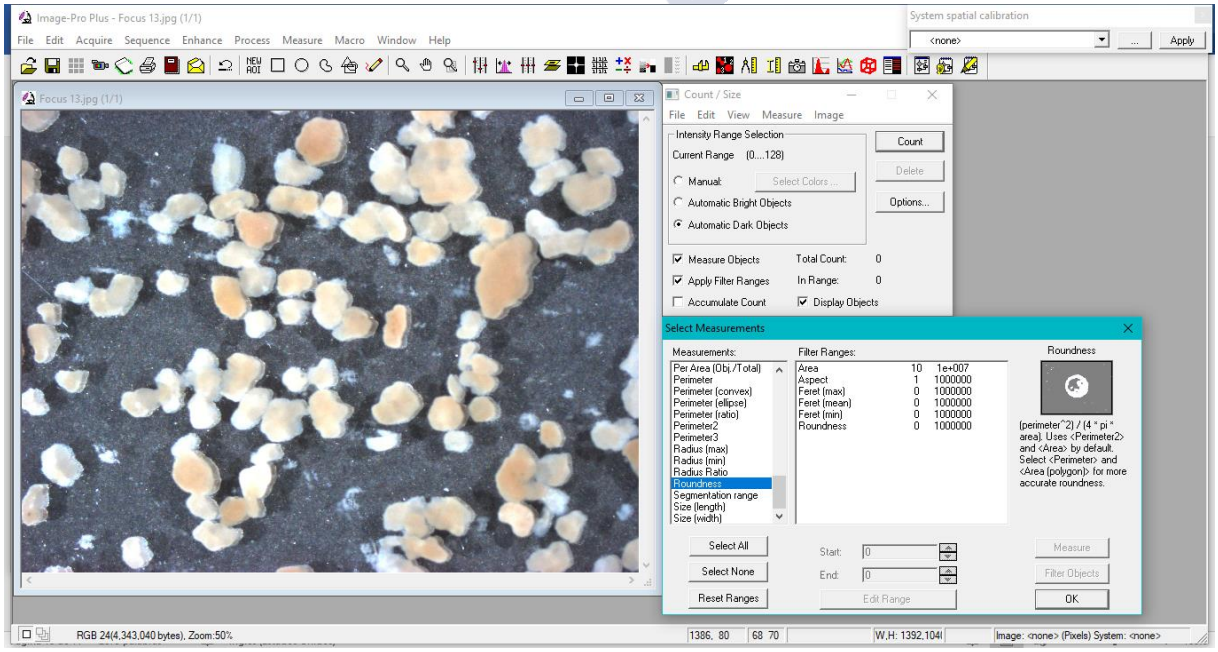

Figure 2.8: Original image of a sample of granules processed by the software.

2.2.5. Extracellular Polymeric Substances (EPS)

The measurement of the Extracellular Polymeric Substances (EPS) content of biomass samples included two main steps: the extraction of the EPS and the characterisation of the extracted compounds. Regarding the extraction step, a thermic method was followed (Le-Clech et al., 2006). For the characterisation of the EPS, only proteins and carbohydrates were measured, according to the methods described in sections 2.1.7 and 2.1.8, respectively, since they are considered the main compounds of the EPS.

The extraction of EPS by the thermic method was performed following the protocol described by Le-Clech et al. (2006), which differentiates between two fractions of EPS: Soluble Microbial Products (SMPs) and Bound EPS (B-EPS).

Firstly, the SMP fraction was separated by centrifuging 50 mL of representative sample of biomass (centrifuge Eppendorf 5430) at 5000 rpm for 5 minutes at room temperature and filtering the supernatant through a 0.20 μm pore-size filter (MF-Millipore, Millipore). Then, the precipitate was resuspended with distilled water to its original volume of 50 mL. Next, it was heated in a thermal bath (Transsonic 570/H) at 80 °C for 10 minutes to extract the B-EPS of the sample. Afterwards, the sample was centrifuged at 7000 rpm for 10 min at 4 °C and the supernatant was filtered through a 0.20 μm pore-size filter (MF-Millipore, Millipore).

The composition of the EPS was assumed to be the sum of both proteins and carbohydrates and was calculated, referred to the VSS content of the biomass, by the Eq. 2.14.

$$\text{EPS [mg EPS/g VSS]} = \frac{\text{PN} + \text{PS}}{\text{VSS}} \qquad \text{Eq. 2.14}$$

Where PN is the concentration of the extracted proteins (mg/L), PS is the concentration of the extracted carbohydrates (mg/L) and VSS is the Volatile Suspended Solids concentration of the biomass (g/L).

2.3. IDENTIFICATION OF BACTERIAL POPULATIONS BY FLUORESCENT *in situ* HYBRIDISATION

The Fluorescent *In Situ* Hybridisation (FISH) technique allows the identification of microorganisms at any desired taxonomical level, just depending on the specificity of the used probe. The quantification of the relative abundance of the identified populations is based on the use of the software Daime (Digital Image Analysis in Microbial Ecology), which measures the total biovolume fraction of a specifically characterised population (Daims et al., 2006).

2.3.1. Identification of bacterial populations

The FISH technique uses fluorescent-labelled probes to detect specific regions in the 23S to 16S rRNA of the targeted bacterial populations. The probes hybridise with the targeted sequence of any desired taxonomical level (domain, phylum, genus or specie) to be later detected microscopically. The protocol included four steps (Amann et al., 1995): (1) the fixation and permeabilisation of the sample; (2) the hybridisation of the targeted sequence to the probe; (3)

the washing steps to remove the unbound probe; and (4) the detection of labelled cells by microscopy.

Reagents preparation

- PBS (3x): 0.49 g of KH_2PO_4 was dissolved in 80 mL of distilled water. Then, 2.3 g of NaCl was added and the pH value was adjusted to 4.2. Finally, the volume was filled up to 100 mL. PBS (1x) was prepared by a dilution 1:3 of PBS (3x) in distilled water.
- Fixative solution: 6.5 mL of distilled water was heated to 60 °C and 0.4 g of paraformaldehyde was added. Then, one drop of NaOH 1 M was added while the solution was vigorously shaken for 1 – 2 minutes until its complete solubilisation. A volume of 3.3 mL of PBS (3x) was added and the pH value was adjusted to 7.2 with HCl (about one drop of HCl 1 M). Finally, the solution was filtered through a 0.2 µm membrane filter.
- Hybridisation buffer: 360 µL of 5 M NaCl solution and 40 µL of 1 M Tris/HCl (pH 8.0) were mixed in a 2 mL Eppendorf tube. The amount of formamide (vol %) for the hybridisation buffer was selected depending on the probe used (Table 2.3). Finally, 4 µL of sodiumdodecylsulphate 10 % (w/v) was added to the mixture.

Table 2.3: Formamide and water addition to the hybridisation buffer.

Formamide (vol %)	Formamide (µL)	MilliQ (µL)
0	0	1600
5	100	1500
10	200	1400
15	300	1300
20	400	1200
25	500	1100
30	600	1000
35	700	900
40	800	800
45	900	700
50	1000	600
55	1100	500
60	1200	400

- Washing buffer: 1 mL of Tris/HCl (pH 8.0), and the required volume of 5 M NaCl and 0.5 M EDTA (pH 8.0), depending on the percentage of formamide used with the applied probe (Table 2.4), were mixed in a 50 mL Falcon tube. The tube was filled up to 50 mL with distilled water and preheated at 48 °C before its use.

Table 2.4: NaCl and EDTA addition to the washing buffer.

Formamide (vol %)	5 M NaCl (µL)	0.5 M EDTA (µL)
0	9000	-
5	6300	-
10	4500	-
15	3180	-
20	2250	500
25	1590	500
30	1120	500
35	800	500
40	560	500
45	400	500
50	280	500
55	200	500
60	80	500

Procedure

1. Fixation of cells. Biomass was washed in PBS (1x), then three volumes of fixative solution were added to one volume of suspension. The solution was kept in ice for 2 h. After this time, it was washed again with PBS (1x) and the cells were resuspended in PBS (1x). Iced 98 % ethanol was added to the biomass suspension in a ratio 1.25:1. Samples were stored at -20 °C.

2. Immobilisation of cells on microscope slides. After fixation, the suspension in ethanol of the fixed biomass was spread in each well of a coated Teflon/glass microscope slide (5 – 10 µL). The slide was dried at 46 °C for 10 min. Then, the cells were dehydrated by successively rinsing the slides, 3 times for 3 minutes, with 50 %, 80 % and 98 % ethanol and dried with air.

3. Hybridisation. The hybridisation buffer was prepared and kept at room temperature. The hybridisation tube was prepared by placing a folded tissue inside a 50 mL Falcon tube. Part of the hybridisation buffer (10 µL) was pipetted into the wells of the slides with the biomass and the rest was poured onto the tissue inside the Falcon tube. The FISH probe was added to the wells of the slides (1 µL of stock solution with a final concentration of 30 ng/µL for Cy3 and Cy5-labelled probes and 50 ng/µL for FITC labelled probes). Then, each slide was placed inside the hybridisation tube and incubated for 1.5 h at 46 °C. In the meantime, the washing buffer was prepared and preheated in a water bath at 48 °C.

4. Washing. This step was performed rapidly. The slide was transferred into the Falcon tube containing the washing buffer and incubated for 15 minutes at 48 °C. Then, the slide was transferred from the washing buffer to cold distilled water for a few seconds and dried with air.

5. Microscopy and image acquisition. The targeted organisms could be detected by the characteristic fluorescence of the dye (fluorochrome) attached to the probe. The fluorochromes used to detect the hybridised rRNA were FLUOS (5(6)-carboxyfluorescein-Nhydroxysuccinimide ester) and Cy3 (indo-carbocyanine). The stain DAPI dye (4,6-diamino-2-phenylindole) was used for the visualisation of all the cells present in the sample. Slide wells were embedded with Vectashield H-1200, which amplified the fluorescence, avoided fading and contained DAPI dye,

and the coverslip was placed on the slide. For the analysis of the slides, an epifluorescence microscope (Axioskop 2 plus, Carl-Zeiss, USA) in combination with a digital camera (Coolsnap, Roper Scientific Photometrics, USA) was used. An acquisition software RSI image v 1.7.3 (Roper Scientific Photometrics, USA) was used to collect and process the images taken from the analysed samples.

For the characterisation of the microbial populations of the present thesis, the following probes were used (Table 2.5): AOB (NSO190), NOB (NTI3), PAO (PAO462, PAO651, PAO846), GAO (GAOQ989, GAOQ431).

Table 2.5: List of oligonucleotide probes and targeted microbial groups for FISH analysis in this thesis.

Probe	Fluorochrome	Formamide (%)	Target organisms
EUB338I[a]	FITC	0 – 50	*Bacteria* domain
EUB338II[a]	FITC	0 – 50	*Planctomycetales*
EUB338III[a]	FITC	0 – 50	*Verrucomicrobiales*
PAO462	Cy3	35	*Candidatus* Accumulibacter Phosphatis
PAO651	Cy3	35	Most members of the *Candidatus* Accumulibacter cluster
PAO846	Cy3	35	*Candidatus* Accumulibacter Phosphatis
GAOQ989	Cy3	35	*Candidatus* Competibacter Phosphatis
GAOQ431	Cy3	35	*Candidatus* Competibacter Phosphatis
NSO190	Cy3	55	Betaproteobacterial ammonia-oxidising bacteria
NTI3	Cy3	40	*Nitrobacter* spp.

[a] EUB338I, EUB338II and EUB338III were applied as an equimolar mix ($EUB338_{mix}$).

2.3.2. Quantification of bacterial populations

The quantification of bacterial populations is based on the use of DAIME software, by measuring the relative abundances (fractions of the total biovolume) of probe labelled populations in digital images (Daims et al., 2006). Although the DAIME software recommends the use of images acquired by using a confocal microscope, in the present thesis, this specific software was used with images acquired by using an epifluorescence microscope, to have an approximate idea of the percentages of certain populations. The quantification was performed by comparing the positive area obtained with a specific probe with the area corresponding to the control made with the DAPI dye.

2.4. CALCULATIONS

The calculations regarding the nitrogen and carbon mass balances applied to the operations of the different reactors are presented in this section, together with the calculations related to the specific activities.

2.4.1. Hydraulic and sludge retention time (HRT and SRT)

The Hydraulic Retention Time (HRT) was calculated following Eq. 2.15:

$$\text{HRT (d)} = \frac{V_{useful}}{F_{cycle} \cdot n} = \frac{V_{min} + V_{eff}}{F_{cycle} \cdot n} \quad \text{Eq. 2.15}$$

Where V_{useful} is the useful volume (L) for the biological processes inside the reactor (i.e., the total liquid volume), V_{min} is the minimum liquid volume (L) provided inside the reactor (which depends on the height of the discharge port), V_{eff} is the exchange volume of the effluent for each cycle (L), F_{cycle} is the volumetric flow of the feeding for one cycle (L/cycle) and n is the number of cycles in one operational day (cycles/d).

The Sludge Retention Time (SRT), which measures the average time that biomass remains inside the reactor, was calculated following Eq. 2.16:

$$\text{SRT (d)} = \frac{X_r}{X_{eff}} \cdot \text{HRT} \quad \text{Eq. 2.16}$$

Where X_r is the biomass concentration in the reactor (g VSS/L) and X_{eff} is the biomass concentration of the effluent (g VSS/L).

2.4.1. Carbon

Organic Loading Rate (OLR)

The Organic Loading Rate (OLR), which indicates the organic matter load applied to the AGS system, was calculated from Eq. 2.17.

$$\text{OLR}\left(\frac{\text{g COD}_S}{\text{L} \cdot \text{d}}\right) = \frac{\text{COD}_{S,inf}}{\text{HRT}} \quad \text{Eq. 2.17}$$

Where $COD_{S,inf}$ is the concentration of soluble COD in the influent (g COD_S/L), and HRT the hydraulic retention time of operation of the reactor (d).

Chemical Oxygen Demand (COD) removal

The COD removal efficiency, which indicates the global total removal of organic matter in the system, due to heterotrophic bacteria or phosphate-accumulating organisms activities, was calculated from the influent-effluent mass balances for the COD, following Eq. 2.18:

$$\%\ \text{COD} = \frac{\text{COD}_{inf} - \text{COD}_{eff}}{\text{COD}_{inf}} \cdot 100 \quad \text{Eq. 2.18}$$

Where COD_{inf} and COD_{eff} are the COD concentrations in the influent and effluent, respectively (mg COD/L). Eq. 2.18 was used to calculate both total and soluble COD removal.

Chemical Oxygen Demand (COD) removed during anaerobic feeding

The fraction of COD removed during the anaerobic feeding phase was calculated following Eq. 2.19:

$$\%\ \mathrm{COD_{An}} = \frac{\mathrm{COD_{T-60t}} - \mathrm{COD_{T-60}}}{\mathrm{COD_{T-60t}}} \cdot 100 \qquad \text{Eq. 2.19}$$

Where $COD_{T\text{-}60t}$ is the theoretical COD concentration, as a result of the mixture of the remaining COD of the reactor and the COD provided with the influent of the following cycle after feeding, if there was no reaction, and $COD_{T\text{-}60}$ is the COD measured after the anaerobic feeding phase (mg COD/L).

2.4.2. Nitrogen

Nitrogen Loading Rate (NLR)

The nitrogen loading rate (NLR) was calculated from the influent concentrations of the nitrogen species and the HRT (Eq. 2.20):

$$\mathrm{NLR}\left(\frac{\mathrm{g\ N}}{\mathrm{L \cdot d}}\right) = \frac{\left(\mathrm{NH_4^+ - N}\right)_{\mathrm{inf}} + \left(\mathrm{NO_2^- - N}\right)_{\mathrm{inf}} + \left(\mathrm{NO_3^- - N}\right)_{\mathrm{inf}}}{\mathrm{HRT}} \cdot \frac{1}{1000} \qquad \text{Eq. 2.20}$$

Where $(NH_4^+\text{-}N)_{inf}$, $(NO_2^-\text{-}N)_{inf}$ and $(NO_3^-\text{-}N)_{inf}$ are the concentrations of ammonium, nitrite and nitrate in the influent (mg N/L), respectively, and HRT the hydraulic retention time (d).

Ammonium removal (% NH_4^+-N)

The ammonium removal efficiency was calculated from the influent-effluent mass balances for the ammonium removed in the system (Eq. 2.21):

$$\%\ \mathrm{NH_4^+ - N} = \frac{\left(\mathrm{NH_4^+ - N}\right)_{\mathrm{inf}} - \left(\mathrm{NH_4^+ - N}\right)_{\mathrm{eff}}}{\left(\mathrm{NH_4^+ - N}\right)_{\mathrm{inf}}} \cdot 100 \qquad \text{Eq. 2.21}$$

Where $(NH_4^+\text{-}N)_{inf}$ is the ammonium concentration in the effluent (mg N/L). The same procedure was used to calculate the Total Nitrogen removal efficiency (% TN).

Carbon to nitrogen ratio

The COD/N ratio was calculated from the influent concentrations of COD_S and TN, according to Eq. 2.22.

$$\mathrm{COD_S/N\ ratio}\left(\frac{\mathrm{g\ COD_S}}{\mathrm{g\ N}}\right) = \frac{\mathrm{COD_{S,inf}}}{\mathrm{TN_{inf}}} \qquad \text{Eq. 2.22}$$

Where $COD_{S,inf}$ and TN_{inf} are the influent concentrations of COD_S and TN, respectively.

Free ammonia (FA) and Free Nitrous Acid (FNA) concentrations

The concentration of Free Ammonia (NH_3) and Free Nitrous Acid (HNO_2) were calculated with Eq. 2.23 and Eq. 2.24, according to Anthonisen et al. (1976):

$$\mathrm{FA}\left(\frac{\mathrm{mg\ NH_3 - N}}{\mathrm{L}}\right) = \frac{\left(\mathrm{NH_4^+ - N}\right)\cdot 10^{\mathrm{pH}}}{\left(e^{6344/(273+\mathrm{T})} + 10^{\mathrm{pH}}\right)} \qquad \text{Eq. 2.23}$$

$$\mathrm{FNA}\left(\frac{\mathrm{mg\ HNO_2 - N}}{\mathrm{L}}\right) = \frac{\left(\mathrm{NO_2^- - N}\right)}{\left(e^{-2300/(273+T)} + 10^{\mathrm{pH}} + 1\right)} \qquad \text{Eq. 2.24}$$

Where T is the temperature (°C).

2.4.3. Phosphorus

Phosphorus Loading Rate (PLR)

The phosphorus loading rate (PLR) was calculated from the influent concentrations of phosphorus and the HRT (Eq. 2.25):

$$\mathrm{PLR}\left(\frac{\mathrm{g\ P}}{\mathrm{L\cdot d}}\right) = \frac{\left(\mathrm{PO_4^{-3} - P}\right)_{\mathrm{inf}}}{\mathrm{HRT}} \cdot \frac{1}{1000} \qquad \text{Eq. 2.25}$$

Where $(PO_4^{-3}\text{-}P)_{inf}$ is the concentration of phosphorus in the influent (mg P/L) and HRT the hydraulic retention time (d).

Phosphorus removal (% PO_4^{-3}-P)

The phosphorus removal percentage, associated with the activity of phosphate-accumulating organisms, was calculated from the influent-effluent mass balances for the phosphorus removed in the system (Eq. 2.26):

$$\%\ \mathrm{PO_4^{-3} - P} = \frac{\left(\mathrm{PO_4^{-3} - P}\right)_{\mathrm{inf}} - \left(\mathrm{PO_4^{-3} - P}\right)_{\mathrm{eff}}}{\left(\mathrm{PO_4^{-3} - P}\right)_{\mathrm{inf}}} \cdot 100 \qquad \text{Eq. 2.26}$$

Where $(PO_4^{-3}\text{-}P)_{inf}$ and $(PO_4^{-3}\text{-}P)_{eff}$ are the phosphorous concentrations in the influent and effluent, respectively (mg P/L).

2.4.4. Biomass growth

Nitrogen and phosphorus removed by assimilation

The amounts of nitrogen and phosphorus assimilated for biomass growth were determined according to Mosquera-Corral et al. (2005a). For a selected operational period, the amount of biomass produced due to growth (ΔW_G, g VSS) was estimated from the biomass increase in the reactor and the amount of biomass washed out in the effluent using Eq. 2.27:

$$\Delta W_G = \Delta X_r \cdot V_r + \overline{X_{eff}} \cdot F \cdot \Delta t \qquad \text{Eq. 2.27}$$

Where ΔX_r is the variation of the biomass concentration inside the reactor during the selected period (mg VSS/L), V_r is the volume of the reactor (L), X_{eff} is the average solids concentration of the effluent (mg VSS/L), F is the effluent flow (L/d) and Δt is the duration of the selected period (d).

Considering a biomass composition of $C_{60}H_{87}O_{23}N_{12}P$ (Tchobanoglous et al., 2014), the average amount of nitrogen and phosphorus assimilated for biomass growth was calculated using Eq. 2.28 and Eq. 2.29, respectively:

$$\Delta W_N = \Delta W_G \frac{12 \cdot 14 \text{ g} - \text{mol N}}{186.2 \text{ kg} - \text{mol biomass}} \qquad \text{Eq. 2.28}$$

$$\Delta W_P = \Delta W_G \frac{31 \text{ g} - \text{mol N}}{186.2 \text{ kg} - \text{mol biomass}} \qquad \text{Eq. 2.29}$$

Biomass production yield

The biomass production yield of the aerobic granules, expressed in terms of gram of biomass produced per gram of organic matter removed, was calculated according to Eq. 2.30.

$$Y = \frac{\Delta W_G}{(\overline{COD_{inf}} - \overline{COD_{eff}}) \cdot F \cdot \Delta t} \qquad \text{Eq. 2.30}$$

Where Y is the biomass yield (g VSS/g COD), ΔW_G is the produced biomass (g VSS), $\overline{COD_{inf}}$ and $\overline{COD_{eff}}$ are average concentrations in the influent and effluent (g COD/L, calculated from the experimental data), F is the flow rate (L/d) and Δt is the duration of the selected period (d).

2.4.5. Consumption and production rates of the nitrogen compounds

The activities of the different microbial populations present in the AGS reactor were calculated using the concentration profiles obtained during an operational cycle measurement, based on the procedure described by Mosquera-Corral et al. (2005b) (Figure 2.9).

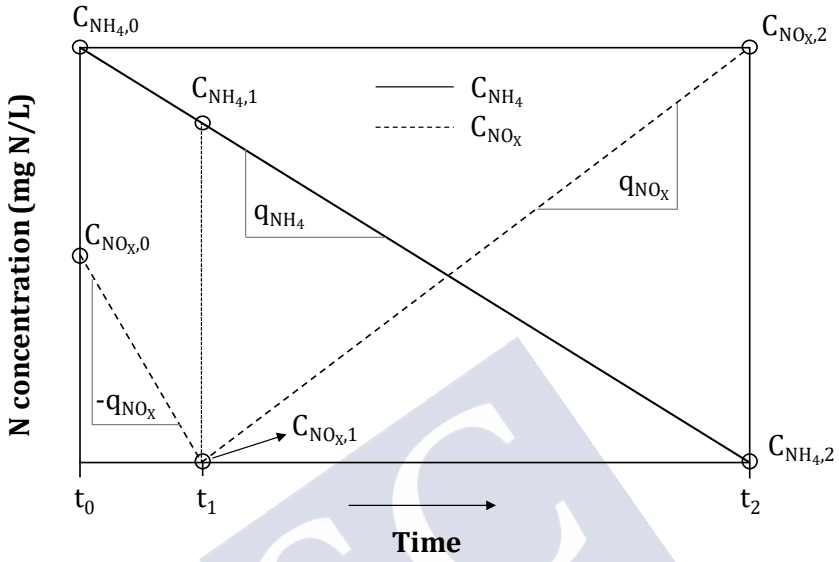

Figure 2.9: Scheme of the nitrogen compounds concentration along the cycle and definition of the calculated parameters (adapted from Mosquera-Corral et al. (2005b)).

The specific consumption rates of ammonia ($-q_{NH4}$) and nitrogen oxides ($-q_{NOX}$), as well as the specific production rate of nitrogen oxides (q_{NOX}), were calculated using Eq. 2.31, Eq. 2.32 and Eq. 2.33, respectively.

$$-q_{NH4} = \frac{C_{NH4,1} - C_{NH4,2}}{(t_2 - t_1) \cdot X_r} \quad \text{Eq. 2.31}$$

$$-q_{NOX} = \frac{C_{NOX,0} - C_{NOX,1}}{(t_1 - t_0) \cdot X_r} \quad \text{Eq. 2.32}$$

$$q_{NOX} = \frac{C_{NOX,2} - C_{NOX,2}}{(t_2 - t_1) \cdot X_r} \quad \text{Eq. 2.33}$$

Where t_0 is the time at the beginning of the cycle (h), t_1 is the time at the end of the feast phase (h), t_2 is the time at the end of the famine phase (h), $C_{c,t}$ is the concentration of each compound (C) at a certain time (t) (mg N/L), X_r is the biomass concentration (g VSS/L) and q_C is the specific rate of each compound (C) (g N/(g VSS·h))

2.4.7. Salinity (g NaCl/L)

The salinity, expressed as g NaCl/L, was estimated from the concentrations of Na^+ and Cl^- determined experimentally, according to Eq. 2.34 and Eq. 2.35, respectively. The concentration of the salt was estimated based on the ion which limits its formation.

$$\text{Salinity (from } Na^+) = C_{Na^+} \frac{58.5 \text{ g} - \text{mol NaCl}}{23 \text{ g} - \text{mol } Na^+} \quad \text{Eq. 2.34}$$

$$\text{Salinity (from } Cl^-) = C_{Cl^-} \frac{58.5 \text{ g} - \text{mol NaCl}}{35.5 \text{ g} - \text{mol } Na^+} \quad \text{Eq. 2.35}$$

Where C_{Na+} is the sodium concentration (g/L) and C_{Cl-} is the chloride concentration (g/L).

2.5. REFERENCES

Amann, R.I., Ludwig, W., Schleifer, K.H., 1995. Phylogenetic identification and in situ detection of individual microbial cells without cultivation. Microbiol. Rev. https://doi.org/10.1128/mmbr.59.1.143-169.1995

Anthonisen, a C., Srinath, E.G., Loehr, R.C., Prakasam, T.B.S., 1976. Inhibition of nitrification and nitrous acid compounds. J. Water Pollut. Control Fed. 48, 835–852. https://doi.org/10.2307/25038971

APHA/AWWA/WEF, 2012. Standard Methods for the Examination of Water and Wastewater. Stand. Methods 541. https://doi.org/ISBN 9780875532356

Beun, J.J., Van Loosdrecht, M.C.M., Heijnen, J.J., 2002. Aerobic granulation in a sequencing batch airlift reactor. Water Res. https://doi.org/10.1016/S0043-1354(01)00250-0

Bower, C.E., Holm-Hansen, T., 1980. A Salicylate–Hypochlorite Method for Determining Ammonia in Seawater. Can. J. Fish. Aquat. Sci. https://doi.org/10.1139/f80-106

Daims, H., Lücker, S., Wagner, M., 2006. daime, a novel image analysis program for microbial ecology and biofilm research. Environ. Microbiol. https://doi.org/10.1111/j.1462-2920.2005.00880.x

Dreywood, R., 1946. Qualitative Test for Carbohydrate Material. Ind. Eng. Chem. - Anal. Ed. https://doi.org/10.1021/i560156a015

Le-Clech, P., Chen, V., Fane, T.A.G., 2006. Fouling in membrane bioreactors used in wastewater treatment. J. Memb. Sci. https://doi.org/10.1016/j.memsci.2006.08.019

Lowry, O.H., Rosebrough, N.J., Farr, A.L., Randall, R.J., 1951. Protein measurement with the Folin phenol reagent. J. Biol. Chem.

Mosquera-Corral, A. Vázquez, J.R., Arrojo, B., Campos, J.L., Méndez, R., 2005a. Nitrifying granular sludge in a Sequencing Batch Reactor. Aerob. Granul. Sludge 63–70

Mosquera-Corral, A., De Kreuk, M.K., Heijnen, J.J., Van Loosdrecht, M.C.M., 2005b. Effects of oxygen concentration on N-removal in an aerobic granular sludge reactor. Water Res. 39, 2676–2686. https://doi.org/10.1016/j.watres.2005.04.065

Soto, M., Veiga, M.C., Méndez, R., Lema, J.M., 1989. Semi-micro C.O.D. determination method for high-salinity wastewater. Environ. Technol. Lett. https://doi.org/10.1080/09593338909384770

Tchobanoglous, G., Stensel, H.D., Tsuchihashi, R., Burton, F., Abu-Orf, M., Bowden, G., Pfrang, W., 2014. Wastewater Engineering: Treatment and Resource Recovery, Fifth Edition (International Edition), Metcalf & Eddy I AECOM, McGraw-Hill Education

Tijhuis, L., van Loosdrecht, M.C.M., Heijnen, J.J., 1994. Formation and growth of heterotrophic aerobic biofilms on small suspended particles in airlift reactors. Biotechnol. Bioeng. https://doi.org/10.1002/bit.260440506

USC
UNIVERSIDADE
DE SANTIAGO
DE COMPOSTELA

Chapter 3

Implementation of pulsed aeration in an aerobic-fed AGS reactor

Summary

In this chapter, a new aeration strategy based on pulsed aeration was evaluated. For this purpose, two anaerobic-fed Aerobic Granular Sludge (AGS) Sequencing Batch Reactors (SBRs) with cycles of 3 hours (112 min of aeration phase) were operated treating low-strength wastewater (Organic Loading Rate of 0.8 kg COD/(m^3·d)) with different aeration strategies: pulses of 1s ON/2s OFF (R1) and continuous aeration (R2, which served as control).

Initially, different Superficial Gas Velocities (SGV) of 3.6 cm/s (R1) and 1.2 cm/s (R2) were imposed for the same airflow (448 L/cycle). The granulation process was completed in 38 days for R1 whereas it took 48 days for R2. Denser and smaller granules were formed with pulsed regime and Phosphate Accumulating Organisms (PAOs) were developed faster. Additionally, the settleability of the granules was better with pulsed aeration (SVI_5 of 45 mL/g TSS) compared to continuous regime (SVI_5 of 62 mL/g TSS). The removal efficiencies were practically the same in both SBRs, being of 85 % for COD, 95 % for P and 30 % for N.

After granules formation, the airflow in both reactors was reduced. For an SGV value of 1.2 cm/s, both systems behaved similarly. The minimum SGV required to maintain a uniform mixture of the biomass inside the reactor was 1.2 (R1) and 0.5 cm/s (R2), meaning less air consumption in the pulsed system (149 L/cycle) compared to the continuous one (179 L/min). Therefore, pulsed aeration successfully reduced granulation periods and aeration requirements in AGS systems.

The obtained granules were stored in tap water at 4 °C for two years. The results of the reactivation assays after long-term storage showed no big differences between pulsed and continuous aeration. Heterotrophic and Ammonia Oxidising Bacteria activity were recovered after 2 and 12 days, respectively, but PAO and Nitrite Oxidising Bacteria activity were not detected.

OUTLINE

Chapter 3 67

3.1. INTRODUCTION 69

3.2. OBJECTIVES 70

3.3. MATERIALS AND METHODS 70

3.3.1. Experimental set-up 70

3.3.2. Operational conditions 72

3.3.3. Analytical and microbiological methods 73

3.4. RESULTS AND DISCUSSION 74

3.4.1. Pulsed vs continuous aeration 74

3.4.2. Evaluation of the minimum air consumption 82

3.4.3. Reactivation of the granules 85

3.5. CONCLUSIONS 87

3.6. REFERENCES 88

3.1. INTRODUCTION

In Aerobic Granular Sludge (AGS) systems, air has a triple role: it is important not only to ensure the development of the biological reactions but also to provide enough shear stress to enhance biomass granulation. In addition, it is responsible for a uniform mixture inside the reactor to maintain the biomass in suspension (Wan et al., 2011). Previous studies indicate that a minimum shear stress, usually expressed in terms of Superficial Gas Velocity (SGV), is necessary for the granulation process, establishing a SGV of 1.2 cm/s as the minimum value (Tay et al., 2001). Lower values lead to unstable and breakable aggregates (Zhu et al., 2015), whereas values between 2.4 and 3.2 cm/s were optimal to maintain stable granules and achieve good removal performances at long-term operation (Chen et al., 2007). However, the process implies significant energy consumption associated to the aeration requirements to granulate the biomass (Gao et al., 2013; Wan et al., 2009; Zhang et al., 2011).

Studies have been conducted to reduce the air supply, which diminishes energy costs and promotes the development of the denitrification process (Yuan and Gao, 2010). Nevertheless, in these cases, granules with worse settling properties were developed and longer start-up periods were required due to the diminishment of the applied shear stress. Jiang et al. (2016) introduced an anoxic stage after the aeration period in a reactor enriched in Phosphate Accumulating Organisms (PAOs). Despite the high removal efficiencies achieved (88.5 % of nitrogen, 90 % of phosphorus and 80 % of Chemical Oxygen Demand, COD), the granulation process was slow, and 80 days were necessary to achieve a full granular system. Wan et al. (2009) needed 175 days to obtain mature granules with SGV values between 0.6 and 2.2 cm/s.

To maintain the appropriate shear stress for granulation and reduce the start-up periods associated to low air supply, an additional unit (mainly mechanical stirrers) is included, but it has associated relevant energy costs (He et al., 2017a; Yilmaz et al., 2008). Zhang et al. (2011) needed a mechanical stirrer to assure a good mixing during the anoxic phase. The combination of mechanical stirring and an on-off regulator of air has been also tested (Dobbeleers et al., 2017). Other strategies to reduce the aeration include: 1) a constant Dissolved Oxygen (DO) concentration by controlling the airflow, 2) headspace gas recirculation, 3) alternation of high and low DO concentrations, maintaining a constant gas flow by adding N_2 gas in the periods of low DO concentration and 4) intermittent aeration (Lochmatter et al., 2013).

An alternative to these strategies could be the use of a pulsed regime, with alternation of seconds of aeration and no aeration. The pulsed strategy has been proven helpful to improve the properties of the biomass in other biological systems. However, the pulsed regime was applied to the feeding, not as an aeration strategy. For example, Franco et al. (2006) used a strategy of pulsed feeding in UASB (Upflow Anaerobic Sludge Blanket) reactors. This regime enhanced higher solid concentrations in the reactor (47.6 g VSS/L), in comparison with a reactor without pulses (16 g VSS/L), due to the faster settling velocity of the biomass. In another study, UAFs (Upflow Anaerobic Filters) were operated with pulsed feeding. The granulation of the biomass was promoted, the useful volume was increased and allowed the treatment of higher Organic Loading Rates (OLRs) in comparison with a UAF without pulsed feeding (Franco et al., 2007).

The pulsed aeration regime must guarantee a minimum airflow of the pulses to maintain a uniform mixture inside the reactor during the non-aeration times. Furthermore, the non-aerated periods need to be defined so that the settling of the biomass is avoided. For a fixed SGV, the pulsed regime will imply a lower air consumption at the end of the aeration stage compared to a continuous mode, since the time of aeration is shorter. Pulsed aeration has never been applied in AGS to remove carbon, nitrogen and phosphorus. It was only applied to the cultivation of nitrifying granules by Belmonte et al. (2009), but without success, since air pulses were not enough to suspend the biomass.

Another aspect that limits the practical application of AGS is the loose of physical properties and biological activity under long-term storage (Wang et al., 2008). For that reason, different research works have addressed the maintenance of granules stability during long-term storage and the recovery of the biological activities and physical properties of the biomass. Different temperatures (-25 °C – 26 °C), substrates (glucose, ethanol, NaCl solution, distilled water) and times (58 days – 12 months) have been tested during long-term storage (Gao et al., 2012; He et al., 2017b; Wan et al., 2014; Wang et al., 2008). Reactivation times of 24 h – one month were reported after long-term storage (Chen et al., 2017; Wan et al., 2014; Yuan et al., 2012).

3.2. OBJECTIVES

The objective of this research work was to study for the first time the impact of pulsed aeration on aerobic biomass granulation and PAO development and, once the granular biomass was established, the removal efficiencies and stability at long-term operation. Furthermore, the SGV was gradually reduced to determine the minimum SGV that can be applied and optimise the aeration requirements in systems with both types of aeration, pulsed and continuous. Additionally, the pulsed aeration was evaluated during the reactivation of aerobic granules after long-term storage.

3.3. MATERIALS AND METHODS

3.3.1. Experimental set-up

Two SBR with a working volume of 1.7 L and a height to diameter (H/D) ratio of 4 were used. The Volumetric Exchange Ratio (VER) was of 50 %, and the hydraulic retention time was 6 h (Figure 3.1). Both reactors were fed from the bottom in plug-flow mode.

a) b)

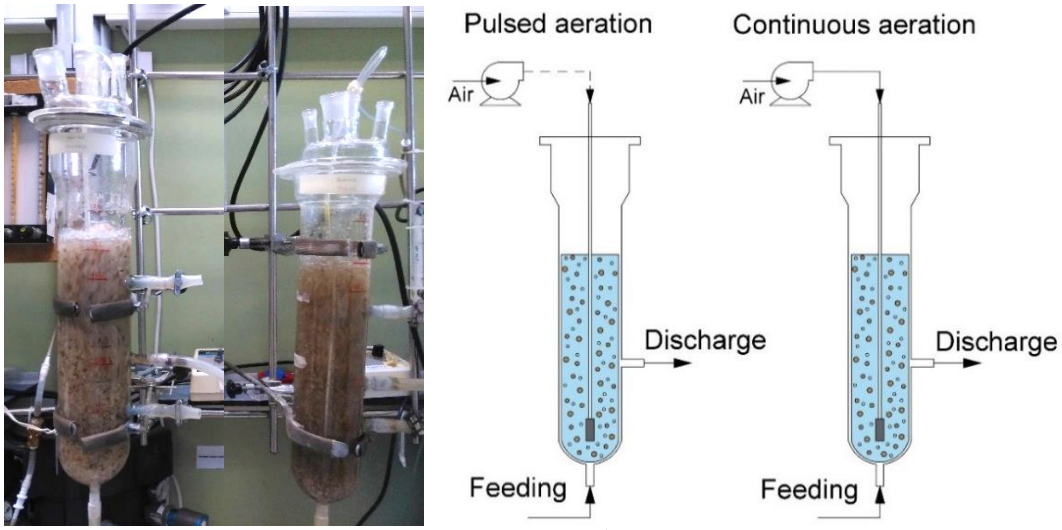

Figure 3.1: Photo of the experimental set-up (a) and scheme (b) of the aerobic granular sludge reactors.

The length of the operational cycle was 3 hours, distributed as follows: 60 minutes of anaerobic feeding-reaction, 112 minutes of aerobic reaction, 7 – 1 minutes of settling and 1 – 7 minutes of effluent withdrawal (Table 3.1). The settling time was gradually decreased from 7 to 2 minutes (day 99) and finally 1 minute (day 128), in both reactors, to increase the hydraulic selection pressure. The time reduced in the settling phase was added to the withdrawal stage, so that the anaerobic and aerobic phases were not affected by the change.

Table 3.1: Scheme of the SBR cycle phases distribution.

				Feeding
				Aerobic phase
				Settling
				Withdrawal
60	112	7 – 1	1 – 7	Time (min)

The air was introduced by fine bubble diffusers located at the bottom of the reactors and it was supplied by the compressed air main line of the building. The airflow was firstly controlled by pressure reducers, located at the end of the main line, and then the fine adjustment was made by a flowmeter. In both reactors, the working time of the aeration was regulated with electrovalves. The activation of the electrovalves and the pumps (for feeding and effluent discharge) in the different cycle phases was controlled by a Programmable Logic Controller (PLC, Siemens model S7-224CPU). In Reactor 1 (R1), air was provided in pulsed regime, consisting of air pulses of 1 second followed by 2 seconds without aeration (1 s ON / 2 s OFF). In Reactor 2 (R2), the air was supplied in a continuous regime during the aerobic phase. The duration of the pulses (ON/OFF) was selected so that a complete mixing (uniform suspension and distribution of the biomass) in the reactor was assured without the need of a mechanical stirrer.

3.3.2. Operational conditions

Both reactors were operated for 486 days, and their operation was divided into different operational stages depending on the supplied airflow, according to Table 3.2. The aeration strategy, in the different stages, was selected to compare the pulsed and the continuous aeration modes, considering the following scenarios: granulation with the same air volume in the cycle (Stage I for both reactors); stability of the granules at 1.2 cm/s (Stage II for R1 and Stage I for R2); stability of the granules at 0.7 cm/s (Stage III for R1 and Stage II for R2).

Table 3.2: Characteristics of the operational stages of R1 and R2.

Reactor	Operational days	Aeration regime	Airflow (L/min)	SGV (cm/s)	Total air volume per cycle (L)	Air saving (%)**
R1	Stage I (0 – 397)	Pulsed: 1 s ON/2 s OFF	12*	3.6*	448	0
	Stage II (398 – 464)		4.0*	1.2*	149	66.7
	Stage III (465 – 486)		2.4*	0.7*	89	80.1
R2	Stage I (0 – 397)	Continuous	4.0	1.2	448	0
	Stage II (398 – 464)		2.4	0.7	269	40.0
	Stage III (465 – 486)		1.6	0.5	179	60.0

*Values corresponding to each air pulse.

** Determined using as a basis the total air volume per cycle applied in the granulation stage (Stage I).

During Stage I (days 0 – 397), the airflow of both reactors was fixed to provide the same air volume during a cycle (448 L/cycle). This involved air pulses of 12 L/min in R1 and a continuous supply of 4 L/min in R2. Therefore, during the 112 minutes of the aeration period, in R1 the SGV of each pulse was 3 times higher (3.6 cm/s) in comparison with R2 (1.2 cm/s, the minimum value to develop stable granules).

In Stage II (days 398 – 464), the airflow of each pulse in R1 was reduced to 4.0 L/min, corresponding to an air consumption of 149 L/cycle, to evaluate the pulsed regime at the established threshold value for SGV of 1.2 cm/s and to compare with R2 in Stage I. The airflow of R2 was reduced from 4.0 to 2.4 L/min (269 L/cycle) and the SGV was set to 0.7 cm/s.

In Stage III (days 465 – 486), the airflow of R1 was reduced from 4.0 to 2.4 L/min (89 L/cycle), to evaluate the pulsed regime at a SGV value of 0.7 cm/s (lower than the recommended one) and compare with R2 in Stage II. In R2 a reduction from 2.4 to 1.6 L/min was applied (179 L/cycle) and the SGV was set to 0.5 cm/s.

The reactors were seeded with 1.7 L of activated sludge from a Wastewater Treatment Plant (WWTP) located in Galicia (NW of Spain), characterised by a Sludge Volume Index (SVI_{30}) of 187 mL/g TSS, and biomass concentrations of 5.25 g TSS/L and 4.33 g VSS/L.

Both reactors were initially fed with synthetic wastewater, according to de De Kreuk et al. (2005) (without allylthiourea addition), containing 380 mg COD/L, 47.2 NH_4^+-N/L and 26 mg PO_4^-

^{3}-P/L. A volume of 1 mL of trace solution was added per litre of feeding. The trace solution composition was prepared according to Vishniac and Santer (1957). From day 27 onwards until the end of the experimental period, the concentration of the feeding was decreased by half to feed 190 mg COD/L, 23.6 mg NH_4^+-N/L and 13 mg PO_4^{-3}-P/L. This composition corresponded to an OLR of only 0.8 kg COD/(m^3·d), Nitrogen Loading Rate (NLR) of 0.1 kg N/(m^3·d) and Phosphorus Loading Rate (PLR) of 0.3 g P/(m^3·d).

Reactivation assays

The aerobic granules enriched in PAOs obtained in the operation described in this chapter, were stored during almost two years in tap water. The storage temperature was 4 °C since it was more suitable to maintain the structural integrity of granules and allowed the best recovery performance, according to Gao et al. (2012).

In order to study their recovery capacity, the granules from R1 and R2 were mixed and divided into two equal fractions. Then, they were introduced in the same reactors, which were operated during 21 days, with the same feeding and operational conditions as Stage I. R1 had a pulsed regime as aeration strategy (airflow of 12 L/min and SGV of 3.6 cm/s in each pulse) and R2 continuous aeration (airflow of 4 L/min and SGV of 1.2 cm/s). The evolution of the reactors was followed by performing cycle analysis and characterising the biomass.

3.3.3. Analytical and microbiological methods

Analytical determination of ammonium (NH_4^+), nitrite (NO_2^-), nitrate (NO_3^-), phosphate (PO_4^{-3}), soluble COD, Total Suspended Solids (TSS), Volatile Suspended Solids (VSS) concentrations and SVI was carried out according to the Standard Methods (APHA/AWWA/WEF, 2012). Cation and anion concentrations were determined by ion chromatography with an Advanced Compact IC system (861, Metrohm). The pH was measured with an electrode (52-03, Crison Instruments, USA) and the dissolved oxygen concentration was measured with an on-line probe (Hach® HQ40D).

The density of the granules was measured with dextran blue following the methodology proposed by Beun et al. (2002). The morphology and size distribution of the granules was measured with a stereomicroscope (Stemi 2000-C, Zeiss) and using an image analysis procedure (Tijhuis et al., 1994). Main microbial populations were identified by FISH analysis. The targeted organisms were PAO (probes PAO462, PAO651 and PAO846) and GAO (probes GAOQ989 and GAOQ431). Detailed information about the probes is provided in Chapter 2. Fluorescence signals were observed under an epifluorescence microscope (Axioskop 2, Zeiss, Germany) and registered with an acquisition system (Coolsnap, Roper Scientific Photometrics). To determine the relative abundance of each population, referred to the total bacteria domain, at least 15 images from each sample were taken and processed using DAIME software (Daims et al., 2006).

Full description of the analytical methods and calculations is provided in Chapter 2.

3.4. RESULTS AND DISCUSSION

3.4.1. Pulsed vs continuous aeration

Granulation process

The same air volume of 448 L/cycle was added in Stage I to R1 and R2 while the imposed pulsing conditions in R1 fixed a SGV value of 3.6 cm/s. The continuous aeration in R2 provided a SGV of 1.2 cm/s. During the first days of Stage I an important decrease of the biomass concentration in both reactors took place, from 4.33 to 1.04 and 1.23 g VSS/L in R1 and R2, respectively. This reduction was due to the imposed settling time to favour the washout of the flocculent sludge and promote the granulation process. This strategy led to a fully granular biomass on day 38 in R1 (pulsed aeration), in the form of white and small granules (Figure 3.2.a), whereas in R2 (continuous aeration) the granulation process was not completed by that time (Figure 3.2.b). In R2 it took ten more days (until day 48) to achieve the complete biomass granulation (Figure 3.2.d), while at the same time in R1 the aggregates evolved, and a small fraction of big granules coexisted with small ones (Figure 3.2.c). Average particle diameter of the granules of 1.2 ± 0.2 and 1.1 ± 0.3 mm were registered on day 48 in R1 and R2, respectively.

Only a few studies have succeeded in cultivating aerobic granules with low-strength wastewater (< 200 mg COD/L). Li et al. (2011) needed to add granulated carbon to form granules using a feeding containing 200 mg COD/L. Ni et al. (2009), feeding 35 – 120 mg/L of soluble COD, observed the first granules after 80 days of operation and were able to obtain an 85 % of the biomass as granules after 300 days. With respect to the applied OLR, 75 days were needed to obtain granular biomass with applied OLRs of 1.05 – 1.68 kg COD/(m^3·d) (Wang et al., 2009) and 90 days to get a fully granular system applying an OLR of 0.76 kg COD/(m^3·d) (Coma et al., 2010). In comparison with these studies, the granulation period in both reactors, R1 and R2, was shorter (38 – 48 days) for an OLR of 1.6 – 0.8 kg COD/(m^3·d). The different results could be related to the different selected strategies to obtain granular biomass. In the abovementioned studies the SBR cycle was fully aerobic whereas in the present research work an anaerobic feeding period was used, promoting the growth of PAOs.

Biomass properties

Once the granulation process was completed, the biomass concentration increased in both reactors to 3 – 4 g TSS/L (day 70). Then, it reached a value of 7 – 8 (day 300) and 6 – 7 g TSS/L (day 300) in R1 and R2, respectively (Figure 3.3.a,b). The reduction of the settling time on day 99 to 2 minutes and on day 128 to 1 minute mainly affected the particle diameter, which increased up to the maximum value of approximately 3.5 mm, while the SVI_5 decreased to 50 – 60 mL/g TSS (Figure 3.4.a,b).

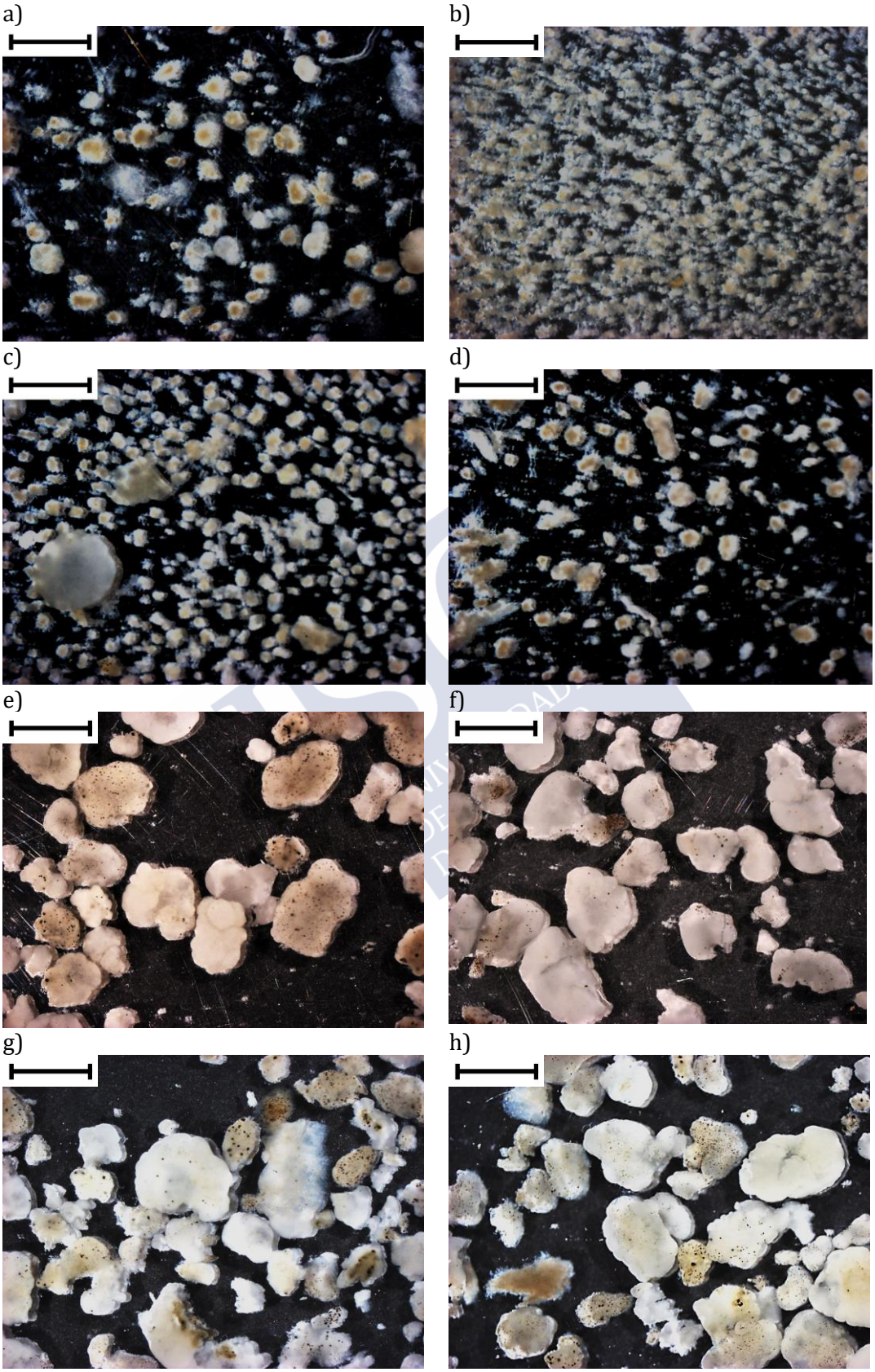

Figure 3.2: Images of the biomass of R1 on days 38 (a), 48 (c), 373 (e) and 462 (g) and biomass of R2 on days 38 (b), 48 (d), 373 (f) and 462 (h). The size bar indicates 2 mm.

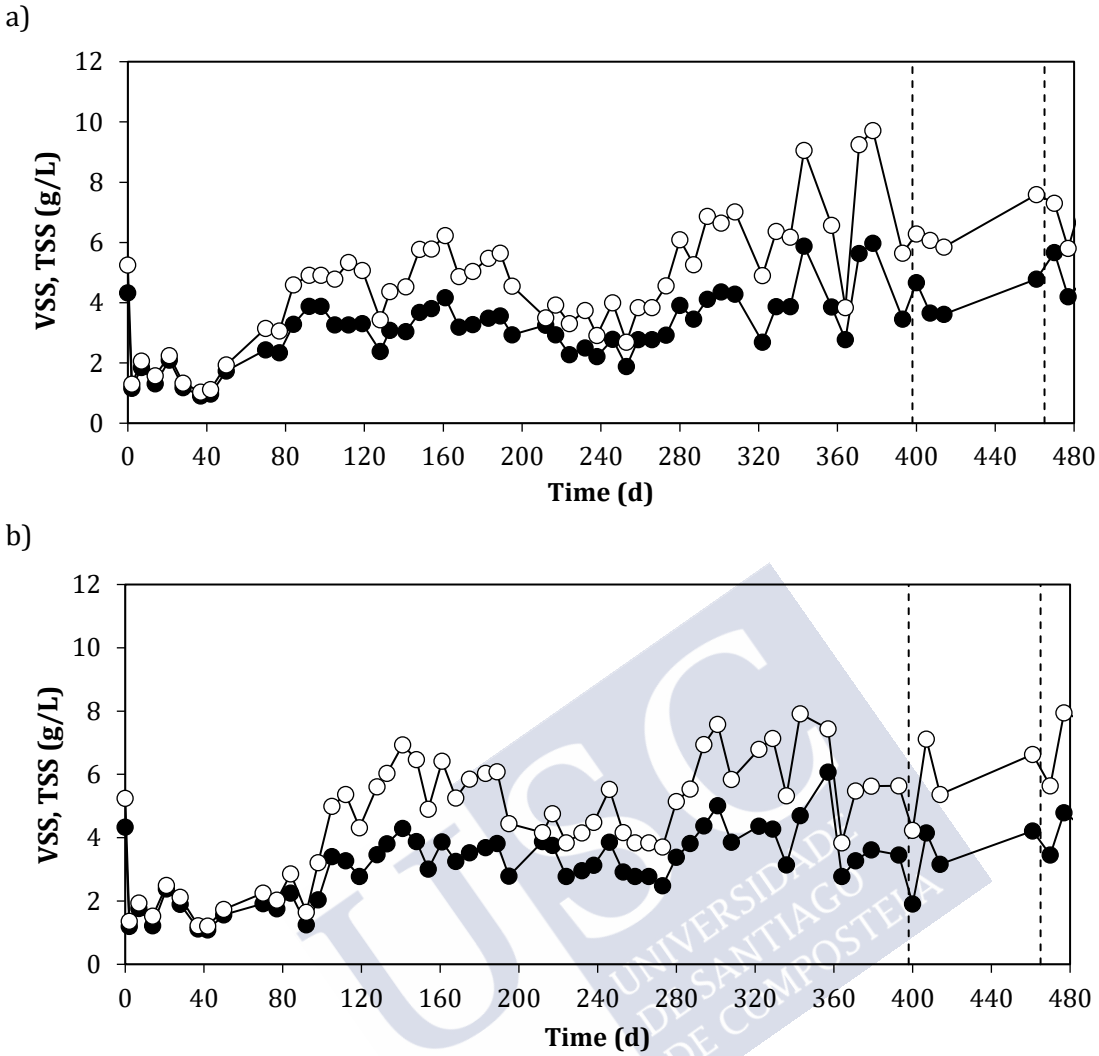

Figure 3.3: (a) Evolution of TSS (○) and VSS (●) in R1 (b) Evolution of TSS (○) and VSS (●) in R2. The discontinuous lines indicate the change of stage.

At the end of Stage I, the differences in density and SVI_5 values between R1 and R2 became significant. In R1 denser granules with better settling properties than in R2 were obtained (Figure 3.4.a,b), which enhanced the retention of biomass in R1. On day 373, the biomass concentration was of 5.63 g VSS/L, the density of 86 g VSS/$L_{granule}$, the SVI_5 of 45 mL/g TSS and the average diameter of 2.3 ± 0.9 mm (Figure 3.2.e). In the case of R2, the biomass reached a concentration of 3.28 g VSS/L on day 373, and was characterised by values of SVI_5 of 62 mL/g TSS, density of 60 g/$L_{granule}$ and particle diameter of 3.4 ± 0.9 mm (Figure 3.2.f).

The higher shear stress (SGV) produced by the air pulses applied to R1 could explain the differences between the properties of the granules in R1 and R2. This is in accordance with the research of Chen et al. (2007), who observed that the higher the applied shear force the denser and more compact granules are obtained. This could be also the explanation for the faster granulation of the biomass in R1 in comparison to R2.

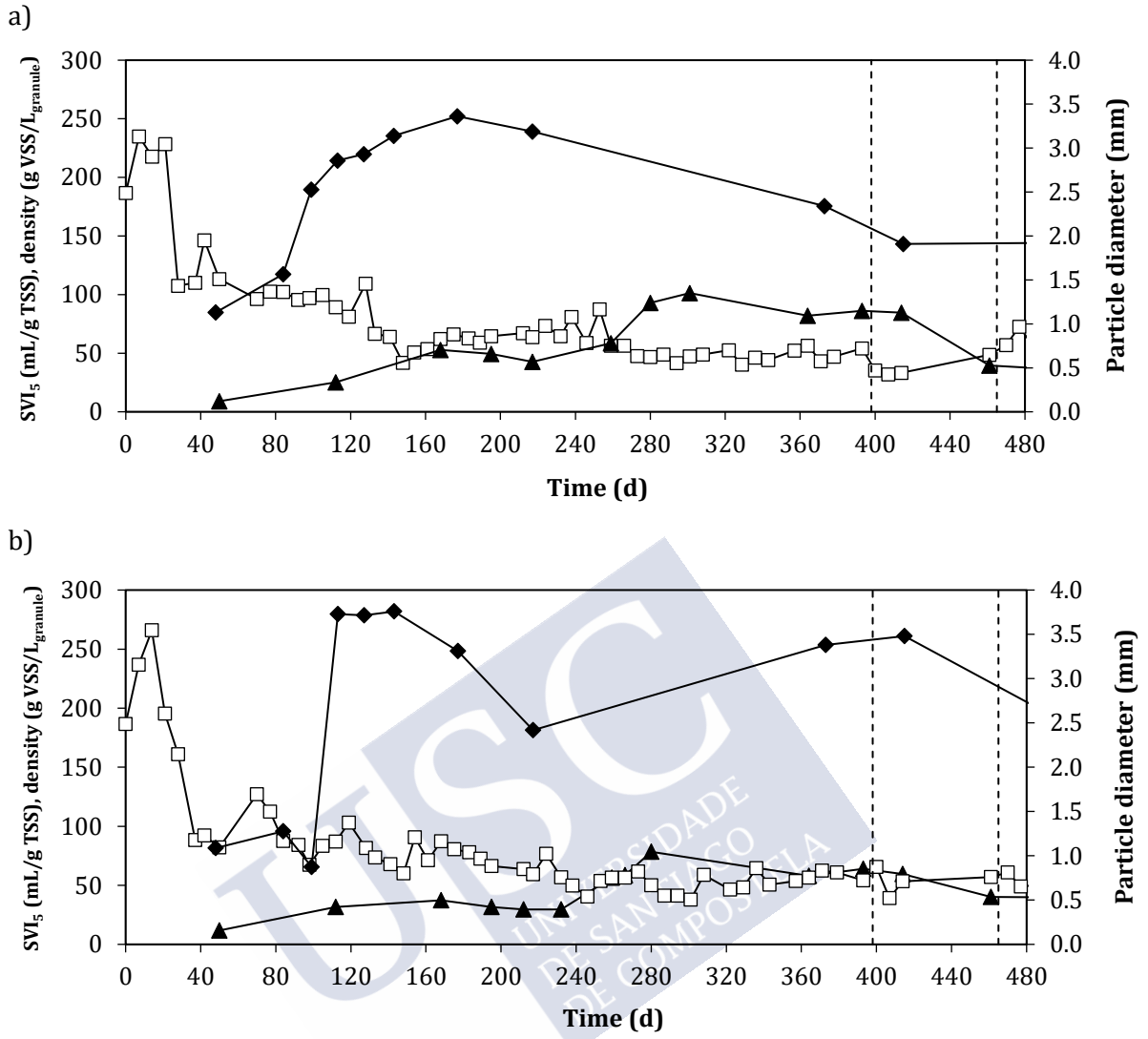

Figure 3.4: (a) Evolution of SVI_5 (□), particle diameter (♦) and density (▲) in R1 (b) Evolution of SVI_5 (□), particle diameter (♦) and density (▲) in R2. The discontinuous lines indicate the change of stage.

Reactors performance

The removal efficiencies of COD reached values of 70 – 80 % in a few days from the start-up in both reactors during Stage I (Figure 3.5.a,b). During the start-up period, COD was mainly removed during the aerobic stage, and phosphorus removal did not occur. Once PAOs were developed (confirmed by FISH analysis), the COD depletion took place mainly during the anaerobic stage coupled to phosphorus release to the bulk. The phosphorus concentration varied between 30 – 40 mg PO_4^{-3}-P/L at the end of the anaerobic feeding (Figure 3.6). The PAO content of the inoculum was insignificant (not detected by FISH analysis). Due to their slow growth, 60 days in R1 and 80 days in R2 were necessary to achieve a stable PAO activity and high percentages of COD removed during the anaerobic stage of 85 % in R1 and R2 (Figure 3.6.a,b). The achieved phosphorus removal efficiencies were of 95 %. In both reactors, a small fraction of COD remained in the effluent probably due to the presence of non-biodegradable substances in the feeding, like

EDTA (present in the trace solution), corresponding to approximately 30 mg COD/L (Wang et al., 2017a). Ammonia was completely oxidised to nitrate in both reactors, but due to the absence of denitrification, nitrogen removal was only attributed to biomass growth, with average values of 32 and 28 % in R1 and R2, respectively (Figure 3.5.a,b).

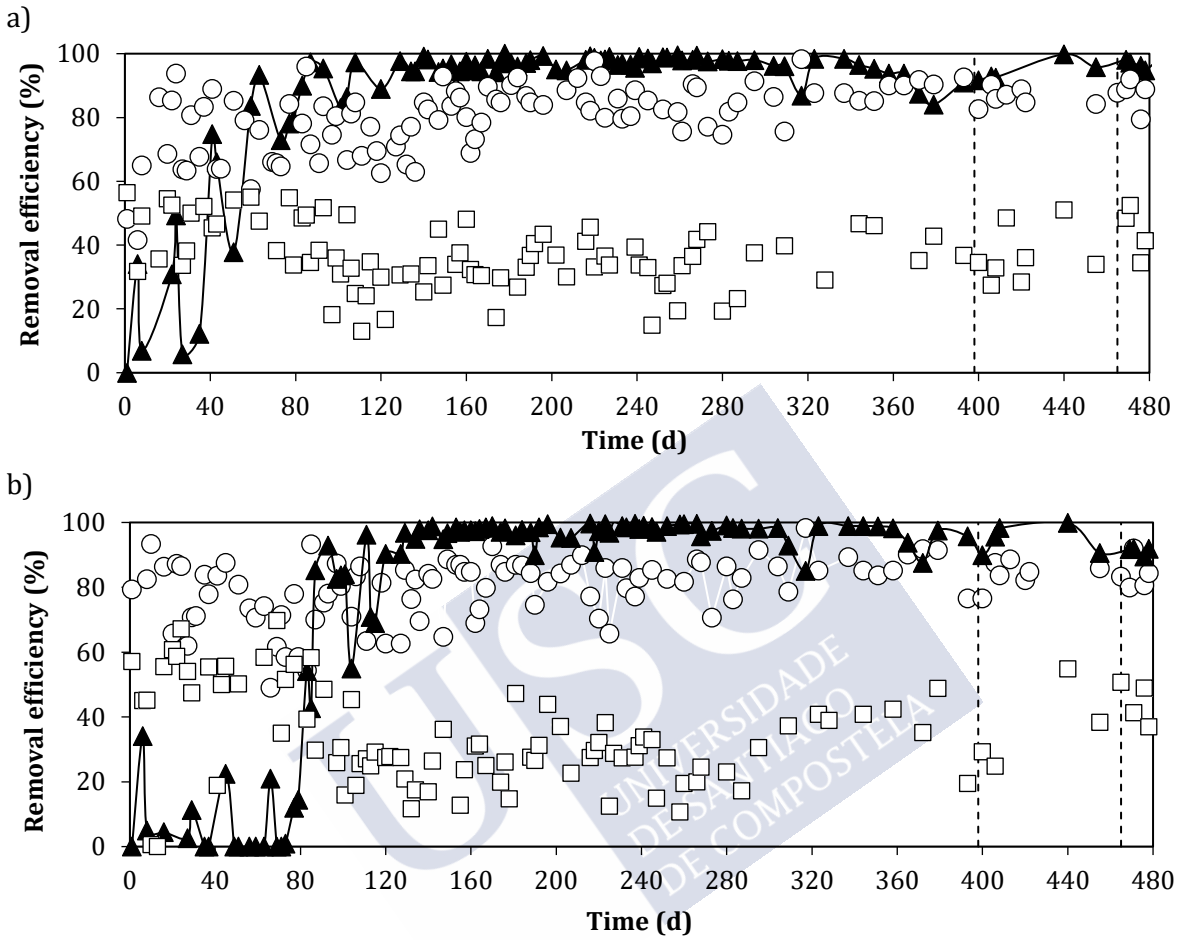

Figure 3.5: Removal percentages of COD (○), nitrogen (□) and phosphorus (▲) in R1 (a) and R2 (b).

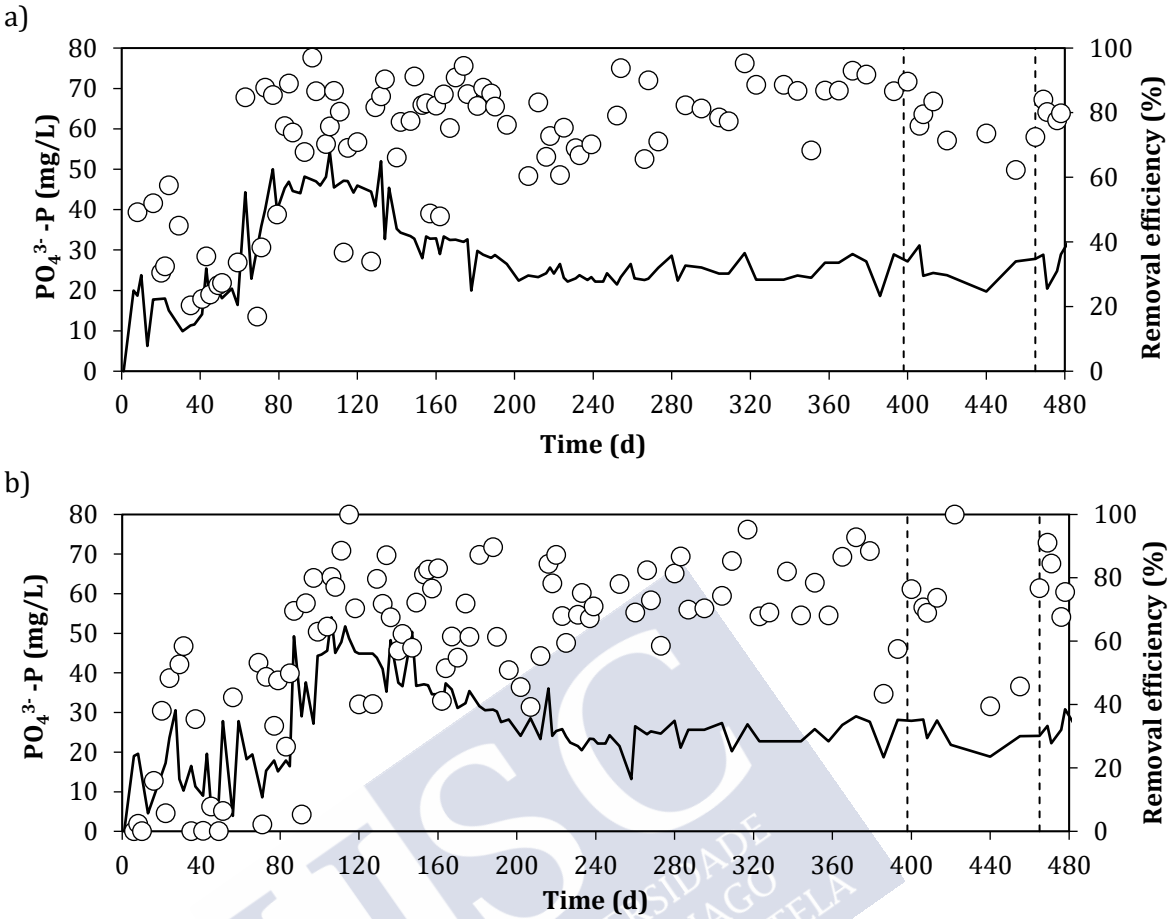

Figure 3.6: Phosphorus concentration at the end of the anaerobic phase (-) and % of the COD removal occurred during the anaerobic stage (○) of R1 (a) and R2 (b). NOTE: the COD removal (%) during the anaerobic stage was calculated as the ratio between the COD removed on the anaerobic stage and the COD removed during the entire cycle.

The faster increase of PAO abundance in R1 compared to R2 was confirmed by FISH analysis. It was at the end of Stage I when the PAO abundance was similar in both reactors and represented 70 – 80 % of the total bacteria domain (Figure 3.7.a). However, in R1 a gradual increase of GAO abundance was registered, reaching a 6 % of the total bacteria domain on day 374, whereas in R2 GAOs were not detected until day 465 (Figure 3.7.b).

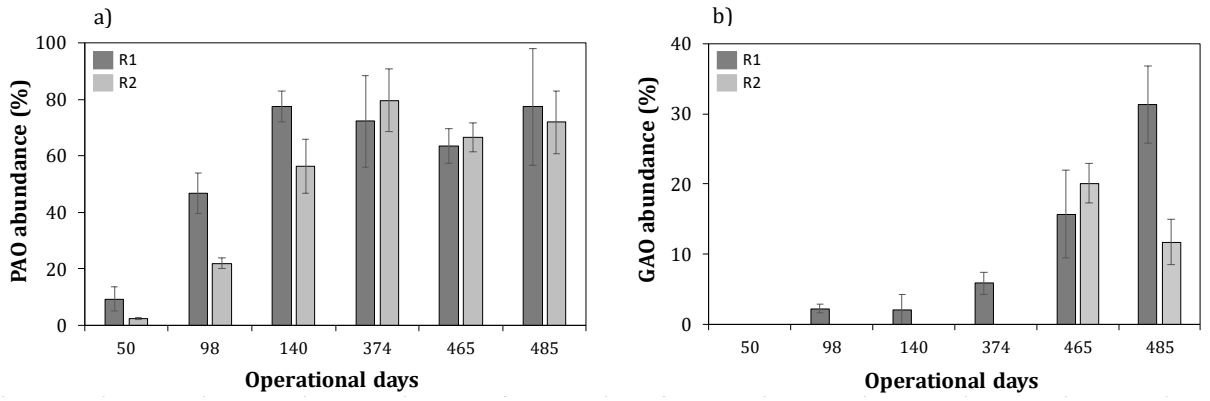

Figure 3.7: Relative abundances at different operational days of (a) PAO (probes PAO462, PAO651 and PAO846) and (b) GAO (probes GAOQ989 and GAOQ431) in the microbial community of R1 and R2.

The differences observed in the operation of the two reactors were evaluated by the monitoring of respective operational cycles of day 91. Phosphorus release took place, in both reactors, during the anaerobic feeding phase, followed by its uptake during the aerobic phase (Figure 3.8.a,c). A small fraction of the COD remained at the end of the anaerobic phase (Figure 3.8b,d) and slightly decreased during the aerobic period. The aerobic COD removal represented 15 % and 30 % of the total COD removed for R1 and R2, respectively. Complete ammonia oxidation to nitrate took place during the aerobic phase (Figure 3.8.a,c). Heterotrophic denitrification did not occur in this period due to the low COD concentration in the bulk, which was previously removed in the anaerobic feeding phase. The limited availability of a carbon source (Guimarães et al., 2017) and consequently the low COD/N ratio hindered the presence of an external electron donor to make heterotrophic denitrification occur (Wei et al., 2013). In addition, the high oxygen concentration, almost up to the saturation value (Figure 3.8.b,d), hindered the existence of enough anoxic zones inside the granules for the denitrification to take place. The same performance was observed by De Kreuk et al. (2005) and Zhong et al. (2014). Only in those systems provided with an anoxic phase the development of denitrifying PAOs (dPAOs) occurred as they use nitrite and nitrate as electron acceptors to uptake the phosphorus released to the bulk (Kuba et al., 1996; Zhong et al., 2014). In the cycle of R2 (continuous aeration) both ammonia oxidation and phosphorus uptake took place slower than in R1 (pulsed aeration).

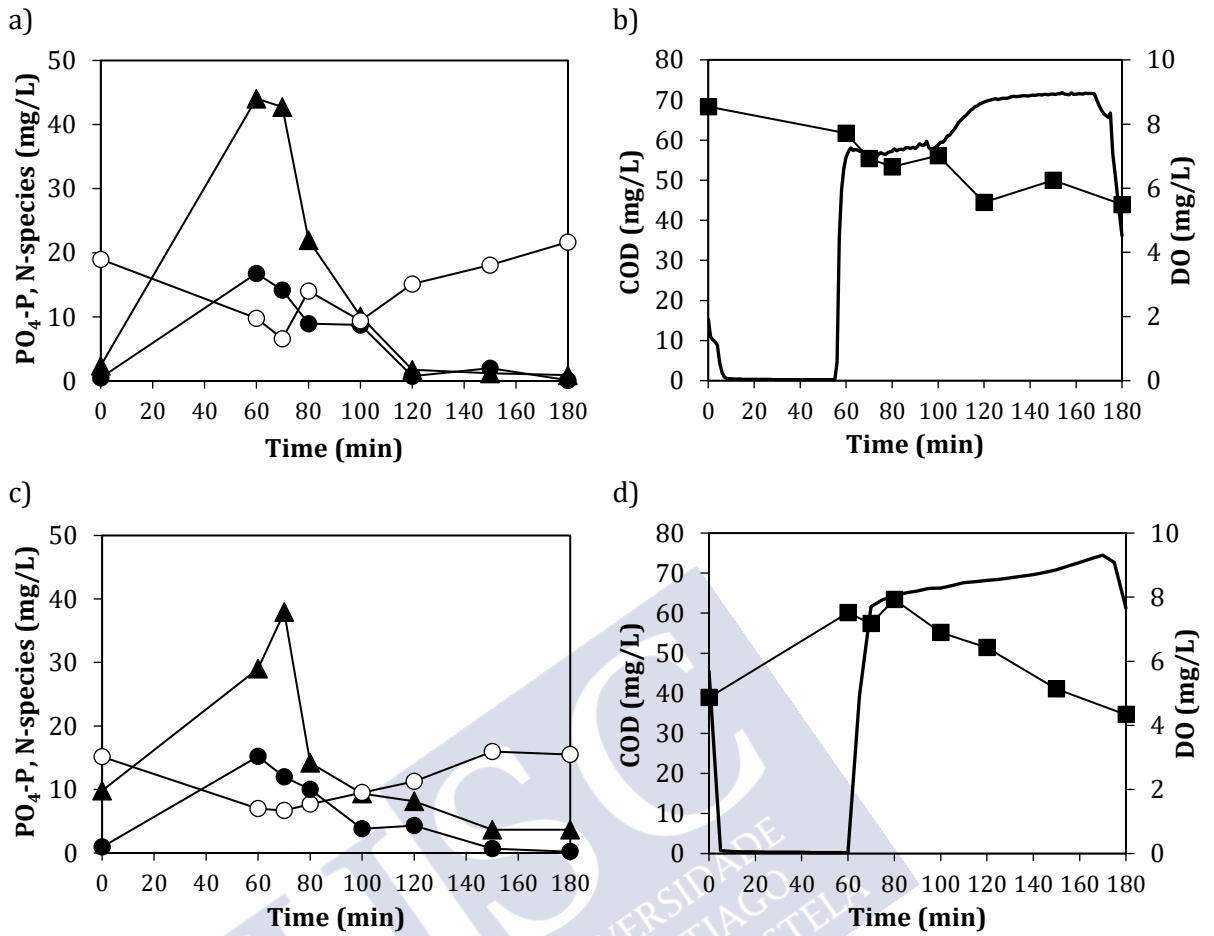

Figure 3.8: Cycle measurements on day 91 of R1 (a, b) and R2 (c, d). The profiles of COD (■), phosphorus (▲), ammonia (●), nitrate (○) and dissolved oxygen (-) are represented. NOTES: a) The initial point is the concentration of each compound measured in the effluent of the previous cycle; b) the nitrate concentration decrease in the anaerobic phase was due to dilution effect of the feeding.

These differences between the cycles of both reactors can be attributed not only to the faster development of PAOs in R1 but also to the different biomass concentrations of 3.88 and 2.04 g VSS/L in R1 and R2, respectively. These different concentrations could be linked to the different properties of the biomass, which favoured its retention in R1, as discussed previously.

Therefore, the results obtained in Stage I showed that, with the same volume of air, the pulsed aeration regime, in comparison with the continuous mode, reduced the time of the granulation process and enhanced a faster development of PAO activity. In addition, smaller and denser granules with better settling properties were obtained in R1, which means a higher retention of biomass in the pulsed aerated system than in the continuous one. In terms of removal efficiencies, the achieved values were practically the same at long-term operation (Table 3.3).

Table 3.3: Summary of the aerobic granular sludge properties and removal efficiencies of each reactor in stationary state at the different operational stages. Provided data are average values plus standard deviation corresponding to the operational days analysed in each stage.

	R1			R2		
	Stage I	**Stage II**	**Stage III**	**Stage I**	**Stage II**	**Stage III**
SGV (cm/s)	3.6	1.2	0.7	1.2	0.7	0.5
Granulation (days)	38	-	-	48	-	-
PAO development (days)	60	-	-	80	-	-
SVI_5 (mL/g TSS)	81 ± 47	37 ± 8	62 ± 9	82 ± 48	54 ± 11	53 ± 6
Density (g VSS/$L_{granule}$)	60.0 ± 30.2	62.1 ± 31.9	38.5 ± 1.4	44.2 ± 19.9	49.9 ± 13.7	40.0 ± 0.3
Particle diameter (mm)	2.56 ± 0.76	1.91 ± 0.67	1.92 ± 0.47	2.61 ± 1.22	3.48 ± 0.97	2.69 ± 0.19
TSS (g/L)	4.60 ± 1.97	6.45 ± 0.78	6.84 ± 0.90	4.58 ± 1.84	5.83 ± 1.30	7.12 ± 1.28
VSS (g/L)	3.12 ± 1.12	4.18 ± 0.75	4.85 ± 0.75	3.12 ± 1.08	3.36 ± 1.08	4.24 ± 0.70
COD removal (%)	84.3 ± 7.2	86.3 ± 2.7	86.9 ± 4.3	82.8 ± 7.0	84.1 ± 4.0	84.3 ± 4.3
N removal (%)	32.9 ± 9.6	36.6 ± 8.7	44.3 ± 6.5	28.3 ± 10.3	36.8 ± 13.3	39.6 ± 7.0
P removal (%)	95.6 ± 6.2	94.6 ± 3.3	96.6 ± 1.2	96.3 ± 7.2	94.8 ± 4.5	91.1 ± 1.2

3.4.2. Evaluation of the minimum air consumption

In Stage II and III experiments were performed to determine the minimum air volume consumption which allows maintaining the stress required for granules stability and aerobic activity of the biomass in both reactors.

Effect of progressive airflow reduction

The progressive reduction of the airflow had effects in the biomass properties of the pulsed aerated system. In Stage II the reduction of airflow supplied to R1 involved the decrease of SGV to 1.2 cm/s and a reduction of the air consumption to 0.73 $L_{air}/(L_{reactor}\cdot min)$. This change caused the loss of density of the granules from 86 to 40 g VSS/$L_{granule}$ (Stage II) and the decrease of the average diameter from 2.3 ± 0.9 to 1.9 ± 0.7 mm (Figure 3.2.g, Figure 3.4.a). However, both the SVI_5 and the solid concentration remained in the same values (48 mL/g TSS and 4.79 g VSS/L on day 461).

The further reduction of the air supply (SGV of 0.7 cm/s) in R1 (Stage III), which supposed an air consumption of 0.44 $L_{air}/(L_{reactor}\cdot min)$, resulted in a low airflow not being enough to maintain the biomass in suspension inside the reactor during the aeration stage. This was presumably due to the good settling properties of the biomass and the high solid concentration in the reactor (around 5 g VSS/L). The same behaviour was observed by Belmonte et al. (2009) in an aerobic granular system. Since it was not possible to achieve a good mixture inside the reactor, it was only operated for 20 days. The lack of mixture and shear stress caused the worsening of the biomass

properties, increasing the SVI_5 to 72 mL/g TSS on day 484. The density and the concentration of the biomass with values of 4.67 g VSS/L and 38 g VSS/$L_{granule}$ were similar to Stage II at a SGV of 1.2 cm/s (Figure 3.3.a,b). The particle diameter was also maintained, with a value of 1.9 ± 0.5 mm. Due to the bad suspension of the biomass in R1 at 0.7 cm/s no more SGV reductions were applied in this system.

In R2 (continuous aeration) the properties of aerobic granular sludge operating with 0.7 cm/s (Stage II) were maintained in comparison with Stage I (1.2 cm/s), which meant that the reduction of the SGV to 0.7 cm/s did not have an important impact in the mature granules (Figure 3.2.h). On day 461, an average particle diameter of 3.5 ± 0.9 mm, a density of 40 g/$L_{granule}$, SVI_5 of 57 mL/g TSS and 4.21 g VSS/L were measured. With the reduction of the SGV from 0.7 cm/s (1.32 L_{air}/($L_{reactor}$·min), Stage II) to 0.5 cm/s (0.88 L_{air}/($L_{reactor}$·min), Stage III) the SVI_5 remained stable while the biomass concentration slightly increased and the density and particle diameter decreased (Figure 3.4.b). However, the differences in the values were not relevant and the operation of the reactor remained stable.

With respect to the removal efficiencies, no significant differences were observed in the COD, N and P removal percentages of both reactors (Table 3.3). COD, P and N removal efficiencies ranged in both reactors between 93 – 87 %, 92 – 97 %, 36 – 44 %, respectively. The effluent quality fulfilled the discharge requirements for sensitive areas except for the Total Nitrogen (TN) concentration, which was still above 10 mg TN/L.

Regarding the presence of slow-growing microorganisms, PAO abundance decreased in R1 and R2 from 70 – 80 to 60 – 65 % (Stage II) of the total bacteria domain. GAO abundance progressively increased in R1 (pulsed aeration), being 10 % on day 465 and 25 % on day 485, while in R2 (continuous aeration) remained at 10 %.

Comparison between pulsed and continuous aeration at the same SGV

The SGV was fixed as a comparison parameter between both reactors and it was of 1.2 cm/s (Stage II for R1 and Stage I for R2) and 0.7 cm/s (Stage III for R1 and Stage II for R2). These fixed values corresponded to different airflow and consumed air volumes in both reactors (Table 3.1).

The main differences between the granular biomass in R1 and R2 with the SGV of 1.2 cm/s were the average diameter of the granules and the SVI_5 (Table 3.3). Both were lower in R1 with pulsed aeration than in R2 with continuous air supply (Figure 3.4). However, the density of the granules diminished in R1 and became lower than that of the granules from R2 of 64 g VSS/$L_{granule}$ on day 393 (Stage I).

The operational cycle of day 455 (Stage II) was measured for R1 to compare its performance with a cycle of R2 at the same SGV of 1.2 cm/s (day 366, Stage I). In R1 (Figure 3.9.a, b) no COD removal was registered during the aerobic phase, the complete oxidation of ammonia to nitrate took place, and denitrification did not occur, as discussed previously. In the cycle of R2 on day 366 (Figure 3.9.c,d), the aerobic COD consumption was reduced in comparison to the cycle of day 91. In terms of nitrogen, the behaviour of the system was similar to the cycle of R1. The DO concentration in both reactors was still too high (almost 8 mg/L) to allow denitrification processes (Figure 3.9.b, d). Consequently, both systems need to be optimised in order to increase the nitrogen removal efficiencies. Since it was not feasible a higher reduction of the airflow of the

pulses, the decrease of the frequency could an alternative to reduce the oxygen concentration (evaluated in Chapter 4).

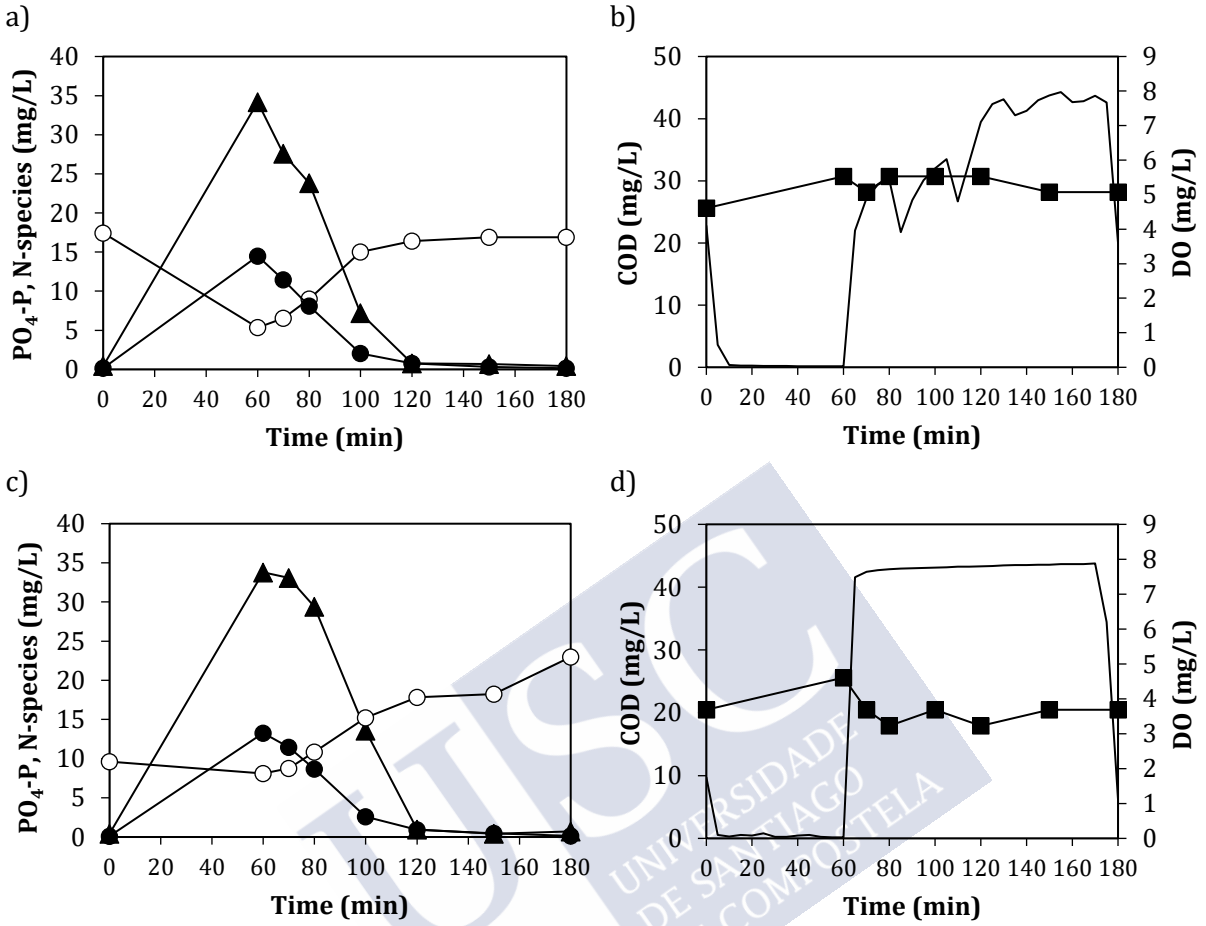

Figure 3.9: Cycle measurements at 1.2 cm/s on day 455 of R1 (a, b) and on day 366 of R2 (c, d). The profiles of COD (■), phosphorus (▲), ammonia (●), nitrate (○) and dissolved oxygen (-) are represented. NOTES: 1) The initial point is the concentration of each compound measured in the effluent of the previous cycle; 2) the nitrate concentration decrease in the anaerobic phase was due to dilution effect of the feeding.

Regarding the performance of the reactors with the SGV of 0.7 cm/s, it was not possible to maintain the biomass in suspension inside the reactor in R1, whereas R2 remained operating in a stable mode, like in the previous stages.

Implications of the minimum airflow requirements in pulsed and continuous aeration systems

Obtained results indicated that the fixed SGV seemed to affect the physical properties of the biomass more than the air pulsation itself. For a fixed SGV the pulsed regime had the beneficial effect of involving less air consumption, and consequently saving costs. However, it was necessary a minimum airflow to assure the uniform mixture in the reactor and maintain the granular biomass in suspension, including the non-aerated periods. Although the minimum required value

of SGV was higher with pulsed mode (1.2 cm/s) than with continuously aerated mode (0.5 cm/s), the total consumption of air in the cycle was still lower with pulsed aeration (Table 3.2).

Both reactors operated satisfactorily with SGVs equal or lower than the minimum recommended of 1.2 cm/s once granules were formed. Therefore, high shear stress was apparently less necessary to maintain the stability of systems with anaerobic feeding. Similar results were obtained by Devlin et al. (2017), suggesting that it is not necessary a high hydrodynamic shear to granulate the biomass, it is just necessary the selection of slow-growing microorganisms able to store the COD during the anaerobic stage. Shear stress could be just necessary to avoid the growth of filamentous bacteria when the biomass is not able to remove all the COD during the anaerobic phase.

3.4.3. Reactivation of the granules

The stored granules maintained their structure during the time of storage, but when seeded into the reactors they were disintegrated in the first days. The settling properties became worse (SVI_5 of 160 – 300 mL/g TSS) and there was a decrease of the biomass concentration in the reactor (from 4.15 on day 0 to 1.74 and 1.34 g TSS/L on day 21 in R1 and R2, respectively). In addition, the high fraction of Inorganic Suspended Solids (ISS) of the biomass in the previous operation (40 %) due to PAO activity, was decreased to values lower than 5 %. This indicated the lack of polyphosphate accumulation, and thus the absence of PAO activity. After 21 days, neither the well-shaped granules nor the good settleability were recovered (Figure 3.10.a,c). In this case, the different aeration strategies did not cause differences regarding the biomass properties.

Although the first day there was no COD removal, the COD removal capacity was rapidly recovered, being of almost 90 % on days 2 and 5, and 70 % at the end of the experiment (Figure 3.10.b, d). However, it was mainly removed during the aerobic stage, instead of the anaerobic one. This, in addition to the lack of phosphorus release and uptake, indicated that PAO activity was not recovered during the operation of the reactors, which led to phosphorus removal efficiencies of only 10 – 15 %. AOB activity was recovered after 12 days in both R1 and R2, whereas no NOB activity was detected. The total nitrogen removal efficiencies were of 40 – 45 %, indicating that almost all the nitrogen removed was due to biomass growth, and probably a small percentage was removed by denitritation.

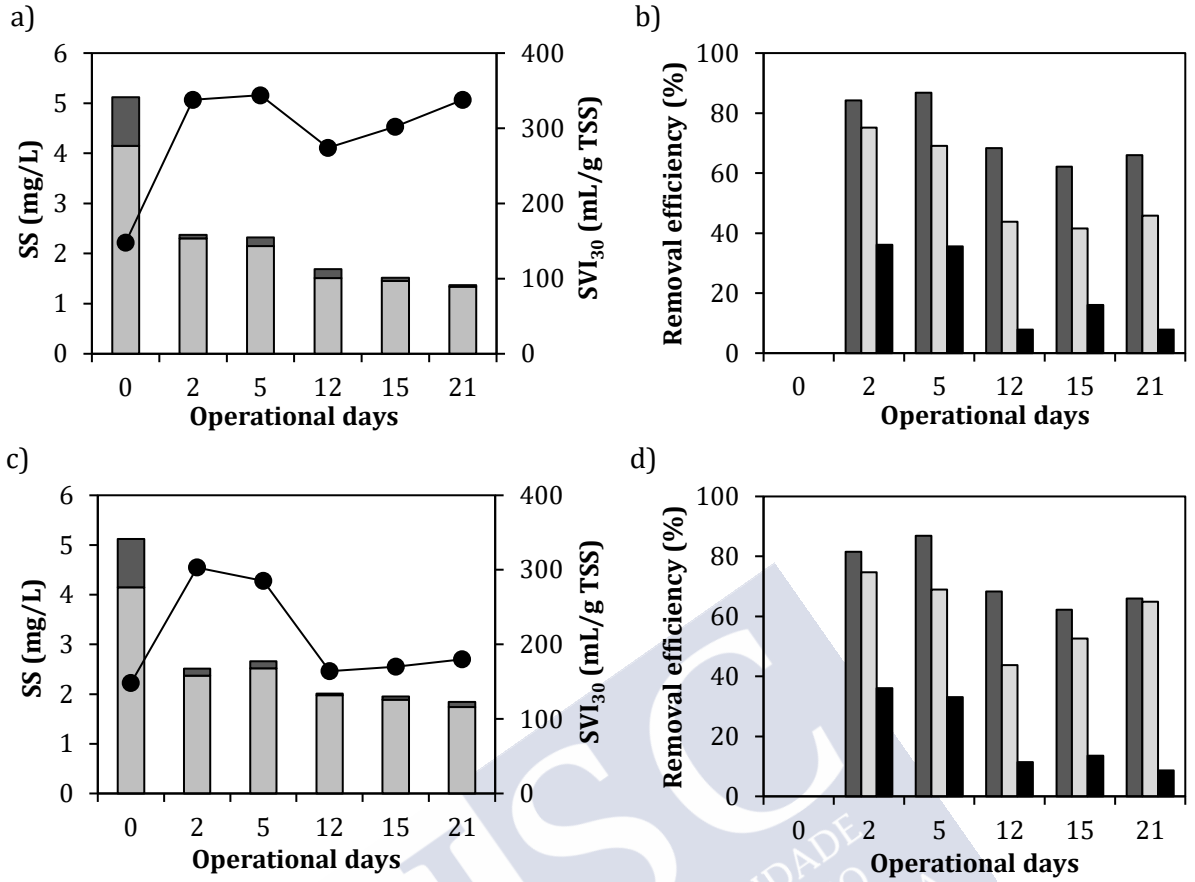

Figure 3.10: VSS (light grey), ISS (dark grey) and SVI_{30} (●) measurements in R1 (a) and R2 (c). COD (dark grey), nitrogen (light grey) and phosphorus (black) removal efficiencies of R1 (b) and R2 (d).

Previous research works have reported also the reactivation of the biological activity in a few days after long-term storage. Wan et al. (2014) stored heterotrophic granules (able to remove organic matter) at 4 °C in a 5 % NaCl solution during 187 days. Then, reactivation assays were performed in a SBR at different COD concentrations (2500, 1000 and 200 mg/L). They observed that heterotrophic activity was recovered after 15 days. Gao et al. (2012) cultivated granules able to remove organic matter and nitrogen in a fully aerobic reactor. They stored the granules during 8 months at different temperatures (-25 °C, 4 °C and room temperature) with different solutions (distilled water and a 400 mg/L solution of glucose). After 5 days of reactivation, both COD and ammonia removal were recovered. Yuan et al. (2012) stored granules (cultivated in a fully aerobic reactor) with tap water at room temperature during 6 and 12 months. They performed reactivation tests at different OLR and ammonia concentrations and SGV. They observed a recovery of 80 % of the activity after 3 days with the granules stored during 6 months. With the optimal operational conditions, granules stored during 12 months were recovered in 7 days. Wang et al. (2008) stored granules capable of removing organic matter and nitrogen during 7 months in tap water. To reactivate them, they stepwise increased the COD and ammonia concentration of the influent, and achieved the full recovery of heterotrophs and autotrophs in 16 and 11 days, respectively.

In the present study, the storage time (almost 2 years) was considerably larger than in the previous research works. Nevertheless, the heterotrophic and Ammonia Oxidising Bacteria (AOB) activities were recovered after 2 and 12 days, respectively, which agrees with the recovery times observed in the previous works. However, neither Nitrite Oxidising Bacteria (NOB) nor PAO activities were recovered, indicating that these bacteria might be more sensitive to long-term storage. In addition, in this case, the selection of different aeration strategies (pulsed and continuous) did not lead to a different recovery of the biomass.

3.5. CONCLUSIONS

Biomass granulation was possible in a SBR where COD, N and P were removed and the air was supplied in pulses (1 s ON / 2 s OFF) even at low COD concentrations in the feeding of 190 mg COD/L. The supply of the same volume of air (448 L/cycle) by pulsed aeration was found to be a better option to speed up the granulation process and achieve denser granules than continuous aeration, because the SGV applied (3.6 cm/s) was higher than without pulses (1.2 cm/s). In addition, this regime favoured the faster development of PAOs and the presence of GAOs.

Regarding the treatment performance, no significant differences in the COD, P and N removal efficiencies were measured in the pulsed and continuously aerated systems.

Required supplied air volume was significantly lower in the case of the pulsed regime than in the continuous one. However, the minimum SGV required was higher in the pulsed regime system than in the continuous one to guarantee the biomass suspension inside the reactor. The pulsed-aerated SBR was operated satisfactorily with a consumption of 0.73 $L_{air}/(L_{reactor} \cdot min)$.

After a long-term storage of almost 2 years, heterotrophic and AOB activities were recovered after 2 and 12 days of operation. Nevertheless, neither PAO nor NOB activities were recovered after 21 days. No significant differences regarding the aeration regime, in the process performance and biomass properties, were observed during the reactivation process.

3.6. REFERENCES

APHA/AWWA/WEF, 2012. Standard Methods for the Examination of Water and Wastewater. Stand. Methods 541. https://doi.org/ISBN 9780875532356

Belmonte, M., Vázquez-Padín, J.R., Figueroa, M., Franco, A., Mosquera-Corral, A., Campos, J.L., Méndez, R., 2009. Characteristics of nitrifying granules developed in an air pulsing SBR. Process Biochem. 44, 602–606. https://doi.org/10.1016/j.procbio.2009.02.019

Beun, J.J., Van Loosdrecht, M.C.M., Heijnen, J.J., 2002. Aerobic granulation in a sequencing batch airlift reactor. Water Res. https://doi.org/10.1016/S0043-1354(01)00250-0

Chen, Y., Jiang, W., Liang, D.T., Tay, J.H., 2007. Structure and stability of aerobic granules cultivated under different shear force in sequencing batch reactors. Appl. Microbiol. Biotechnol. 76, 1199–1208. https://doi.org/10.1007/s00253-007-1085-7

Chen, Y., Zhu, J.Y., Zhang, Z.M., Qin, Y., Yuan, S.C., 2017. Reactivation of hypersaline aerobic granular sludge after Low-temperature storage. Tecnol. y Ciencias del Agua 8, 61–70. https://doi.org/10.24850/j-tyca-2017-02-06

Coma, M., Puig, S., Balaguer, M.D., Colprim, J., 2010. The role of nitrate and nitrite in a granular sludge process treating low-strength wastewater. Chem. Eng. J. 164, 208–213. https://doi.org/10.1016/j.cej.2010.08.063

Daims, H., Lücker, S., Wagner, M., 2006. daime, a novel image analysis program for microbial ecology and biofilm research. Environ. Microbiol. https://doi.org/10.1111/j.1462-2920.2005.00880.x

De Kreuk, M.K., Heijnen, J.J., Van Loosdrecht, M.C.M., 2005. Simultaneous COD, nitrogen, and phosphate removal by aerobic granular sludge. Biotechnol. Bioeng. 90, 761–769. https://doi.org/10.1002/bit.20470

Devlin, T.R., di Biase, A., Kowalski, M., Oleszkiewicz, J.A., 2017. Granulation of activated sludge under low hydrodynamic shear and different wastewater characteristics. Bioresour. Technol. 224, 229–235. https://doi.org/10.1016/j.biortech.2016.11.005

Dobbeleers, T., D'aes, J., Miele, S., Caluwé, M., Akkermans, V., Daens, D., Geuens, L., Dries, J., 2017. Aeration control strategies to stimulate simultaneous nitrification-denitrification via nitrite during the formation of aerobic granular sludge. Appl. Microbiol. Biotechnol. 101, 6829–6839. https://doi.org/10.1007/s00253-017-8415-1

Franco, A., Roca, E., Lema, J.M., 2007. Enhanced Start-Up of Upflow Anaerobic Filters by Pulsation. J. Environ. Eng. 133, 186–190. https://doi.org/10.1061/(ASCE)0733-9372(2007)133:2(186)

Franco, A., Roca, E., Lema, J.M., 2006. Granulation in high-load denitrifying upflow sludge bed (USB) pulsed reactors. Water Res. 40, 871–880. https://doi.org/10.1016/j.watres.2005.11.044

Gao, D., Yuan, X., Liang, H., 2012. Reactivation performance of aerobic granules under different storage strategies. Water Res. 46, 3315–3322. https://doi.org/10.1016/j.watres.2012.03.045

Gao, D.W., Liu, L., Liang, H., 2013. Influence of aeration intensity on mature aerobic granules in sequencing batch reactor. Appl. Microbiol. Biotechnol. 97, 4213–4219. https://doi.org/10.1007/s00253-012-4226-6

Guimarães, L.B., Mezzari, M.P., Daudt, G.C., da Costa, R.H.R., 2017. Microbial pathways of nitrogen

removal in aerobic granular sludge treating domestic wastewater. J. Chem. Technol. Biotechnol. 92, 1756–1765. https://doi.org/10.1002/jctb.5176

He, Q., Zhang, W., Zhang, S., Wang, H., 2017a. Enanced nitrogen removal in an aerobic granular sequencing batch reactor performing simultaneous nitrification, endogenous denitrification and phosphorus removal with low superficial gas velocity. Chem. Eng. J. 326, 1223–1231. https://doi.org/10.1016/j.cej.2017.06.071

He, Q., Zhang, W., Zhang, S., Zou, Z., Wang, H., 2017b. Performance and microbial population dynamics during stable operation and reactivation after extended idle conditions in an aerobic granular sequencing batch reactor. Bioresour. Technol. 238, 116–121. https://doi.org/10.1016/j.biortech.2017.03.181

Jiang, X., Yuan, Y., Ma, F., Tian, J., Wang, Y., 2016. Enhanced biological phosphorus removal by granular sludge in anaerobic/aerobic/anoxic SBR during start-up period. Desalin. Water Treat. 57, 5760–5771. https://doi.org/10.1080/19443994.2015.1004114

Kuba, T., Murnleitner, E., Van Loosdrecht, M.C.M., Heijnen, J.J., 1996. A metabolic model for biological phosphorus removal by denitrifying organisms. Biotechnol. Bioeng. 52, 685–695. https://doi.org/10.1002/(SICI)1097-0290(19961220)52:6<685::AID-BIT6>3.3.CO;2-M

Li, A.J., Li, X.Y., Yu, H.Q., 2011. Granular activated carbon for aerobic sludge granulation in a bioreactor with a low-strength wastewater influent. Sep. Purif. Technol. https://doi.org/10.1016/j.seppur.2011.05.006

Lochmatter, S., Gonzalez-Gil, G., Holliger, C., 2013. Optimized aeration strategies for nitrogen and phosphorus removal with aerobic granular sludge. Water Res. 47, 6187–6197. https://doi.org/10.1016/j.watres.2013.07.030

Ni, B.J., Xie, W.M., Liu, S.G., Yu, H.Q., Wang, Y.Z., Wang, G., Dai, X.L., 2009. Granulation of activated sludge in a pilot-scale sequencing batch reactor for the treatment of low-strength municipal wastewater. Water Res. 43, 751–761. https://doi.org/10.1016/j.watres.2008.11.009

Tay, J.H., Liu, Q.S., Liu, Y., 2001. The effects of shear force on the formation, structure and metabolism of aerobic granules. Appl. Microbiol. Biotechnol. 57, 227–233. https://doi.org/10.1007/s002530100766

Tijhuis, L., van Loosdrecht, M.C.M., Heijnen, J.J., 1994. Formation and growth of heterotrophic aerobic biofilms on small suspended particles in airlift reactors. Biotechnol. Bioeng. https://doi.org/10.1002/bit.260440506

Vishniac, W., Santer, M., 1957. Thiobacilli. Bacteriol. Rev. 21, 195–213

Wan, C., Lee, D.J., Yang, X., Wang, Y., Lin, L., 2014. Saline storage of aerobic granules and subsequent reactivation. Bioresour. Technol. 172, 418–422. https://doi.org/10.1016/j.biortech.2014.08.103

Wan, J., Bessière, Y., Spérandio, M., 2009. Alternating anoxic feast/aerobic famine condition for improving granular sludge formation in sequencing batch airlift reactor at reduced aeration rate. Water Res. 43, 5097–5108. https://doi.org/10.1016/j.watres.2009.08.045

Wan, J., Mozo, I., Filali, A., Liné, A., Bessière, Y., Spérandio, M., 2011. Evolution of bioaggregate strength during aerobic granular sludge formation. Biochem. Eng. J. 58–59, 69–78. https://doi.org/10.1016/j.bej.2011.08.015

Wang, S.G., Gai, L.H., Zhao, L.J., Fan, M.H., Gong, W.X., Gao, B.Y., Ma, Y., 2009. Aerobic granules for low-strength wastewater treatment: Formation, structure, and microbial community. J. Chem. Technol. Biotechnol. 84, 1015–1020. https://doi.org/10.1002/jctb.2127

Wang, X., Zhang, H., Yang, F., Wang, Y., Gao, M., 2008. Long-term storage and subsequent reactivation of aerobic granules. Bioresour. Technol. 99, 8304–8309. https://doi.org/10.1016/j.biortech.2008.03.024

Wang, Z., van Loosdrecht, M.C.M., Saikaly, P.E., 2017. Gradual adaptation to salt and dissolved oxygen: Strategies to minimize adverse effect of salinity on aerobic granular sludge. Water Res. 124, 702–712. https://doi.org/10.1016/j.watres.2017.08.026

Wei, D., Qiao, Z., Zhang, Y., Hao, L., Si, W., Du, B., Wei, Q., 2013. Effect of COD/N ratio on cultivation of aerobic granular sludge in a pilot-scale sequencing batch reactor. Appl. Microbiol. Biotechnol. https://doi.org/10.1007/s00253-012-3991-6

Yilmaz, G., Lemaire, R., Keller, J., Yuan, Z., 2008. Simultaneous nitrification, denitrification, and phosphorus removal from nutrient-rich industrial wastewater using granular sludge. Biotechnol. Bioeng. 100, 529–541. https://doi.org/10.1002/bit.21774

Yuan, X., Gao, D., 2010. Effect of dissolved oxygen on nitrogen removal and process control in aerobic granular sludge reactor. J. Hazard. Mater. 178, 1041–1045. https://doi.org/10.1016/j.jhazmat.2010.02.045

Yuan, X., Gao, D., Liang, H., 2012. Reactivation characteristics of stored aerobic granular sludge using different operational strategies. Appl. Microbiol. Biotechnol. 94, 1365–1374. https://doi.org/10.1007/s00253-011-3660-1

Zhang, H., Dong, F., Jiang, T., Wei, Y., Wang, T., Yang, F., 2011. Aerobic granulation with low strength wastewater at low aeration rate in A/O/A SBR reactor. Enzyme Microb. Technol. 49, 215–222. https://doi.org/10.1016/j.enzmictec.2011.05.006

Zhong, C., Wang, Y., Li, Y., Lv, J., Hao, W., Zhu, J., 2014. The characteristic and comparison of denitrification potential in granular sequence batch reactor under different mixing conditions. Chem. Eng. J. 240, 589–594. https://doi.org/10.1016/j.cej.2013.10.078

Zhu, L., Zhou, J., Yu, H., Xu, X., 2015. Optimization of hydraulic shear parameters and reactor configuration in the aerobic granular sludge process. Environ. Technol. (United Kingdom) 36, 1605–1611. https://doi.org/10.1080/09593330.2014.998717

Chapter 4

Implementation of pulsed aeration in a fully aerobic AGS reactor

Summary

Two fully aerobic granular sludge reactors with cycles of 3 hours (167 min of aeration phase) were operated to treat wastewater with an average Organic Loading Rate (OLR) of 2 kg COD/(m^3·d). One of them was aerated by a pulsed regime (R1), with pulses of 1 s ON/2 s OFF, whereas the other was aerated in a continuous mode (R2). Two different Superficial Gas Velocities (SGV) of 3.6 (R1) and 1.2 cm/s (R2) were imposed for the same air volume per cycle (668 L/cycle).

The granulation time was almost the same in both reactors, being lower than a month. Nevertheless, the properties of the biomass were completely different. In R1, despite the low OLR, well-shaped granules (average diameter of 2.1 mm) with good settleability (SVI_5 of 70 mL/g TSS) were obtained. In R2, the growth of filamentous bacteria was observed, as a consequence of both the low OLR and SGV applied. However, filamentous bacteria acted as a carrier for granules, and the big aggregates (average diameter of 1 – 2 cm) formed in R2 still presented good settling properties (SVI_5 of 70 mL/g TSS). The removal efficiencies of both reactors were similar, being of 90 % and 65 % for COD and nitrogen, respectively.

The decrease in the frequency of the air pulses in R1 was also evaluated. The non-aeration time was increased from 2 to 4 and 6 s, to establish the lower value necessary to maintain the stability of the system. The pulsed regime with 1 s ON/4 s OFF allowed the maintenance of the performance and stability of the system. With this frequency, the air consumption was reduced a 40 % with respect to the frequency of 1 s ON/2 s OFF. However, the reduction to 1 s ON/6 s OFF provoked the destabilisation of the system due to the low dissolved oxygen concentration (lower than 2 mg O_2/L).

OUTLINE

Chapter 4 91

4.1. INTRODUCTION 93

4.2. OBJECTIVES 94

4.3. MATERIALS AND METHODS 94

4.3.1. Experimental set-up 94

4.3.2. Operational periods 95

4.3.3. Analytical methods 95

4.4. RESULTS AND DISCUSSION 96

4.4.1. Pulsed vs continuous aeration 96

4.4.2. Evaluation of the decrease of the air pulses frequency 101

4.4.3. Evaluation of the pulsed aeration with different feeding strategies 103

4.5. CONCLUSIONS 105

4.6. REFERENCES 106

4.1. INTRODUCTION

Most of the research studies of Aerobic Granular Sludge (AGS) technology have been based on cultivating aerobic granules by the use of anaerobic-fed Sequencing Batch Reactors (SBR), to select slow-growing organisms like Phosphate Accumulating Organisms (PAOs) or Glycogen Accumulating Organisms (GAOs). This system presents the advantage of lower energy consumption compared to fully aerobic systems and it enables the removal of phosphorus in addition to organic matter and nitrogen (de Kreuk and van Loosdrecht, 2004).

A fully aerobic SBR also allows the cultivation of AGS, by establishing an aerobic feast-famine regime. It has been reported that the AGS cultivated under fully aerobic conditions is less stable than that from anaerobic-fed reactors, since the fast consumption of organic matter on the outer layers of the granule promotes filamentous growth (Beun et al., 1999; Pronk et al., 2015). However, this configuration has been successfully applied to treat different kinds of wastewater.

Granules were successfully cultivated treating industrial wastewater with OLRs between 1 – 10 kg/(m^3·d) of Chemical Oxygen Demand (COD) (Farooqi and Basheer, 2017; Morales et al., 2013; Su and Yu, 2005; Truong et al., 2018). Stable granules with good settleability (Sludge Volume Index (SVI) values of 30 – 70 mL/g TSS) were obtained after 46 – 180 days. Besides, the AGS system presented a high removal capacity (75 – 99 % COD, 60 – 90 % N). In addition, the fully aerobic configuration was also used to treat low-strength municipal sewage (OLR of 0.6 – 1 kg COD/(m^3·d)). Although the granulation process lasted 300 days, the system was able to remove 85 – 95 % and almost 100 % of the COD and nitrogen from the fed wastewater (Ni et al., 2009).

This system has also been reported to be easier to control, as observed by Pishgar et al. (2019). They evaluated the performance of three SBRs with different operation modes. The first one included a short feeding followed by an anaerobic stage and aerobic reaction. In the middle of the aerobic phase, another short feeding took place followed by an anoxic period. The second option was a reactor with static anaerobic feeding, and the third one presented a short feeding followed by an aerobic reaction. They observed that the more complex the operation, the lower the degree of granule compactness, the higher the flocculent fraction of the AGS, and the more instability in maturation phase. The fully aerobic system was found to present the most stable operation, with lower washout of biomass.

Nevertheless, in fully aerobic AGS reactors, the aerobic phase represents a higher fraction of the operational cycle compared to anaerobic-fed systems. In addition, in fully-aerobic configuration, the shear stress is more necessary to assure the maintenance of stable granules. This implies higher energy consumption associated with aeration compared to anaerobic-fed reactors. Therefore, it is even more necessary to apply strategies to reduce the energy requirements during the aerobic stage if the fully aerobic configuration is used. In Chapter 3, a new strategy based on the use of pulsed aeration was successfully implemented in an anaerobic-fed reactor. It speeded up the granulation process and enabled the selection of PAOs and the formation of stable granules. However, this pulsed pattern has not been applied in fully aerobic AGS reactors.

4.2. OBJECTIVES

The aim of this Chapter was to study if the pulsed aeration strategy was advantageous in a fully aerobic reactor, as well as the comparison of the results with those obtained in Chapter 3, where the impact of pulsed aeration was studied in an anaerobic-fed aerobic granular system, enriched in PAOs. Once the granular biomass was established, another objective was to evaluate the effect of the reduction of the frequency of the air pulses.

4.3. MATERIALS AND METHODS

4.3.1. Experimental set-up

Two SBR with a working volume of 1.7 L and a height to diameter (H/D) ratio of 4 were operated in parallel (Figure 4.1). The volumetric exchange ratio was of 50 %, and the hydraulic retention time of 6 h.

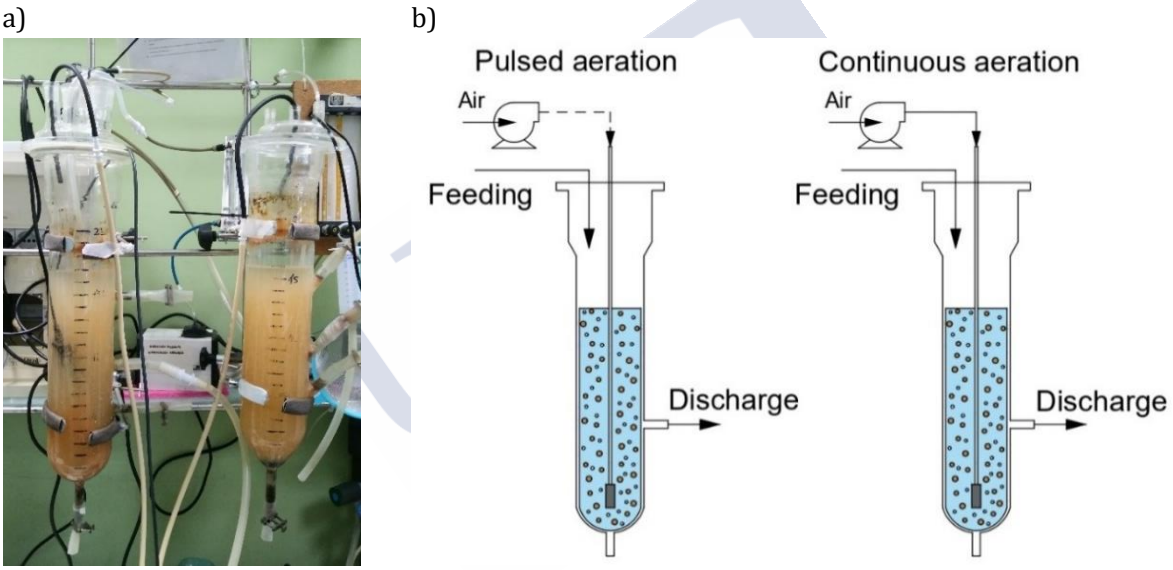

Figure 4.1: Photo of the experimental set-up (a) and scheme (b) of the aerobic granular sludge reactors.

The length of the operational cycle was 3 hours, distributed as follows: 5 min of feeding, 167 min of aerobic reaction, 7 – 1 minutes of settling and 1 – 7 minutes of effluent withdrawal (Table 4.1). The settling time was gradually decreased from 7 to 3 minutes (day 9) and finally 1 minute (day 29), in both reactors, to increase the hydraulic selection pressure. The time reduced in the settling phase was added to the withdrawal stage so that the aerobic phase was not affected by the change. Both reactors were fed from the top.

Table 4.1: Distribution of the SBR cycle phases.

				Feeding
				Aerobic phase
				Settling
				Withdrawal
5	167	7 – 1	1 – 7	Time (min)

The air was introduced by fine bubble diffusers located at the bottom of the reactors and it was supplied by the compressed air main line of the building. The airflow was firstly controlled by pressure reducers, located at the end of the mainline, and then the fine adjustment was made by a flowmeter. In both reactors, the working time of the aeration was regulated with electrovalves. The activation of the electrovalves and the pumps (for feeding and effluent discharge) in the different cycle phases was controlled by a Programmable Logic Controller (PLC, Siemens model S7-224CPU). In Reactor 1 (R1), air was provided in pulsed regime, consisting of air pulses of 1 second followed by 2 seconds without aeration (1 s ON / 2 s OFF). In Reactor 2 (R2), the air was supplied in a continuous regime during the aerobic phase. The same volume of air per cycle was provided in both reactors (668 L/cycle). However, the airflow and the Superficial Gas Velocity (SGV) were different, with values of 12 L/min and 3.6 cm/s, respectively, in R1, and 4 L/min and 1.2 cm/s, respectively, in R2.

4.3.2. Operational periods

Both reactors were operated in parallel for 110 days. Afterwards, R2 was stopped and in R1 two reductions of the air pulses frequency were tested, with an operational time of 20 days for each reduction (Table 4.2).

Table 4.2: Strategy of air pulses frequency reduction in R1.

Operational days	Aeration regime	Airflow (L/min)*	Total air volume per cycle (L)	Air saving (%)**
0 – 110	1 s ON/2 s OFF	12	668	0
111 – 130	1 s ON/4 s OFF	12	401	40
131 – 150	1 s ON/6 s OFF	12	286	57

*Values corresponding to each air pulse.

** Determined using as a basis the total air volume per cycle applied in the granulation stage (668 L).

The reactors were seeded with 1.7 L of activated sludge from a Wastewater Treatment Plant (WWTP) located in Galicia (NW of Spain), characterised by an SVI_{30} of 387 mL/g TSS, and solids concentrations of 2.47 g TSS/L and 2.15 g VSS/L.

Both reactors were initially fed with synthetic wastewater, containing 500 mg COD/L and 52.3 mg NH_4^+-N/L. A volume of 1 mL of trace solution was added per litre of feeding. The composition of the simulated wastewater was: 1.20 g/L Na·Ac·$3H_2O$, 0.20 g/L NH_4Cl, 0.10 g/L K_2HPO_4, 0.03 g/L KH_2PO_4, 0.04 g/L $MgSO_4$, 0.07 g/l $CaCl_2$·H2O and 0.019 g/L KCl. The trace solution composition was prepared according to (Vishniac and Santer, 1957). From day 62 onwards until the end of the experimental period, the concentration of the feeding increased to feed 750 mg COD/L and 69.7 mg NH_4^+-N /L. The applied loading rate was initially of 1.8 kg COD/(m^3·d), and after the increase of the feeding concentration (day 62) it increased to 2.3 kg COD/(m^3·d).

4.3.3. Analytical methods

Analytical determination of ammonium (NH_4^+), nitrite (NO_2^-), nitrate (NO_3^-), soluble COD, total suspended solids (TSS) and volatile suspended solids (VSS) concentrations and SVI was

carried out according to the standard methods (APHA/AWWA/WEF, 2012). Cation and anion concentrations were determined by ion chromatography with an Advanced Compact IC system (861, Metrohm).

The density of the granules was measured with dextran blue following the methodology proposed by Beun et al. (2002). The morphology and size distribution of the granules was measured with a stereomicroscope (Stemi 2000-C, Zeiss) and using an image analysis procedure (Tijhuis et al., 1995). The pH was measured with an electrode (52-03, Crison Instruments, USA) and the dissolved oxygen concentration was measured with an on-line probe (Hach® HQ40D).

Full description of the analytical methods and the calculations is provided in Chapter 2.

4.4. RESULTS AND DISCUSSION

4.4.1. Pulsed vs continuous aeration

Granulation process and effect of the OLR

The settleability of the biomass rapidly improved during the first operational days in both reactors (SVI_5 reduced from 398 on day 0 to 190 and 160 mL/g TSS on day 7 in R1 and R2, respectively). After 8 days of operation, the first granules were observed in both reactors with particle diameter of 0.55 and 0.47 mm in R1 and R2, respectively (Figure 4.2.a,d). After 27 days of operation, the biomass was in form of small granules with a particle diameter of 0.40 and 0.39 mm in R1 and R2, respectively.

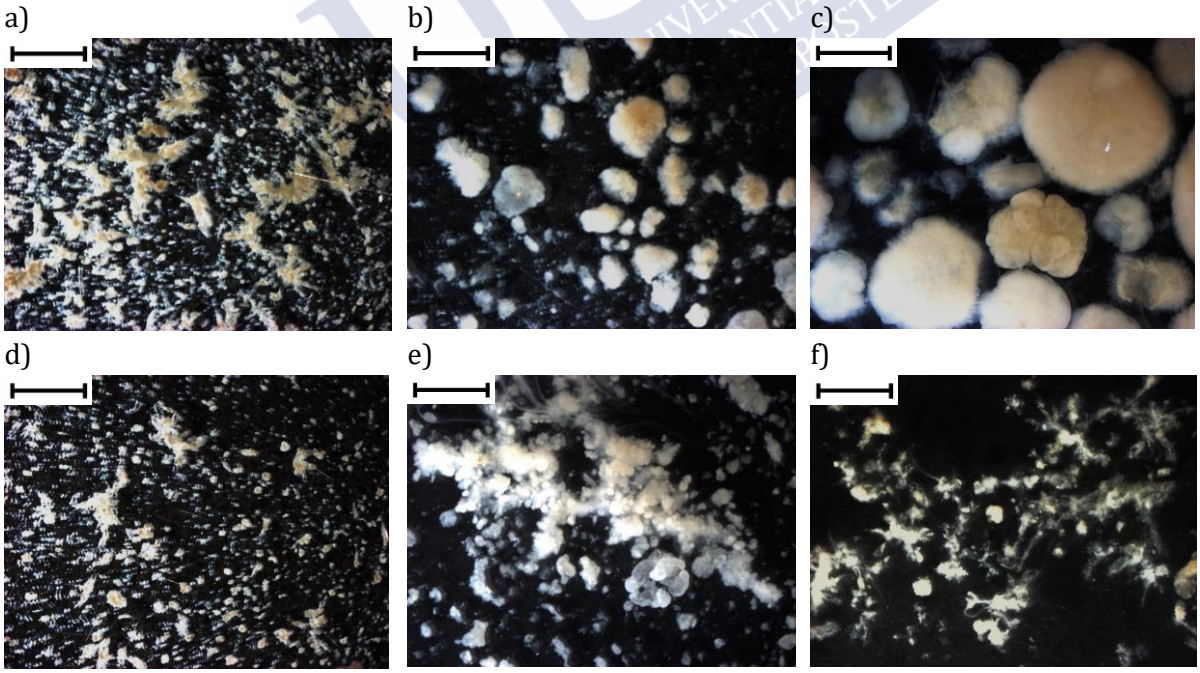

Figure 4.2: Images of the granules of R1 on days 8 (a), 50 (b) and 97 (c), and R2 on days 8 (d), 50 (e), 97 (f). The size bar indicates 2 mm.

The first settling time reduction (from 7 to 3 min, day 9) did not have a big impact on the biomass, but after the second one (from 3 to 1 min, day 29) there was a loss of flocculent biomass in both reactors and a consequent improvement of the settleability. In R1, granules increased their size (0.63 mm on day 36), while the biomass concentration remained almost constant (1.3 g VSS/L on day 51) (Figure 4.3.a). In R2, the increase of the size of the granules was also observed (0.57 mm on day 36), but on day 50 the growth of filamentous bacteria occurred, probably because of the low applied OLR. Small granules with a particle diameter of 0.58 mm coexisted with aggregates of filamentous bacteria with an average diameter of 8.19 mm (Figure 4.2.e). However, the settling properties were not severely affected (SVI_5 of 37 mL/g TSS on day 51, Figure 4.3.b). Filamentous bacteria seemed to act as a carrier over which the granules grew and remained entrapped. Aqeel et al. (2016) also observed the formation of structures with filaments integrated and enmeshed in granules, which presented good settling properties and caused biomass accumulation in the reactor. In R1, this kind of aggregates was not observed, the biomass was only in form of well-shaped granules with a particle diameter of 0.91 mm (Figure 4.2.b).

Previous research works have also reported the presence of filamentous bacteria and the difficulties to achieve granular biomass in fully aerobic reactors when the applied OLR was lower than 2 kg COD/(m^3·d). Tay et al. (2004) tested different OLRs (1, 2, 3 and 4 kg COD/(m^3·d)) and they did not observe granules with 1 and 2 kg COD/(m^3·d). Li et al. (2011) observed the formation of small aggregates, but not a 100 % granular system with an OLR of 0.8 kg COD/(m^3·d) and a SGV of 1.18 cm/s. Wang et al. (2009) obtained a system constituted by a mixture of aggregates and filamentous bacteria with an OLR of 1.05 – 1.68 kg COD/(m^3·d) and a SGV of 2.5 cm/s. Kim et al. (2008) needed to increase the OLR from 1.76 to 2.52 and 2.84 kg COD/(m^3·d) to granulate the biomass. Nevertheless, if the OLR is low, the increase of the SGV can help to maintain the integrity of the granules. That was the difference between R1 and R2. In R1, the SGV of 3.6 cm/s was high enough to avoid the growth of filamentous bacteria, whereas in R2 the SGV of 1.2 cm/s was not enough. Thus, the combination of low OLR and SGV caused the loss of stability of the granules and the appearance of filamentous bacteria in R2.

After the increase of the OLR (day 62), in R1 there was an increase of the biomass concentration from 1.8 g VSS/L on day 64 to 6.7 g VSS/L on day 86, and big granules with an average diameter of 2.1 mm (day 97) were observed until the end of the operation (Figure 4.2.c). The settleability of the biomass was good, with SVI_5 values around 70 mL/g TSS, and a density of 30 g TSS/$L_{granule}$ on day 114. In R2, the filamentous aggregates increased their size to 1 – 2 cm (impossible to determine with the microscope) with the increase of the OLR. Besides, the biomass concentration increased up to 5 g TSS/L on day 71. However, after 90 days of operation, the big filamentous structures broke, and a small number of granules was observed in addition to small filamentous aggregates (Figure 4.2.f). The increase of the OLR might have helped to reduce the size of the filamentous structures and favoured the growth of granules. At the end of the operation, the density of the biomass in R2 (19 g TSS/$L_{granule}$ on day 114) was lower than in R1, but the settleability was similar, also with SVI_5 values around 70 mL/g TSS.

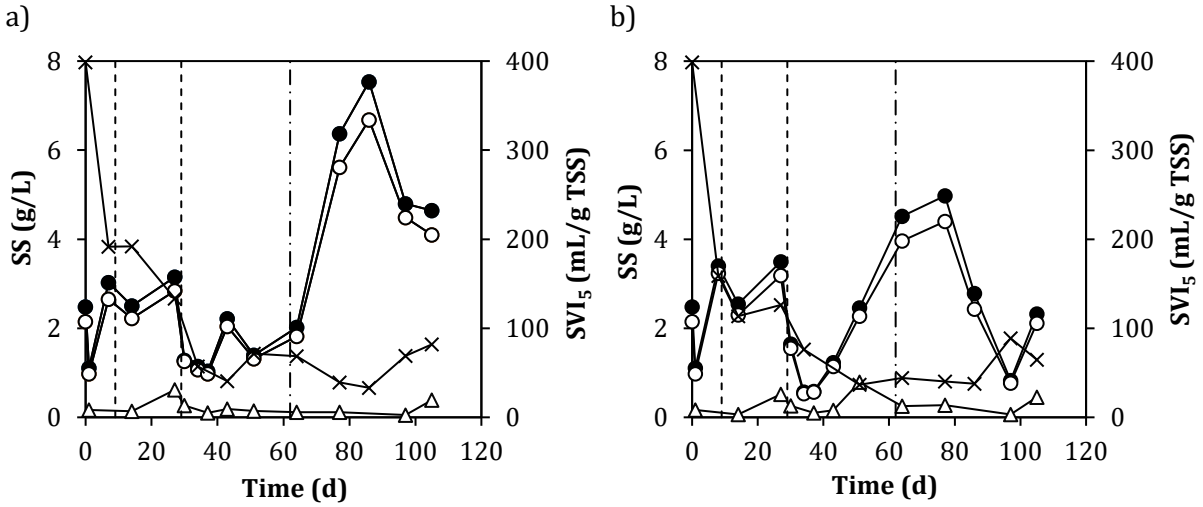

Figure 4.3: Evolution of VSS (●) and TSS (○) inside the reactors, and TSS of the effluent (△) and SVI_5 (x) in R1 (a) and R2 (b). The discontinuous lines (- -) indicate the reductions of the settling time. The discontinuous line (- · -) indicates the change in the OLR.

Therefore, there were no big differences regarding the appearance of the first aggregates, being necessary almost the same time in the pulsed and continuous aerated reactor to achieve a granular system (27 days). Nevertheless, due to the low applied OLR, in R2 the overgrowth of filamentous bacteria occurred whereas in R1 it did not. For the same volume of air per cycle applied, the pulsed aeration helped to avoid the growth of filamentous bacteria, promoted the growth of denser granules, and favoured the biomass retention, leading to higher concentrations inside the reactor. This was due to the higher hydrodynamic stress applied during the air pulses, because of the higher SGV. The same behaviour was observed in Chapter 3 with anaerobic-fed granular reactors. In addition, the use of pulsed aeration allowed the achievement of a stable granular system at a low OLR (1.8 kg COD/(m^3·d)) in R1, whereas with continuous aeration (R2) higher OLRs were needed.

Reactors performance

The COD removal efficiencies in both reactors were higher than 90 % during their entire operation (Figure 4.4.a,b), and they were not affected by the increase of the loading rate. The feast – famine regime was observed in both reactors from almost the beginning of the operational period (around day 6), with a feast duration of 30 – 40 min.

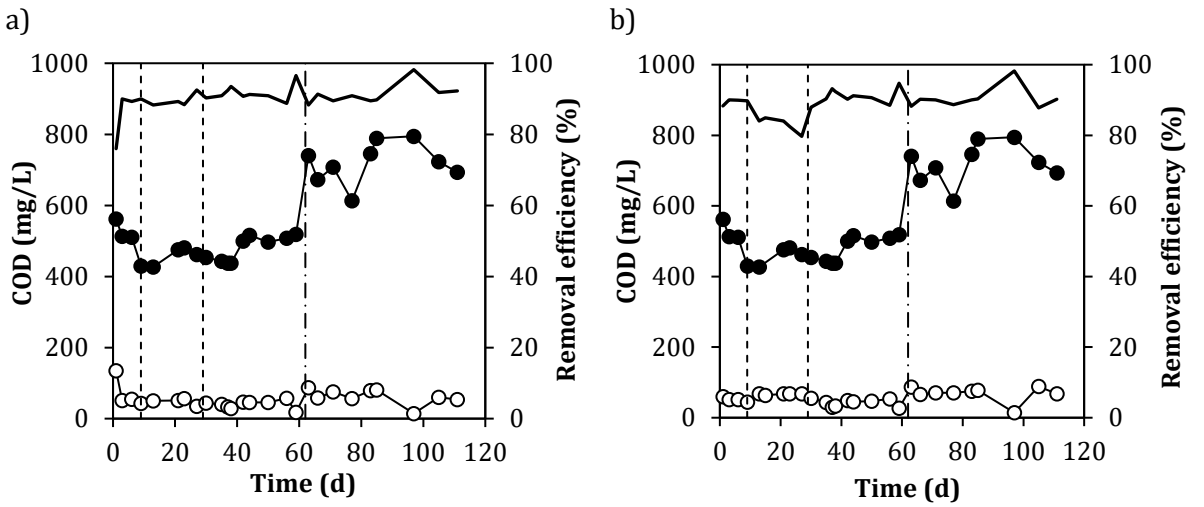

Figure 4.4: COD concentration of the influent (●), effluent (○), and removal efficiency (-) in R1 (a) and R2 (b). The discontinuous lines (- -) indicate the reductions of the settling time. The discontinuous line (- · -) indicates the change in the OLR.

Regarding the nitrogen removal, after 21 days a 100 % of ammonia oxidation was observed in both reactors with nitrite accumulation (Figure 4.5.a,b). During the next days, the nitrite concentration in the effluent gradually decreased and nitrate concentration increased. The increase of nitrate concentration was a bit faster in R1, indicating a faster development of Nitrite Oxidising Bacteria (NOB) activity. From day 35 onwards the effects of the settling time reduction were observed. As a consequence of a lower biomass content in both reactors, the ammonia concentration of the effluent increased, and nitrate concentration was reduced. The profiles of the nitrogen species seemed to indicate that Ammonia Oxidising Bacteria (AOB) were partially washed out from the system, whereas there was a higher washout of NOB.

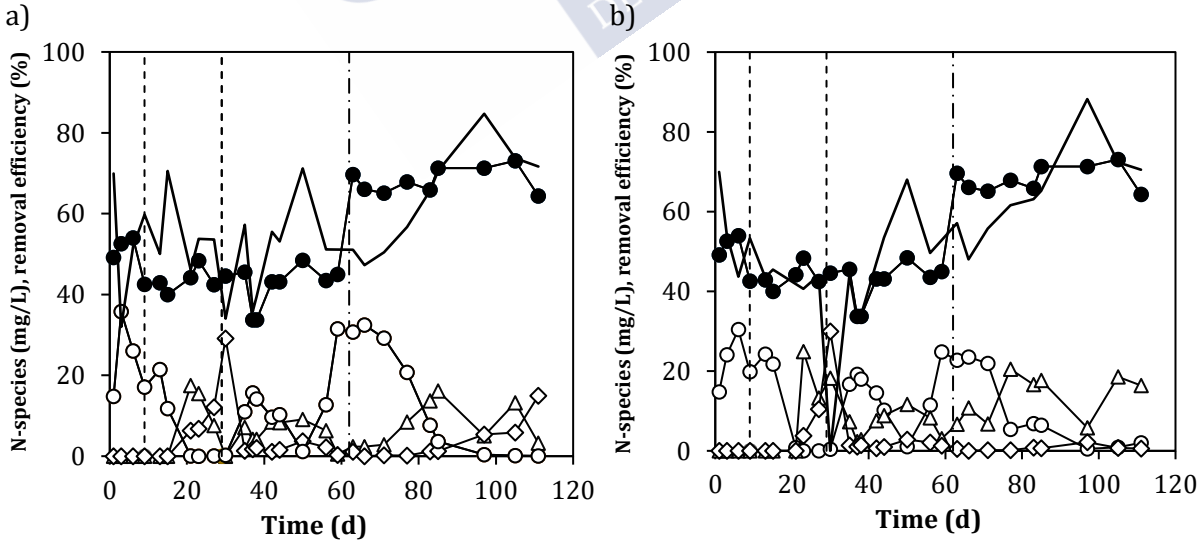

Figure 4.5: Ammonia concentration of the influent (●), ammonia (○), nitrite (△) and nitrate concentration (◇) of the effluent, and total nitrogen removal efficiency (-) in R1 (a) and R2 (b).

The increase of the nitrogen loading rate on day 62 provoked an increase of the ammonia concentration in the effluent, but it was gradually reduced until zero. In R1, from day 85 onwards, the nitrate concentration of the effluent gradually increased, whereas in R2, it was no more detected. Nevertheless, the total nitrogen removal efficiencies were similar in both reactors (70 – 80 %).

The differences observed in the operation of the two reactors were evaluated by the monitoring of respective operational cycles at day 110 (Figure 4.6). Regarding COD consumption, the COD uptake was a bit faster in R1, with a feast period shorter (30 min) than R2 (40 min). In addition, the ammonia oxidation was faster in R1, leading to the complete depletion of ammonia after 150 minutes of the cycle, and the production of both nitrite and nitrate. In R2 the ammonia removal was not complete, and only nitrite was detected. Nevertheless, the specific ammonia oxidation activity was a bit higher in R2 (0.111 mg NH_4^+-N/(g VSS·min) than in R1 (0.073 mg NH_4^+-N/(g VSS·min)). The higher conversion velocity in R1 was due to a higher biomass concentration inside the reactor, being of 4.1 g VSS/L in R1 and 2.1 g VSS/L in R2 (day 110). In both reactors, denitrification was observed during the first minutes of the cycle, when the dissolved oxygen concentration was low. Then, during the famine phase, a reduction of 5 – 10 mg/L of total nitrogen occurred, indicating a small fraction of denitrifying activity.

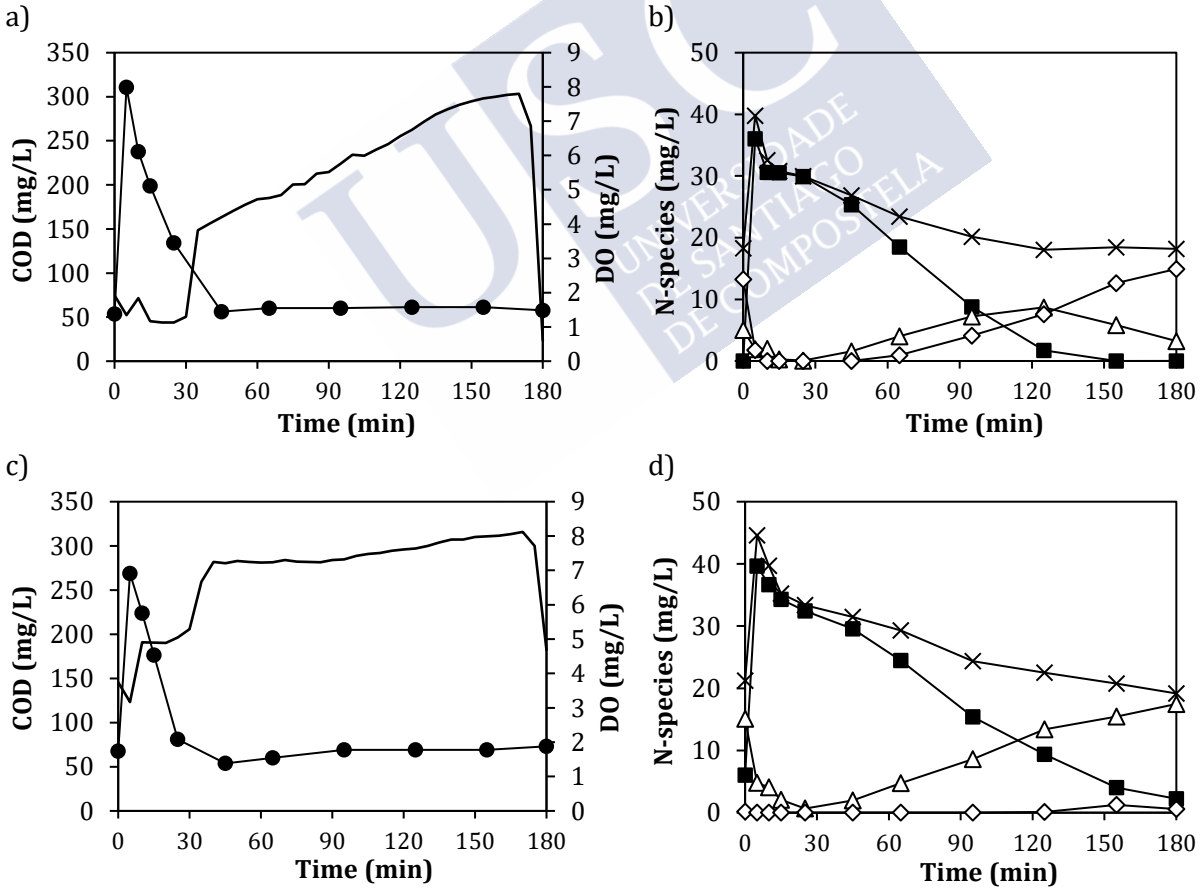

Figure 4.6: Cycle measurements on day 110 of R1 (a, b) and R2 (c, d). The profiles of COD (●), dissolved oxygen (-), ammonia (■), nitrite (△), nitrate (◇) and total nitrogen (x) are represented.

4.4.2. Evaluation of the decrease of the air pulses frequency

After the operation of R1 to compare its performance with R2, two reductions of the frequency of the air pulses were made, in order to evaluate the minimum frequency needed to maintain the stability of the system.

After the first increase of the non-aeration time from 2 to 4 seconds (1 s ON/4 s OFF), a small fraction of flocculent biomass appeared (Figure 4.7.a), the SVI_5 increased from 70 to 105 mL/g TSS (Figure 4.8.a) and the density slightly decreased to 29 mL/g TSS.

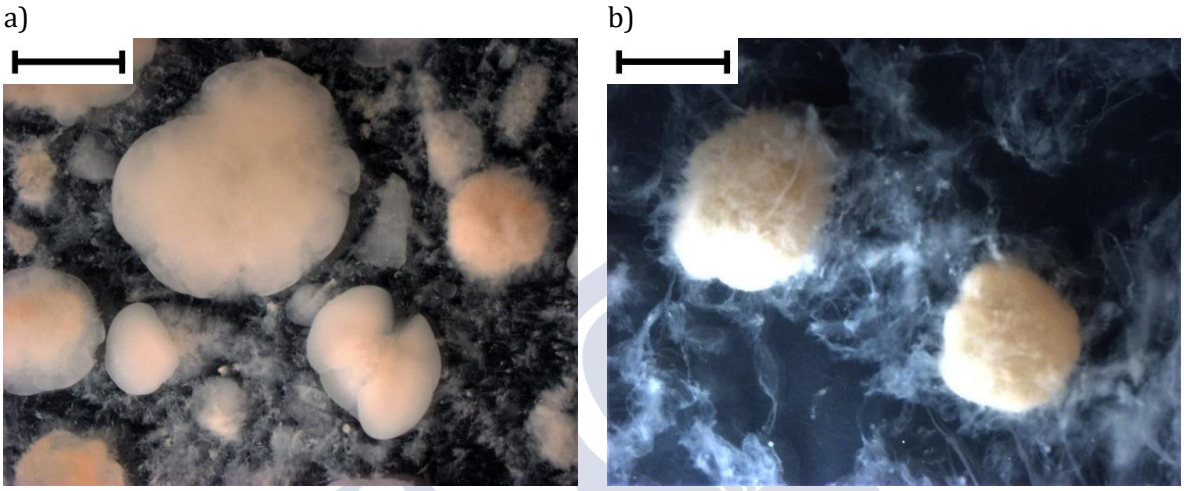

Figure 4.7: Images of the granules of R1 after the first (a) and second (b) reduction of the air pulses frequency. The size bar indicates 2 mm.

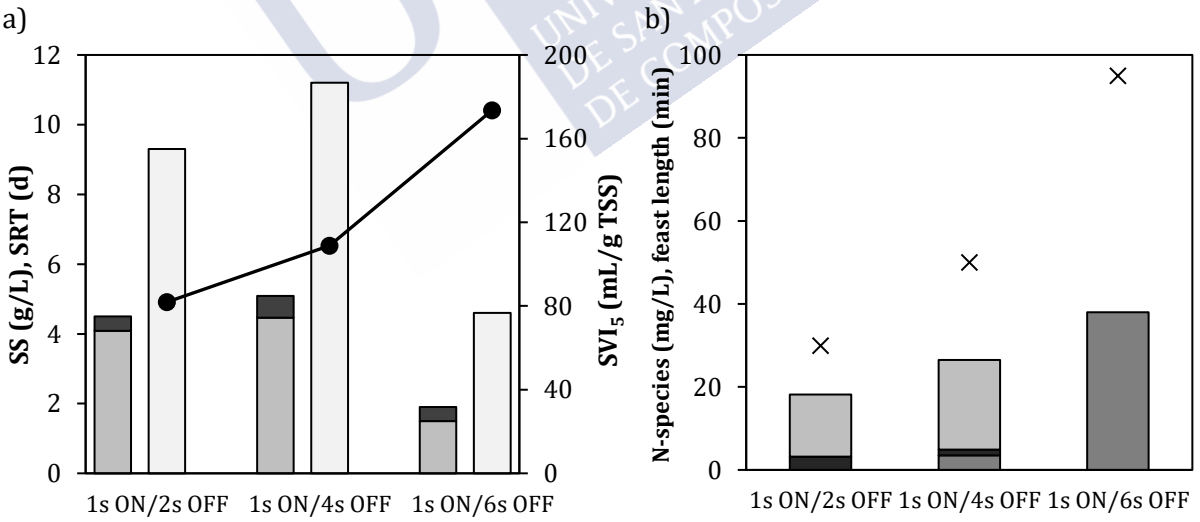

Figure 4.8: (a) VSS (dark grey), ISS (Inorganic Suspended Solids, black), SRT (light grey) and SVI_5 (●) during the tested air pulses frequencies. (b) Ammonia (dark grey), nitrite (black) and nitrate (light grey) concentration of the effluent and feast duration (x) during the tested air pulses frequencies.

The feast phase increased, being of 50 min (Figure 4.8.a). Besides, the specific ammonia oxidation rate decreased in comparison to the previous pulse frequency (0.073 mg NH_4^+-N/(g VSS·min) and 0.031 mg NH_4^+-N/(g VSS·min) with a non-aeration time of 2 s and 4 s, respectively)

(Figure 4.7.b). This was probably due to the lower oxygen concentration in the reactor during the famine, being of 3 – 4 mg O_2/L. Nevertheless, the ammonia was almost completely oxidised at the end of the cycle, and nitrite was completely oxidised to nitrate, indicating a better activity of NOB. During the famine phase (from minute 50 onwards), the total nitrogen concentration remained stable, indicating the absence of denitrifying activity. Both the COD and nitrogen removal efficiencies of 92 and 65 %, respectively, were similar to the previous operational stage. The SRT was a bit higher, which could favour the development of nitrifying bacteria, especially NOBs.

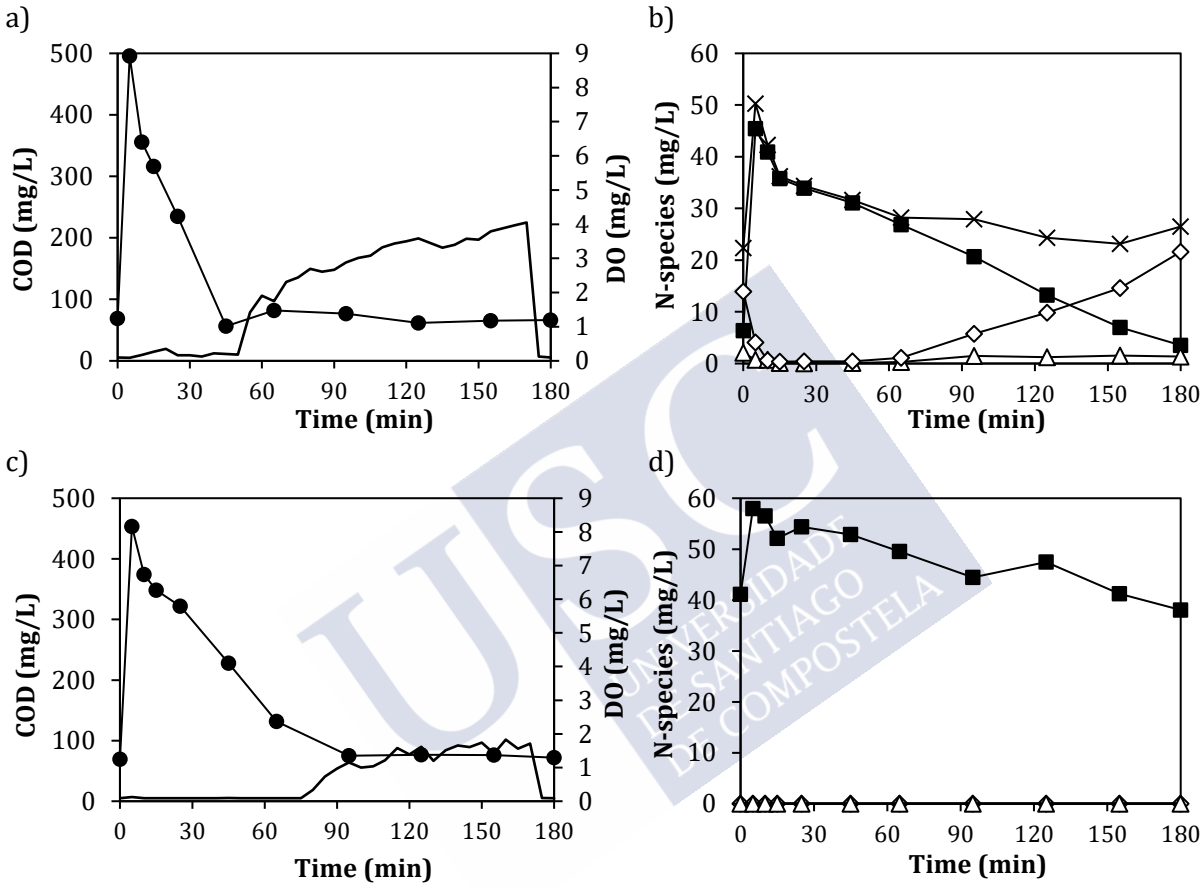

Figure 4.9: Cycle measurements of R1 after the first (a, b) and second (c, d) pulses frequency reduction. The profiles of COD (●), dissolved oxygen (-), ammonia (■), nitrite (△), nitrate (◇) and total nitrogen (x) are represented.

The second increase of the non-aeration time did affect both the biomass and the performance of the reactor. The low oxygen supply caused a longer feast phase, which was increased to 90 min (Figure 4.9.c) and lower oxygen concentrations inside the reactor during the famine phase (lower than 2 mg O_2/L). The feast phase represented the 50 % of all the aeration time, whereas it has been reported that it should be a 20 – 40 % to achieve stable granules (Liu and Tay, 2008; López-Palau et al., 2012). The loss of the balance between the feast and famine phases caused the overgrowth of filamentous bacteria and the disintegration of granules (Figure 4.7.b). As a consequence, the settleability of the biomass worsened, and the SVI_5 increased to 174 mL/g TSS. This caused a big washout of biomass and a considerable decrease of the solids concentration inside the reactor to 1.9 g TSS/L (Figure 4.8.a). The SRT was diminished to 4.6 days and led to a drastic reduction of AOB and NOB activity inside the reactor. Consequently, the

nitrogen removal efficiencies dropped to 47 %, being the biomass growth the main removal pathway (Figure 4.9.d).

Dissolved oxygen concentrations lower than 4 – 5 mg O_2/L during the famine phase have been reported to provoke the disintegration of aerobic granules cultivated in fully aerobic granular systems. Mosquera-Corral et al. (2005) observed the loss of stability of aerobic granules cultivated at 100 % saturation of dissolved oxygen when it was reduced to 40 % of saturation. Sturm and Irvine (2008) observed a decrease of the biomass concentration inside the reactor, the growth of filamentous bacteria and the increase of the feast phase with dissolved oxygen concentrations lower than 5 mg O_2/L.

Therefore, with a non-aeration time of 4 s, there were no big differences compared to the non-aeration time of 2 s. Nevertheless, with the increase to 6 s of non-aeration, the low air supply increased the feast duration and the dissolved oxygen concentration inside the reactor decreased below 2 mg O_2/L during the feast. This caused the disintegration of granules, hindered the nitrifying activity and worsened the effluent quality.

4.4.3. Evaluation of the pulsed aeration with different feeding strategies

The application of pulsed aeration demonstrated to have advantages in both an anaerobic-fed (Chapter 3) and a fully aerobic reactor (this Chapter). These advantages are compared for both systems in the next sections.

Granulation process and properties of the granules

Regarding the granulation time, the differences between pulsed and continuous aeration were bigger in the anaerobic-fed system than in the fully-aerobic one. In the anaerobic-fed system, the pulsed aeration reduced the time necessary to granulate the biomass in almost 21 % (Chapter 3). The granulation time with pulsed aeration was of 38 days, whereas with continuous aeration it was of 48 days (Table 4.3). However, in the fully aerobic system, the use of pulsed aeration did not lead to differences regarding the granulation time. Granules appeared after less than one month of operation, almost at the same time in both the pulsed and continuous aerated reactor. The differences in the granulation time of both systems were attributed to the different growth rates of PAOs and heterotrophic bacteria, being lower in the case of PAOs (the maximum growth rate at 20 °C is 1 d^{-1} for PAOs and 2 d^{-1} for heterotrophic bacteria, according to Henze et al. (2000)). Thus, since in the fully aerobic system the granulation process was faster, no differences between continuous and pulsed aeration were observed.

Table 4.3: Granules properties with pulsed and continuous aeration in the two AGS configurations.

Type of feeding	Aeration regime	Granulation time (days)	SVI_5 / SVI_{30} (mL/g TSS)	Density (mL/g TSS)	Aspect of the biomass
Anaerobic	Pulsed	38	45/45	90	Well-shaped granules
	Continuous	48	50/50	70	Well-shaped granules
Short feeding	Pulsed	27	50/50	30	Well-shaped granules
	Continuous	27	50/50	20	Filamentous aggregates

The differences in shape and aspect of the granules were more important in the fully aerobic system than in the anaerobic-fed comparing continuous and pulsed aeration (Table 4.3). Once granular biomass was obtained, the applied hydrodynamic stress by aeration (expressed in terms of SGV) was more important to maintain well-shaped granules in the fully aerobic system. It was especially important when applying low loading rates, to control the growth of filamentous bacteria. When the system was enriched in slow-growing organisms that anaerobically uptake COD, their capacity of forming aggregates was enough to assure the stability of the granular system, which made hydrodynamic stress in the aerobic phase less relevant.

Therefore, in the anaerobic-fed system, the pulsed regime was useful to reduce the time necessary for the granulation process but did not influence the biomass properties at long-term operation. For this configuration, the pulsed aeration could be more focused on the reduction of the air consumption, reducing the air supply during the cycle compared to a continuous system. In the fully aerobic reactor, the use of pulsed aeration presented more advantages at long-term operation, promoting the growth of smooth and dense granules. In this case, the pulsed aeration could help to provide a higher hydrodynamic stress in the media with the same air supply as the continuous aeration.

Modifications of the pulsed aeration

Two modifications of the pulsed aeration regime were made: the reduction of the airflow maintaining the same pulses frequency (Chapter 3) and the decrease of the frequency of the pulses with the same airflow (Chapter 4) (Table 4.4).

Table 4.4: Tested modifications of the air pulses.

Type of feeding	Pulse frequency	Airflow (L/min)	Air consumed (L/cycle)	Air saving (%)*	Aeration time (min)
Anaerobic	1 s ON/2 s OFF	12	448	0	112
		4	149	66.7	112
		1.7	89	80.1	112
Short feeding	1 s ON/2 s OFF	12	668	0	167
	1 s ON/4 s OFF	12	401	40.0	167
	1 s ON/6 s OFF	12	286	57.1	167

* Determined using as a basis the total air volume per cycle applied in the granulation stage.

The first difference that can be observed between both systems is that the oxygen requirements were different depending on the type of feeding, being lower in the case of the anaerobic-fed reactor for the same cycle length (Table 4.4). In the fully aerobic system, oxygen is needed to uptake the COD and oxidise the ammonia, whereas in the anaerobic-fed system it is only needed during the aerobic stage for ammonia oxidation. Therefore, the reduction of the air pulses frequency and/or airflow, might not have the same effect in both configurations.

In the anaerobic-fed reactor, the best scenario was obtained operating under an airflow of 4 L/min. It was possible to save 66.7 % of the supplied air compared to continuous aeration, while the performance of the reactor and the biomass properties remained stable. In the fully aerobic configuration, the second scenario was also the best option, with a pulse frequency of 1 s ON/4 s OFF, which allowed an air saving of 40 %.

The causes that led to the instability of the system were different depending on the anaerobic-fed system or the fully aerobic one. In the anaerobic-fed system, the reduction of the airflow was studied. In this case, the low airflow tested (1.7 L/min) was not enough to resuspend and mix the biomass. It was a limitation related to the hydrodynamics of the system. In the fully-aerobic system, the increase of the non-aeration time did not suppose problems in terms of mixture inside the reactor. The instability of the system was due to the lack of enough dissolved oxygen to allow the biological reactions, and promoting the growth of filamentous bacteria.

Although two modifications of the pulse were studied (decrease of the airflow and pulses frequency), they were tested in reactors operated with different configurations, and each modification was studied separately. Further research is needed to study: (1) the implementation of both modifications at the same time to find the best scenario for the operation of the AGS reactor and (2) the implementation of the same strategy in the two reactor configurations to study the differences under the same conditions.

4.5. CONCLUSIONS

First aggregates appeared at the same time using continuous and pulsed aeration in aerobic granular reactors with short feeding (fully aerobic reaction). With continuous aeration, the overgrowth of filamentous bacteria occurred, due to a combination of low applied OLR (lower than 2 kg COD/(m^3·d)) and SGV (1.2 cm/s). Maintaining the same volume of air per cycle, the pulsed aeration allowed applying a SGV of 3.6 cm/s. This avoided the growth of filamentous bacteria and led to the production of well-shaped granules with good settleability and higher biomass concentrations inside the reactor.

The achieved removal efficiencies were almost the same with pulsed and continuous aeration, being of 95 and 65 % for COD and nitrogen, respectively. With continuous aeration, only AOB activity was detected, whereas with pulsed aeration there was also NOB activity.

The reactor with pulsed aeration maintained its stability after the increase of the non-aeration time from 2 to 4 s. Nevertheless, when it was increased to 6 s the system lost its stability due to the low concentrations of dissolved oxygen (lower than 2 mg O_2/L).

The pulsed aeration speeded up the granulation process in an anaerobic-fed AGS reactor (Chapter 3), but did not suppose big differences on the overall performance at long term operation with respect to continuous aeration. In fully aerobic systems, the pulsed aeration did not reduce the granulation time, but was crucial to maintain the stability of the granules at long-term operation working with low OLRs (below 2 kg COD/(m^3·d)).

4.6. REFERENCES

APHA/AWWA/WEF, 2012. Standard Methods for the Examination of Water and Wastewater. Stand. Methods 541. https://doi.org/ISBN 9780875532356

Aqeel, H., Basuvaraj, M., Hall, M., Neufeld, J.D., Liss, S.N., 2016. Microbial dynamics and properties of aerobic granules developed in a laboratory-scale sequencing batch reactor with an intermediate filamentous bulking stage. Appl. Microbiol. Biotechnol. https://doi.org/10.1007/s00253-015-6981-7

Beun, J.J., Hendriks, A., Van Loosdrecht, M.C.M., Morgenroth, E., Wilderer, P.A., Heijnen, J.J., 1999. Aerobic granulation in a sequencing batch reactor. Water Res. 33, 2283–2290. https://doi.org/10.1016/S0043-1354(98)00463-1

Beun, J.J., Van Loosdrecht, M.C.M., Heijnen, J.J., 2002. Aerobic granulation in a sequencing batch airlift reactor. Water Res. https://doi.org/10.1016/S0043-1354(01)00250-0

de Kreuk, M.K., van Loosdrecht, M.C.M., 2004. Selection of slow growing organisms as a means for improving aerobic granular sludge stability. Water Sci. Technol. 49, 9–17

Farooqi, I.H., Basheer, F., 2017. Treatment of Adsorbable Organic Halide (AOX) from pulp and paper industry wastewater using aerobic granules in pilot scale SBR. J. Water Process Eng. 19, 60–66. https://doi.org/10.1016/j.jwpe.2017.07.005

Henze, M., Gujer, W., Mino, T., Loosdrecht, M. van, 2000. Activated Sludge Models ASM1, ASM2, ASM2d and ASM3 IWA Scientific and Technical Report No.9, Journal of Chemical Information and Modeling. https://doi.org/10.1017/CBO9781107415324.004

Kim, I.S., Kim, S.M., Jang, A., 2008. Characterization of aerobic granules by microbial density at different COD loading rates. Bioresour. Technol. 99, 18–25. https://doi.org/10.1016/j.biortech.2006.11.058

Li, A.J., Li, X.Y., Yu, H.Q., 2011. Granular activated carbon for aerobic sludge granulation in a bioreactor with a low-strength wastewater influent. Sep. Purif. Technol. 80, 276–283. https://doi.org/10.1016/j.seppur.2011.05.006

Liu, Y.Q., Tay, J.H., 2008. Influence of starvation time on formation and stability of aerobic granules in sequencing batch reactors. Bioresour. Technol. https://doi.org/10.1016/j.biortech.2007.03.011

López-Palau, S., Pinto, A., Basset, N., Dosta, J., Mata-Álvarez, J., 2012. ORP slope and feast-famine strategy as the basis of the control of a granular sequencing batch reactor treating winery wastewater. Biochem. Eng. J. https://doi.org/10.1016/j.bej.2012.08.002

Morales, N., Figueroa, M., Fra-Vázquez, A., Val Del Río, A., Campos, J.L., Mosquera-Corral, A., Méndez, R., 2013. Operation of an aerobic granular pilot scale SBR plant to treat swine slurry. Process Biochem. 48, 1216–1221. https://doi.org/10.1016/j.procbio.2013.06.004

Mosquera-Corral, A., De Kreuk, M.K., Heijnen, J.J., Van Loosdrecht, M.C.M., 2005. Effects of oxygen concentration on N-removal in an aerobic granular sludge reactor. Water Res. 39, 2676–2686. https://doi.org/10.1016/j.watres.2005.04.065

Ni, B.J., Xie, W.M., Liu, S.G., Yu, H.Q., Wang, Y.Z., Wang, G., Dai, X.L., 2009. Granulation of activated sludge in a pilot-scale sequencing batch reactor for the treatment of low-strength municipal wastewater.

Water Res. 43, 751–761. https://doi.org/10.1016/j.watres.2008.11.009

Pishgar, R., Dominic, J.A., Sheng, Z., Tay, J.H., 2019. Influence of operation mode and wastewater strength on aerobic granulation at pilot scale: Startup period, granular sludge characteristics, and effluent quality. Water Res. 160, 81–96. https://doi.org/10.1016/j.watres.2019.05.026

Pronk, M., Abbas, B., Al-zuhairy, S.H.K., Kraan, R., Kleerebezem, R., van Loosdrecht, M.C.M., 2015. Effect and behaviour of different substrates in relation to the formation of aerobic granular sludge. Appl. Microbiol. Biotechnol. https://doi.org/10.1007/s00253-014-6358-3

Sturm, B.S.M.S., Irvine, R.L., 2008. Dissolved oxygen as a key parameter to aerobic granule formation. Water Sci. Technol. https://doi.org/10.2166/wst.2008.393

Su, K.Z., Yu, H.Q., 2005. Formation and characterization of aerobic granules in a sequencing batch reactor treating soybean-processing wastewater. Environ. Sci. Technol. 39, 2818–2827. https://doi.org/10.1021/es048950y

Tay, J.-H., Pan, S., He, Y., Tay, S.T.L., 2004. Effect of Organic Loading Rate on Aerobic Granulation. II: Characteristics of Aerobic Granules. J. Environ. Eng. https://doi.org/10.1061/(asce)0733-9372(2004)130:10(1102)

Tijhuis, L., Huisman, J.L., Hekkelman, H.D., van Loosdrecht, M.C.M., Heijnen, J.J., 1995. Formation of nitrifying biofilms on small suspended particles in airlift reactors. Biotechnol. Bioeng. 47, 585–595. https://doi.org/10.1002/bit.260470511

Truong, H.T.B., Nguyen, P. Van, Nguyen, P.T.T., Bui, H.M., 2018. Treatment of tapioca processing wastewater in a sequencing batch reactor: Mechanism of granule formation and performance. J. Environ. Manage. 218, 39–49. https://doi.org/10.1016/j.jenvman.2018.04.041

Vishniac, W., Santer, M., 1957. Thiobacilli. Bacteriol. Rev. 21, 195–213

Wang, S.G., Gai, L.H., Zhao, L.J., Fan, M.H., Gong, W.X., Gao, B.Y., Ma, Y., 2009. Aerobic granules for low-strength wastewater treatment: Formation, structure, and microbial community. J. Chem. Technol. Biotechnol. 84, 1015–1020. https://doi.org/10.1002/jctb.2127

USC
UNIVERSIDADE
DE SANTIAGO
DE COMPOSTELA

Chapter 5

Influence of the OLR and salt fluctuations on AGS stability treating fish-canning wastewater

Summary

The development and stability of Aerobic Granular Sludge (AGS) was studied in a fully aerobic SBR treating fish-canning wastewater with variable salt concentrations (4.97 – 13.45 g NaCl/L) and Organic Loading Rates (OLR, 1.80 – 6.65 kg $COD_S/(m^3 \cdot d)$). The granulation process was completed after 90 days and the biomass was stable against the variable feeding composition. As a consequence, high Sludge Retention Times (SRT), up to 15.2 days were achieved, which helped the retention of nitrifying organisms and increased the nitrogen removal efficiencies up to 80 %. The COD_S removal was also high (75 – 80 %), with feast phase lengths of 10 – 40 min (total reaction time of 167 – 227 min), depending on the applied OLR.

The performance of the fully aerobic configuration (R1) was compared with the operation of an anaerobic-fed reactor (R2, study from Campo, 2018), operated in the same conditions but with different feeding strategy. The granulation process was faster in R2 (100 % granules on day 34) but more instability episodes were observed with the fluctuations of the feeding. In addition, the low retention of the biomass (SRT < 6 days) did not allow the growth of nitrifying bacteria in R2, so that the nitrogen removal efficiencies were low (40 %) compared to R1. However, the presence of an anaerobic feeding phase increased the organic matter removal efficiency (80 – 90 %), which was slightly higher than in R1 with a fully aerobic phase. In terms of AGS properties, an anaerobic feeding phase is not beneficial, but it enables the production of a better-quality effluent.

OUTLINE

Chapter 5 109
5.1. INTRODUCTION 111
5.2. OBJECTIVES 112
5.3. MATERIALS AND METHODS 112
5.3.1. Experimental set-up 112
5.3.2. Operational conditions 113
5.3.3. Analytical and microbiological methods 114
5.4. RESULTS AND DISCUSSION 115
5.4.1. Operation of the reactor 115
5.4.2. Evaluation of different feeding strategies to treat saline industrial wastewater 123
5.5. CONCLUSIONS 126
5.6. REFERENCES 127

5.1. INTRODUCTION

Spain is the main producer of canned fish of the European Union. Among all the production of the food-processing industry, almost the 40 % corresponds to the processing and canning of seafood. In particular, the fish-canning sector of Galicia (NW region of Spain) represents the 85 % of the Spanish production value of fish and shellfish-canning. Galicia is the main exporter, amounting to over the 30 % of the total volume of exported canned seafood (ANFACO-CECOPESCA, 2019). There are 60 factories in Galicia, including the three most important ones of Spain, all of them located in coastal areas. As a consequence of the strong activity of this sector, large volumes of wastewater are produced, which put pressure over the Galician marine ecosystems. Therefore, it is necessary an efficient treatment of these effluents, which are characterised by high complexity and variability. Globally, they contain high concentrations of organic matter and nutrients. In addition, the considerable and variable salt concentrations (2 – 36 g NaCl/L) represent the main constraints for the activities of the microbial populations in the biological treatments such as nitrification, denitrification and phosphorus removal (Cristóvaõ et al., 2015; Kargi, 2002; Moussa et al., 2006).

The lower footprint of Aerobic Granular Sludge (AGS) systems in comparison with conventional activated sludge processes (Bengtsson et al., 2018), makes them an attractive alternative to treat industrial wastewater. This is of special importance in the fish-canning sector as these industries normally lack space to expand their facilities and to implement wastewater treatments. However, the instability of the granular sludge is one of the reported bottlenecks that hinder the application of AGS technologies. The growth of flocculent biomass, in addition to other factors such as organic overloads or the presence of toxic compounds like salts, is one of the causes responsible for granules integrity loss (Figueroa et al., 2015; Meunier et al., 2016). The maintenance of the stability of the aggregates is, even today, of major concern for AGS systems application (Bassin et al., 2019; Val Del Río et al., 2013; Wagner et al., 2015; Zhao et al., 2012). In order to protect the discharge bodies, it is crucial for the fish canneries to produce treated effluents fulfilling the emission limits in terms of solids, organic matter and nutrient concentrations. For this reason, the assessment of different reactor configurations to avoid and/or limit the instability episodes is of interest.

As explained in the previous chapters, two cycle configurations are preferentially used to produce AGS: (1) a fully aerobic; or (2) an anaerobic feeding followed by an aerobic reaction phase. Franca et al. (2017) studied the stability of AGS in a Sequencing Batch Reactor (SBR) provided with an initial anaerobic feeding phase, performed in static conditions or plug-flow regime. They found that the latter was better to cope with industrial wastewater variability and to minimise the AGS instability. Thwaites et al. (2017) compared the use of long anaerobic and split anaerobic-aerobic feedings and concluded that the formation and stability of AGS did not require a conventional long anaerobic feeding. In Chapter 4, a fully aerobic configuration was compared with an anaerobic feeding followed by an aerobic stage. However, there are no studies comparing these two configurations treating saline industrial wastewater.

Salt concentration of the treated effluents, in special if they are variable, is recognised as one of the reasons for the AGS instability. Although many research studies were conducted to evaluate the effects of high salinity on granule formation and biological activity inhibition (Bassin et al., 2011; Pronk et al., 2014; van den Akker et al., 2015; Wang et al., 2017), few studies investigated the influence of the variable salinity on biological processes and metabolic activities (Sun et al.,

2010; Wang et al., 2009). Moreover, most of these studies have been performed with synthetic media and under a gradual increase of salinity. Studies that address the issue of granule stability under fluctuations (increase and decrease) of salinity and Organic Loading Rate (OLR) have not been found yet in case of industrial wastewater treatment.

5.2. OBJECTIVES

The present study aimed to evaluate the performance of an AGS reactor at laboratory scale, operated in fully aerobic conditions (short feeding) to treat fish-canning wastewater with variable composition in terms of salt and organic matter concentrations. Its performance was compared with an AGS reactor with anaerobic feeding followed by aerobic reaction.

5.3. MATERIALS AND METHODS

5.3.1. Experimental set-up

An AGS laboratory-scale Sequencing Batch Reactor (SBR) with a working volume of 1.7 L (inner diameter of 9 cm) was started-up (Figure 5.1). It was fed from the top and the Volume Exchange Ratio (VER) of each cycle was 50 %. A fine bubble diffuser located at the bottom of the reactor supplied an airflow of 7 L/min, corresponding to a Superficial Gas Velocity (SGV) of 2 cm/s. A Programme Logic Controller (PLC) Siemens model S7-224 CPU was used to control the activation of the different devices (pumps, valves, aeration system) and the length of the cycle. The reactor was operated at 25 ± 1 °C in a thermostatic room and without pH control.

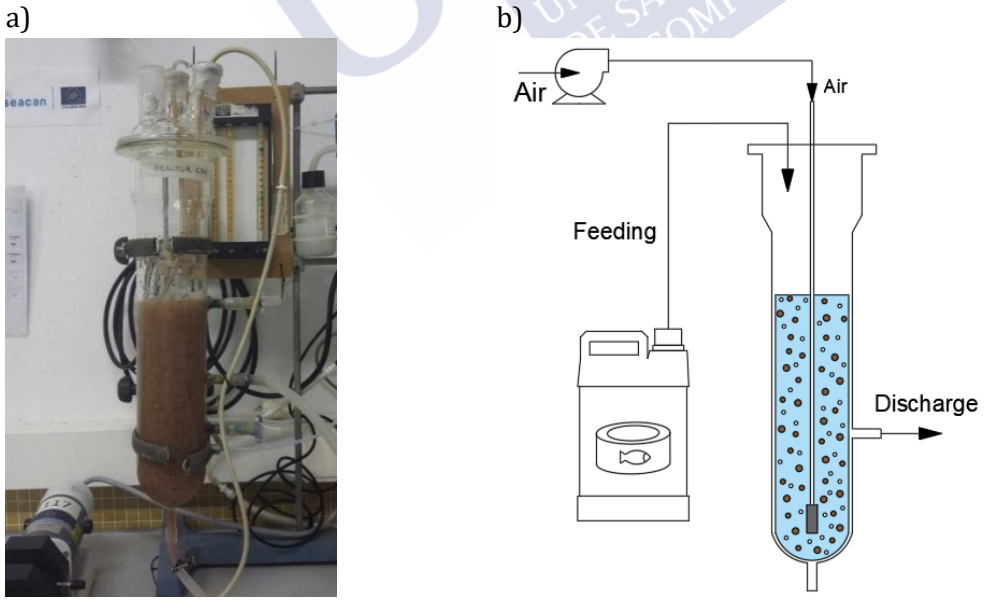

Figure 5.1: Photo of the experimental set-up (a) and scheme (b) of the aerobic granular sludge reactor.

Each operational cycle included a short feeding phase, an aerobic phase where the biological reactions took place, a short settling stage and the withdrawal of the effluent (Table 5.1). Two cycle lengths were tested: 3 h (days 0 – 92) and 4 h (days 93 – 226). The cycle length was changed to 4 h to increase the length of the aerobic phase, promote the retention of biomass inside the reactor and the growth of autotrophic bacteria.

Table 5.1: Scheme of the SBR cycle.

				Feeding
				Aerobic phase
				Settling
				Withdrawal
5	167 – 227	7 – 1	1 – 7	Time (min)

In order to increase the hydraulic selection pressure and improve the properties of the biomass, the settling time was gradually reduced, starting with 7 minutes (days 0 – 15), 4 minutes (days 15 – 22) and 1 minute (from day 23 onwards). With this reduction, a higher settling velocity was imposed to the granules to remain in the system, being 1.33 m/h (7 min of settling), 2.33 m/h (4 min) and 9.30 m/h (1 min).

5.3.2. Operational conditions

The reactor was operated for 226 days treating wastewater from a fish cannery located on the coast of Galicia (NW region of Spain). The industrial wastewater was collected from the outflow stream of the DAF (Dissolved Air Flotation) system in operation in the factory. The different batches of collected wastewater were fully characterised, due to their significant fluctuations associated with the seasonal variations of the processed fish products. The operational period was divided into four stages, depending on the salt concentration of the collected batches of wastewater (Table 5.2).

In Stages II and III, two sub-stages were defined on days 93 and 152, respectively. In Stage II the cycle length was extended from 3 h (Sub-Stage II.a) to 4 h (Sub-Stage II.b), resulting in an increase of the Hydraulic Retention Time (HRT) from 6.0 h to 8.0 h. During Stage III, the applied OLR was diminished from 4.3 kg/(m^3·d) of soluble COD (COD_S) (Sub-Stage III.a) to 1.8 kg COD_S/(m^3·d) (Sub-Stage III.b) associated to a decrease of the Chemical Oxygen Demand (COD) concentration in the fed wastewater.

The SBR was inoculated with 875 mL of flocculent sludge, enriched in microorganisms adapted to high saline conditions, collected from a SBR installed in the fish cannery. The inoculum contained 3.23 g TSS/L and 2.27 g VSS/L and presented poor settling properties, with an SVI_{30} (Sludge Volume Index) of 300 mL/g TSS.

Table 5.2: Characteristics of the wastewater and operational conditions in the different stages.

Stage	**I**	**II.a**	**II.b**	**III.a**	**III.b**	**IV**
Days	**0-35**	**36-92**	**93-102**	**103-151**	**152-182**	**183-226**
Wastewater composition						
Salinity (g NaCl/L)	10.19 ± 0.63	5.48 ± 0.59		13.33 ± 0.57		4.97 ± 0.52
SO_4^{2-} (mg/L)	386.97 ± 108.58	240.87 ± 58.50		208.29 ± 134.77	263.47 ± 158.26	137.27 ± 75.55
COD_T (g/L)	2.17 ± 0.24	1.21 ± 0.23		1.81 ± 0.32	0.78 ± 0.15	0.91 ± 0.08
COD_S (g/L)	1.71 ± 0.22	0.96 ± 0.07		1.47 ± 0.24	0.61 ± 0.12	0.84 ± 0.07
TOC (mg/L)	537.60 ± 75.07	236.15 ± 36.27		506.72 ± 83.46	156.10 ± 54.64	300.06 ± 36.42
TN (mg/L)	99.13 ± 13.81	129.86 ± 12.43		106.78 ± 18.09	77.36 ± 6.95	107.64 ± 53.23
NH_4^+-N (mg/L)	90.55 ± 7.77	102.13 ± 27.03		86.08 ± 14.32	72.56 ± 7.15	105.80 ± 5.30
PO_4^{3-}-P (mg/L)	22.34 ± 9.10	15.78 ± 4.89		20.17 ± 9.55	10.55 ± 2.23	13.65 ± 3.45
TSS (mg/L)	237.51 ± 49.07	108.13 ± 35.79		194.18 ± 98.47	160.71 ± 60.52	58.66 ± 26.45
VSS (mg/L)	167.77 ± 27.30	81.69 ± 33.98		120.92 ± 83.75	78.59 ± 39.50	41.50 ± 25.19
pH (-)	5.89 ± 0.35	7.37 ± 0.26		6.64 ± 0.30	7.34 ± 0.31	7.46 ± 0.16
Operational conditions						
HRT (h)	6.0	6.0*	8.00*	8.00		8.00
OLR ($kg\ COD_S/(m^3 \cdot d)$)	6.65 ± 0.83	3.22 ± 0.32		4.28 ± 0.70**	1.80 ± 0.38**	2.37 ± 0.16
NLR ($kg\ NH_4^+$-N $/(m^3 \cdot d)$)	0.37 ± 0.03	0.45 ± 0.07		0.25 ± 0.22	0.22 ± 0.02	0.31 ± 0.02
PLR ($g\ PO_4^{3-}$-P$/(m^3 \cdot d)$)	88.7 ± 36.5	53.15 ± 42.45		59.7 ± 29.8	31.6 ± 7.0	38.9 ± 9.9
COD/N (g/g)	19.28 ± 3.52	7.62 ± 1.60		17.66 ± 4.05	8.39 ± 2.40	7.93 ± 0.55

*Stage II had two sub-stages corresponding to the modification of the HRT due to the change in the operational cycle length from 3 to 4 h.

**Stage III had two sub-stages corresponding to the shift of OLR provoked by the change of the industrial wastewater composition, mainly of COD concentration.

5.3.3. Analytical and microbiological methods

The concentrations of ammonium (NH_4^+), nitrite (NO_2^-), nitrate (NO_3^-), Total Nitrogen (TN), phosphate (PO_4^{3-}), Total Suspended Solids (TSS) and Volatile Suspended Solids (VSS) and Sludge Volume Index (SVI) were measured according to the Standard Methods (APHA/AWWA/WEF, 2012). The concentrations of chloride (Cl^-), sulphate (SO_4^{2-}) and sodium (Na^+) ions were determined through Ion Chromatography (Metrohm 816 Advanced Compact IC). The COD concentration was determined according to Soto et al. (1989) taking into account the different salt concentrations of the sample. Total COD concentration (COD_T) was determined in the sample without filtering, whereas COD_S was measured in samples filtered through 0.45 μm pore size filters. The pH was measured with an electrode (Crison Instruments GLP22), as well as the conductivity (HACH Lange 50 60, Platinum Cell). The dissolved oxygen concentration was

measured with an on-line probe (HACH HQ40D). The proteins concentration was determined according to the Lowry's method (Lowry et al., 1951), and the carbohydrates concentration with the anthrone method (Dreywood, 1946).

The density of the granules was measured with dextran blue following the methodology proposed by Beun et al. (2002). The morphology and size distribution of the granules was measured with a stereomicroscope (Stemi 2000-C, Zeiss) and using an image analysis procedure (Tijhuis et al., 1994). Extracellular Polymeric Substances (EPS) were extracted from granular biomass samples following the thermic method described by Le-Clech et al. (2006). Proteins and carbohydrates of the extracted EPS were characterised as previously described.

The main microbial populations were identified by FISH analysis. The targeted organisms were AOB (NSO190) and NOB (NTI3). Detailed information about the probes is given in Chapter 2. Fluorescence signals were observed under an epifluorescence microscope (Axioskop 2, Zeiss, Germany) and registered with an acquisition system (Coolsnap, Roper Scientific Photometrics). To determine the relative abundance of each population, referred to the total bacteria domain, at least 15 images from each sample were taken and processed using DAIME software (Daims et al., 2006).

A detailed description of the analytical methods, as well as the calculations, is provided in Chapter 2.

5.4. RESULTS AND DISCUSSION

5.4.1. Operation of the reactor

Granulation process under variable composition feeding

The biomass used as inoculum (from the fish-canning treatment plant) was supposed to be acclimated to the wastewater conditions and for this reason, it was chosen despite its bad settling properties (SVI_{30} of 300 mL/g TSS) (Figure 5.2.a). As a consequence of the imposed selection pressure, the settling properties of the biomass were rapidly improved and the first aggregates were observed on day 22 of operation (Figure 5.3.a).

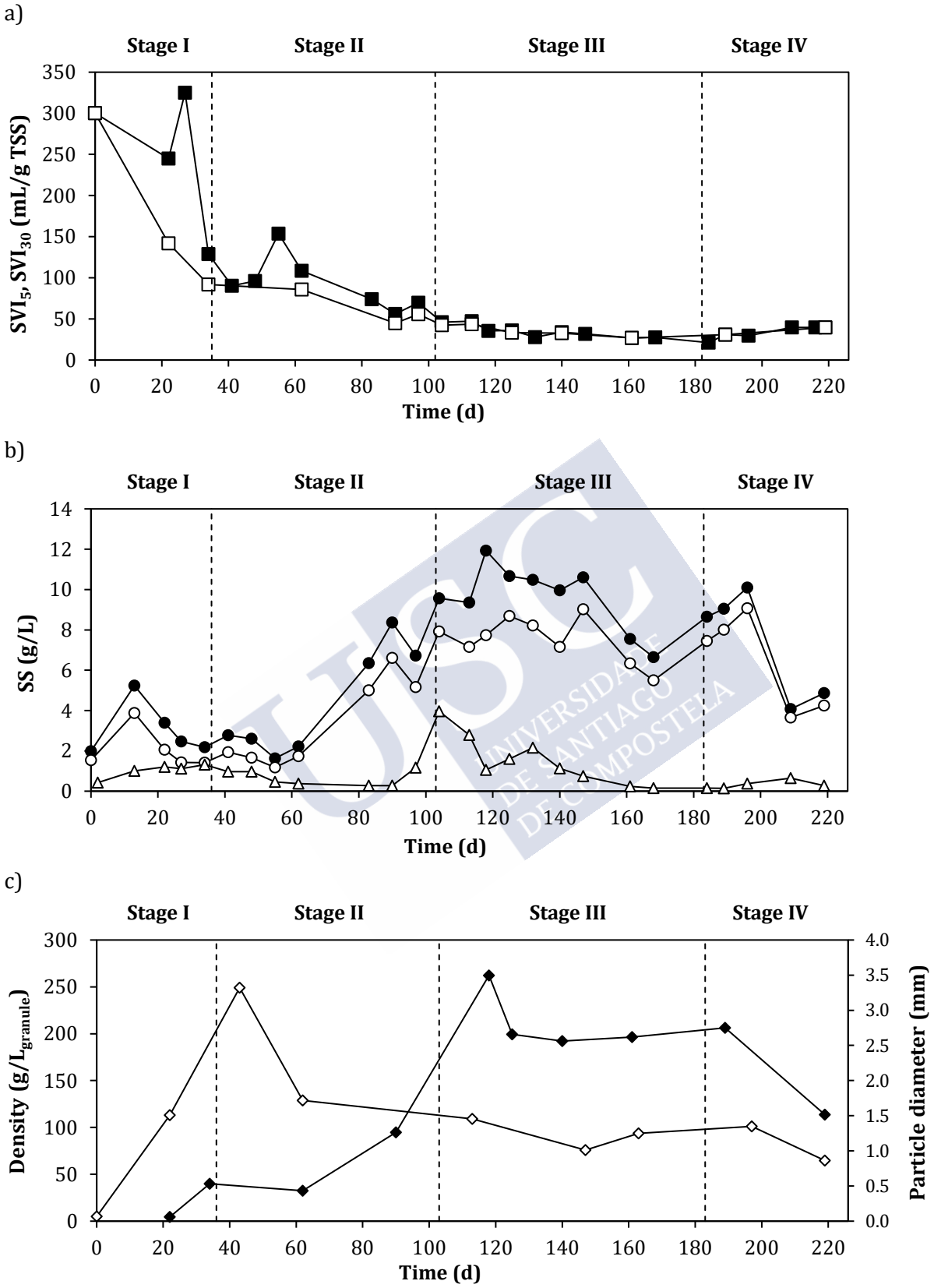

Figure 5.2: (a) Evolution of the SVI_5 (■) and SVI_{30} (□) of the granular sludge. (b) Evolution of the concentrations of TSS (●) and VSS (○) in the reactor and TSS (△) in the effluent of the reactor. (c) Evolution of the density (◆) and particle diameter (◇) of the granules.

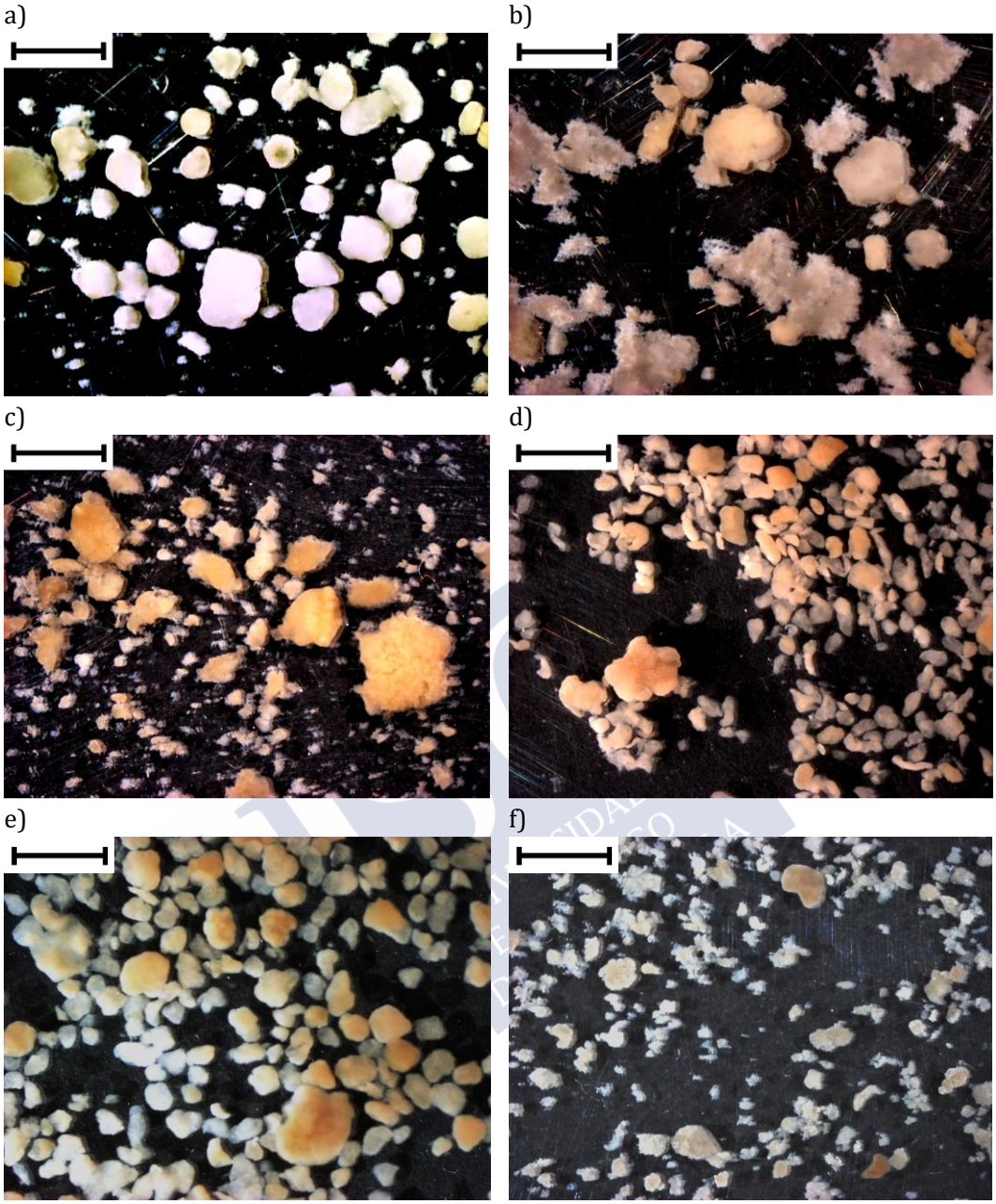

Figure 5.3: Images of the granules on day 22 (a), 43 (b), 100 (c), 147 (d), 197 (e) and 222 (f). The size bar corresponds to 2 mm.

After only one month, the composition of the industrial wastewater changed (Stage II), mainly characterised by a decrease of salt concentration from 10.2 to 5.5 g NaCl/L (Table 5.2). The biomass concentration remained stable (1.3 – 1.9 g VSS/L between days 27 – 48, Figure 5.2.b), but the change of salinity provoked a significant increase of the size of the aggregates, from 1.51 to 3.22 mm (Figure 5.2.c). At the beginning of this stage, the biomass consisted of a mixture of big flocs and granules (Figure 5.3.b), which gradually improved their settleability (SVI_5 from 90 mL/g TSS on day 43 to 45 mL/g TSS on day 90) and evolved to a fully granular system. Therefore, the

salinity change did not affect the evolution of the granulation process and on day 90 it was considered complete, since the SVI_5 was similar to the SVI_{30} (Figure 5.2.a). The biomass concentration on that day was of 6.61 g VSS/L, with a density of 94.7 g TSS/$L_{granule}$. On day 93 the cycle length was extended to 4 h. However, this change did not have significant effects on the biomass properties.

Similar results regarding the granulation process were obtained in previous research works treating fish-canning wastewater with AGS. Figueroa et al. (2008) obtained mature granules after 75 days of operation with an OLR of 1.5 kg $COD_S/(m^3 \cdot d)$, with high density (60 g VSS/L) and good settleability (30 mL/g VSS). Val Del Río et al. (2013) observed the first aggregates after 21 days and obtained mature granules with similar properties (SVI_5 of 30 mL/g TSS, density of 65 mL/g VSS) after 170 days, operating under alternating OLRs (2.5 – 13 kg $COD_S/(m^3 \cdot d)$).

In Stage III, the salinity of the wastewater increased suddenly up to 13.4 g NaCl/L. This change implied a higher buoyancy force in the mixed liquor and, consequently, occasional events of biomass washout took place (Stage III.a). The maximum solids concentration in the effluent, of 3.96 g TSS/L, was registered at the beginning of the stage (day 104). However, granules presented better settleability (SVI_{30} of 33 mL/g TSS and equal to SVI_5 from day 125 onwards) and higher density (190 g TSS/$L_{granule}$) than in previous stages. In addition, the granules, with irregular surface at the beginning of the stage (Figure 5.3.c), became well-shaped with smooth surface (Figure 5.3.d). Then, the reduction of the applied OLR (Stage III.b) provoked the decrease of the biomass concentration, from 9.0 to 5.5 g VSS/L. However, no significant effect was observed in the AGS characteristics. In both sub-stages, the Inorganic Suspended Solids (ISS) to TSS ratio presented the highest values, between 20 – 30 %, corresponding to the highest salinity of the wastewater. This result agrees with Figueroa et al. (2008), who observed ISS/TSS ratios of 7 – 25 % when the system treated an effluent with a salt concentration of 13 g NaCl/L. Therefore, the higher salt concentration of Stage III had a beneficial effect on the physical properties of the granules, favouring the biomass retention inside the reactor, with solid concentrations of 6 – 10 g TSS/L.

In Stage IV the salt concentration in the feeding suddenly decreased again down to 5.0 g NaCl/L (as in Stage II). However, due to the fact that the granular biomass was at that moment more "mature" than in Stage II, the effect of this change was not immediately observed and did not significantly influence the AGS properties or granule shape (Figure 5.3.e). The SVI_{30} and average diameter were similar to those measured before the change, while the biomass concentration increased a little (Figure 5.2.a,b,c). Nevertheless, the granules partially broke up into smaller aggregates (Figure 5.3.f) and the washout of biomass took place between days 196 – 209.

To study the evolution of EPS content of the granular sludge, samples were taken during the different operational stages. The extracted amount of EPS oscillated between 20 – 140 mg EPS/g VSS, containing a protein to polysaccharide ratio (PN/PS) of 0.01 – 20, which increased throughout the operation of the reactor (Figure 5.4). During Stage I, when the biomass was still acclimating to the imposed operational conditions, the PN/PS ratio was low (Figure 5.4), and the PN content increased with the granulation process. This trend agrees with the results obtained by Campo et al. (2018), who observed a low PN content during the start-up of an AGS reactor that increased when the biomass was acclimated to the operational conditions. The highest PN/PS

ratio, as well as the extracted EPS content, was observed during Stage III (Figure 5.4). In this stage, the granules presented the best properties (highest density and lowest SVI) and the salt concentration was the highest one (13.4 g NaCl/L). The high PN content could be responsible for the increase of the hydrophobicity of the biomass and led to the production of compact and stable granules, as observed by Zhu et al. (2012). During Stage IV, due to the partial destabilisation of the biomass caused by the decrease of salinity, the PS content increased, decreasing the PN/PS ratio.

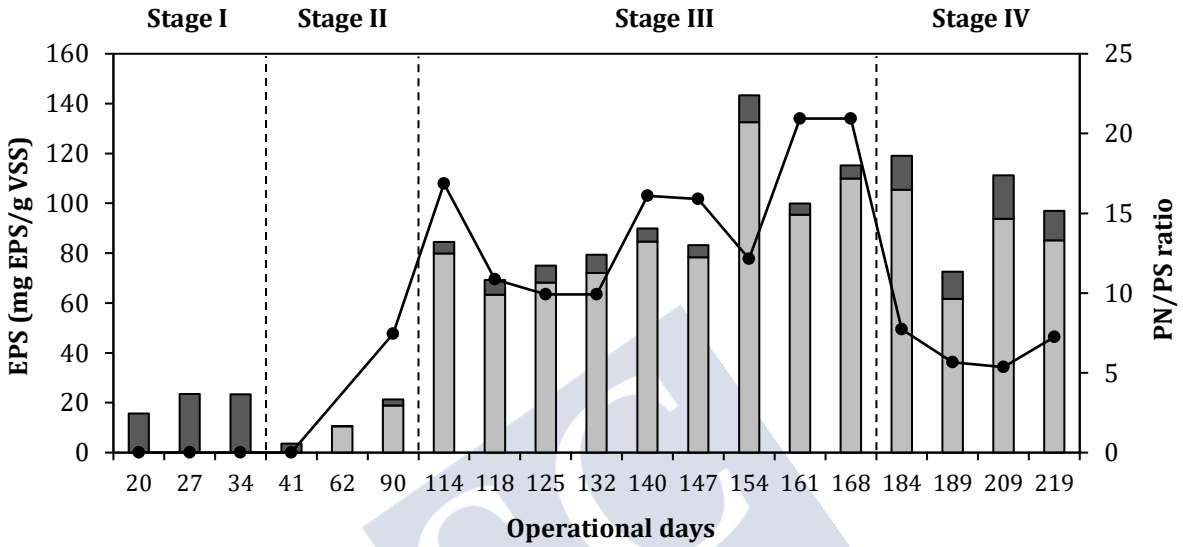

Figure 5.4: Evolution of the EPS content (PN light grey, PS dark grey) and the PN/PS ratio (●) of the granular biomass.

Reactor performance

During the first days of Stage I the COD_S removal gradually increased up to an average value of 80 % (Figure 5.5.a). Although the applied OLR varied during the entire operational time, the removal efficiencies remained almost constant (Stages I to IV), so COD removal seemed to be not affected by the fluctuating applied OLR. Only in Stage III, when the OLR decreased from 4.3 to 1.8 kg $COD_S/(m^3 \cdot d)$, a slight decrease of the removal efficiencies occurred, probably due to these transient conditions and the decrease of biomass concentration in the reactor. The feast phase gradually shortened throughout the operation of the reactor. During Stage I it lasted 40 – 60 min, and after the increase of biomass concentration as a consequence of the granulation process, it shortened to 10 – 20 min, depending on the applied OLR. The shortest feast phase was obtained in stages III.b and IV, coinciding with the lowest OLR. The trends of the COD_T removal efficiencies were similar (Figure 5.5.b). The higher COD_T concentrations were measured in the effluent at the beginning of the operational time (Stage I) and in Stage III.a, due to the washout of biomass associated to the granulation process and the increase of salinity in the influent, respectively.

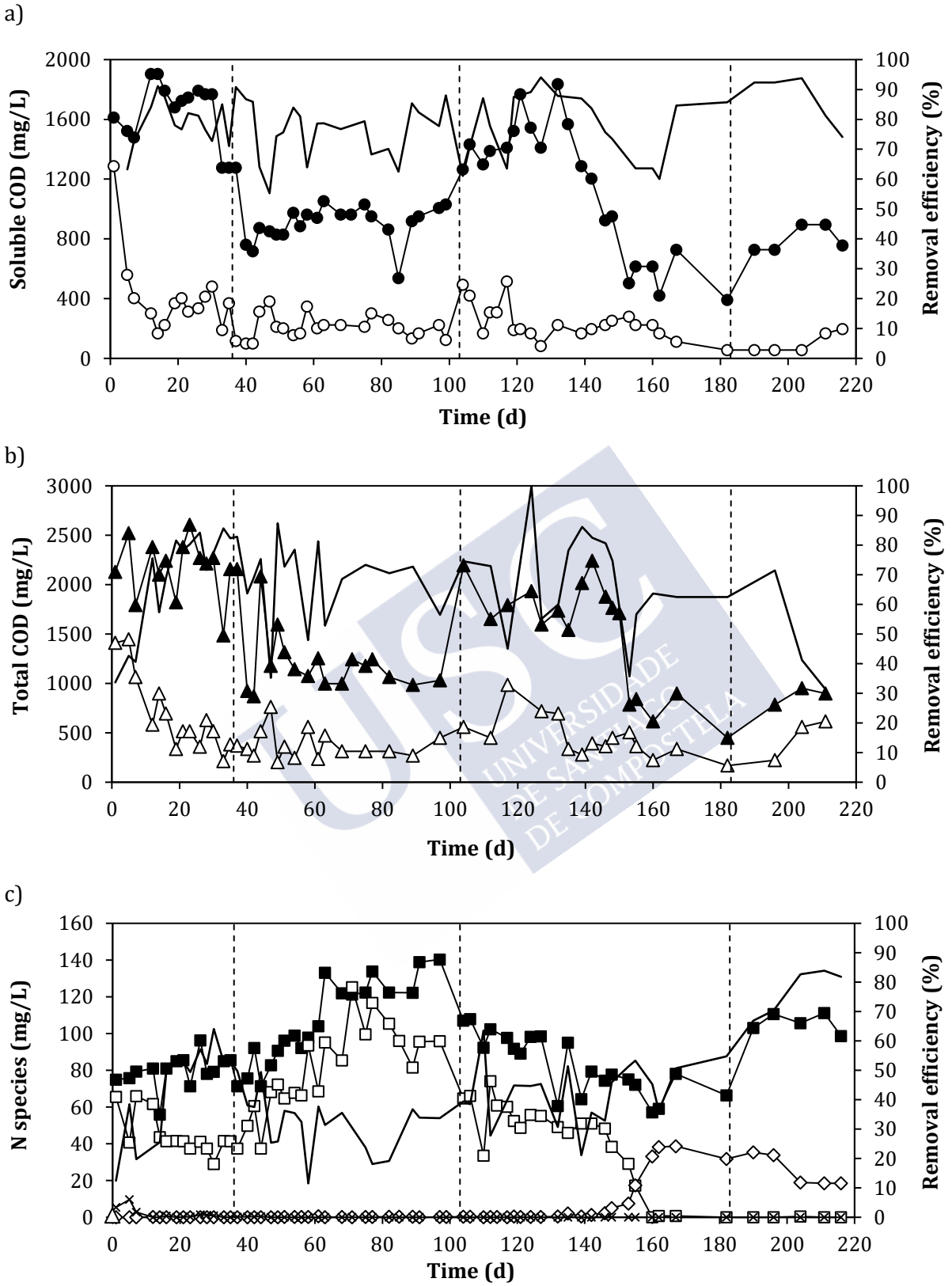

Figure 5.5: (a) COD_S concentration of the influent (●) and effluent (○) of the reactor and removal efficiency (-). (b) COD_T concentration of the influent (▲) and effluent (△) of the reactor and removal efficiency (-). (c) Ammonium concentration in the influent (■), ammonium (□), nitrite (◇) and nitrate (x) concentrations of the effluent and removal efficiency (-).

Nitrogen removal occurred due to heterotrophic biomass growth during most part of the operation of the reactor (Stage I to Sub-Stage III.a). The removal efficiencies ranged between 20 and 40 % depending on the load of COD removed and the corresponding ammonium concentration (Figure 5.5.c). In order to study the cause of the absence of nitrifying bacteria, two parameters were analysed: the Free Ammonia (FA) concentration and the Sludge Retention Time (SRT).

The highest FA concentrations were of 20 – 23 mg N/L and corresponded to the operational stage with the highest ammonia concentration in the influent (Stage III). However, these values were not high enough to cause the complete inhibition of the nitrifying activity, as observed by Yang et al. (2004). These authors managed to nitrify in an AGS reactor where FA concentrations were below 23.5 mg N/L. In addition, the reported FA inhibition threshold of AOB was of 10 – 150 mg N/L for *Nitrosomonas* and of 0.1 – 4 mg N/L for *Nitrobacter* bacteria (Anthonisen et al., 1976).

The SRT oscillated between 1.5 – 3.0 days in Stages I and III.a. In these stages, neither nitrite nor nitrate were measured in the effluent. Then, when the SRT increased over 5 – 7 days (from day 153 onwards, Stage III), nitrite production considerably increased to values between 3.72 mg NO_2-N/g VSS and 7.05 mg NO_2-N/g VSS. Therefore, the short SRTs of the first operational stages were presumably the main cause of the absence of detectable nitrifying bacteria activities, as found by (Wagner et al., 2015). They observed that when SRT values were lower than 3 days only 15 % of ammonia was removed, whereas with SRTs of 7 days it increased up to 70 %.

Furthermore, nitrite oxidation to nitrate did not take place throughout the whole experiment, probably because of the salt concentration in the reactor. Previous research works have reported the complete inhibition of NOBs with salinities of 20 – 30 g NaCl/L (Bassin et al., 2011; Pronk et al., 2014; Wang et al., 2017). Although in the present study the maximum salt concentration of the incoming wastewater was lower (13 g NaCl/L), other factors might have contributed to the inhibition of NOBs, like the complexity of the industrial wastewater, the presence of other ions or the chosen operational cycle distribution. The accumulation of Free Nitrous Acid (FNA) due to the combination of the produced nitrite and the pH inside the reactor, could also provoke the inhibition of NOB. Thresholds of 0.2 – 2.8 mg/L have been reported to provoke the inhibition of NOB (Anthonisen et al., 1976). However, in the present work, when nitritation occurred, the nitrite concentrations at the end of the cycle were of 5 – 39 mg NO_2-N/L. The pH values were of 7.3 – 8.5 inside the reactor. With these conditions, the FNA concentrations were considerably lower than the inhibition values, so that FNA was not a cause of the NOB inhibition.

The proliferation of AOB was confirmed by the results of the FISH analysis (Figure 5.6). In AGS samples from days 0 (inoculum), 34 (Stage I) and 92 (Stage II.b) no positive signal for AOB was detected. However, on samples from days 145 (Stage III.a), 163 (Stage III.b) and 222 (Stage IV) the results for AOB were positive and their relative abundance had an increasing trend with values of 1.3 %, 2.3 % and 4.8 %, respectively, corresponding to SRTs over 5 days (Figure 5.6).

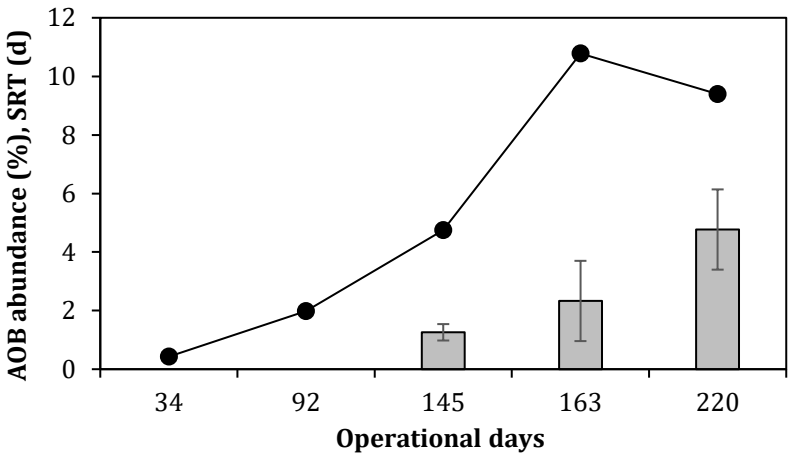

Figure 5.6: Relative abundance (grey bars) of AOB in the microbial community of granular sludge samples collected at different operational days: 34 (Stage I), 92 (Stage II.a), 145 (Stage III.a), 163 (Stage III.b) and 220 (Stage IV) and corresponding SRTs (d) (●).

The differences among the operational stages were studied through the comparison of operational cycles from days 91 and 162 (Figure 5.7). On day 91, the fully granular system was recently achieved, and the retention of biomass was not very efficient (SRT of 3 days), whereas on day 163 the biomass was in the form of mature granules and the corresponding SRT was relatively long (15 days).

Regarding the COD_S removal, on day 91, a feast phase of 40 min was determined (OLR of 2.9 kg $COD_S/(m^3 \cdot d)$), whereas on day 162 (OLR of 1.8 kg $COD_S/(m^3 \cdot d)$), only 15 min were necessary to remove the soluble COD from the liquid phase (Figure 5.7.a,c). These differences might be due to the decrease of the applied OLR, caused by the different batches of wastewater used to feed the reactor.

Regarding nitrogen removal, on day 91 the ammonia oxidation was negligible (Figure 5.7.b). However, on day 162, when the SRT increased to 15 days, complete ammonia oxidation to nitrite took place, and the nitrite formed was removed by denitritation during the feast period of the next cycle (Figure 5.7.d). This removed nitrogen, in addition to the ammonia removal due to biomass growth, allowed for the improvement of the nitrogen removal efficiencies to 49 % and 77 % in Stages III and IV, respectively (Figure 5.5.c). The fact that nitrite is the resulting compound from ammonia oxidation may be considered as an advantage as its denitrification will need less amount of organic matter from that fed at the beginning of the cycle. In this way, the use of COD for denitritation is expected more efficient than in the case of having complete denitrification from nitrate.

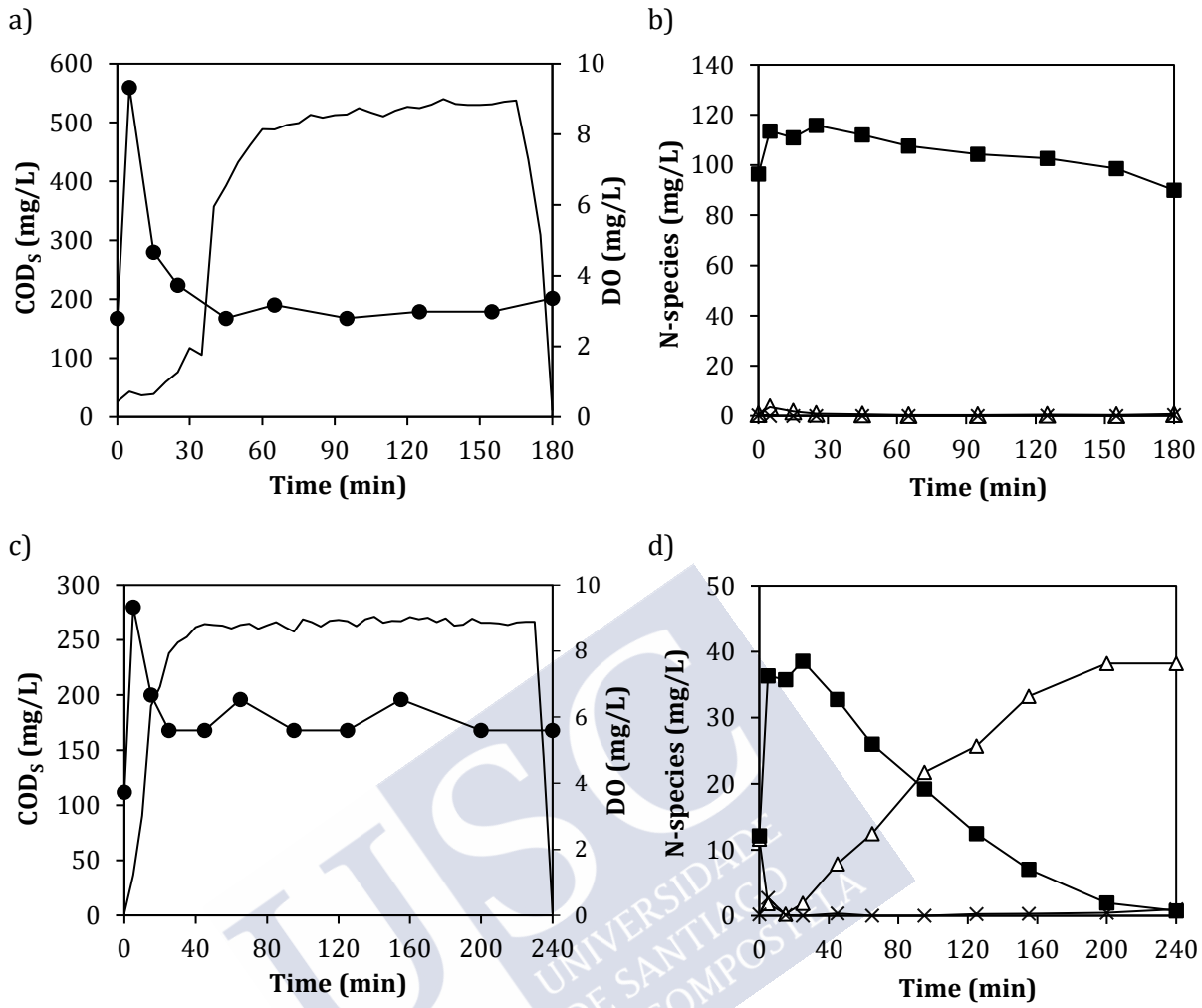

Figure 5.7: Concentration profiles of COD (●), dissolved oxygen (-), NH_4^+-N (■), NO_2^--N (△) and NO_3^--N (x) throughout single operational cycles measured in the reactor on days 91 (Stage II.a) (a, c) and 163 (Stage III.b) (b, d).

5.4.2. Evaluation of different feeding strategies to treat fish-canning wastewater

In order to determine the influence of the feeding strategy on the granulation and performance of AGS, the operation of the reactor described in this chapter (fully aerobic, R1) was compared with the operation of a reactor with anaerobic feeding followed by aerobic reaction (R2), described by Campo (2018). Both reactors were operated simultaneously. The operational conditions, as well as the feeding composition, were the same in both reactors, being the feeding strategy the only difference between them.

The dynamic behaviour, due to the industrial wastewater variability, of the aggregation process of the biomass was observed in both SBRs (Table 5.3).

Table 5.3: Biomass properties of R1 (the present study) and R2 (operated by Campo (2018)) in the different operational stages.

Stage		**I**	**II.a**	**II.b**	**III.a**	**III.b**	**IV**
NaCl (g/L)		10.19	5.49	5.49	13.45	13.45	5.00
Applied OLR (kg COD_S/(m^3·d))		6.65	3.54	2.90	4.28	1.80	2.37
Change from previous stage		Start-up	Salt decrease	HRT increase	Salt increase	OLR decrease	Salt decrease
Main features	R1	-	granulation	-	biomass loss (quick)	nitrification	biomass loss
	R2	granulation	instability (flocculent growth)	-	biomass loss (slow)	better settleability	instability (flocculent growth)
VSS_R (g/L)	R1	2.06 ± 1.05	3.02 ± 2.23	5.17 ± 0.56	7.98 ± 0.72	5.91 ± 0.60	6.48 ± 2.40
	R2	1.44 ± 0.26	2.82 ± 1.60	3.40 ± 0.84	3.99 ± 0.68	3.04 ± 0.70	2.56 ± 0.61
VSS_{eff} (g/L)	R1	0.66 ± 0.20	0.40 ± 0.23	0.92 ± 0.26	1.39 ± 0.97	0.15 ± 0.05	0.27 ± 0.19
	R2	0.69 ± 0.37	0.26 ± 0.17	0.08 ± 0.03	0.55 ± 0.40	0.17 ± 0.06	0.50 ± 0.29
SVI_5/SVI_{30} (mL/g TSS)	R1	250/178	96/65	70/56	37/38	27/27	33/33
	R2	127/88	115/95	136/109	103/77	68/62	93/73
Density ($g\ TSS/L_{granule}$)	R1	22.3 ± 25.1	63.6 ± 44.1	70.5 ± 0.0	217.9 ± 38.5	196.4 ± 20.5	156.0 ± 65.5
	R2	11.4 ± 0.5	38.6 ± 18.0	72.6 ± 0.0	68.4 ± 11.2	106.9 ± 20.6	93.8 ± 13.8
Average diameter (mm)	R1	1.51 ± 0.53	2.52 ± 1.13	1.72 ± 0.57	1.23 ± 0.31	1.25 ± 0.39	1.10 ± 0.34
	R2	0.89 ± 0.51	1.63 ± 0.18	1.38 ± 0.05	1.18 ± 0.19	0.94 ± 0.11	1.12 ± 0.25
SRT (d)	R1	0.78 ± 0.41	2.88 ± 3.05	1.98 ± 0.03	2.56 ± 1.46	15.18 ± 4.50	11.60 ± 10.54
	R2	1.00 ± 0.38	3.06 ± 1.64	5.93 ± 0.05	3.07 ± 1.94	4.04 ± 2.49	2.26 ± 1.20

Sub-indexes: R – reactor; eff – effluent.

In the fully aerobic configuration (R1), the granulation process was slower (completed on day 90) than in the anaerobic-fed configuration (R2, completed on day 34). However, the granules obtained in the former were more stable against alternating OLR and salinity concentrations in the industrial wastewater (Table 5.3). In R2, instability episodes associated with flocculent growth and biomass washout were observed. In general, the granular biomass of the fully aerobic configuration presented lower SVI_5/SVI_{30} ratios, higher density and larger average diameter than that from the anaerobic feeding configuration. In addition, both the biomass concentration and the SRT were higher in R1 (Table 5.3).

Concerning the reactor performance, R2 responded slightly better in terms of COD_S removal (80 – 90 %) than R1 (75 – 85 %). Nitrogen removal was significantly larger in R1 (80 %) when the values of SRT were high enough to promote nitrification, while in R2 nitrification did not occur, probably due to the instability episodes of the AGS, which led to low values of the SRTs (< 6 days).

Table 5.4: Performance and effluent quality of R1 (the present study) and R2 (operated by Campo (2018)) during the different operational stages.

Stage		**I**	**II.a**	**II.b**	**III.a**	**III.b**	**IV**
Reactor performance							
COD_S removal (%)	R1	78.6 ± 7.6	75.9 ± 9.6	82.9 ± 7.3	79.9 ± 10.4	71.5 ± 12.6	86.7 ± 8.7
	R2	81.9 ± 6.0	82.4 ± 11.3	92.3 ± 3.4	85.3 ± 6.7	68.9 ± 15.0	78.5 ± 8.4
COD_T removal (%)	R1	68.6 ± 17.7	68.8 ± 14.0	56.5 ± 1.2	73.6 ± 15.3	56.2 ± 11.8	47.9 ± 20.9
	R2	57.6 ± 16.5	70.8 ± 14.1	87.3 ± 1.8	84.3 ± 6.0	63.8 ± 13.9	48.4 ± 4.9
NH_4^+-N removal (%)	R1	44.0 ± 16.7	28.7 ± 11.4	31.7 ± 0.0	39.3 ± 11.9	89.2 ± 16.6	99.9 ± 0.2
	R2	45.4 ± 17.0	26.4 ± 11.3	29.5 ± 16.3	20.1 ± 13.3	22.3 ± 4.4	31.8 ± 3.3
TN removal (%)	R1	44.6 ± 15.7	27.8 ± 11.4	31.7 ± 0.0	39.3 ± 11.9	89.2 ± 16.6	77.1 ± 7.9
	R2	46.2 ± 18.3	39.3 ± 9.9	44.3 ± 15.7	16.8 ± 15.5	19.7 ± 3.4	36.3 ± 3.3
Effluent quality							
COD_S (mg/L)	R1	416.0 ± 273.0	211.9 ± 79.8	173.6 ± 71.3	261.0 ± 125.8	177.3 ± 82.4	106.4 ± 69.7
	R2	458.6 ± 281.3	163.9 ± 105.5	78.4 ± 38.8	223.7 ± 93.9	217.8 ± 113.5	190.4 ± 75.1
COD_T (mg/L)	R1	682.4 ± 386.0	368.8 ± 149.7	448.0 ± 0.0	522.5 ± 218.6	319.2 ± 130.7	466.7 ± 212.0
	R2	1099.2 ± 535.7	422.0 ± 294.4	212.8 ± 0.0	357.4 ± 187.7	315.0 ± 98.9	504.0 ± 79.2
TN (mg/L)	R1	39.1 ± 8.0	102.1 ± 26.3	114.3 ± 0.0	63.8 ± 12.2	36.7 ± 10.6	48.1 ± 17.9
	R2	65.6 ± 20.7	70.3 ± 4.9	84.4 ± 0.0	73.1 ± 7.0	69.8 ± 2.3	76.2 ± 2.8

The effluent composition of both reactors (Table 5.4) was compared with the threshold limits suggested in the "Reference Document on Best Available Techniques in the Food, Drink and Milk Industries" (European IPPC Bureau, 2019) (50 mg TSS/L, 125 mg COD/L and 10 mg TN/L). The configuration with a previous anaerobic feeding phase presented lower concentrations of TSS during the whole experiment, whereas in the fully aerobic reactor there were important fluctuations due to the quick washout of the biomass with the change of the wastewater conditions. In this sense, the slower washout of flocculent biomass in R2 when fluctuations occurred, avoided the peaks of solids in the effluent but provoked the instability of the aggregates, which remained entrapped in it. However, none of the configurations respected the discharge limit for TSS (50 mg/L), which was probably related to the difficulty to achieve stable AGS when treating a wastewater characterised by high fluctuating values of salinity and OLR. Therefore, for industrial application, both configurations would require a posterior separation system. With this alternative, both the solid content and the COD_T concentration could be reduced.

Regarding the COD_S removal, the fully aerobic reactor (R1) did not fulfil the discharge requirements (125 mg COD/L), except for Stage IV, reaching values below 90 mg COD/L. The COD_S concentration in the effluent was lower in the anaerobic-fed reactor and with less fluctuations during the whole operational period. It fulfilled the discharge requirements in each stage, very often in Stage II, characterised by low salinity and low OLR.

In terms of TN, the concentration in the effluent was similar in both configurations, with the exception of the operational periods when the SRT was higher than 10 days in the fully aerobic reactor (Stage III.b and Stage IV, Table 5.3). At that moment, the TN concentration in the effluent was lower than in the anaerobic-fed system due to the ammonia oxidation to nitrite and its further denitritation, but it was still above the discharge requirements for TN (10 mg N/L). The improvement of the nitrogen removal would imply a change in the operational conditions like the decrease of the dissolved oxygen concentration which might enhance the denitrification process (Mosquera-Corral et al., 2005).

5.5. CONCLUSIONS

The formation of aerobic granular sludge was feasible after 90 days of operation treating fish-canning wastewater in a fully aerobic reactor. The obtained granules were stable against alternating OLRs and salinity concentrations of the industrial wastewater (1.80 – 6.65 kg $COD_S/(m^3 \cdot d)$ and 4.97 – 13.45 g NaCl/L, respectively). Furthermore, the highest salinity tested in the treated wastewater of 13 g NaCl/L improved the physical properties of the granules and the biomass retention inside the reactor.

Regarding the reactor performance, high COD_S removal efficiencies were achieved (75 – 85 %). Nitrogen removal was significantly larger at the end of the operation (up to 80 % removal) when the values of the SRT were high enough (above 5 days) to promote nitrification. At this point nitritation – denitritation was the main nitrogen removal process.

Although the granulation process was longer in a fully aerobic configuration (R1) than in an anaerobic-fed one (R2, study from Campo (2018)) the obtained granular biomass was more stable against the fluctuations of the feeding and presented lower SVI_5/SVI_{30} ratios, higher density and larger average diameters.

Nitrification and denitrification processes succeeded in R1 and nitrogen removal percentages of 80 % were achieved, whereas in R2 nitrifying activity was not observed and the nitrogen removal efficiencies were lower (17 – 46 %). In order to improve the N removal, actions like DO control should be explored to enhance the denitrification processes.

5.6. REFERENCES

ANFACO-CECOPESCA, 2019. Datos del sector 2018

Anthonisen, A.C., Loehr, R.C., Prakasam, T.B.S., Srinath, E.G., 1976. Inhibition of nitrification by ammonia and nitrous acid. J. Water Pollut. Control Fed. https://doi.org/10.1016/0168-6496(92)90072-2

APHA/AWWA/WEF, 2012. Standard Methods for the Examination of Water and Wastewater. Stand. Methods 541. https://doi.org/ISBN 9780875532356

Bassin, J.P., Pronk, M., Muyzer, G., Kleerebezem, R., Dezotti, M., van Loosdrecht, M.C.M., 2011. Effect of elevated salt concentrations on the aerobic granular sludge process: Linking microbial activity with microbial community structure. Appl. Environ. Microbiol. https://doi.org/10.1128/AEM.05016-11

Bassin, J.P., Tavares, D.C., Borges, R.C., Dezotti, M., 2019. Development of aerobic granular sludge under tropical climate conditions: The key role of inoculum adaptation under reduced sludge washout for stable granulation. J. Environ. Manage. https://doi.org/10.1016/j.jenvman.2018.09.072

Bengtsson, S., de Blois, M., Wilén, B.M., Gustavsson, D., 2018. Treatment of municipal wastewater with aerobic granular sludge. Crit. Rev. Environ. Sci. Technol. 48, 119–166. https://doi.org/10.1080/10643389.2018.1439653

Beun, J.J., Van Loosdrecht, M.C.M., Heijnen, J.J., 2002. Aerobic granulation in a sequencing batch airlift reactor. Water Res. https://doi.org/10.1016/S0043-1354(01)00250-0

Campo, R., 2018. Aerobic Granular Sludge technology for the treatment of industrial saline wastewater. PhD thesis. Universitá degli Studi di Enna "Kore."

Campo, R., Corsino, S.F., Torregrossa, M., Di Bella, G., 2018. The role of extracellular polymeric substances on aerobic granulation with stepwise increase of salinity. Sep. Purif. Technol. https://doi.org/10.1016/j.seppur.2017.11.074

Cristóvaõ, R.O., Botelho, C.M., Martins, R.J.E., Loureiro, J.M., Boaventura, R.A.R., 2015. Fish canning industry wastewater treatment for water reuse - A case Study. J. Clean. Prod. 87, 603–612. https://doi.org/10.1016/j.jclepro.2014.10.076

Daims, H., Lücker, S., Wagner, M., 2006. daime, a novel image analysis program for microbial ecology and biofilm research. Environ. Microbiol. https://doi.org/10.1111/j.1462-2920.2005.00880.x

Dreywood, R., 1946. Qualitative Test for Carbohydrate Material. Ind. Eng. Chem. - Anal. Ed. https://doi.org/10.1021/i560156a015

European IPPC Bureau, 2019. Best Available Techniques Reference document on food, drink and milk industries, European Commission.

Figueroa, M., Mosquera-Corral, A., Campos, J.L., Méndez, R., 2008. Treatment of saline wastewater in SBR aerobic granular reactors. Water Sci. Technol. https://doi.org/10.2166/wst.2008.406

Figueroa, M., Val Del Río, A., Campos, J.L., Méndez, R., Mosquera-Corral, A., 2015. Filamentous bacteria existence in aerobic granular reactors. Bioprocess Biosyst. Eng. 38, 841–851. https://doi.org/10.1007/s00449-014-1327-x

Franca, R.D.G., Ortigueira, J., Pinheiro, H.M., Lourenço, N.D., 2017. Effect of SBR feeding strategy and feed composition on the stability of aerobic granular sludge in the treatment of a simulated textile wastewater. Water Sci. Technol. 76, 1188–1195. https://doi.org/10.2166/wst.2017.300

Kargi, F., 2002. Enhanced biological treatment of saline wastewater by using halophilic bacteria. Biotechnol. Lett. https://doi.org/10.1023/A:1020379421917

Le-Clech, P., Chen, V., Fane, T.A.G., 2006. Fouling in membrane bioreactors used in wastewater treatment. J. Memb. Sci. https://doi.org/10.1016/j.memsci.2006.08.019

Lowry, O.H., Rosebrough, N.J., Farr, A.L., Randall, R.J., 1951. Protein measurement with the Folin phenol reagent. J. Biol. Chem.

Meunier, C., Henriet, O., Schroonbroodt, B., Boeur, J.M., Mahillon, J., Henry, P., 2016. Influence of feeding pattern and hydraulic selection pressure to control filamentous bulking in biological treatment of dairy wastewaters. Bioresour. Technol. 221, 300–309. https://doi.org/10.1016/j.biortech.2016.09.052

Mosquera-Corral, A., De Kreuk, M.K., Heijnen, J.J., Van Loosdrecht, M.C.M., 2005. Effects of oxygen concentration on N-removal in an aerobic granular sludge reactor. Water Res. https://doi.org/10.1016/j.watres.2005.04.065

Moussa, M.S., Sumanasekera, D.U., Ibrahim, S.H., Lubberding, H.J., Hooijmans, C.M., Gijzen, H.J., Van Loosdrecht, M.C.M., 2006. Long term effects of salt on activity, population structure and floc characteristics in enriched bacterial cultures of nitrifiers. Water Res. https://doi.org/10.1016/j.watres.2006.01.029

Pronk, M., Bassin, J.P., De Kreuk, M.K., Kleerebezem, R., Van Loosdrecht, M.C.M., 2014. Evaluating the main and side effects of high salinity on aerobic granular sludge. Appl. Microbiol. Biotechnol. 98, 1339–1348. https://doi.org/10.1007/s00253-013-4912-z

Soto, M., Veiga, M.C., Mendez, R., Lema, J.M., 1989. Semi-micro C.O.D. determination method for high-salinity wastewater. Environ. Technol. Lett. 10, 541–548

Sun, C., Leiknes, T.O., Weitzenböck, J., Thorstensen, B., 2010. Salinity effect on a biofilm-MBR process for shipboard wastewater treatment. Sep. Purif. Technol. https://doi.org/10.1016/j.seppur.2010.03.010

Thwaites, B.J., Reeve, P., Dinesh, N., Short, M.D., van den Akker, B., 2017. Comparison of an anaerobic feed and split anaerobic–aerobic feed on granular sludge development, performance and ecology. Chemosphere 172, 408–417. https://doi.org/10.1016/j.chemosphere.2016.12.133

Tijhuis, L., van Loosdrecht, M.C.M., Heijnen, J.J., 1994. Formation and growth of heterotrophic aerobic biofilms on small suspended particles in airlift reactors. Biotechnol. Bioeng. https://doi.org/10.1002/bit.260440506

Val Del Río, A., Figueroa, M., Mosquera-Corral, A., Campos, J.L., Méndez, R., 2013. Stability of aerobic granular biomass treating the effluent from a seafood industry. Int. J. Environ. Res. https://doi.org/10.22059/ijer.2013.606

van den Akker, B., Reid, K., Middlemiss, K., Krampe, J., 2015. Evaluation of granular sludge for secondary treatment of saline municipal sewage. J. Environ. Manage. 157, 139–145. https://doi.org/10.1016/j.jenvman.2015.04.027

Wagner, J., Guimarães, L.B., Akaboci, T.R.V., Costa, R.H.R., 2015. Aerobic granular sludge technology and nitrogen removal for domestic wastewater treatment. Water Sci. Technol. 71, 1040–1046. https://doi.org/10.2166/wst.2015.064

Wagner, Jamile, Weissbrodt, D.G., Manguin, V., Ribeiro da Costa, R.H., Morgenroth, E., Derlon, N., 2015. Effect of particulate organic substrate on aerobic granulation and operating conditions of sequencing batch reactors. Water Res. https://doi.org/10.1016/j.watres.2015.08.030

Wang, P., Qu, Y., Zhou, J., 2009. Biodegradation of mixed phenolic compounds under high salt conditions and salinity fluctuations by arthrobacter sp. W1, in: Applied Biochemistry and Biotechnology. https://doi.org/10.1007/s12010-008-8494-7

Wang, X., Yang, T., Lin, B., Tang, Y., 2017. Effects of salinity on the performance, microbial community, and functional proteins in an aerobic granular sludge system. Chemosphere. https://doi.org/10.1016/j.chemosphere.2017.06.047

Wang, Z., van Loosdrecht, M.C.M., Saikaly, P.E., 2017. Gradual adaptation to salt and dissolved oxygen: Strategies to minimize adverse effect of salinity on aerobic granular sludge. Water Res. https://doi.org/10.1016/j.watres.2017.08.026

Yang, S.F., Tay, J.H., Liu, Y., 2004. Inhibition of free ammonia to the formation of aerobic granules. Biochem. Eng. J. 17, 41–48. https://doi.org/10.1016/S1369-703X(03)00122-0

Zhao, X., Feng, H.X., Jiang, F., Chen, N.L., Wang, X.C., 2012. Research of carbon and nitrogen ratio and sludge stability in aerobic granular sludge bioreactor, in: Advanced Materials Research. https://doi.org/10.4028/www.scientific.net/AMR.518-523.473

Zhu, L., Lv, M. Le, Dai, X., Yu, Y.W., Qi, H.Y., Xu, X.Y., 2012. Role and significance of extracellular polymeric substances on the property of aerobic granule. Bioresour. Technol. https://doi.org/10.1016/j.biortech.2011.12.008

USC
UNIVERSIDADE
DE SANTIAGO
DE COMPOSTELA

Chapter 6

Pilot-scale AGS reactor design for *in situ* fish-canning wastewater treatment

Summary

In this chapter, a pilot-scale sequencing batch reactor was designed to be located in a fish cannery to treat the produced wastewater by Aerobic Granular Sludge (AGS) technology. Firstly, the produced effluents of the factory were characterised. It produced 400 m^3/d of wastewater, which was divided into two streams: low-strength wastewater (LS-WW) and high-strength wastewater (HS-WW). The former represented the 95 % of the total volume of produced wastewater and contained low concentrations of both COD and nutrients (average values of 0.5 g COD_S/L and 8 mg NH_4^+-N/L). The latter represented only a 5 % of volume, but concentrations of the different pollutants were considerably higher (average values of 7.3 g COD_S/L and 0.5 g NH_4^+-N/L). The current wastewater treatment of the factory was designed to treat the LS-WW stream, and consisted of a Dissolved Air Flotation (DAF) unit, followed by a physicochemical tank and another DAF. The HS-WW was stored in a tank and small volumes (between 0 – 4 % of the volume) were mixed with the LS-WW to be treated in the wastewater treatment plant.

To treat the produced industrial wastewater by AGS technology, it was necessary to include a pre-treatment in the pilot plant to avoid operational problems in the AGS reactor. The pre-treatment of the LS-WW was designed to remove big solids, by using a rotary drum. The pre-treatment of the HS-WW was focused on the removal of greases, with a grease separation tank. The AGS reactor was designed to treat a maximum Organic Loading Rate (OLR) of 6 kg COD_S/(m^3·d). The length of the operational cycles was modified depending on the treated wastewater (LS-WW, HS-WW or a mixture of both). The operational strategy of the reactor was defined to cope with the routines of the factory, and the operational cycles were adapted to the non-working days of the fish cannery. To assure the production of a good-quality effluent, a small settler was included in the pilot plant, to remove the solids of the AGS reactor effluent.

OUTLINE

Chapter 6 131

6.1. INTRODUCTION 133

6.2. OBJECTIVES 134

6.3. MATERIALS AND METHODS 134

6.4. INDUSTRIAL WASTEWATER CHARACTERISATION 134

6.4.1. Low-strength wastewater (LS-WW) 135

6.4.2. High-strength wastewater (HS-WW) 136

6.4.3. Current wastewater treatment of the factory 137

6.5. AGS PILOT PLANT DESCRIPTION 137

6.5.1. Pilot AGS reactor pre-treatments 138

6.5.2. Pilot plant reactor 141

6.5.3. Pilot AGS reactor post-treatment 143

6.5.4. Control system 143

6.6. OPERATIONAL STRATEGY 144

6.7. CONCLUSIONS 146

6.8. REFERENCES 147

APPENDIX A: Scheme of the wastewater treatment plant of the fish-canning factory 148

APPENDIX B: Scheme of the AGS pilot plant 149

APPENDIX C: Dimensions of the units of the pilot plant 150

6.1. INTRODUCTION

The fish canneries can process a wide range of products, and their processing schemes in terms of raw material, source of utility water and unit processes vary between factories (Chowdhury et al., 2010). Fish processing operations generate large volumes of wastewater, which is characterised by presenting organic pollutants in soluble, colloidal and particulate form and eventually high salt concentration. Depending on the raw material and specific processing activity, wastewater with different degrees of contamination can be produced (AMEC Earth & Environmental Limited, 2003). Washing operations produce wastewater with low degree of pollution, while processes like fish filleting generate wastewater with mild degree of contamination. Bloodwater from fish storage tanks and fish evisceration, as well as water from the cookers, produce streams with a heavy degree of pollution. The produced wastewater streams are usually divided into two categories: high volume – low strength and low volume – high strength streams (Colic et al., 2012). In general, they contain greases and oils, proteins and solids coming from wastes from the fish processing units. The nitrogen content is likely due to the presence of proteins in the wastewater, whereas the phosphorus might come from the seafood and its processing and cleaning compounds (AMEC Earth & Environmental Limited, 2003). In addition, if seawater is used as processing water in the processing activities, salt concentrations are also present in the produced effluents. In order to protect the environment this kind of wastewater must be treated in the fish-cannery previous to its discharge.

The most common treatments applied to these streams consist of a primary treatment to remove insoluble suspended matter, based on physicochemical processes, that can be followed or not by a biological treatment to remove soluble organic matter and nutrients. Primary treatment includes processes like screening, sedimentation, Dissolved Air Flotation (DAF) or flow equalisation (Hung et al., 2005). The screening is usually the first step, to remove relatively large solids (larger than 0.7 mm), through tangential screenings or rotary drums. Sedimentation is used to separate heavy and small solids, in settling tanks. Greases, oil and particulate matter are usually removed in DAF systems. To avoid big fluctuations in the influent to the DAF unit, it is recommendable to locate a previous equalisation tank. If the particulate matter is difficult to separate, coagulants and/or flocculants like metal salts, acids or synthetic polyelectrolytes are added (Cristóvão et al., 2014).

Different types of biological reactors have been used to treat fish-processing wastewater, including anaerobic and aerobic systems (Chowdhury et al., 2010). Both suspended and attached growth biomass technologies have been applied. Implemented anaerobic processes included anaerobic digesters (the most common ones), anaerobic filters, or Upflow Anaerobic Sludge Blanket (UASB) reactors. The main advantage of the anaerobic systems is the possibility of resource recovery by the production of biogas. In addition, they have low operational costs, space requirements and sludge generation. However, both the pH and ammonia concentration of the wastewater can provoke the inhibition of the process, if the free ammonia reaches concentrations above 500 mg NH_3-N/L (Appels et al., 2008). Salinity can also affect the process, since sodium concentrations above 3.5 g/L can inhibit methanogenic bacteria (Appels et al., 2008). In addition, in anaerobic processes nitrogen is not removed, being necessary an additional unit afterwards to comply with the required quality for the effluent discharge.

Applied aerobic processes include conventional activated sludge reactors, aerated lagoons or rotating biological contactors (Chowdhury et al., 2010). The main disadvantage of aerobic technologies compared to anaerobic ones is that resource recovery is not possible, since biogas is not produced. Nevertheless, aerobic systems can remove nutrients in addition to organic matter, and they are less sensitive to pH and ammonia concentrations. Aerobic Granular Sludge (AGS) is proposed as an alternative treatment, since it is a compact technology with high treatment capacity, and it can withstand the presence of salt (Figueroa et al., 2008). It could be suitable for factories with the need of treating high-loaded wastewater and with low space availability.

6.2. OBJECTIVES

In Chapter 5, the feasibility of AGS technology was demonstrated at laboratory scale, so the next step was the scale-up of the process. The objective of the present Chapter was the design of an AGS pilot plant, located in a fish cannery, to treat the produced effluents. To do that, the current operation of the fish cannery was studied, and the produced wastewater streams were characterised.

6.3. MATERIALS AND METHODS

The concentrations of ammonium (NH_4^+), nitrite (NO_2^-), nitrate (NO_3^-), Total Nitrogen (TN), phosphate (PO_4^{3-}), Volatile Fatty Acids, Total Suspended Solids (TSS) and Volatile Suspended Solids (VSS) were measured according to the Standard Methods (APHA/AWWA/WEF, 2012). The concentrations of chloride (Cl^-), sulphate (SO_4^{2-}) and sodium (Na^+) ions were determined by means of Ion Chromatography (Metrohm 816 Advanced Compact IC). The Chemical Oxygen Demand (COD) concentration was determined according to Soto et al., (1989) taking into account the different salt concentrations of the sample. Total COD concentration (COD_T) was determined in the sample without filtering, whereas soluble COD concentration (COD_S) was measured in samples filtered through 0.45 μm pore size filters. The pH was measured with an electrode (Crison Instruments GLP22), as well as the conductivity (HACH Lange 50 60, Platinum Cell). The protein concentration was measured according to the Lowry's method (Lowry et al., 1951), and the carbohydrates concentration with the anthrone method (Dreywood, 1946). Fats were determined with the gravimetric method, according to the Standard Methods (APHA/AWWA/WEF, 2012). The COD fractionation was done in a BM-T respirometer (SURCIS L model). The soluble readily biodegradable (S_S), soluble inert (S_I), particulate slowly biodegradable (X_S) and particulate inert (X_I) COD fractions were determined. The density of the sludge from the grease separation unit was estimated by weighting a known volume of sludge. More details about the analytical methods are given in Chapter 2.

6.4. INDUSTRIAL WASTEWATER CHARACTERISATION

The selected fish-canning company produced two types of effluents: Low-Strength wastewater (LS-WW) and High-Strength wastewater (HS-WW). The former presented low concentrations of

pollutants and represented a 95 % of the total volume of wastewater produced. The latter contained high concentrations of pollutants and represented only a 5 % of the wastewater effluent. The total volume of wastewater produced by the factory was 400 m^3/d.

6.4.1. Low-strength wastewater (LS-WW)

The LS-WW was produced as a result of washing processes. It presented a variable composition, depending on the product that was being processed, that could be tuna, octopus, common cockle, mussels, squid, vegetables or sauce. The composition could vary not only daily, but also hourly. Most of the time, the produced stream was a mixture of washing wastewater of different products. This wastewater was characterised by low concentrations of soluble COD and nitrogen and the presence of greases and solids. In addition, it also contained high salt concentrations, since the factory used seawater in some of the cleaning processes. The wastewater produced from the washing processes of common cockle presented the lowest concentrations of pollutants, whereas the wastewater from tuna and squid presented the highest ones (Table 6.1).

Table 6.1: Characterisation of LS-WW generated by the processing of two different products and average values from samples collected at different days.

Parameter	Unit	Common cockle	Tuna	Average value
Conductivity	mS/cm	37.7	20.9	22.1 ± 12.5
pH	-	7.53	5.91	6.26 ± 0.85
Total Suspended Solids	g/L	0.174	0.225	0.250 ± 0.137
Volatile Suspended Solids	g/L	0.105	0.217	0.213 ± 0.140
Total COD	mg/L	195.8	1183.2	1203.8 ± 671.9
Soluble COD	mg/L	179.2	691.2	507.4 ± 282.0
Greases	mg/L	30.02	311.41	145.7 ± 120.3
Volatile Fatty Acids	mg COD/L	26.62	44.46	169.7 ± 206.2
Ammonia	mg N/L	2.83	3.40	8.18 ± 7.45
Total nitrogen	mg N/L	8.98	18.73	21.23 ± 8.36
Phosphate	mg P/L	0	2.1	3.05 ± 2.46
Proteins	mg/L	31.73	102.76	86.46 ± 48.08
Carbohydrates	mg/L	10.35	72.31	46.28 ± 29.76
Chloride	g Cl^-/L	14.72	8.41	7.37 ± 5.6
Sulphate	g SO_4^{-2}/L	2.02	1.13	1.00 ± 0.77
Sodium	g Na^+/L	7.99	4.49	4.24 ± 2.90
Salt	g NaCl/L	20.3	11.4	14.35 ± 5.76

The COD fractions also varied depending on the day that the wastewater was collected (Figure 6.1). In general, this type of wastewater contained at least a 25 % of inert COD and the biodegradable fraction (calculated as the sum of the soluble and particulate biodegradable COD) oscillated between 27 – 75 %.

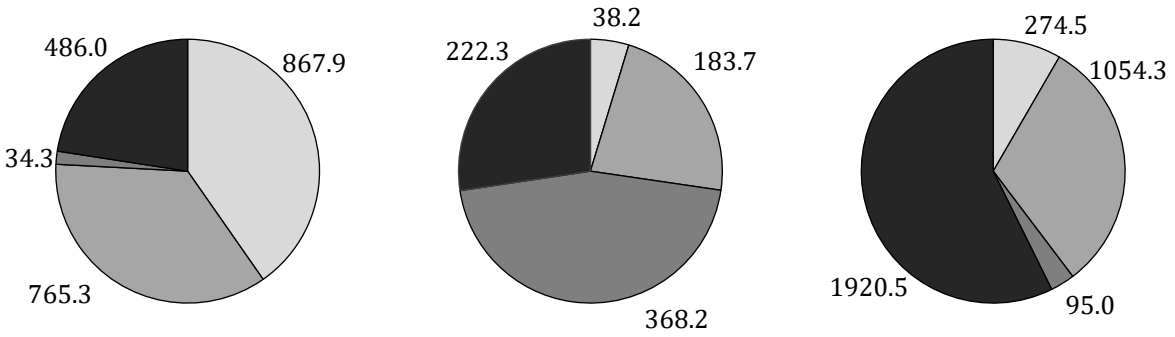

Figure 6.1: COD fractions S_S (light grey), X_S (grey), S_I (dark grey) and X_I (black) of LS-WW collected in three different days, expressed in mg/L.

6.4.2. High-strength wastewater (HS-WW)

The HS-WW came from the boilers of the factory, as well as the processing of liquid-by products containing fats and oils. Thus, the concentrations of all the pollutants were considerably higher compared to the LS-WW. It presented less variability and lower salt concentrations (Table 6.2). In addition, the biodegradable fraction was considerably higher, being more than a 90 % of the total COD (Figure 6.2). The main product that was cooked in the boilers was tuna.

Table 6.2: average values of the characterisation of HS-WW.

Parameter	Unit	Value
Conductivity (mS/cm)	mS/cm	18.0 ± 3.6
pH	-	6.59 ± 0.23
Total Suspended Solids	g/L	2.37 ± 1.79
Volatile Suspended Solids	g/L	1.07 ± 0.26
Total COD	g/L	10.8 ± 4.9
Soluble COD	g/L	7.3± 2.2
Greases	g/L	1.6 ± 1.2
Volatile Fatty Acids	g COD/L	3.3 ± 2.3
Ammonia	g N/L	0.56 ± 0.39
Total nitrogen	g N/L	1.02 ± 0.12
Phosphate	g P/L	0.13 ± 0.07
Proteins	g/L	2.06 ± 0.30
Carbohydrates	g/L	0.51 ± 0.72
Chloride	g Cl^-/L	4.21 ± 1.01
Sulphate	g SO_4^{-2}/L	0.25 ± 0.04
Sodium	g Na^+/L	2.77 ± 0.60
Salt	g NaCl/L	7.41 ± 2.06

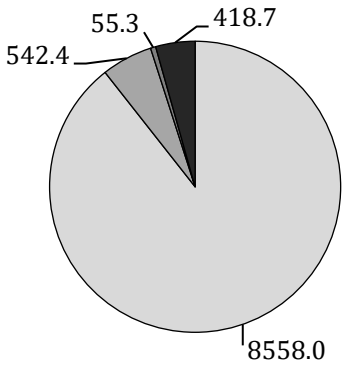

Figure 6.2: COD fractions S_S (light grey), X_S (grey), S_I (dark grey) and X_I (black) of HS-WW, expressed in mg/L.

6.4.3. Current wastewater treatment of the factory

The current wastewater treatment of the factory was designed to treat the LS-WW stream and consisted of four units (Appendix A). Firstly, the wastewater passed through a rotary drum, to remove the big solids, and small volumes of HS-WW (0:100 – 4:96 % v/v ratio) were added sometimes to this stream. Then, a Dissolved Air Flotation (DAF-1) unit removed the suspended solids and greases. The effluent of the DAF was pumped to a physicochemical unit (PCh-2), where coagulants and flocculants were added to remove the particulate matter of the water. Then, the last unit of the treatment was another DAF (DAF-3), where the sludge produced in the previous unit was removed. The total amount of sludge separated from the DAF units of the wastewater treatment plant (DAF-1 + DAF-3) was of 1 t/week. The residence time of the wastewater in this treatment plant (DAF-1 + PCh-2 + DAF-3) was about 30 min.

The produced HS-WW was stored in a tank of 250 m^3 (STO-4). When the volume of wastewater was near the maximum capacity of the tank, a part of the wastewater was mixed with the LS-WW and treated in the previously described wastewater treatment plant. The volume of wastewater, as well as the frequency of emptying of the tank, depended on the specific production of the plant.

6.5. AGS PILOT PLANT DESCRIPTION

The design and operation of the pilot plant were part of the activities performed in the frame of the LIFE SEACAN project (LIFE14 ENV/ES/000852). The main objective of the project was the reduction of the pressure applied by the fish canneries on the Galician marine ecosystem. To do that, two aerobic biofilm-based technologies were selected to be tested at pilot scale, located in a factory of the coast of Galicia. The selected alternatives were Moving Bed Biofilm Reactor (MBBR) and AGS technology. Afterwards, the effect of the wastewater treatment was studied in the benthic ecosystem near the point of discharge of the specific company. The partners of the project were CETaqua Galicia (coordinators of the project), CETaqua Barcelona (experts in MBBR technology),

University of Santiago de Compostela (experts in AGS technology) and University of Vigo (experts in benthic ecosystems monitoring).

The design of the AGS pilot plant was done in collaboration with CETaqua Galicia, considering the characteristics of the wastewater that was going to be treated. The prototype was constructed in a 20-ft standard container. It was constituted by 5 units: a rotary drum, a grease separator tank, a buffer tank, the AGS reactor and a settler. A scheme of the pilot plant and the dimensions of the units are provided in Appendix B and C. The buffer tank and the settler were located inside the container, whereas the rest of the units were outside.

6.5.1. Pilot AGS reactor pre-treatments

Depending on the type of incoming wastewater, different pre-treatments were needed before feeding the AGS reactor, to avoid operational problems. The aim of the pre-treatment scheme was the removal of solids and greases.

Low-strength wastewater

The LS-WW was collected from DAF-1 of the wastewater treatment of the factory (pump P-01). It was taken from a point located at mid-height of the tank, to avoid the presence of the solids from the bottom and the greases from the upper part of the liquid column.

The pre-treatment of the LS-WW in the pilot plant consisted of a rotary drum (RD-01, Appendix B) to remove the solids of the wastewater. The filter had a grating mesh of 0.15 mm. It was located outside the container and in an elevated position (1 m over the container), to let the outlet stream move by gravity to the next unit.

This unit removed the big solids present in the wastewater, like pieces of vegetables, fish or fishbone. The presence of this kind of solids after the DAF-1 of the factory was due to the short residence time, so that part of the solids from the wastewater was not removed. Approximately 60 g of solids per m^3 of wastewater were separated. It was necessary to clean the rotary drum with water at least once a week, to avoid the clog of the grating mesh due to the presence of greases.

High-strength wastewater

The HS-WW was collected from the storage tank of the factory (STO-4). A submersible pump (P-02) was introduced inside the tank, in the middle of the liquid column, to avoid the layer of greases from the top and the layer of solids from the bottom. The pump had a buoy, to avoid the collection of greases and solids if the level of water was too low.

The greases and solids content of the HS-WW was considerably high compared to the LS-WW. Since the factory did not have a unit to remove the greases and the solids of this stream, it was necessary to add one in the pre-treatment line of the pilot plant.

The unit consisted of a grease-separation tank (GS-02, Appendix B), with a useful volume of 3 m^3 (diameter of 1.72 m), located outside the container. It was fed from the top and the outlet was located at mid-height of the tank. In this tank, the remaining solids settled to the bottom and

the greases floated to the upper part. The minimum hydraulic retention time was of 2 h. After that, the wastewater was pumped (pump P-03) to the next unit of the pilot plant.

To determine the hydraulic retention time of the grease separator, laboratory tests were previously performed. Firstly, a static test was done, to determine the optimal retention time to achieve high grease separation efficiencies. Then, the determined retention time was imposed in a dynamic test, to confirm that the removal efficiency was maintained operating in a continuous mode. Afterwards, a comparison between a continuous aerated and non-aerated system was done, to study the effect of aeration in the greases separation. The operational conditions, as well as the composition of the wastewater used in the tests, are shown in Table 6.3.

Table 6.3: Operational conditions and wastewater composition of the grease-separation tests.

	Test 1	**Test 2**	**Test 3**
Operational conditions of the test			
Type of test	Static	Continuous mode	Continuous with and without aeration
Volume (L)	25	5	3
Duration (h)	24	8	8 each test
Hydraulic retention time (h)	-	2	2
Temperature (°C)*	25	25	37
Airflow (L/min)	-	-	2 (only in the test with aeration)
Characterisation of the wastewater			
Total COD (g/L)	18.6	18.6	6.6
Greases (g/L)	3.0	3.0	0.4
Proteins (g/L)	2.5	2.5	1.9
Carbohydrates (g/L)	0.4	0.4	1.5
VFAs (g COD/L)	4.6	4.6	0.6
TSS (g/L)	4.4	4.4	0.9

*The temperature of the test was selected to reproduce the conditions of the wastewater when it was taken from the storage tank of the factory.

In the first test, done in static conditions, a volume of 25 L of wastewater was introduced in a tank, and time was given to let the solids settle and the greases float. Samples were taken within time at mid-height of the water column to determine the separation of solids and greases. The results showed grease removal of 80 % and solids removal of 68 % after 2 h (Figure 6.3). This time was selected for the appropriated separation of solids and grease.

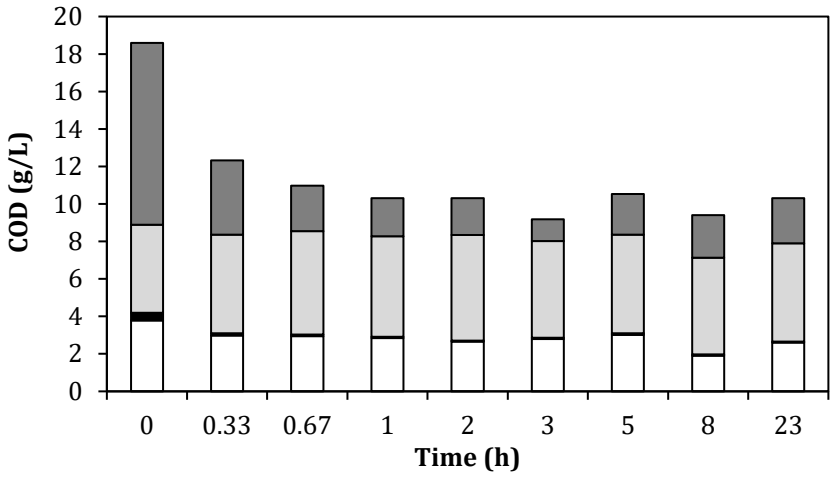

Figure 6.3: Evolution of the different fractions of COD within time of the static test. Proteins (white), carbohydrates (black), volatile fatty acids (light grey) and greases (dark grey) were measured throughout time during the experiment.

In the second test, in dynamic conditions, a tank (5 L) was fed and discharged in a continuous mode, at a hydraulic retention time of 2 h (determined as adequate time in the previous test). The wastewater came from the same batch as that of the previous test, and the effluent was characterised to determine the solids and greases concentration. The results of the test were similar to the previous one, with grease removal efficiencies of 86 % and solids removal of 67 % (Figure 6.4.a).

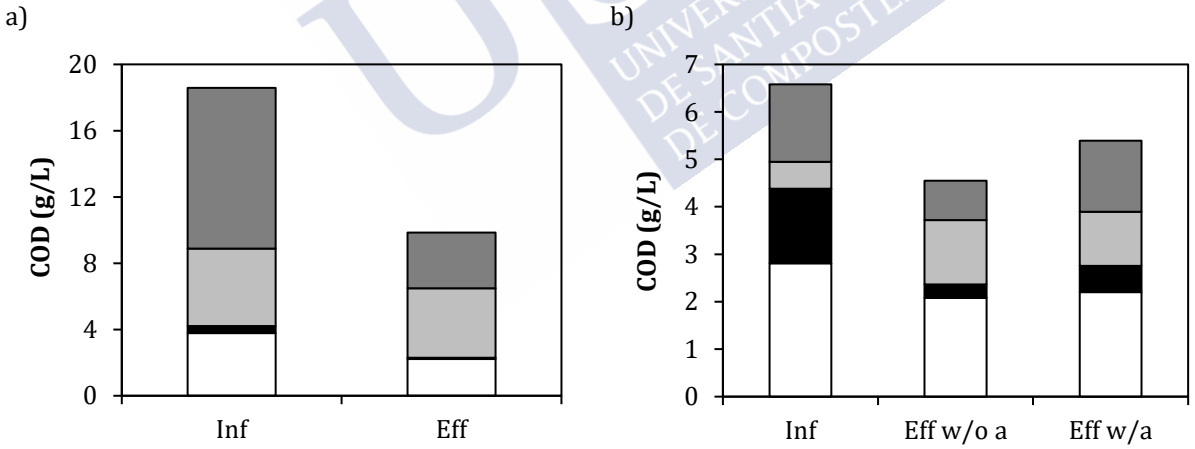

Figure 6.4: (a) Fractions of COD of the influent (Inf) and effluent (Eff) of the first dynamic test. (b) Fractions of COD of the influent (Inf), effluent without aeration (Eff w/o a) and effluent with aeration (Eff w/a) of the second dynamic test. Proteins (white), carbohydrates (black), volatile fatty acids (light grey) and greases (dark grey) were measured.

In the third test, a tank of 3 L was fed and discharged in a continuous mode. It was firstly operated without aeration, and then the experiment was repeated with air supply. The fed wastewater, in this case, came from a different batch, and the effluent characterisation with and without aeration was compared. In this case, the removal efficiencies were lower than in the previous tests, because the initial content of both greases and solids was lower. The results

showed that aeration did not suppose an improvement in the separation (Figure 6.4.b). Without aeration, removal efficiencies of 24 and 28 % were achieved for greases and solids, respectively. In the aerated test, there was no grease removal and the solid removal was of 19 %.

In the grease separator, the upper layer of greases was removed manually from the tank twice a week. Approximately 1.78 kg of sludge was separated per m^3 of wastewater. This sludge presented a density of 0.86 g/L and a total and volatile solid content of 0.13 and 0.12 g/L, respectively. In addition, a purge of solids was made from the bottom of the reactor once a week.

The outlet of both the rotary drum and the grease separator was pumped to a buffer tank (BT-03, Appendix B) previous to the reactor, located inside the container. It had a working volume of 3 m^3 (diameter of 1.72 m), with capacity to store water for two AGS operational cycles, operating at a 100 % of the useful volume of the reactor. It had a valve at the bottom to remove the settled solids, and a mechanical stirrer (MS-02) to mix the wastewater after its collection.

To control the loading rate applied to the reactor, the fraction of each type of wastewater (% v/v) added to the buffer tank was selected in the control system. Images of all the pre-treatment units of the pilot plant are provided in Figure 6.5.

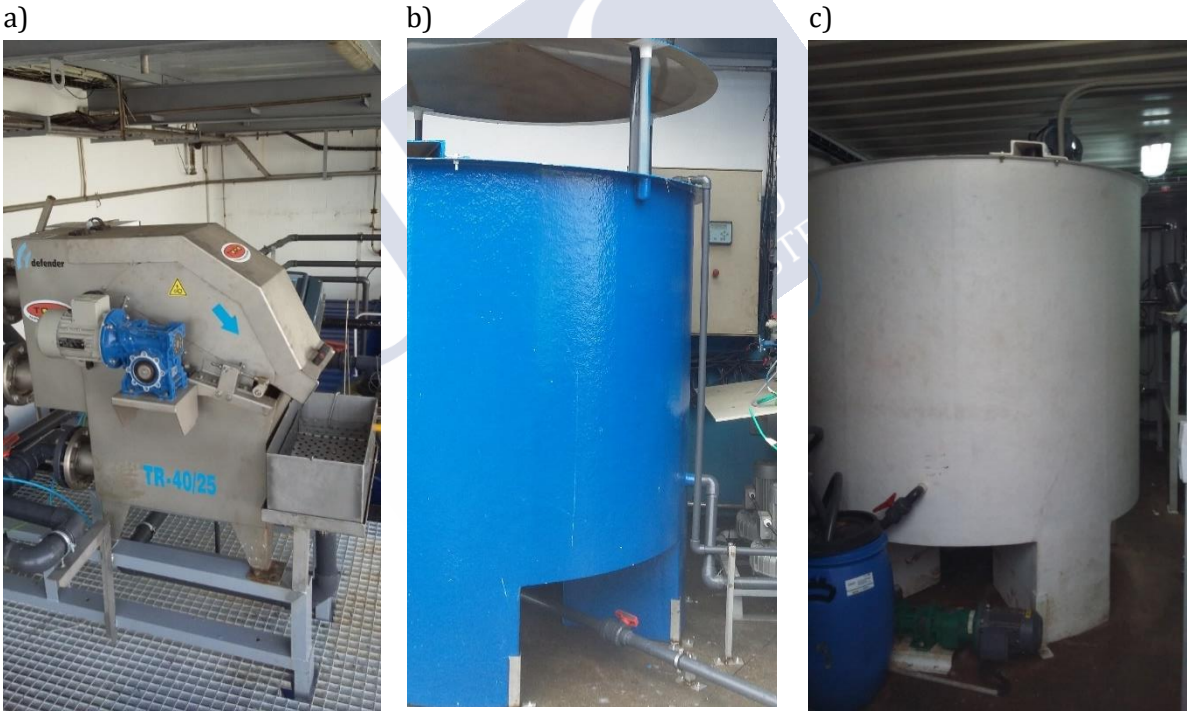

Figure 6.5: Images of: (a) rotary drum (RD-01) of the LS-WW pre-treatment; (b) grease separator (GS-02) of the HS-WW pre-treatment; (c) buffer tank (BT-03).

6.5.2. Pilot plant reactor

The AGS reactor (GR-04, Appendix B) was located outside the container (Figure 6.6.a). It was designed to have a maximum total height of 4 m, because of requirements of the factory. It had a useful volume of 3 m^3, with a useful height of 3 m and a diameter of 1.42 m. In the factory, it was

located in a place where it was possible to access to the upper part by stairs and a platform, that were already installed in the factory.

The reactor was fed from the top (pump P-04), and had five outlet ports at different heights, corresponding to the 20, 40, 60, 80 and 100 % of the working volume. Thus, it was possible to vary the Volume Exchange Ratio (VER) by choosing different outlet ports, and to take samples at different heights as well. In addition, the bottom was conical and provided with a valve to allow the purge of solids. A mechanical stirrer was installed (MS-03), to be used in case of the application of low airflows to assure a good mixture inside the reactor. Furthermore, in the upper part four probes were located, to measure in a continuous mode pH, conductivity, redox potential and dissolved oxygen concentration (Figure 6.6.b).

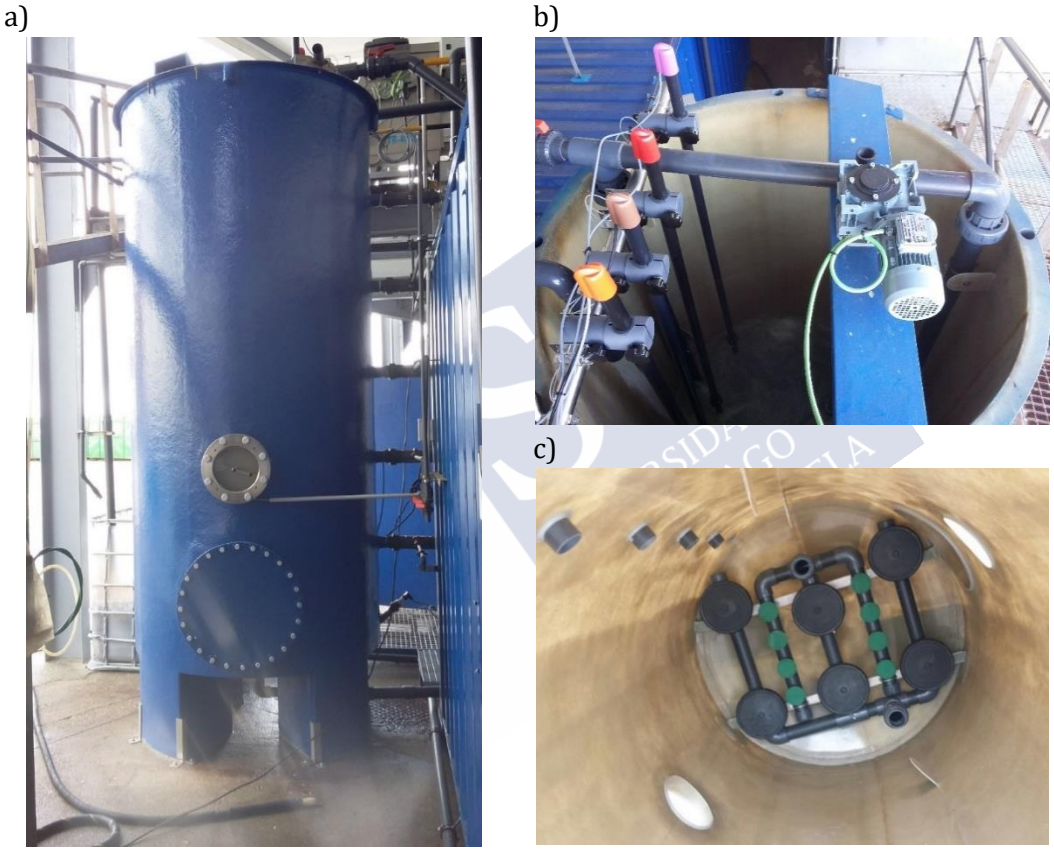

Figure 6.6: Images of: (a) aerobic granular sludge reactor (GR-04); (b) upper part of the reactor; (c) air diffusers distribution.

The air diffusers were located at the bottom (Figure 6.6.c). A mixture of fine and coarse bubble diffusers was selected, to assure a high airflow, as well as a good mass transfer. Each type of diffusers had an independent pipeline, to avoid the formation of preferential paths due to the different pressure drops. Different configurations of the diffusers were initially proposed, and the final option was selected after a study by Computational Fluid Dynamics made by a subcontracted institution subcontracted within the framework of the LIFE SEACAN project.

6.5.3. Pilot AGS reactor post-treatment

The effluent of the reactor was pumped (P-05) to a settler (ST-05, Appendix B), located inside the container, with the purpose of reducing the solids and total COD content to produce an effluent with good quality. It had a working volume of 3 m^3, with a diameter of 1.5 m. To discharge the effluent, it had a buoy connected to the discharge tube, so that the effluent was always discharged from the top of the liquid column (Figure 6.7). With this system, the discharge of solids present in the lower layers of the settler was avoided.

a) b)

Figure 6.7: Images of (a) settler (ST-05); (b) buoy of the settler.

6.5.4. Control system

To control de operation of the pilot plant, a Programmable Logic Controller (PLC) Siemens SIMATIC S2-300 was used. All the equipment connected to the PLC (pumps, mechanical stirrers, air blower, valves) could work in automatic or manual mode, and there was also the possibility to stop them. The automatic mode was activated by default, the manual mode was only used in specific cases, and the stop mode was activated during the stops of the plant and the non-working times of each equipment.

All the tanks were provided with a level sensor and low and high-level alarms, to stop the functioning of their respective pumps, mechanical stirrers and/or air blower. In addition, the PLC allowed the definition of the filling volume of the buffer tank of each type of wastewater, as well as the working volume of the reactor and the specific outlet to discharge the effluent. In the PLC it was also possible to define the working time of each unit of the plant. It allowed for the definition of the different stages of the operational cycle of the reactor, as well as the working time of units dedicated to secondary activities, like the filling or emptying of the tanks (Table 6.4).

Table 6.4: Example of an operational cycle distribution of the AGS pilot plant, corresponding to the treatment of HS-WW.

	Feeding	**Aerobic reaction**						**Settling**	**Discharge**	**Idle**
P-01										
P-02										
P-03										
MS-01										
P-04										
MS-02										
B-01										
MS-03										
P-05										
VA-02										
VA-03										
VA-04										
VA-05										
VA-06										
VA-07										
Time (min)	**10**	**90**	**60**	**60**	**2**	**75**	**47**	**5**	**10**	**1**

The first stage of the cycle was the feeding of the reactor (pump P-04). Then, during the aerobic reaction stage, air was provided to the reactor by B-01. At the beginning of this stage, P-03 was activated to pump the HS-WW from the grease separation unit to the buffer tank. Then, the LS-WW was also pumped (P-02) to the buffer tank. At the same time, P-01 was switched on to fill the grease separator with HS-WW. The incoming HS-WW was mixed with the remaining wastewater of the separation tank (MS-01 switched on). At the end of the aeration stage, the settler was emptied by opening the valve VA-07. In the discharge phase, the pump P-05 and the valve VA-05 (mid-height of the reactor), were activated to withdraw the effluent of the reactor. During the settling stage, as well as the idle phase, all the devices were switched off. When the influent of the pilot plant was only LS-WW, the cycle distribution was the same, but all the devices associated with the pretreatment of the HS-WW (P-02, P-03, MS-01) were deactivated.

6.6. OPERATIONAL STRATEGY

The AGS pilot plant treated the two produced streams of the factory: LS-WW and HS-WW. Its operation was divided in different stages, depending on the type of incoming wastewater (the experimental results will be presented in the next chapter). The cycle length, as well as the VER, were selected to avoid applied OLRs higher than 6 kg $COD_S/(m^3 \cdot d)$.

The strategy of operation was designed to cope with the fluctuating production of wastewater in the factory associated with the non-working days. The company stopped its production during weekends and holidays. In the short stops, the production was stopped but the DAF of the LS-WW treatment and the storage tank of HS-WW remained full of water. In July and December, the factory was closed for two weeks, and all the tanks were emptied and cleaned.

When LS-WW was treated, operational cycles of 3 h with a VER of 50 % were selected to remove the COD and nitrogen. During the short stops, the available wastewater to feed the pilot plant corresponded to the capacity of the DAF of the factory (14 m^3). To avoid the stop of the pilot plant, during the weekends the cycle length was extended to 6 h. If the plant stopped the production for more than 3 days, the VER was also reduced, and the settling time was modified to maintain the same imposed settling velocity. The VER depended on the number of non-working days of the plant, but it was always higher than 30 %.

When HS-WW was treated, it was diluted with LS-WW (in a ratio 25/75 – 50/50 % v/v) (Table 6.5), and operational cycles of 6 h with a VER of 50 % were selected. When the AGS reactor was operated at maximum OLR (6 kg COD_S /(m^3·d)), the mixture of the feeding was of 50 – 50 (% v/v) of HS-WW – LS-WW. During weekends, and other short stops, the volume of available LS-WW was of 14 m^3 (capacity of the DAF), whereas the volume of available HS-WW corresponded to the storage capacity of the tank of the factory (250 m^3). However, the availability of HS-WW was not always guaranteed, since the storage tank was not always full of water (it depended on the production of the factory). During the short stops, the cycle length of the reactor was extended to 8 h, with the consequent modification of the settling time to maintain the same settling velocity.

Table 6.5: HS-WW / LS-WW mix used as feeding of the pilot plant.

Type of treated wastewater	**HS-WW / LS-WW mix (% v/v)**	**Mixing point**
LS-WW	0/100 – 4/96	Inlet of the WWTP of the factory (mix done by the factory)
HS-WW	25/75 – 50/50	Buffer tank of the AGS pilot plant

During summer and winter holidays (stops of 2 weeks), the same strategy was applied when treating LS-WW and HS-WW to avoid the stop of the pilot plant. Before the stop, 4 – 5 containers of 1 m^3 were filled with HS-WW. During the stops, the reactor was manually fed, by using a submersible pump, with the stored wastewater, and longer cycles were established (1 – 3 days). The manual feeding consisted of the addition of HS-WW from the storage containers to the buffer tank, located previously to the reactor of the pilot plant, with a submersible pump.

6.7. CONCLUSIONS

To treat the wastewater of a fish cannery by AGS technology the pilot-scale plant designed was constituted by five units: a rotary drum, a grease separator, a buffer tank, an AGS reactor and a settler.

The LS-WW needed a pre-treatment to remove the solids present in the wastewater before being fed to the reactor, which consisted of a rotary drum with a grating-mesh filter of 0.15 mm. The HS-WW also needed a pre-treatment consisting of the removal of grease and solids. The experiments performed to design the grease separation unit indicated that the minimum residence time was of 2 h, in order to obtain removal efficiencies above 80 %.

The cycle distribution of the AGS reactor included a short feeding, followed by aerobic reaction, settling, discharge of the effluent and idle phase. In addition, the working time of units dedicated to secondary activities was defined.

The operational strategy of the AGS reactor was designed to cope with the routines of the factory and avoid a complete stop of the AGS during the non-working days. To do that, the length of the cycles was modified depending on the duration of the stops.

6.8. REFERENCES

AMEC Earth & Environmental Limited, 32 Troop Ave, U. #301, 2003. Management of Wastes from Atlantic Seafood Processing Operations, B3B 1Z1. ed. Dartmouth, Nova Scotia

APHA/AWWA/WEF, 2012. Standard Methods for the Examination of Water and Wastewater. Stand. Methods 541. https://doi.org/ISBN 9780875532356

Appels, L., Baeyens, J., Degrève, J., Dewil, R., 2008. Principles and potential of the anaerobic digestion of waste-activated sludge. Prog. Energy Combust. Sci. https://doi.org/10.1016/j.pecs.2008.06.002

Chowdhury, P., Viraraghavan, T., Srinivasan, A., 2010. Biological treatment processes for fish processing wastewater - A review. Bioresour. Technol. https://doi.org/10.1016/j.biortech.2009.08.065

Colic, M., Morse, W., Hicks, J., Lechter, A., Miller, J.D., 2012. Case Study: Fish Processing Plant Wastewater Treatment. Proc. Water Environ. Fed. https://doi.org/10.2175/193864707787781557

Cristóvão, R.O., Botelho, C.M., Martins, R.J.E., Loureiro, J.M., Boaventura, R.A.R., 2014. Primary treatment optimization of a fish canning wastewater from a Portuguese plant. Water Resour. Ind. https://doi.org/10.1016/j.wri.2014.07.002

Dreywood, R., 1946. Qualitative Test for Carbohydrate Material. Ind. Eng. Chem. - Anal. Ed. https://doi.org/10.1021/i560156a015

Figueroa, M., Mosquera-Corral, A., Campos, J.L., Méndez, R., 2008. Treatment of saline wastewater in SBR aerobic granular reactors. Water Sci. Technol. https://doi.org/10.2166/wst.2008.406

Hung, Y.-T., Show, K.-Y., Tay, J.-H., 2005. Seafood Processing Wastewater Treatment, in: Waste Treatment in the Food Processing Industry. https://doi.org/10.1201/9781420037128.ch2

Lowry, O.H., Rosebrough, N.J., Farr, A.L., Randall, R.J., 1951. Protein measurement with the Folin phenol reagent. J. Biol. Chem.

Soto, M., Veiga, M.C., Mendez, R., Lema, J.M., 1989. Semi-micro C.O.D. determination method for high-salinity wastewater. Environ. Technol. Lett. 10, 541–548

APPENDIX A: Scheme of the wastewater treatment plant of the fish-canning factory

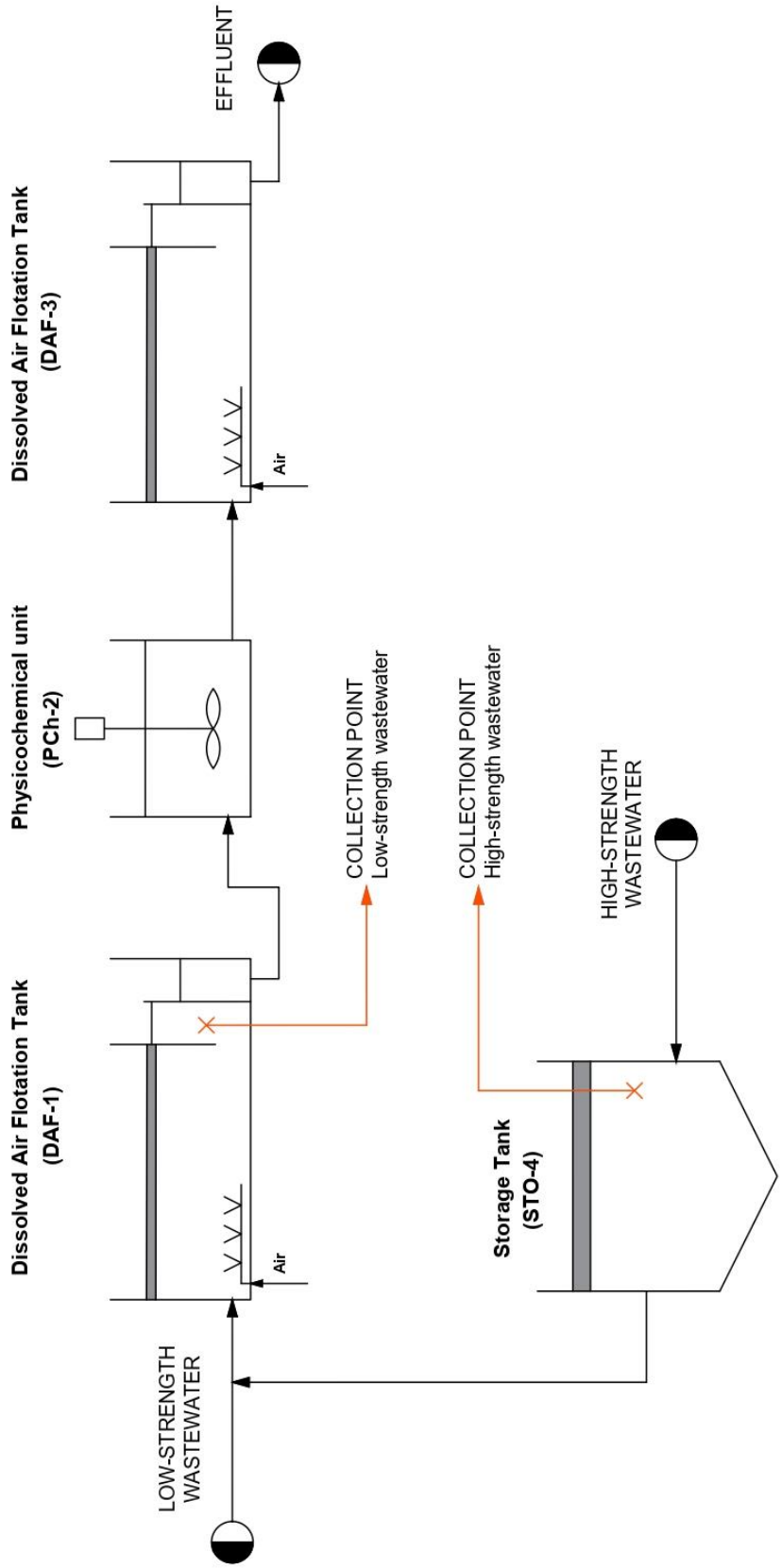

APPENDIX B: Scheme of the AGS pilot plant

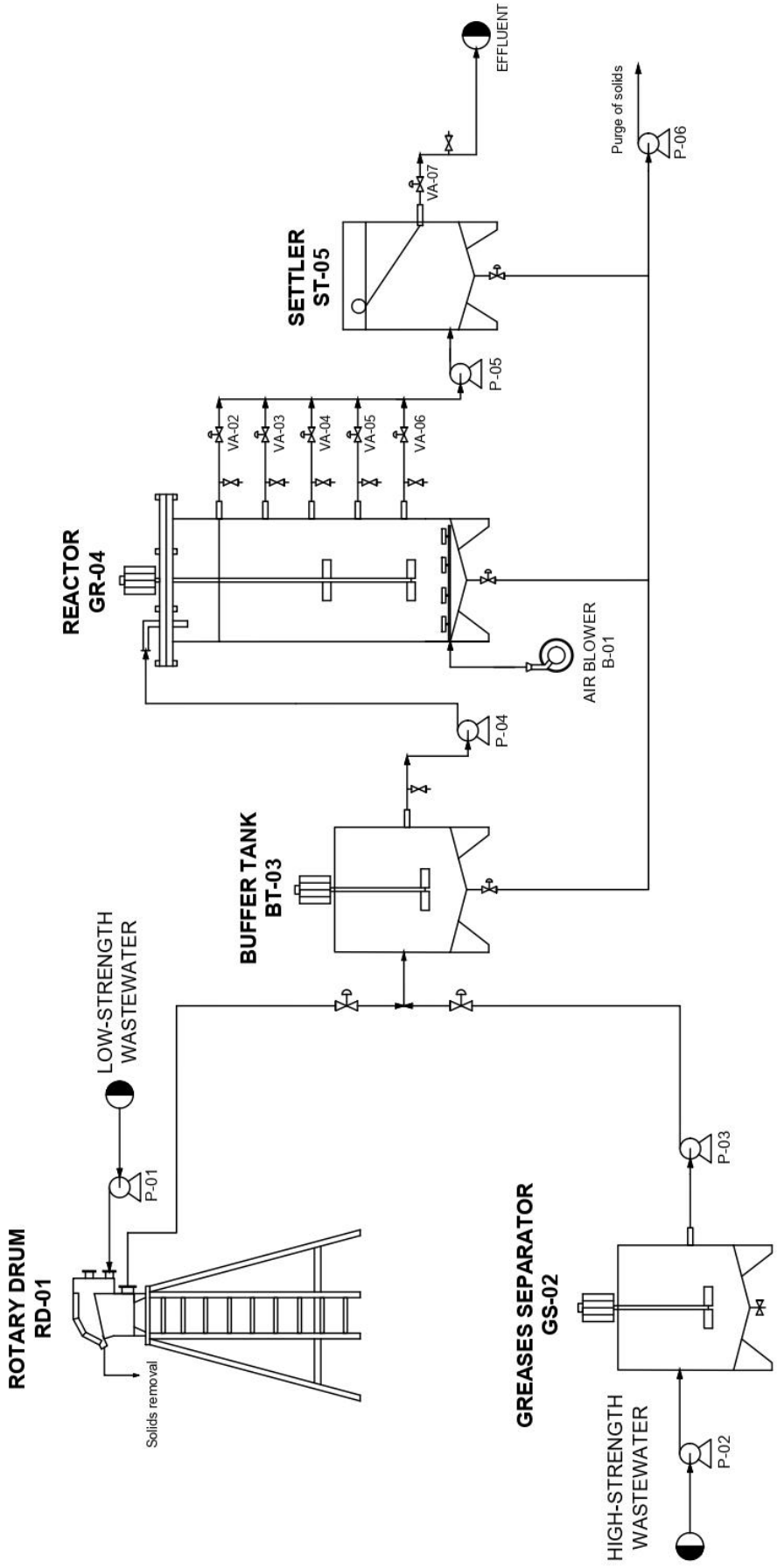

APPENDIX C: Dimensions of the units of the pilot plant

	GS-02	BT-03	GR-04	ST-05
Working volume (m^3)	3	3	3	3
Diameter (m)	1.72	1.72	1.42	1.5
Total height (m)	2	2	3.5	1.5
Working height (m)	1.5	1.5	3	1
Mechanical stirrer*	Yes	Yes	Yes	No
Location	Outside the container	Inside the container	Outside the container	Inside the container

*Mechanical agitation was provided by a centrally-mounted axial impeller.

Chapter 7

Pilot-scale AGS reactor operation for *in situ* fish-canning wastewater treatment

Summary

In this chapter, the operation of the pilot-scale Aerobic Granular Sludge (AGS) sequencing batch reactor designed in Chapter 6 was described. The fully aerobic pilot-scale AGS reactor had a working volume of 3 m^3 and was located in a fish cannery to treat the produced wastewater. Two streams of the factory were treated: low-strength (LS-WW, Stages I and II) and high-strength wastewater (HS-WW, Stage III). The results of the operation showed how the use of different streams as feeding led to the growth of biomass with different properties, so that the influent composition was found to be crucial to select appropriate organisms to form granules.

When using LS-WW as feeding (Stages I and II), the first granules were observed after 1 month of operation. However, the overgrowth of filamentous bacteria occurred, due to the low concentration organic matter (COD) and nitrogen in the wastewater. Nevertheless, high COD and N removal efficiencies of 70 – 80 % were achieved. When the reactor was fed with HS-WW (Stage III), dense flocs with good settleability and small aggregates appeared, but more time was needed to achieve well-formed granules. The COD removal efficiencies were high (80 – 90 %) and more stable than in Stage I, but the N removal efficiencies were lower (30 %), only attributed to biomass growth.

The changes in the cycle length during stops of the factory on the weekends did not have a big impact on the overall performance of the reactor. The average removal efficiencies before and after the stops were similar. When treating LS-WW they were 56 and 60 % on Fridays and Mondays, respectively. When the reactor was fed with HS-WW they were of 89 % on Fridays and 86 % on subsequent Mondays. The long stops (summer and winter holidays) affected the physical properties more than the removal efficiencies of the biomass. However, the system was able to recover after one week of normal operation.

OUTLINE

Chapter 7 151

7.1. INTRODUCTION 153

7.2. OBJECTIVES 154

7.3. MATERIALS AND METHODS 154

7.3.1. Experimental set-up 154

7.3.2. Operational conditions 154

7.3.3. Analytical methods 156

7.4. RESULTS AND DISCUSSION 156

7.4.1. Low-strength wastewater treatment. Stages I and II 156

7.4.2. High-strength wastewater treatment. Stage III 167

7.4.3. AGS effluent post-treatment 169

7.4.4. Effluent quality 170

7.5. CONCLUSIONS 171

7.6. REFERENCES 172

7.1. INTRODUCTION

Different laboratory-scale research works have demonstrated the suitability of Aerobic Granular Sludge (AGS) technology for the treatment of industrial wastewater, including fish-canning wastewater, as discussed in Chapter 5. In all the studies that used AGS to treat effluents from fish canneries (Carrera et al., 2019; Corsino et al., 2016; Val Del Río et al., 2013), the granulation process was completed after 70 – 170 days. The achieved removal efficiencies were of 80 – 100 % and 40 – 80 % for Chemical Oxygen Demand (COD) and Nitrogen (N), respectively.

The scale-up of the AGS technology to pilot-scale has been reported to have issues which are not present at laboratory-scale, and granule formation courses are different. First of all, in laboratory-scale reactors, environmental factors like the wastewater influent concentrations or temperature can be precisely controlled and the feeding characteristics are very stable (Liu et al., 2010). When operating at pilot-scale, there are more fluctuations in the feeding associated with the operational changes of the factory. In addition, at laboratory-scale, it is possible to inoculate or bioaugment with aerobic granules, whereas at pilot-scale it is not feasible. Moreover, the scale-up involves changes in the hydrodynamic conditions inside the reactor, which can affect the granulation process. The aeration pattern, as well as the gas distribution inside the reactor, need to be optimised and, if it is not the case, this fact might eventually hinder biomass granulation (Pishgar et al., 2018).

Only a few studies addressed the wastewater treatment with pilot-scale AGS reactors. The granulation and performance of the AGS system were studied using as influent synthetic, urban and industrial wastewater. Depending on the type of wastewater and the COD concentration of the influent, the length of the granulation periods oscillated between a few days and several months, although a correlation between both parameters is not evident.

The works addressing municipal sewage treatment with AGS have reported granulation periods between 80 – 300 days with applied Organic Loading Rates (OLRs) of 0.5 – 2 kg $COD_S/(m^3 \cdot d)$ and influent soluble COD (COD_S) concentrations of 270 – 500 mg/L (De Kreuk et al., 2006; Ni et al., 2009; Rocktäschel et al., 2015). When treating septic tank sewage, the granulation time was shorter (40 – 50 days) due to higher OLRs between 2.7 – 4.5 kg COD_S $/(m^3 \cdot d)$ (COD_S of 200 – 800 mg/L) (Li et al., 2014; Long et al., 2014). In general, the use of municipal sewage as feeding led to the production of small granules, with average particle diameters of 1 mm or less. In all the studies, the removal efficiencies oscillated between 75 – 85 % and 60 – 70 % for COD and N, respectively.

Regarding the industrial wastewater treatment, the OLRs were often higher than sewage treatment (2 – 4.5 kg $COD_S/(m^3 \cdot d)$) due to higher influent COD_S concentrations (1 – 3 g/L) (Dobbeleers et al., 2020; Farooqi and Basheer, 2017; Morales et al., 2013; Wei et al., 2013). The granulation time was reported to last between 30 – 180 days, and bigger aggregates were obtained compared to municipal wastewater (average size of 1 – 4 mm). The average removal efficiencies were of 70 – 90 % for both COD and N in all the works.

The main bottlenecks identified when operating at pilot-scale were the long start-up periods and slow granulation process that could take several months. In addition, the long-term stability of the reactor was difficult to maintain, especially when there were fluctuations in the feeding composition and flowrate. Besides, the impact of salinity on the granulation process and the

performance of the reactor at pilot scale has not been studied yet. All the research works previously presented used non-saline wastewater as feeding. In addition to the salt content, some factories, like fish canneries, do not produce wastewater in a continuous mode, since they have stops of the production depending on the availability of processed product. The effects of modifying the operational conditions due to the lack of available wastewater on granulation and the performance of the AGS reactor, have not either been studied yet.

7.2. OBJECTIVES

The objective of this study was to evaluate the feasibility of treatment of fish-canning wastewater in a pilot-scale AGS reactor operated in situ in a fish cannery. Special attention was paid to the influence of the type of wastewater and its fluctuations in composition and flowrate on the granulation process and reactor performance.

7.3. MATERIALS AND METHODS

7.3.1. Experimental set-up

A pilot-scale Sequencing Batch Reactor (SBR), with a working volume of 3 m^3, located in a fish-canning factory in the NW of Spain, was started-up. It was fed from the top, and the Volume Exchange Ratio (VER) of each cycle varied between 37 – 50 %. A mixture of fine and coarse bubble diffusers, located at the bottom of the reactor, provided an airflow of 40 – 75 m^3/h and a Superficial Gas Velocity (SGV) of 0.7 – 1.4 cm/s. A Programme Logic Controller (PLC) Siemens SIMATIC S2-300 was used to control the working time of the different devices and the operational cycles length and distribution. A detailed description of the reactor, as well as the rest of the units of the pilot plant, is given in Chapter 6.

7.3.2. Operational conditions

The factory, where the prototype was located in, produced two types of wastewater: low-strength (LS-WW) and high-strength wastewater (HS-WW). The LS-WW was produced in washing processes, whereas the HS-WW stream came from the fish cookers. The wastewater was pumped directly from the tanks of the factory to the pre-treatment line of the pilot plant and it was conducted to a small buffer tank placed before the reactor, so that the feeding of the AGS reactor fluctuated as the factory production did. Each of the two streams had an independent pre-treatment before being pumped to the buffer tank. Detailed information about the characterisation of the two streams produced in the cannery, as well as the corresponding pre-treatment units, is given in Chapter 6.

The operation of the AGS prototype was divided in three stages. It was firstly operated treating LS-WW with useful volumes of 2 m^3 (Stage I) and 3 m^3 (Stage II), respectively. Then, the reactor was fed with HS-WW, diluted with LS-WW (Stage III). The operational conditions of each stage are shown in Table 7.1. The working capacity of the pilot SBR at maximum loading rate was 12 m^3/day and 4.8 m^3/day for LS-WW and HS-WW, respectively.

Table 7.1: Operational conditions in the different operational stages of the pilot-scale AGS.

	STAGE I	STAGE II	STAGE III
Operational conditions			
Operation time (days)	63	163	178
Useful volume (m^3)	2	3	3
Feeding	LS-WW	LS-WW	HS-WW
Cycle length (h)	3	3	6
VER (%)	37	50	40
Airflow (m^3/h)	40	75	79
SGV (cm/s)	0.7	1.3	1.4
OLR (kg $COD_S/m^3 \cdot d$)	2.0 ± 0.6	1.5 ± 1.3	3.9 ± 2.0
Wastewater characterisation			
COD_T (g/L)	1.47 ± 0.98	1.33 ± 1.18	3.20 ± 1.53
COD_S (g/L)	0.56 ± 0.28	0.37 ± 0.21	2.41 ± 1.28
TN (mg/L)	36.7 ± 22.2	9.2 ± 8.9	269.4 ± 155.9
NH_4^+-N (mg/L)	24.6 ± 19.2	8.8 ± 7.7	265.6 ± 193.9
Salinity (g NaCl/L)	8.4 ± 2.2	10.7 ± 5.4	8.4 ± 3.9

Each operational cycle included a short feeding, followed by an aerobic reaction, a short settling period, the discharge of the effluent and an idle phase (Table 7.2). In order to promote the formation and selection of granular biomass, the settling time was gradually shortened during the operation of the prototype. In this way, fast settling velocities were imposed to the biomass to select for dense biomass with good settleability. The time reduced in the settling stage was added to the reaction period. In Stage I, the settling time was initially 15 min, and was diminished to 5 min on day 17. In Stage II, it started in 30 min and was decreased to 20 min (day 7), 15 min (day 27), 10 min (day 44), 7 min (day 90) and 5 min (day 118). In Stage III, it was reduced from 15 min (day 0) to 10 min (day 7), 7 min (day 28), 5 min (day 37) and 3 min (day 137).

Table 7.2: AGS reactor operational cycle distribution.

■					Feeding
	■				Aerobic phase
		■			Settling
			■		Withdrawal
				■	Idle phase
9	131 – 336*	30 - 3	9	1	Time (min)

*131 min corresponds to the 3-h cycle, 336 min corresponds to the 6-h cycle.

The operational strategy was designed to cope with the fluctuating production of wastewater in the fish-canning factory associated with the non-working days. Consequently, during the weekends and holiday periods, the cycle length was extended, taking into account the volume of available wastewater, to assure a continuous operation of the reactor. In Stages I and II, the cycle length was increased from 3 to 6 h. In Stage III, it was changed from 6 to 8 h.

In summer and winter periods, the factory stopped its production during 2 weeks and emptied and cleaned all the storage tanks and units of the wastewater treatment plant. To avoid

the complete stop of the prototype, it was manually fed with diluted high-strength wastewater from the factory, previously collected and stored in containers of 1 m^3. Moreover, longer cycles were established (1 – 3 days).

7.3.3. Analytical methods

The concentrations of ammonium (NH_4^+), nitrite (NO_2^-), nitrate (NO_3^-), Total Nitrogen (TN), phosphate (PO_4^{3-}), Volatile Fatty Acids (VFAs), Total Suspended Solids (TSS), Volatile Suspended Solids (VSS) and Sludge Volume Index (SVI) were measured according to the Standard Methods (APHA/AWWA/WEF, 2012). The concentrations of chloride (Cl^-), sulphate (SO_4^{2-}) and sodium (Na^+) ions were determined through Ion Chromatography (Metrohm 816 Advanced Compact IC). The COD concentration was determined according to Soto et al., (1989) taking into account the different salt concentrations of the sample. Total COD (COD_T) concentration was determined in the sample without filtering, whereas soluble COD (COD_S) concentration was measured in samples filtered through 0.45 μm pore size filters. The pH of the samples was measured with an electrode (Crison Instruments GLP22), as well as the conductivity (HACH Lange 50 60, Platinum Cell). The Dissolved Oxygen (DO) was continuously monitored with an LDO sc probe (HACH Lange) connected to a universal multichannel controller SC1000. The morphology and size distribution of the aggregates was measured with a stereomicroscope (Stemi 2000-C, Zeiss) and using an image analysis procedure (Tijhuis et al., 1994). More details about the analytical methods are given in Chapter 2.

7.4. RESULTS AND DISCUSSION

7.4.1. Low-strength wastewater treatment. Stages I and II

Stage I

The reactor was inoculated with 1 m^3 (50 % of the working volume) of activated sludge from a wastewater treatment plant adapted to salt concentrations of 15 g/L (Figure 7.1). The inoculum contained 5.00 g TSS/L and 3.67 g VSS/L, and was characterised by an SVI_5 value of 194 mL/g TSS and SVI_{30} of 86 mL/g TSS. The concentration of COD of the LS-WW ranged from 300 to 800 mg COD_S/L.

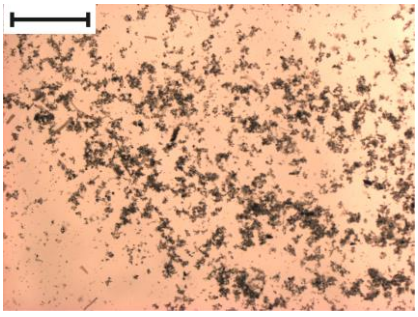

Figure 7.1: Image of the inoculum of the AGS reactor in Stage I. The size bar corresponds to 2 mm.

During the first two weeks after inoculation (days 0 – 13) there was a continuous failure of the air blowers, so that the reactor was not properly aerated. Once the problem was solved and the reactor operated normally, there was an important washout of biomass attributed to the imposed selection pressure, by means of a short settling time (reduced to 5 min on day 17), to promote the granulation process. On day 28, the biomass concentration inside the reactor decreased to 0.97 g VSS/L and remained stable until the plant was stopped on day 63 (Figure 7.2.a). Although granules were not observed, the settling properties of the biomass were considerably improved compared to those at the beginning of the operation, with salt concentrations of 6 – 10 g NaCl/L. The SVI_5 and SVI_{30} were reduced from 194 and 86 mL/g TSS on day 0 to 39 mL/g TSS (SVI_5 equal to SVI_{30}) on day 63 (Figure 7.3.a).

On day 63, samples were taken during aeration at different heights of the reactor (corresponding to the 33 and 67 % of the useful volume) to determine if the biomass concentration was homogeneous inside it. At the point corresponding to the 33 % of the volume, dark brown flocs were observed, with a biomass concentration of 0.90 g VSS/L and 1.96 g TSS/L and a SVI_5 of 48 mL/g TSS. The sample corresponding to the 66 % of the useful volume consisted of yellowish flocs, with 0.66 g VSS/L, 1.50 g TSS/L and a SVI_5 of 57 mL/g TSS. These results showed a clear stratification of biomass inside the reactor, meaning that the supplied airflow (SGV of 0.7 cm/s) was not high enough to assure a good mixing.

Long granulation periods have been previously reported in pilot-scale studies treating wastewater with low COD_S concentrations. Ni et al. (2009) operated an AGS reactor of 1 m^3 with short feeding and fully aerobic conditions to treat municipal wastewater with a COD concentration of 35 – 120 mg COD_S/L. They observed the first small aggregates after 80 days of operation, and it took approximately 10 months to achieve a system with 80 % of granules (particle size of 0.2 – 0.8 mm). Mature granules presented SVI_5 values of 30 – 40 mL/g, and biomass concentrations of 8 – 9 g VSS/L. Rocktäschel et al, (2015) treated municipal wastewater in a reactor of 0.1 m^3 with short feeding and anaerobic mixing previous to aeration. With a COD_S of 290 mg/L in the influent and the addition of acetate there were necessary approximately 100 days to complete the granulation process. In steady-state conditions, granules with an average diameter of 1.1 mm were obtained, and biomass concentrations of 3 – 8 g TSS/L were measured. Derlon et al. (2016) operated a reactor of 0.19 m^3, with anaerobic feeding, using municipal sewage as feeding with a COD_S concentration of around 130 mg/L. They obtained a system where granules represented a 60 – 70 % of the total biomass, with average SVI_{30} of 84 mL/g TSS and solids concentrations higher than 6 g TSS/L. Isanta et al. (2012) treated synthetic wastewater with COD_S concentrations of 400 mg/L in a reactor of 100 L with anaerobic feeding. They did not observe the formation of granules with an SGV of 0.8 cm/s, but the granulation process was completed after 51 days subsequent to increasing the SGV to 1.6 cm/s.

In the present research work, the SVI of the biomass (39 mL/g TSS) was in the range of abovementioned pilot-scale studies treating wastewater with low COD_S (SVI between 30 – 80 mL/g TSS). However, lower concentrations of biomass were obtained (average of 1 g VSS/L), since the operational time was shorter and a granular system was not achieved. In addition, the feeding strategies were different (most of the previous studies included an anaerobic period previous to aeration) and the treated wastewater was municipal sewage or synthetic wastewater instead of an industrial effluent. The absence of granules was presumably due to the combination of various

factors. First, the COD concentrations of the feeding were low, like in the previously described pilot-scale works. In addition, there were high fluctuations in composition, flow, salinity and changes in the operation during the weekends. Moreover, the SGV of the reactor was only of 0.7 cm/s, since the capacity of the air blower did not allow the supply of higher airflows. This value of SGV did not provide enough hydrodynamic stress to promote the granulation of the biomass, as observed by Isanta et al. (2012), and caused the stratification of biomass.

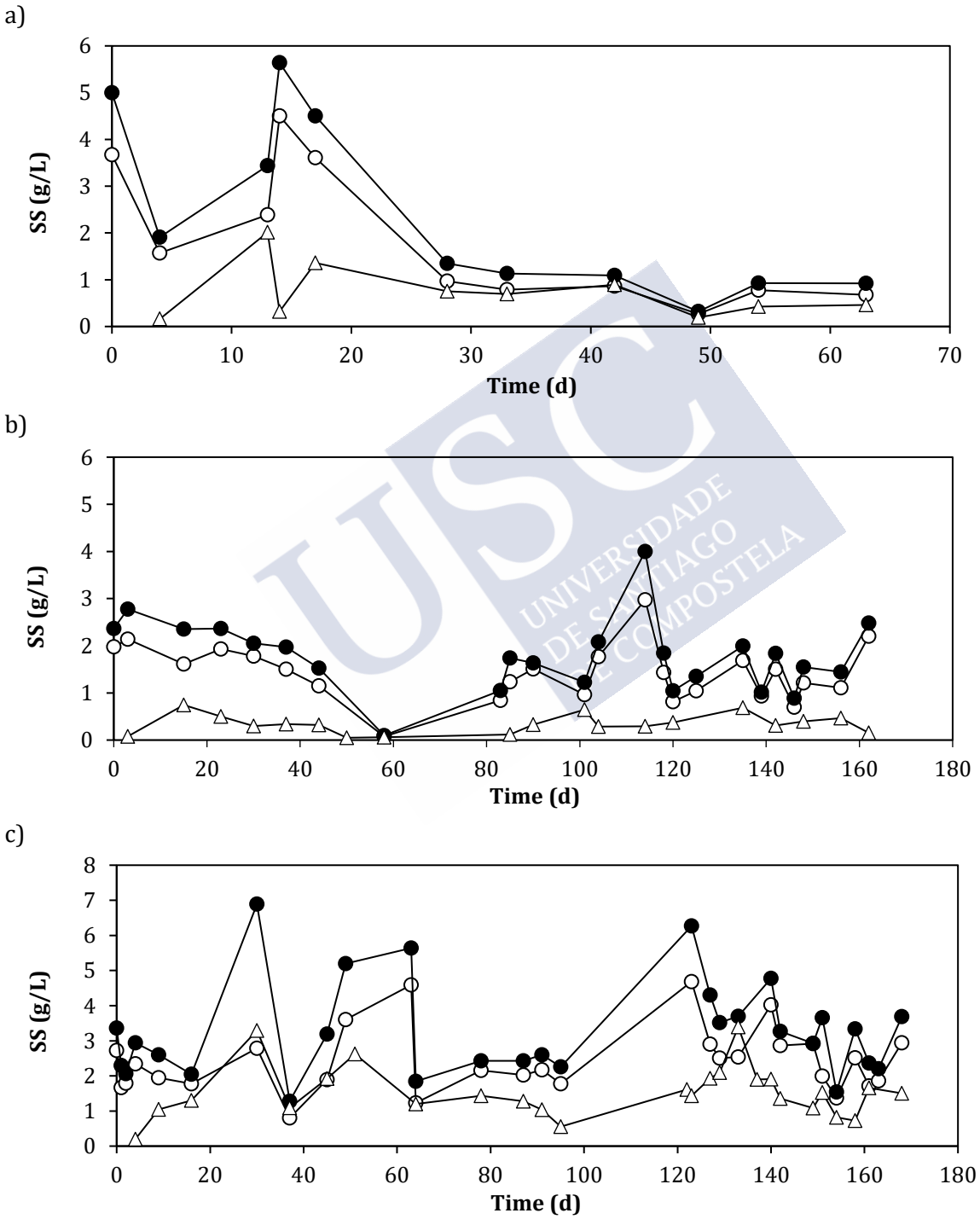

Figure 7.2: Evolution of the TSS (●) and VSS (○) concentrations in the AGS reactor and TSS concentrations of the effluent (△) in Stages I (a), II (b) and III (c).

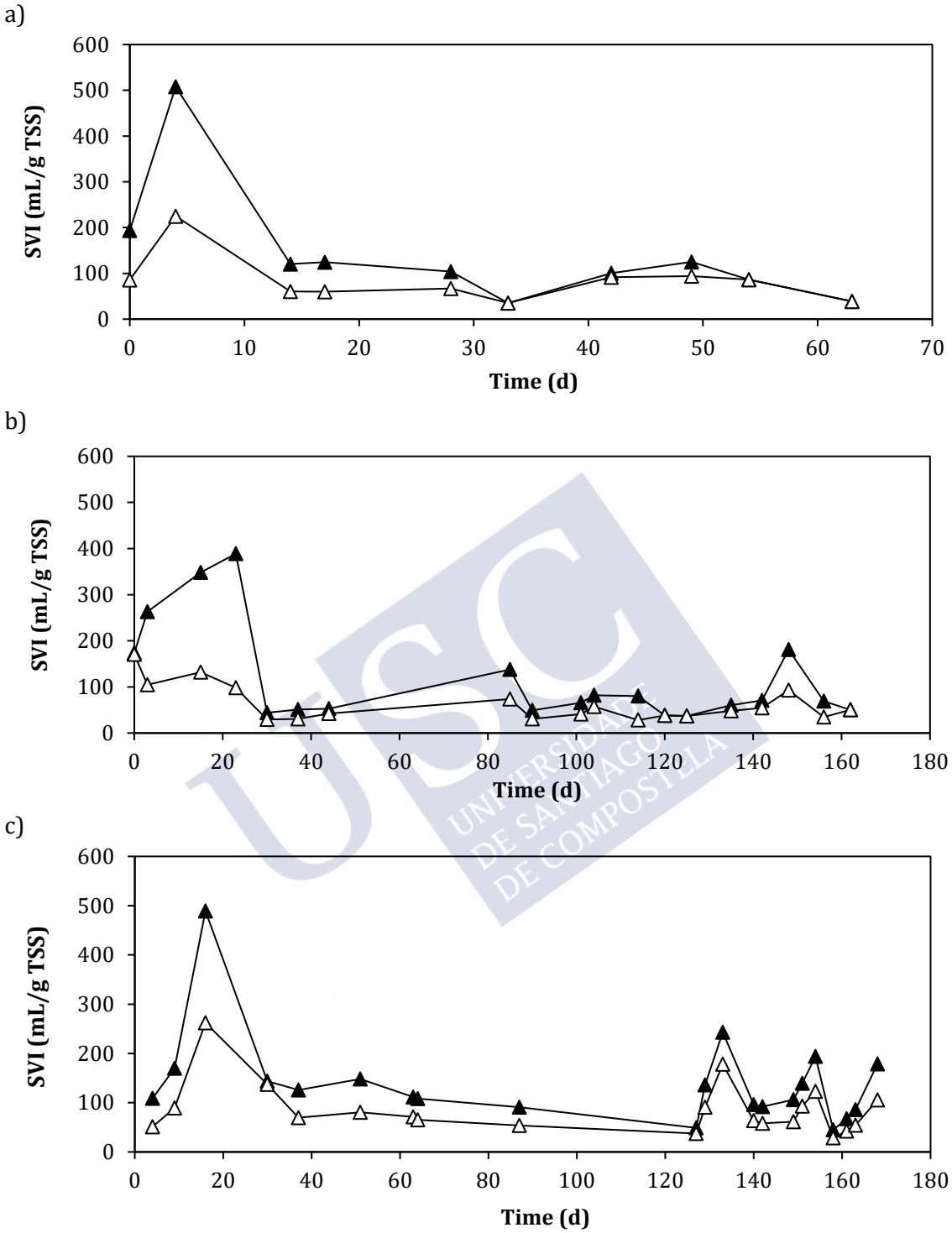

Figure 7.3: Evolution of the SVI_5 (▲) and SVI_{30} (△) in the AGS reactor in Stages I (a), II (b) and III (c).

Regarding the removal efficiencies, the achieved COD_S removal was of 70 – 80 % (Figure 7.4.a), and the COD_S concentration of the effluent stabilised in 150 – 200 mg/L. A feast-famine regime was established in the reactor from day 20 onwards, with a length of 40 min. The removal of COD_T was irregular at the beginning of the operation, but it reached a stable value of 40 % from day 50 onwards (Figure 7.5.a).

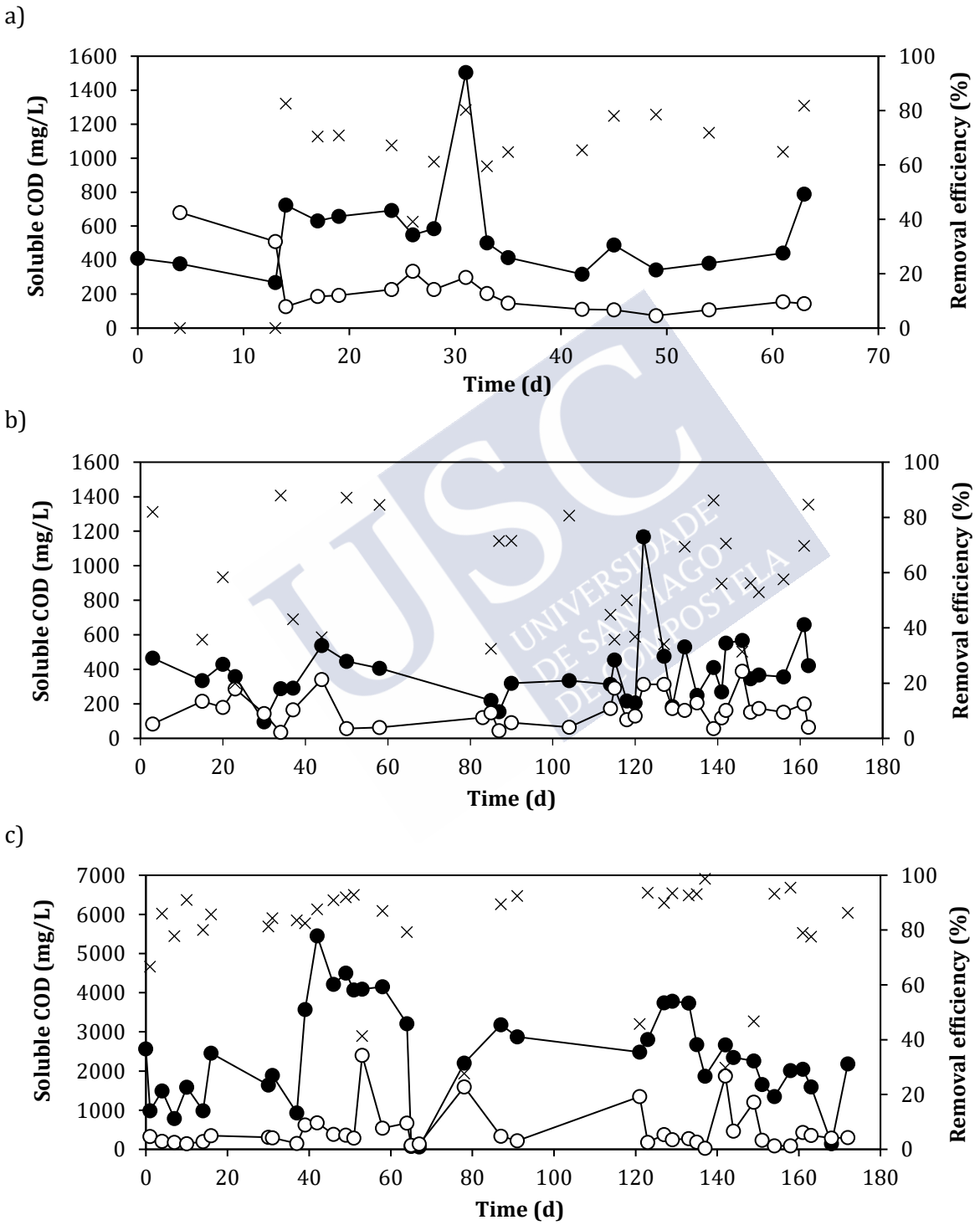

Figure 7.4: Profile of the soluble COD concentration in the influent (●), effluent (○) and removal efficiency (x) of the AGS reactor in Stages I (a), II (b) and III (c).

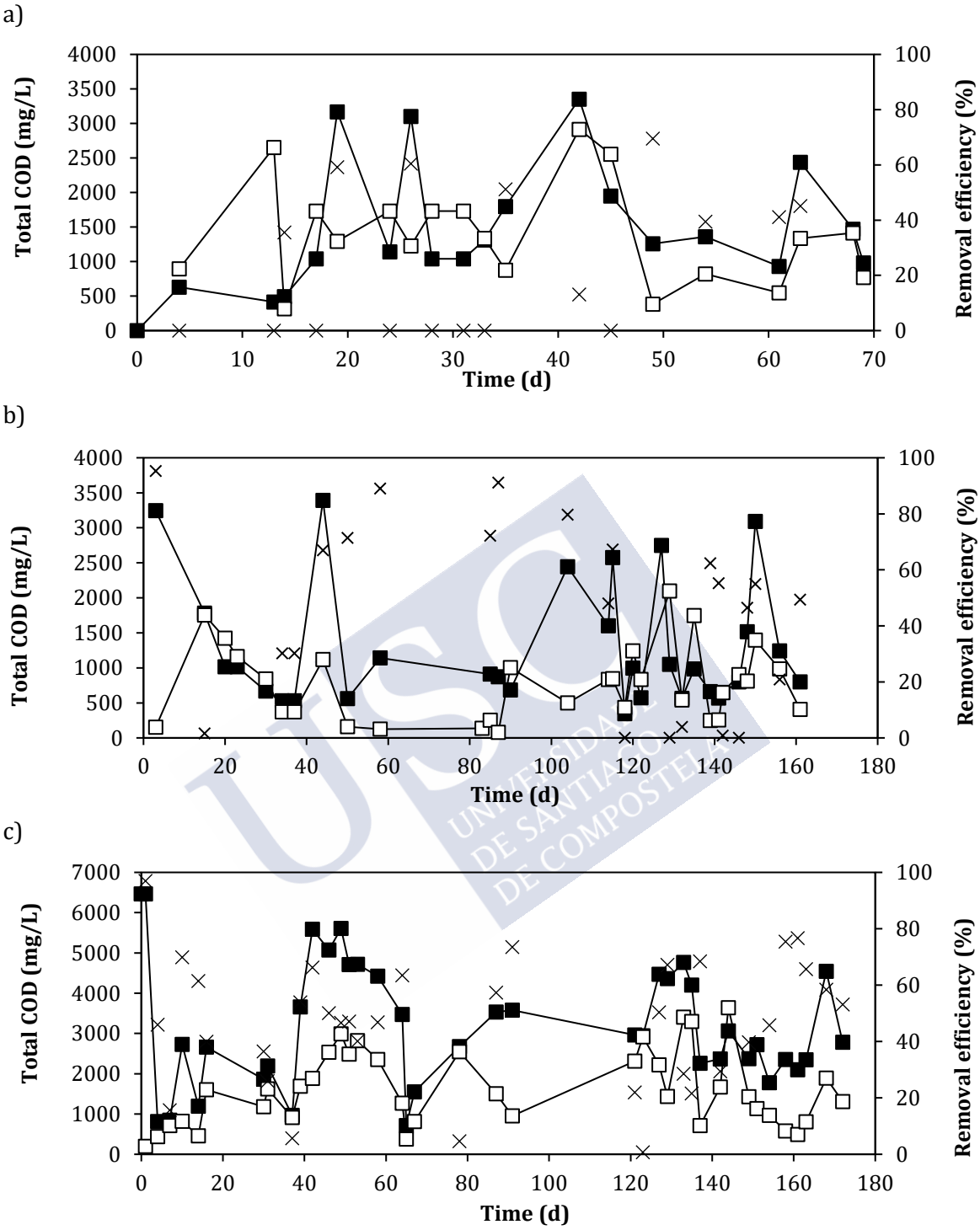

Figure 7.5: Profile of the total COD concentration in the influent (■), effluent (□) and removal efficiency (x) of the AGS reactor in Stages I (a), II (b) and III (c).

High N removal efficiencies of 80 – 90 % were achieved (Figure 7.6.a). However, the removal pathway was only biomass growth, since nitrite and nitrate were not detected in the effluent. This is logical, since the biomass concentration and the Sludge Retention Time (SRT) were too low to allow development of nitrifying bacteria. Wagner et al. (2015) observed that the growth of

nitrifying bacteria occurred in an AGS reactor when the SRT was of, at least 5 – 7 days. In this operation the SRT was of 2 – 3 days.

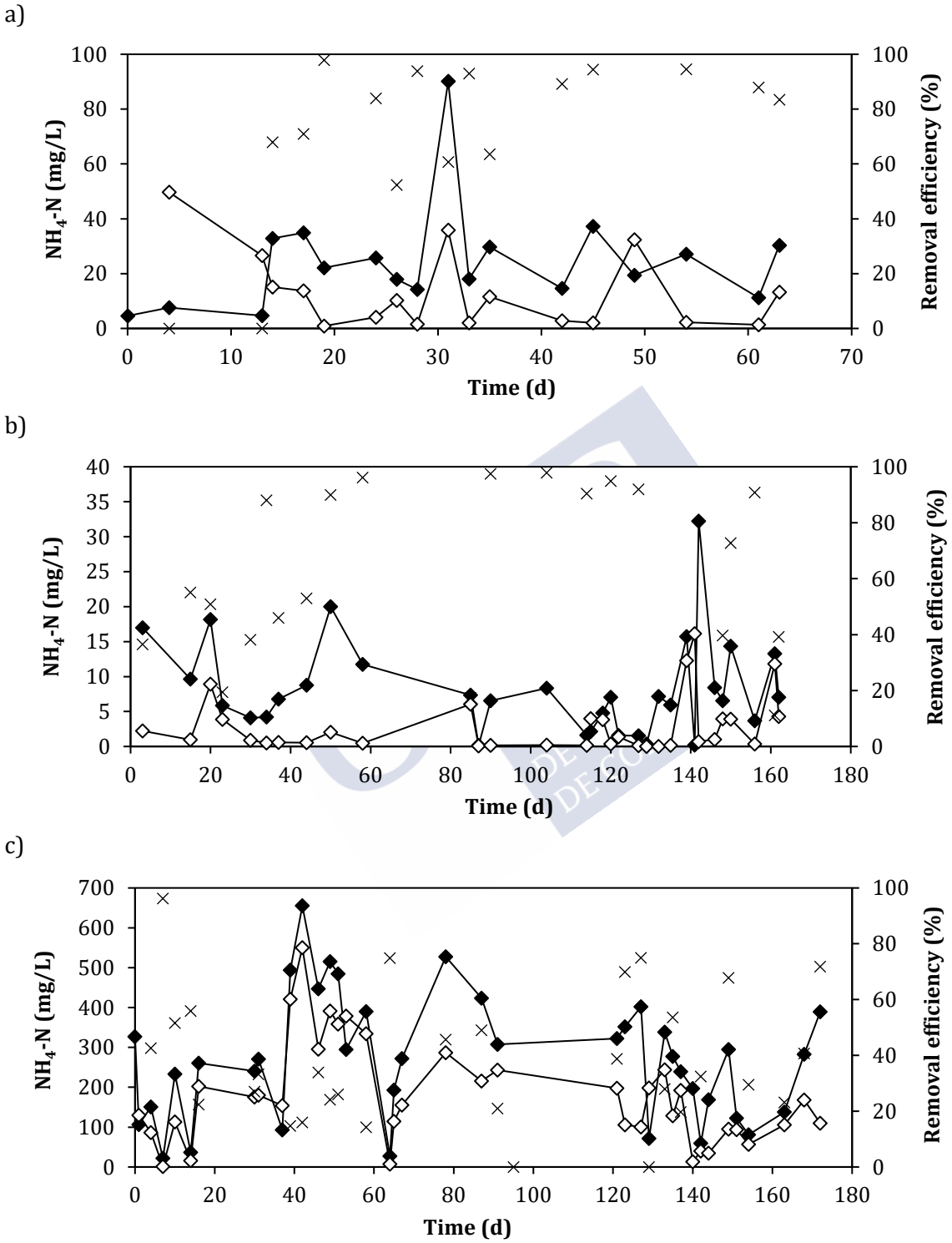

Figure 7.6: Profile of NH_4^+-N concentration in the influent (◆), effluent (◇) and removal efficiency (x) in the AGS reactor in Stages I (a), II (b) and III (c).

Therefore, the biomass concentration inside the AGS reactor stabilised and the settling properties were improved, but the length of the operational period and the applied operational conditions of this stage were not enough to allow for the formation of granular biomass.

Stage II

The AGS reactor was re-started. It was inoculated with 0.3 m^3 of sludge (10 % of the AGS reactor useful volume), from the thickener of the same wastewater treatment plant as the previous stage, adapted to salt concentrations of 15 g NaCl/L (Figure 7.7.a). The inoculum contained 22.5 g TSS/L and 18.8 g VSS/L, and was characterised by an SVI_5 of 174 mL/g TSS and SVI_{30} of 171 mL/g TSS.

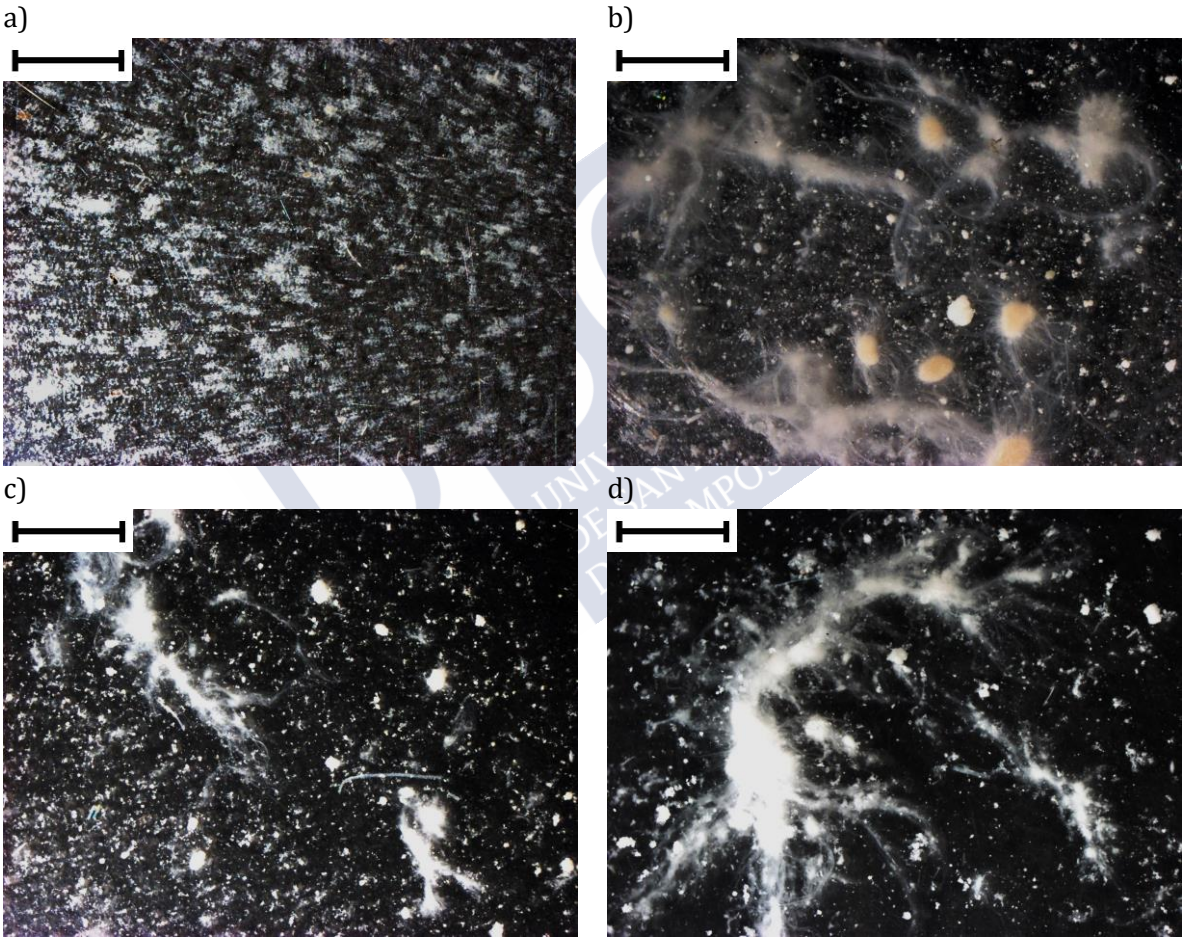

Figure 7.7: Images of the biomass samples collected on days 0 (a), 30 (b), 120 (c) and 153 (d) of Stage II. The size bar corresponds to 2 mm.

In this case, the biomass washout was inferior compared to Stage I, and a stable concentration of biomass between 1.2 – 1.7 g VSS/L was obtained after 30 days of operation (Figure 7.2.b). Due to the better operational conditions of this stage (larger VER and higher SGV), the selection of biomass was better, and the first granules appeared after 30 days. Filamentous bacteria were observed growing on the surface of the granules (Figure 7.7.b), due to the low applied loading rate (1 – 1.5 kg $COD_S/(m^3 \cdot d)$). From this point forward, the biomass was in the form of a mixture of

small granules and big flocs, with good settling properties. The SVI_5 was considerably reduced compared to the beginning of the operation, reaching stable values of 30 – 40 mL/g TSS (Figure 7.3.b).

However, this stability was lost on day 58 because of an episode of almost complete biomass washout, due to the presence of detergents and other chemical compounds in the wastewater, associated to washing activities performed in the factory. In addition, on day 59, the factory stopped its activity until day 83, so that there was no available LS-WW to be used as feeding. Nevertheless, the reactor was fed with HS-WW with longer cycles, as explained in Section 7.3.2.

When the factory restarted its activity (day 83), the biomass concentration in the reactor was of 0.9 g VSS/L (Figure 7.2.b), and the SVI_5 increased to 74 mL/g TSS (Figure 7.3.b) as a consequence of the change in the operational conditions during the stop. However, the biomass rapidly recovered the same properties as it had before the washout, and after only a week (day 90) granules were observed again. The biomass concentration increased to 1.7 g VSS/L and the SVI_5 was reduced again to 30 mL/g TSS. The biomass concentration in the reactor progressively increased, achieving a value of 2.9 g VSS/L on day 114, and it decreased again after the reduction of the settling time on day 118 to 1.4 g VSS/L.

However, on day 130 the overgrowth of filamentous bacteria was observed (Figure 7.7.c). This led to a worsening of the settling properties, increasing the SVI_5 from 37 mL/g TSS (equal to SVI_{30}) on day 125 to 180 mL/g TSS on day 148 (SVI_{30} of 93 mL/g TSS). The aggregates of filamentous bacteria gradually increased their size (Figure 7.7.d) and their poor settleability caused the continuous washout of biomass in the effluent. This fact, as well as the low biomass concentrations inside the reactor, implied SRTs of 1 – 3 days during the entire operation.

Some research works have reported the overgrowth of filamentous bacteria and consequently the instability of the AGS system, due to different factors. Large and uncontrolled SRTs, higher than 10 – 20 days (Moura et al., 2018; Yang et al., 2016) provoke the appearance of big granules with filamentous bacteria in their surface. Low dissolved oxygen concentrations inside the reactor, lower than the 40 % of the saturation level, also provoke the growth of filamentous bacteria in the surface of the granules (de Kreuk and van Loosdrecht, 2004; Mosquera-Corral et al., 2005a). High COD/N ratios and ammonia concentrations lower than 1.5 mg/L can suppose a nutrient deficit, which also favours the development of filamentous bacteria (Liu and Liu, 2006). In addition, OLRs lower than 1 kg $COD_S/(m^3 \cdot d)$, can provoke low substrate gradients inside the aggregates, which favour the growth of filamentous over granule-forming bacteria (Peyong et al., 2012). Moreover, in Chapter 4 of the present thesis, the combination of low OLR (1.8 kg COD_S /(m^3·d)) and SGV (1.2 cm/s) has been reported to provoke the overgrowth of filamentous bacteria.

In the present research work, the combination of some factors could have provoked the uncontrolled growth of filamentous bacteria, as suggested by Figueroa et al. (2015). The COD concentrations in the feeding were low (300 – 500 mg/L, average OLR of 1.5 kg $COD_S/(m^3 \cdot d)$) and the shear stress in the reactor (SGV of 1.3 cm/s) might have not been sufficient to favour the formation of aggregates with smooth surface. However, the main reason that caused the appearance of filamentous bacteria was probably the low nitrogen concentration of the feeding between days 114 – 129 of operation. The wastewater presented most of the operational days

COD/N ratios of 100/1.4 – 100/3.3. However, between days 114 – 129, the ammonia concentration of the feeding was of 1.5 – 2 mg N/L, with a COD/N ratio of 100/0.5 – 100/0.2. Previous studies have reported the absence of filamentous bacteria with at least COD/N ratios of 100/5 (considered the appropriate ratio), 100/2.5 and 100/2 (Yin et al., 2019). However, in the present study, the ratio was considerably lower, indicating a clear nutrient deficit in the feeding.

Some strategies have been proposed in literature to control the presence of filamentous bacteria in AGS reactors, including: decreasing the biomass retention inside the reactor by shortening the SRT (lower than 10 days), ensuring sufficient supply of dissolved oxygen as well as COD and nutrients, and short feeding phases (Liu and Liu, 2006). In the present study, a short feeding phase was applied, and the length of the operational cycles was short (3 h), to try to maximise the applied OLR. However, it was not possible to control the overgrowth of filamentous bacteria, which continued being dominant until the end of operation. Since the nitrogen deficit was a problem associated to the characteristics of the wastewater, the feeding of the reactor was changed in the next operational stage, and a stream with higher concentrations of N was used as feeding (Stage III).

Regarding the removal efficiencies, the COD_S concentration of the effluent achieved stable values, similar to those from Stage I, of 100 – 150 mg/L. The removal efficiencies oscillated between 60 – 80 %, depending on the concentration of the influent (Figure 7.4.b). The feast – famine regime was established, with feast durations of 40 min at the beginning of the Stage II, and 10 – 15 min on the last operational days. The COD_T removal, like in Stage I, was irregular at the beginning, due to the washout of biomass associated to the granulation process, but it was increased and maintained from day 44 onwards, in a range of 70 – 80 % (Figure 7.5.b). However, at the end of the operation, due to the presence of filamentous bacteria, the removal efficiencies decreased to 40 – 70 %. The nitrogen removal pathway, like in Stage I, was its uptake for biomass growth (Figure 7.6.b), and neither nitrite nor nitrate were detected in the effluent because of the low retention of biomass inside the reactor.

On day 162, a cycle measurement was done, by analysing COD, N and dissolved oxygen concentrations at different times of an operational cycle (Figure 7.8). The cycle showed the COD consumption in the first minutes of the cycle, with a feast phase of 30 minutes. The oxygen concentration was low at the beginning of the feast, and it started to increase with the decrease of the COD concentration, achieving a stable value when the famine phase started. The decrease of the nitrogen concentration corresponded to the nitrogen requirements for biomass growth. Oxidised species of nitrogen were not detected.

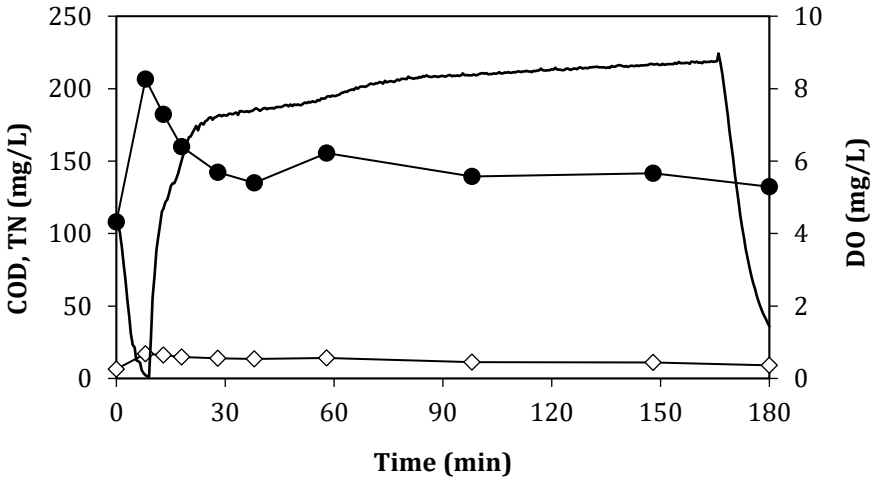

Figure 7.8: Soluble COD (●), total nitrogen (◇) and dissolved oxygen (-) profiles during an operational cycle on day 162.

Influence of the operational conditions in the granulation process

a) Volume exchange ratio and airflow

The different applied operational conditions in Stage I and II, led to the development of biomass with different properties. In Stage II, since the operational conditions were more favourable to select granular biomass, biological aggregates were observed, whereas in Stage I they were not present. The higher VER helped to increase the applied OLR in the system and improved the selection of biomass with good settleability. In addition, the SGV in Stage II was of 1.3 cm/s, which is in the range of recommended SGV values to achieve stable granulation (Liu and Tay, 2004), whereas in Stage I, the SGV was of 0.7 cm/s, below this limit.

b) Operational changes during the production stops of the plant

To determine the influence of the stops during weekends on the reactor performance, the average COD removal efficiencies on Fridays and subsequent Mondays were compared. The average COD_S removal efficiencies were of 56.5 ± 20.8 % on Fridays (OLR of 0.38 – 2.09 kg $COD_S/(m^3 \cdot d)$), and 65.0 ± 24.2 % on Mondays (OLR of 0.78 – 1.19 kg $COD_S/(m^3 \cdot d)$). Therefore, the increase of the cycle length (from 3 to 6 h) during weekends, did not have a big impact on the removal overall performance of the system. However, the combination of these changes during weekends, in addition to the fluctuations and low loads of the feeding, probably hindered the granulation process.

After the long stop of the factory during winter holidays (Stage II, days 59 – 83), the system was able to recover its removal capacity in a few days. The settling properties were affected by the stop, and higher SVI values were observed in the first days after the restart of the normal operation (SVI_{30} and SVI_5 of 138 and 76 mL/g TSS, respectively, on day 85). Nevertheless, they were rapidly recovered (SVI_{30} and SVI_5 of 49 and 31 mL/g TSS, respectively, on day 90).

Therefore, after the long stop, the most affected parameter was the settleability of the biomass, whereas the performance of the system was maintained. Only a few days (less than a

week) were necessary to recover the same conditions as the operation before the stop. Neither the removal efficiencies nor the biomass properties were affected after the short stops.

7.4.2. High-strength wastewater treatment. Stage III

The reactor was inoculated with 0.6 m^3 of sludge (which supposed a 20 % of the AGS reactor useful volume), from the thickener of the same wastewater treatment plant as the previous stages, adapted to a salt concentration of 15 g/L (Figure 7.9.a). The biomass concentration in the reactor after the inoculation was 3.36 g TSS/L and 2.73 g VSS/L, and was characterised by an SVI_5 of 300 mL/g TSS and SVI_{30} of 178 mL/g TSS.

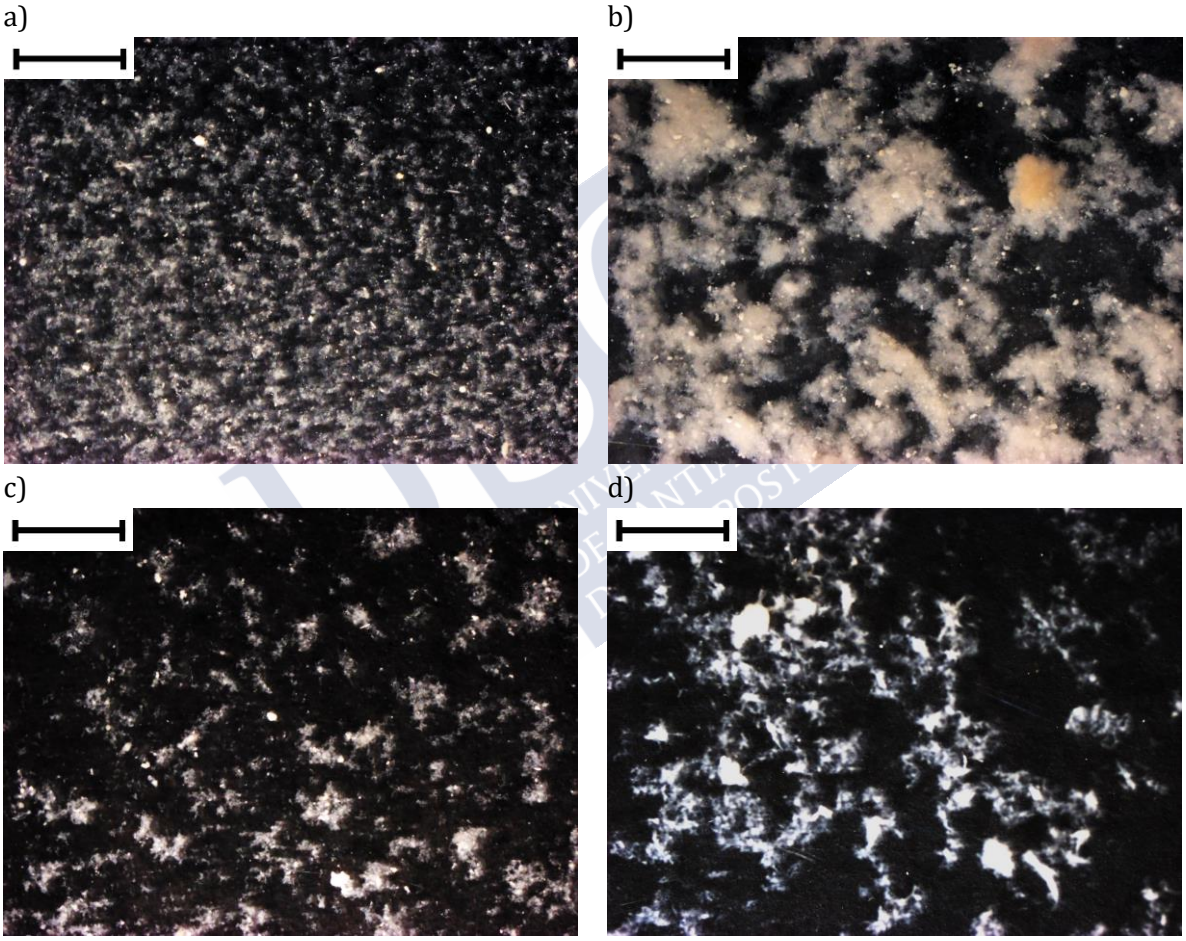

Figure 7.9: Images of the biomass samples collected on days 0 (a), 33 (b), 64 (c) and 178 (d) of Stage III. The size bar corresponds to 2 mm.

The biomass concentration in the reactor reached higher values (2 – 3 g VSS/L) compared to Stage I, associated with a higher COD concentration in the feeding (Figure 7.2.c). After one month of operation, the biomass was in form of big flocs, and a few aggregates appeared, which could be biological aggregates or solids or greases that entered in the reactor with the feeding (Figure 7.9.b). When the OLR was increased to 6 kg COD_S/m^3·d, between days 49 – 64, the highest values of biomass concentrations, up to 4.5 g VSS/L were observed. The granulation process evolved, the size of the flocs decreased and small aggregates were observed on day 64 (Figure 7.9.c). After that,

there was a diminishment of the OLR during days 65 – 95, and a decrease and stabilisation of the biomass concentration to 2 – 3 g VSS/L. In addition, a progressive decrease of the solids of the effluent was observed. The settleability of the biomass remained stable until day 95, with values of SVI_5 of 54 – 70 mL/g TSS (Figure 7.3.c). The good settleability of the biomass and the progressive decrease of the solids in the effluent indicated a good evolution of the biomass.

On day 64, to study the homogeneity of the biomass inside the reactor, samples were taken during aeration at different heights of the reactor (corresponding to the 33 and 67 % of the useful volume). At the point corresponding to the 33 % of the volume, the biomass concentration was of 1.27 g VSS/L and 1.90 g TSS/L, and the SVI_5 was of 105 mL/g TSS. The sample corresponding to the 66 % of the useful volume presented a biomass concentration of 1.23 g VSS/L, 1.84 g TSS/L and a SVI_5 of 108 mL/g TSS. The aspect of the biomass was similar in both samples (Figure 7.9.c). Thus, the SGV of 1.4 cm/s was enough to avoid the stratification of biomass.

From day 95 until day 120 the prototype was stopped, due to a stop of the production of the factory. After that, the biomass rapidly recovered the same properties as before the stop. The biomass concentrations fluctuated between 2.0 – 3.5 g VSS/L, associated with changes in the operational conditions. The settleability of the biomass oscillated between 30 – 178 mL/g TSS. Small aggregates mixed with flocs were observed, which were maintained until the end of the operation (Figure 7.9.d). Although an evolution of the biomass occurred, well-defined granules were not observed, since more time was needed to complete the granulation process. Nevertheless, the overgrowth of filamentous bacteria was not observed, due to the higher loading rates applied to the reactor. The COD/N ratios in this stage were considerably higher than those corresponding to LS-WW, with values of 100/6.7 – 100/20.

Only a few studies addressed the treatment of high OLRs at pilot-scale (most of them were focused on the treatment of low-strength sewage). Farooqi and Basheer (2017) operated a reactor of 3.39 m^3 to treat the effluent of pulp and paper industry, which presented a COD_S of 2000 – 3000 mg/L. They obtained a full granular system after 180 days with a maximum OLR of 4.5 kg $COD_S/(m^3 \cdot d)$. The granules presented a particle diameter of 2 – 4 mm, SVI_5 of 60 – 70 mL/g TSS and biomass concentration of 7 – 8 g VSS/L. Wei et al. (2013) treated wastewater with a COD_S of 1000 – 2000 mg/L (OLR of 2.25 kg COD_S /($m^3 \cdot d$)) in a reactor of 1.47 m^3. The granulation process was completed after 30 days, obtaining granules with an average size of 1.2 – 2 mm. The biomass concentration inside the reactor was of 6 – 7 g TSS/L and the SVI_5 was 43 – 55 mL/g TSS. In the present work, although the SVI_5 (50 – 100 mL/g TSS) was in the range of the values reported in the abovementioned studies, the biomass concentration was lower (2 – 5 g VSS/L). This was presumably because the granulation process was not completed at the end of the operation, and the retention of the biomass was low.

The COD_S removal efficiencies were high during the whole operation (80 – 90 %), and more stable than in the previous stages (Figure 7.4.c). A feast/famine regime was also established, with a feast duration of 1 – 3 h, depending on the applied OLR and the biomass concentration inside the reactor. The removal efficiencies corresponding to COD_T were of 40 – 70 %. The fluctuations were caused by the biomass washout due to the selection of aggregates with good settleability (Figure 7.5.c).

Regarding nitrogen removal, like in the previous stages, it was only due to biomass growth. Nitrifying activity was not observed (neither nitrite nor nitrite were detected in the effluent), because the SRT of the reactor was not high enough to promote the growth of nitrifying bacteria. The SRT in the reactor oscillated between 4 – 5 days, whereas to observe nitrifying activity values higher than 5 – 7 days are required. The Free Ammonia (FA) concentrations (50 – 63 mg N/L) could have contributed to inhibit nitrifying activity (Yang et al. (2004) reported the decrease of the nitrifying activity with FA concentrations above 23.5 mg N/L). However, the short SRT was presumably the main cause of the absence of ammonia oxidation.

Since the influent concentrations of ammonia were high (200 – 300 mg NH_4^+-N/L), the removal efficiencies were of 30 – 40 % (Figure 7.6.c). Although they were lower than the previous stages, the nitrogen removal capacity of the biomass was considerably higher (0.02 kg N/(m^3·d) and 0.14 kg N/(m^3·d) in Stages II and III, respectively).

Regarding the changes in the cycle length during weekends, the same behaviour as Stages I and II was observed. No important changes in the performance or the biomass properties were observed after the short stops. The average COD_S removal efficiencies on Fridays were of 89.3 ± 4.6 % (OLR of 2.45 – 6.94 kg COD_S/(m^3·d)), whereas on subsequent Mondays they were of 86.0 ± 6.9 % (OLR of 1.30 – 6.73 kg COD_S/(m^3·d)).

The long stop took place during days 85 – 120 (stop of production due to summer holidays). The first day after the restart the COD removal was a bit lower than the rest of the days (46 % on day 121), but on day 123 the removal efficiency increased until the same values observed previously (above 90 %). The SVI remained in the same values as before the stop (SVI_5 of 37 mL/g TSS, equal to SVI_{30}). This behaviour was not observed in the operation with LS-WW. This was probably due to the fact that, during the stop of Stage II, the reactor was fed with a different wastewater (HS-WW instead of LS-WW) whereas in Stage III the same wastewater was used.

7.4.3. AGS effluent post-treatment

In all the stages, the effluent of the AGS was treated in a settler, to remove the remaining solids left with the effluent and assure the production of a good-quality effluent.

The solids removal, as well as COD_T removal, were of 60 – 80 % during the whole operation in the settler (Figure 7.10). Therefore, a simple post-treatment like a small settler could be enough to considerably reduce the solids and COD_T concentrations of the effluent of the AGS reactor.

However, sometimes there were problems of greases and/or biomass flotation, which worsened the quality of the effluent. When LS-WW was used as feeding of the AGS reactor, these issues were provoked by a deficient wastewater pre-treatment of the DAF of the factory. When treating HS-WW, these episodes occurred when the wastewater level of the storage tank of the factory was low. This caused the collection of wastewater with higher grease concentrations.

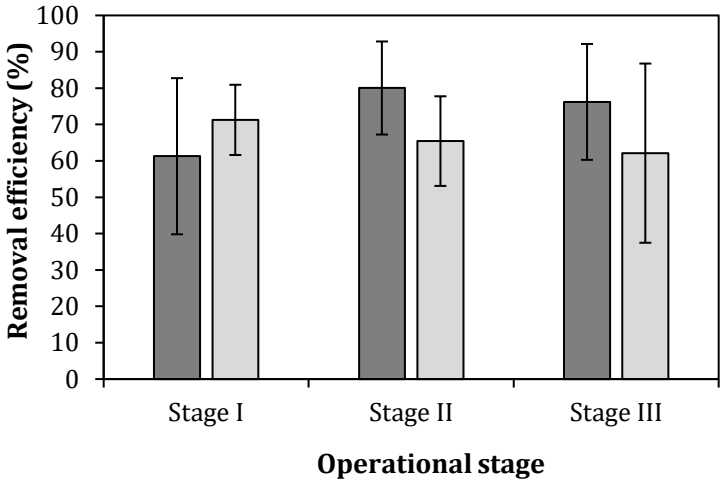

Figure 7.10: Removal efficiencies of TSS (dark grey) and COD (light grey) in the settler during Stages I, II and III.

7.4.4. Effluent quality

The effluent quality of the AGS pilot plant was compared to the discharge limits imposed in the factory where it was located, in order to evaluate the performance of the system in terms of compliance of the discharge requirements (Table 7.3).

Table 7.3: Fulfilment of the discharge requirements in Stages I, II and III of operation.

Parameter	Limit concentration	Stage I	Stage II	Stage III
pH	5.5 – 9.5	6.8 – 7.5	6.5 – 7.2	7.9 – 9.1
Suspended solids (mg/L)	125	100 – 120	70 – 100	200 – 400
Total COD (mg/L)	350	350 – 500	400 – 500	400 – 900
BOD_5 (mg/L)	150	160 – 200	100 – 200	40 – 200
TP (mg/L)	12.5	1 – 2	0.3 – 2.5	50 – 100
NH_4^+-N (mg/L)	25	1.5 – 6	1 – 6	80 – 300
TN (mg/L)	57.5	4 – 10	2 – 8	80 – 320
Greases (mg/L)	25	50 – 70	70 – 200	2 – 10

When treating LS-WW (Stages I and II), there was deficient grease separation in the DAF system of the cannery before feeding the pilot plant. Since greases were not removed neither in the AGS reactor nor the settler, the concentration in the effluent of the prototype was higher than the discharge requirements. Nevertheless, the settler was able to reduce the solids concentration of the effluent until values lower than the imposed limit. The total COD concentration was higher than the required limit, due to, mainly, the presence of greases. The low concentrations of

nutrients in the wastewater implied that their removal for biomass growth was enough to reduce the concentration to comply with the discharge requirements.

When treating HS-WW (Stage III), the high loading of the fed wastewater led to a high production of biomass, and consequently a higher solid washout in the effluent. Although solids were removed in the settler, the concentrations of the effluent were too high. In addition, despite the high COD removal efficiencies of the reactor, only the soluble COD was higher than the discharge permit of total COD. However, the greases concentration was lower compared to the previous stages, due to a better pre-treatment of the wastewater. Since nitrogen removal was only attributed to biomass growth, the removal rates of the AGS reactor were not high enough to reduce the concentration below the limit. If fully developed granular biomass was achieved, the nitrogen removal via nitrification-denitrification processes could take place. This would be expected to help to the achievement of the imposed effluent quality by decreasing the nitrogen and presumably the COD concentrations.

Therefore, when treating LS-WW (Stages I and II), an improvement of the removal efficiency of the DAF of the company could be enough to reduce the COD and greases content before feeding the reactor and meet the discharge limits. However, when treating HS-WW (Stage III), despite the high removal efficiencies of the system, another unit is necessary to remove the remaining COD and nitrogen to accomplish the discharge requirements.

7.5. CONCLUSIONS

The operational conditions imposed in the AGS reactor (short feeding, high air flowrate and low settling time), led to the selection of appropriate organisms to form granules: a feast-famine regime was established in all the operational stages and the settleability of the biomass was improved. However, granules were observed in Stage II (treating LS-WW with an SGV of 1.3 cm/s) and II (treating HS-WW with an SGV of 1.4 cm/s).

The low COD and nitrogen concentrations of the LS-WW hindered the formation of granules: the applied OLR was low, and the lack of enough nitrogen limited the biomass growth. In addition, the low concentrations and high COD/N ratios provoked the overgrowth of filamentous bacteria. Although the treatment of the LS-WW seems difficult, a possible solution would be to mix this stream with another one containing nitrogen, like the high-load stream. The HS-WW was more suitable, but a longer start-up is needed to obtain a fully granular system, due to the complexity of the wastewater. Therefore, the selection of an appropriate influent is important to assure the stability of the reactor.

The system was able to remove COD and nitrogen with high removal efficiencies. When treating LS-WW, the effluent of the plant fulfilled part of the discharge requirements, with the exception of COD, BOD_5 and greases, associated with the deficient operation of the pre-treatment units. When treating HS-WW, the COD, BOD_5, nitrogen and phosphorus concentrations were higher than the discharge limits. Consequently, an additional treatment is needed previous to effluent discharge.

7.6. REFERENCES

APHA/AWWA/WEF, 2012. Standard Methods for the Examination of Water and Wastewater. Stand. Methods 541. https://doi.org/ISBN 9780875532356

Carrera, P., Campo, R., Méndez, R., Di Bella, G., Campos, J.L., Mosquera-Corral, A., Val del Rio, A., 2019. Does the feeding strategy enhance the aerobic granular sludge stability treating saline effluents? Chemosphere. https://doi.org/10.1016/j.chemosphere.2019.03.127

Corsino, S.F., Capodici, M., Morici, C., Torregrossa, M., Viviani, G., 2016. Simultaneous nitritation-denitritation for the treatment of high-strength nitrogen in hypersaline wastewater by aerobic granular sludge. Water Res. 88, 329–336. https://doi.org/10.1016/j.watres.2015.10.041

de Kreuk, M.K., van Loosdrecht, M.C.M., 2004. Selection of slow growing organisms as a means for improving aerobic granular sludge stability. Water Sci. Technol. 49, 9–17

De Kreuk, M.K., Van Loosdrecht, M.C.M., Heijnen, J.J., 2006. Aerobic granular sludge : scaling up a new technology, Department of Biochemical Engineering

Derlon, N., Wagner, J., da Costa, R.H.R., Morgenroth, E., 2016. Formation of aerobic granules for the treatment of real and low-strength municipal wastewater using a sequencing batch reactor operated at constant volume. Water Res. 105, 341–350. https://doi.org/10.1016/j.watres.2016.09.007

Dobbeleers, T., Caluwé, M., Dockx, L., Daens, D., D'aes, J., Dries, J., 2020. Biological nutrient removal from slaughterhouse wastewater via nitritation/denitritation using granular sludge: an onsite pilot demonstration. J. Chem. Technol. Biotechnol. 95, 111–122. https://doi.org/10.1002/jctb.6212

Farooqi, I.H., Basheer, F., 2017. Treatment of Adsorbable Organic Halide (AOX) from pulp and paper industry wastewater using aerobic granules in pilot scale SBR. J. Water Process Eng. 19, 60–66. https://doi.org/10.1016/j.jwpe.2017.07.005

Figueroa, M., Val Del Río, A., Campos, J.L., Méndez, R., Mosquera-Corral, A., 2015. Filamentous bacteria existence in aerobic granular reactors. Bioprocess Biosyst. Eng. https://doi.org/10.1007/s00449-014-1327-x

Isanta, E., Suárez-Ojeda, M.E., Val del Río, Á., Morales, N., Pérez, J., Carrera, J., 2012. Long term operation of a granular sequencing batch reactor at pilot scale treating a low-strength wastewater. Chem. Eng. J. 198–199, 163–170. https://doi.org/10.1016/j.cej.2012.05.066

Li, J., Ding, L. Bin, Cai, A., Huang, G.X., Horn, H., 2014. Aerobic sludge granulation in a full-scale sequencing batch reactor. Biomed Res. Int. 2014. https://doi.org/10.1155/2014/268789

Liu, Y., Liu, Q.S., 2006. Causes and control of filamentous growth in aerobic granular sludge sequencing batch reactors. Biotechnol. Adv. 24, 115–127. https://doi.org/10.1016/j.biotechadv.2005.08.001

Liu, Y., Tay, J.H., 2004. State of the art of biogranulation technology for wastewater treatment. Biotechnol. Adv. https://doi.org/10.1016/j.biotechadv.2004.05.001

Liu, Y.Q., Moy, B., Kong, Y.H., Tay, J.H., 2010. Formation, physical characteristics and microbial community structure of aerobic granules in a pilot-scale sequencing batch reactor for real wastewater treatment. Enzyme Microb. Technol. 46, 520–525.

https://doi.org/10.1016/j.enzmictec.2010.02.001

Long, B., Yang, C. zhu, Pu, W. hong, Yang, J. kuan, Jiang, G. sheng, Dan, J. feng, Li, C. yang, Liu, F. biao, 2014. Rapid cultivation of aerobic granular sludge in a pilot scale sequencing batch reactor. Bioresour. Technol. 166, 57–63. https://doi.org/10.1016/j.biortech.2014.05.039

Morales, N., Figueroa, M., Fra-Vázquez, A., Val Del Río, A., Campos, J.L., Mosquera-Corral, A., Méndez, R., 2013. Operation of an aerobic granular pilot scale SBR plant to treat swine slurry. Process Biochem. 48, 1216–1221. https://doi.org/10.1016/j.procbio.2013.06.004

Mosquera-Corral, A., De Kreuk, M.K., Heijnen, J.J., Van Loosdrecht, M.C.M., 2005. Effects of oxygen concentration on N-removal in an aerobic granular sludge reactor. Water Res. 39, 2676–2686. https://doi.org/10.1016/j.watres.2005.04.065

Moura, L.L., Duarte, K.L.S., Santiago, E.P., Mahler, C.F., Bassin, J.P., 2018. Strategies to re-establish stable granulation after filamentous outgrowth: Insights from lab-scale experiments. Process Saf. Environ. Prot. 117, 606–615. https://doi.org/10.1016/j.psep.2018.06.005

Ni, B.J., Xie, W.M., Liu, S.G., Yu, H.Q., Wang, Y.Z., Wang, G., Dai, X.L., 2009. Granulation of activated sludge in a pilot-scale sequencing batch reactor for the treatment of low-strength municipal wastewater. Water Res. 43, 751–761. https://doi.org/10.1016/j.watres.2008.11.009

Peyong, Y.N., Zhou, Y., Abdullah, A.Z., Vadivelu, V., 2012. The effect of organic loading rates and nitrogenous compounds on the aerobic granules developed using low strength wastewater. Biochem. Eng. J. https://doi.org/10.1016/j.bej.2012.05.009

Pishgar, R., Kanda, A., Gress, G.R., Gong, H., Dominic, J.A., Tay, J.H., 2018. Effect of aeration pattern and gas distribution during scale-up of bubble column reactor for aerobic granulation. J. Environ. Chem. Eng. https://doi.org/10.1016/j.jece.2018.10.006

Rocktäschel, T., Klarmann, C., Ochoa, J., Boisson, P., Sørensen, K., Horn, H., 2015. Influence of the granulation grade on the concentration of suspended solids in the effluent of a pilot scale sequencing batch reactor operated with aerobic granular sludge. Sep. Purif. Technol. 142, 234–241. https://doi.org/10.1016/j.seppur.2015.01.013

Soto, M., Veiga, M.C., Mendez, R., Lema, J.M., 1989. Semi-micro C.O.D. determination method for high-salinity wastewater. Environ. Technol. Lett. 10, 541–548

Tijhuis, L., van Loosdrecht, M.C.M., Heijnen, J.J., 1994. Formation and growth of heterotrophic aerobic biofilms on small suspended particles in airlift reactors. Biotechnol. Bioeng. https://doi.org/10.1002/bit.260440506

Val Del Río, A., Figueroa, M., Mosquera-Corral, A., Campos, J.L., Méndez, R., 2013. Stability of aerobic granular biomass treating the effluent from a seafood industry. Int. J. Environ. Res.

Wagner, J., Guimarã;es, L.B., Akaboci, T.R.V., Costa, R.H.R., 2015. Aerobic granular sludge technology and nitrogen removal for domestic wastewater treatment. Water Sci. Technol. 71, 1040–1046. https://doi.org/10.2166/wst.2015.064

Wei, D., Qiao, Z., Zhang, Y., Hao, L., Si, W., Du, B., Wei, Q., 2013. Effect of COD/N ratio on cultivation of aerobic granular sludge in a pilot-scale sequencing batch reactor. Appl. Microbiol. Biotechnol. https://doi.org/10.1007/s00253-012-3991-6

Yang, S.F., Tay, J.H., Liu, Y., 2004. Inhibition of free ammonia to the formation of aerobic granules. Biochem. Eng. J. 17, 41–48. https://doi.org/10.1016/S1369-703X(03)00122-0

Yang, H.G., Li, J., Liu, J., Ding, L.B., Chen, T., Huang, G.X., Shen, J.Y., 2016. A case for aerobic sludge granulation: From pilot to full scale. J. Water Reuse Desalin. 6, 188–194. https://doi.org/10.2166/wrd.2015.188

Yin, Y., Sun, J., Liu, F., Wang, L., 2019. Effect of nitrogen deficiency on the stability of aerobic granular sludge. Bioresour. Technol. 275, 307–313. https://doi.org/10.1016/j.biortech.2018.12.069

Chapter 8

Modelling of an AGS reactor treating fish-canning wastewater

Summary

In this chapter, the operation of an Aerobic Granular Sludge (AGS) Sequencing Batch Reactor (SBR) treating fish-canning wastewater was simulated with a one-dimensional biofilm model. The biological processes were described according to the Activated Sludge Model no. 3 (ASM3). Two modifications were implemented in the model to accurately describe the biological processes: (1) simultaneous growth and storage processes to describe the COD removal and (2) the split of the nitrification into two steps, including nitrite as an intermediate compound. In addition, an inhibition term to express the inhibition of salinity was considered to be included in the model. The model was calibrated and validated with experimental data from the operation of the laboratory-scale reactor described in Chapter 5. Two different salt concentrations of 13 and 5 g NaCl/L were used for calibration and validation, respectively.

An accurate description of the COD and nitrogen species experimentally measured along cycles was obtained. The calibrated kinetic parameters of heterotrophic bacteria were similar to other research works modelling AGS reactors operation with ASM3. However, the kinetic parameters of nitrifying bacteria after calibration were lower. The causes of these discrepancies were presumably the use of industrial wastewater as feeding, the presence of salt or the sludge retention time of the biomass. The model was able to correctly predict the effluent concentrations of COD and nitrogen species with the operational conditions used as input in the validation step.

The inhibition term associated with salinity showed a reduction of 23 – 37 % of the maximum growth rate of the different bacteria populations under salt concentrations of 13 g NaCl/L. With 5 g NaCl/L the reduction of the growth rates was of 10 – 19 %. However, since the model was tested at moderate-low salinities, it should be desirable to test the inhibition term at higher salt concentrations.

OUTLINE

Chapter 8 175

8.1. INTRODUCTION 177

8.2. OBJECTIVE 178

8.3. MATERIALS AND METHODS 178

8.3.1. Experimental data 178

8.3.2. Simulation set-up 179

8.4. GRANULAR SLUDGE REACTOR MODEL 179

8.4.1. Biological processes 179

8.4.2. Granule characteristics 180

8.4.3. SBR operation 181

8.4.4. Inclusion of salinity effect in the model 181

8.5. RESULTS AND DISCUSSION 183

8.5.1. Calibration of the model 183

8.5.1. Validation of the model 187

8.6. CONCLUSIONS 189

8.7. REFERENCES 190

APPENDIX A: reference case 194

APPENDIX B: bioconversion reactions 196

APPENDIX C: Stoichiometric matrix 198

APPENDIX D: kinetic and stoichiometric parameters 200

APPENDIX E: estimation of the inhibition constants 202

8.1. INTRODUCTION

The Aerobic Granular Sludge (AGS) technology is nowadays regarded as an established way to treat both municipal and industrial wastewater, resulting in significant space and energy savings compared with traditional activated sludge processes (Pronk et al., 2015). In order to profit from these benefits, there has been an increasing interest to also treat saline wastewater with AGS, from both urban areas (Thwaites et al., 2018; van den Akker et al., 2015) as well as from different industrial sectors, such as petrochemical or seafood processing (Campo and Di Bella, 2019; Corsino et al., 2016; Val Del Río et al., 2013). High salt concentrations affect the reactor performance through their effect on the physical properties of the granules and biological activity.

Overall, saline wastewater, with moderate salt concentrations (5 – 15 g NaCl/L), can be beneficial for the formation of dense and smooth aerobic aggregates with good settling properties, as observed in Chapter 5. High salt concentrations provoke an increase of the bulk liquid density and lead to the washout of light and poor settling aggregates (Bassin et al., 2011). As a consequence, there is a reduction of the biomass concentration in the system, where only the dense aggregates with good settleability are present. In addition, the higher shear stress applied to the biomass provokes the growth of granules with a regular and smooth surface and a higher production of Extracellular Polymeric Substances (EPS) (Corsino et al., 2016; Li et al., 2017).

However, high salinity has been reported to have a detrimental effect on biological activity. Different inhibition thresholds have been observed depending on (1) the tolerance of each type of bacteria and (2) the adaptation of the biomass to high salt concentrations. The inhibitory effect of salinity on nitrifying bacteria has been the most studied, whereas there are less research works that pay attention to the inhibition of Heterotrophic Bacteria (HB). In general, salt concentrations lower than 10 g NaCl/L do not significantly affect the biological activity, and it has even been observed a stimulatory effect on the nitrifying activity at salt concentrations up to 5 g NaCl/L (Liu et al., 2008; Wang et al., 2017). However, when the salt content is above 10 g NaCl/L, the biological activity is usually reduced. In the case of biomass without any acclimation, the reported complete inhibition salt concentrations are of 13 – 20 and 10 – 20 g NaCl/L for Ammonia Oxidising Bacteria (AOB) and Nitrite Oxidising Bacteria (NOB), respectively (Bassin et al., 2011; Moussa et al., 2006; Wang et al., 2017). If the biomass is adapted to salinity, the salt inhibitory concentrations for AOB and NOB oscillate between 33 – 80 g NaCl/L and 20 – 35 g NaCl/L, respectively. Regarding autotrophic bacteria, most of the studies agree that NOB are more sensitive than AOB to high salt concentrations (Bassin et al., 2011; Figueroa et al., 2008; Pronk et al., 2014). However, a few have reported the opposite behaviour (Moussa et al., 2006; Wang et al., 2017).

Modelling is a useful tool to gain understanding and optimise the biological processes involved in wastewater treatment (Henze et al., 2008). The bioconversion processes that occur in AGS reactors, can be described by the Activated Sludge Models (ASM). Most of the studies modelling the bioconversion processes of AGS in fully aerobic SBRs, have used ASM3. Ni et al. (2008) used a modified ASM3, to describe simultaneous growth and storage of organic matter, to model the AGS performance treating low-strength wastewater. Zhou et al. (2013) modified ASM3 to include simultaneous growth and storage by heterotrophs, and split the nitrification into two processes: ammonia oxidation to nitrite and nitrite oxidation to nitrate. Vázquez-Padín et al. (2010) used ASM3 to model AGS processes under variable Chemical Oxygen Demand to Nitrogen (COD/N) ratios. They included the simultaneous growth and storage of organic matter by

heterotrophic bacteria and two-step nitrification. Isanta et al. (2013) developed a model to determine the guidelines to enhance biological nitrogen removal in AGS, treating swine wastewater. They modified ASM3, to describe the COD removal by simultaneous growth and storage, and the nitrification as a two-step process. Zhao et al. (2016) modified ASM3 to simulate the treatment of piggery wastewater by AGS with high organic matter and nitrogen concentrations. The model included the simultaneous growth and storage to remove organic matter and heterotrophic nitrification as the nitrogen removal pathway. Among all the abovementioned studies, only one of them has been used to simulate industrial wastewater treatment, whereas there are not models that address the treatment of industrial saline wastewater.

8.2. OBJECTIVES

The present work aimed to set up a model to describe the operation of an aerobic granular SBR treating fish-canning wastewater. Alternative models to describe the biological conversions were compared against each other. The need to consider an inhibition term to include the effect of salinity was investigated as well. The results of the simulations were directly compared to the experimental results from Chapter 5. This work was done in collaboration with Ghent University during a research stay.

8.3. MATERIALS AND METHODS

8.3.1. Experimental data

The operating conditions of the reactor used as a reference scenario for the simulation correspond to the SBR reactor described in Chapter 5. The reactor had a working volume of 1.7 L and a volume exchange ratio of 50 %. It was operated in cycles of 3 – 4 h, distributed as follows: 5 min of feeding, 167 – 227 min of aeration, 1 min of settling and 7 min of withdrawal. During the aeration stage, the dissolved oxygen concentration reached saturation values of 8.6 mg O_2/L. The reactor was fed with industrial saline wastewater (fish-canning wastewater), and its operation was divided into different stages depending on the salt concentration of the incoming wastewater (Figure 8.1). The initial factions of COD were determined experimentally through a COD fractionation test.

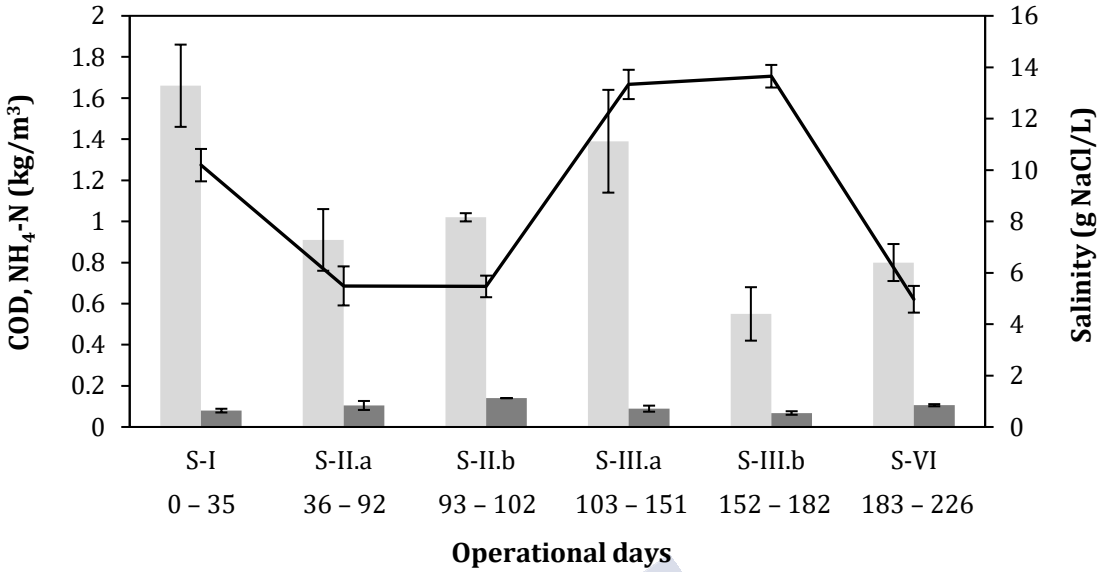

Figure 8.1: Influent characterisation of the AGS reactor operated in Chapter 5 in terms of soluble COD (light grey bars), ammonia (dark grey bars) and salt concentration (black line). The error bars indicate the standard deviations of the influent of each operational stage.

During the first phases (I, II.a and II.b, days 0 – 35 and 36 – 92), the reactor was not operating in steady-state conditions (the granulation process was not completed). Nitrifying activity appeared in Stage III.a (days 103 – 151), and achieved stable removal efficiencies in Stage III.b (days 152 – 182), which were maintained in Stage IV (days 183 – 226). Experimental data of Stages III.b and IV was used to calibrate and validate the model since the reactor was operating in steady-state conditions. For the calibration of the model, the dataset corresponding to Stage III.b was selected, since the reactor was operated with the highest salt concentration (13 g NaCl/L). For validation, the experimental data from Stage IV was used, with an influent salt concentration of 5 g NaCl/L. All the information related to the operational conditions of the reactor used as input of the model is presented in Appendix A.

8.3.2. Simulation set-up

Simulations were done for constant influent composition, detailed in Appendix A. The simulations were first run with the reference operational conditions for 200 days to ensure a steady-state operation and microbial population distribution. The operation was considered at stationary state conditions when the effluent concentrations of each compound, as well as the fractions of each type of bacteria inside the granule, achieved a stable value.

8.4. GRANULAR SLUDGE REACTOR MODEL

8.4.1. Biological processes

The first bioconversion model selected to be implemented was ASM1 (Henze et al., 2000). It describes the biological processes which enable the removal of organic matter and nitrogen. It

includes the growth and decay processes of heterotrophs and autotrophs, and the hydrolysis of organic matter and nitrogen compounds.

Then, the ASM3 model was also implemented (Henze et al., 2000). It is a modification of ASM1, which considers the COD removal by its storage inside the cells of bacteria (all substrates first become stored material and later are assimilated to biomass). Two modifications were made for an accurate description of the biological processes. ASM3 assumes that all the organic matter is first stored and afterwards used for biomass growth. However, in systems where a feast/famine regime is established, this assumption does not provide an accurate description of the process. In reality, both storage and growth take place at the same time under feast conditions. Therefore, the first modification of the model was the introduction of simultaneous growth and storage by heterotrophic bacteria, as proposed by Krishna and Van Loosdrecht (1999). The second modification was the description of nitrification as a two-step process (Isanta et al., 2013; Kaelin et al., 2009), including the oxidation of ammonia to nitrite by AOB, and the subsequent oxidation of nitrite to nitrate by NOB. Therefore, nitrite was included as an intermediate compound in both nitrification and denitrification processes. All the bioconversion reactions included in the model are listed in Appendix B. The stoichiometric matrix of soluble and particulate compounds is presented in Appendix C, following the format proposed by Henze et al. (2000).

The developed model included 8 soluble compounds: dissolved oxygen (S_O), soluble easily biodegradable COD (S_S), inert soluble COD (S_I), soluble COD (S_{COD}), organic nitrogen (S_{ND}), ammonium (S_{NH}), nitrite (S_{NO2}) and nitrate (S_{NO3}). In addition, 5 particulate compounds were included: particulate slowly biodegradable COD (X_S), particulate inert COD (X_I), heterotrophic bacteria (X_H), storage compounds (X_{STO}), AOB (X_A), and NOB (X_N). Alkalinity was not included in the model because it was not a limiting process parameter. In addition, pH and temperature were considered constant, due to the low fluctuations during the SBR operation. The soluble compound S_{COD}, calculated as the sum of S_I and S_S, was included in the model to be able to compare the output of the model with the experimental data, since the experimentally-measured COD concentration included both S_I and S_S.

8.4.2. Granule characteristics

The number of granules (n_g) was calculated according to Eq.8.1 and Eq.8.2. Granules were assumed to be spherical particles with a radius equal to the average value measured experimentally.

$$n_g = \frac{V_X}{4/3\,\pi R_m{}^3} \qquad \text{(Eq.8.1)}$$

$$V_X = \frac{V_R X}{\rho} \qquad \text{(Eq.8.2)}$$

Where R_m is the average radius of the granules (m, determined experimentally), V_X is the total volume of granules (m^3), V_R is the volume of the reactor (m^3), X is the solids concentration (g

VSS/m^3) and ρ is the density of the granules (g VSS/m^3). Both the solids concentration and the density of the granules were determined experimentally. The density of the biomass, expressed in terms of COD (ρ_{COD}), was calculated following Eq.8.3.

$$\rho_{COD} = \rho\left(1 - \frac{ISS_R}{TSS_R}\right)1.3659\left(\frac{1}{1-\varepsilon_w}\right) \quad \text{(Eq.8.3)}$$

Where ρ is the density of the granules (g TSS/m^3, determined experimentally), ISS are the Inert Suspended Solids and TSS the Total Suspended Solids of the reactor, 1.3659 is the ratio COD/VSS of the biomass (g COD/g VSS) and ε_W is the porosity of the granules.

The transport processes inside the granules, which are influenced by diffusion coefficients, conversion rates, density and porosity were described through the biofilm modelling software AQUASIM (Reichert, 1998). Mass transfer resistance from the bulk liquid to the granule surface was neglected. To model the intragranular transport, a compound-specific estimation of the effective diffusion coefficient inside a biofilm matrix was used (Baeten et al., 2018). The granule depth was divided into 20 grid points.

8.4.3. SBR operation

To describe the discontinuous operation of the SBR in AQUASIM, the total reactor volume was divided into a biofilm and a mixed compartment. They were coupled with a diffusive link (exchange coefficient 1000 m^3/h) to let the liquid phase behave as one perfectly mixed water volume and ensure the same bulk liquid concentration in both compartments (Baeten et al., 2017). The volume of the biofilm compartment was fixed at 0.25 L. The completely mixed reactor contained the remaining liquid, and had a variable volume, with a maximum value of 1.7 L during the aeration stage.

8.4.4. Inclusion of salinity effect in the model

Salinity effect on biological activity was considered as a non-competitive inhibition. Different terms have been proposed in literature to describe this type of inhibition caused by different compounds in different types of bacteria (Table 8.1).

Table 8.1: Non-competitive inhibition terms.

Inhibition term		Inhibitor	Affected bacteria	Reference
(1)	$\frac{K_{Inh,50}}{K_{Inh,50} + S_{Inh}}$	Free nitrous acid	AOB	Jiménez et al. (2012); Torà et al., 2010)
		Fluoride	AOB	Carrera et al. (2003)
		Chloramphenicol	Anammox	Phanwilai et al. (2020)
		Cadmium and cooper	HB	Pai et al. (2009)
		Benzene, toluene, phenol, benzoate	Anammox	Peng et al. (2018)
(2)	$1 - \frac{S_{Inh}}{K_{Inh,100}}$	Salinity	HB	Dan et al, (2003)
(3)	$\frac{K_{Inh,50}}{S_{Inh}^{\ m} + K_{Inh,50}}$	Benzene, toluene, phenol, benzoate	Anammox	Peng et al. (2018)
(4)	$1 - (S_{Inh}/K_{IL})^n$	Benzene, toluene, phenol, benzoate	Anammox	Peng et al. (2018)
		Aromatic substances	Anammox	Ramos et al. (2015)
(5)	$1 - \frac{1}{1 + (S_{Inh}/K_{Inh,50})^b}$	Quinoline	Anammox	Chen et al. (2019)
		Nanoparticles	Anammox	Song et al. (2018)
		Copper	Denitrifying bacteria	Chen et al. (2016)

Where $K_{Inh,50}$ is the half-inhibition constant, $K_{Inh,100}$ is the 100 % inhibition constant, and S_{Inh} is the inhibitor concentration. $K_{IL,}$ m, n and b are constants of the different models.

Among all the cited terms, inhibition term (1) was selected to be tested and added to the model, because it is the most reported in literature and it was recommended by ASM3 (Henze et al., 2000) to be used in case of inhibition processes.

The value of the half-inhibition constant was estimated based on activity tests of different research works, that report a reduction of the biological activity with the increase of salinity. Activity tests with biomass non-adapted to salt and adapted to different salinities were considered. The values obtained from literature are shown in Table 8.2. The figures of the works, as well as the estimating procedure, are included in Appendix E.

Table 8.2: Calculated values for the inhibition constant ($K_{Inh,50}$) of the inhibition term ($\frac{K_{Inh,50}}{K_{Inh,50}+S_{Inh}}$) from literature. Data from different research works (Bassin et al., 2011; Dan et al., 2003; Gonzalez-Silva et al., 2016; Moussa et al., 2006; Wang et al., 2015).

Bacteria	$K_{Inh,50}$ (g/L)	Salinity adaptation
AOB	10.7 ± 3.2	Yes
	24.8 ± 9.5	No
NOB	13.5 ± 0.0	Yes
	21.7 ± 5.5	No
HB	23.0 ± 0.0	Yes
	44.3 ± 10.4	No
Denitrifying HB	50.0 ± 0.0	Yes
	40.0 ± 0.0	No

8.5. RESULTS AND DISCUSSION

8.5.1. Calibration of the model

To calibrate the model, the simulation of the process was firstly done with default values of the kinetic parameters, provided by ASM1 and ASM3 (Henze et al., 2000). The COD, NH_4-N, NO_2-N and NO_3-N profiles obtained with the model were compared with a cycle measurement of the experimental data (operational day 163), corresponding to the conditions used as input of the model.

Evaluation of different biological models: ASM1 versus ASM3

The first step for the modelling of the SBR operation was the implementation of the well-established ASM1. The aim was to evaluate if it was possible to obtain the same results as the experimental data with a simpler model compared to ASM3. To fit the experimental data (from Stage III.b), the conversion rate of COD was increased by changing the kinetic parameters of the heterotrophic bacteria. Different values of the maximum growth rate ($\mu_{max,H}$) in a range of 6 – 20 d^{-1} were tested. To reproduce a similar COD velocity consumption, it was necessary to increase the maximum growth rate until a value of 20 d^{-1} (Figure 8.2.a). This value was found to be considerably higher than those of ASM1 and other biological models of AGS, which were in a range of 2 – 13 d^{-1} (Henze et al., 2000; Isanta et al., 2013; Zhou et al., 2013). Therefore, ASM1, in which COD removal is only attributed to biomass growth, did not describe accurately the biological process. Since it was not possible to reproduce the same COD conversion rates of the experimental data, nitrifying activity was not calibrated (Figure 8.2.b). Therefore, ASM1 was discarded and subsequent ASM3 implementation was tested.

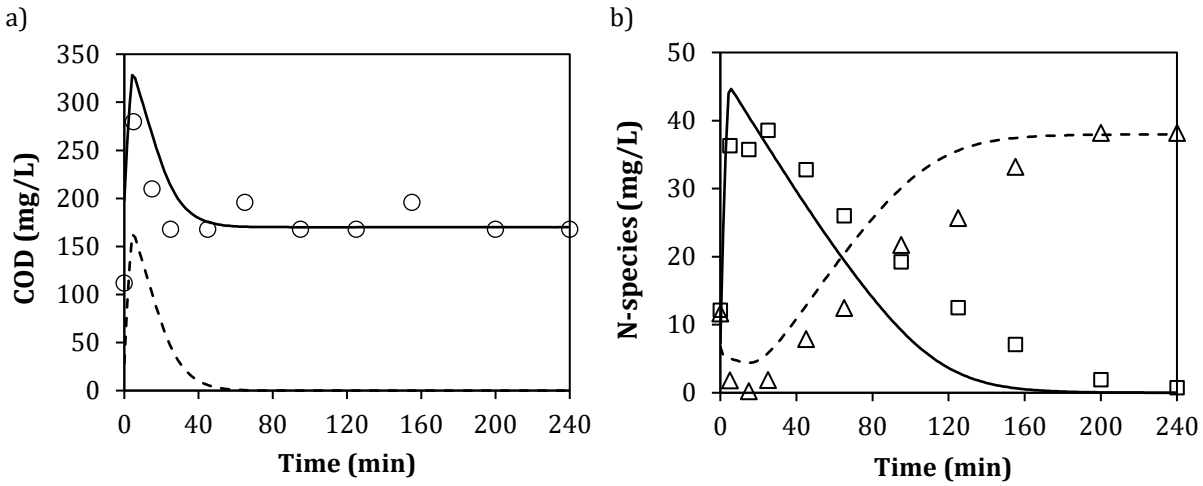

Figure 8.2: (a) S_{COD} (-) and S_S (- -) profiles predicted with ASM1; and S_{COD} (○) profile from experimental data. (b) S_{NH} (-) and S_{NO2} (- -) profiles predicted with ASM1; and S_{NH} (□) and S_{NO2} (△) profiles from experimental data.

Calibration of ASM3

To calibrate ASM3 with experimental data from Stage III.b, the same procedure was applied. The kinetic parameters of both heterotrophic and autotrophic were calibrated to fit the experimental data (Figure 8.3). To do that, the half-saturation coefficients were maintained, whereas the maximum growth rates (which included the inhibition term of salinity) and the storage rate constant were modified (Appendix D).

The results of the calibration of the model showed the consumption of all the biodegradable fraction of COD in the first minutes of the cycle, during the feast phase (Figure 8.3.a). The COD present at the end of the cycle could be attributed to the inert fraction. The ammonia was completely oxidised to nitrite, whereas no nitrate was observed (Figure 8.3.b). In addition, during the first minutes of the cycle, the denitritation of the nitrite from the previous cycle took place.

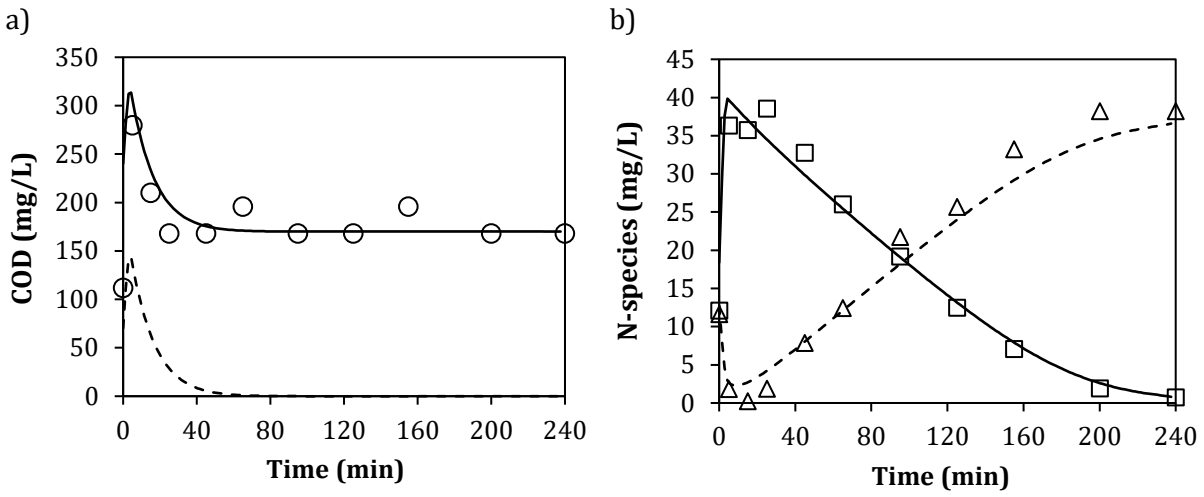

Figure 8.3: (a) S_{COD} (-) and S_S (- -) profiles predicted with ASM3; and S_{COD} (○) profile from experimental data. (b) S_{NH} (-) and S_{NO2} (- -) profiles predicted with ASM3; and S_{NH} (□) and S_{NO2} (△) profiles from experimental data. Cycle profiles corresponding to the results of the model calibration.

Heterotrophic bacteria (X_H) were present in the external layers of the granule, whereas autotrophs (X_A) were located in inner layers of the granule, due to the lower growth rates compared to heterotrophs (Figure 8.4). There was a progressive increase of the inert material (X_I) in direction to the centre of the granule, which indicates an important fraction of the granule which is not active.

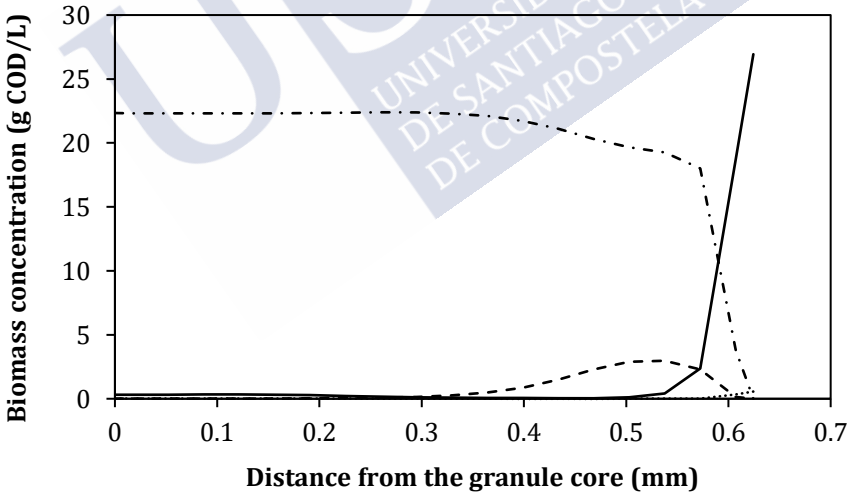

Figure 8.4: X_H (-), X_A (- - -), X_{STO} (· · ·) and X_I (- · -) distribution in the granule predicted by the model.

The calibrated heterotrophic bacteria kinetic parameters ($\mu_{max,H}$ of 6 d^{-1} and k_{STO} of 8 d^{-1}) were similar to those from previous research works modelling AGS with ASM3 (Figure 8.5). However, the calibrated values of nitrifying bacteria ($\mu_{max,A}$ of 0.18 and $\mu_{max,N}$ of 0.10 d^{-1}) were lower than the reported ranges of 1.1 – 1.3 and 0.9 – 1.3 d^{-1} for $\mu_{max,A}$ and $\mu_{max,N}$, respectively (Isanta et al., 2013; Ni et al., 2008; Vázquez-Padín et al., 2010; Zhao et al., 2016; Zhou et al., 2013).

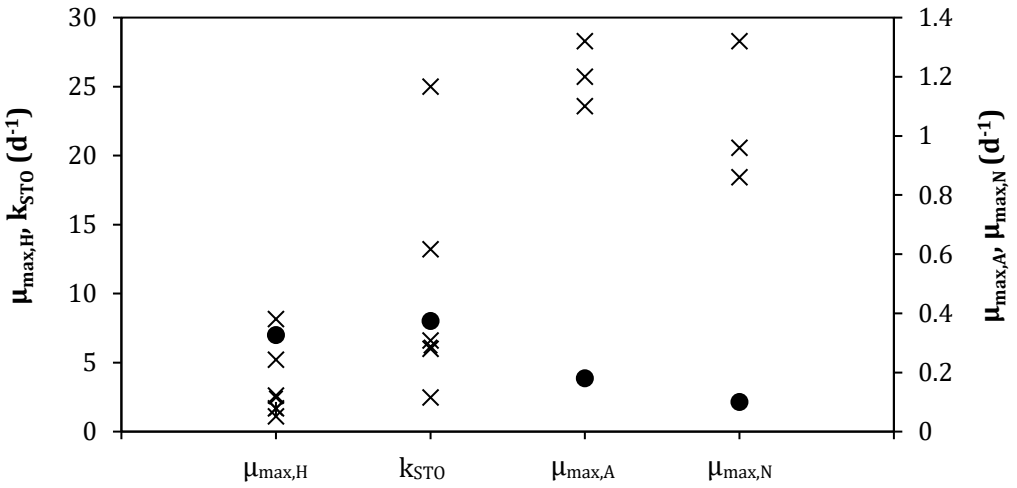

Figure 8.5: Comparison of the kinetic parameters of this model (●) with the values obtained in other works (x) modelling AGS with ASM3 (Henze et al., 2000; Isanta et al., 2013; Ni et al., 2008; Vázquez-Padín et al., 2010; Zhao et al., 2016; Zhou et al., 2013).

A few works have also reported values of $\mu_{max,A}$ lower than those in ASM3. Gao et al. (2010) obtained a value of 0.46 d^{-1}. They explained that it was due to the shortcut nitrification process, with only nitrite production. The biomass production, in this case, was less than in the conventional nitrification process (AOB+NOB), so that the value of μ_{max} was lower than ASM3, which lumps AOB and NOB activity into a single process.

One of the possible causes for low values of $\mu_{max,A}$ might be a high biomass retention inside the reactor. Chiellini et al. (2013) estimated the value of $\mu_{max,A}$ in a Conventional Activated Sludge (CAS) reactor and a Membrane bioreactor (MBR). They observed a lower value of 0.46 d^{-1} in MBR, with a Sludge Retention Time (SRT) of 20 days, whereas in CAS it was of 0.96 d^{-1} (SRT below 10 d). Munz et al. (2010) also established a comparison between CAS and MBR and observed the same results, a $\mu_{max,A}$ of 0.35 d^{-1} in an MBR and of 0.72 d^{-1} in CAS. They pointed out that the cause could be the difference between the SRT of both systems (20 d in the MBR, 8 d in the CAS). In systems with biofilms the higher biomass retention and SRT promote the selection of slow-growing nitrifiers, which present low values of μ_{max}. However, in systems like CAS, with low values of SRT, the development of rapid-growing nitrifiers (high values of μ_{max}) is favoured.

Another factor that could reduce the value of $\mu_{max,A}$ is the salt concentration inside the reactor. Cui et al. (2016) observed that the increase of the salt concentration (30 – 85 g NaCl/L) stimulates the growth of halophilic nitrifiers, characterised by a high affinity for ammonium and low growth rates (low half-saturation constant and low μ_{max}). They determined a μ_{max} of 0.26 d^{-1} with a salt concentration of 30 g NaCl/L and half-saturation coefficient values of 1 – 1.7 mg NH_4^+-N/L. The kinetic parameters showed a decreasing trend with the increase of salinity. They suggested the possibility of a shift in the community composition due to a long-term salinity selection. Gonzalez-Silva et al. (2016) also observed a change with time of the microbial community composition as a response to the variations on salt concentration and its adaptation to saline conditions.

In the present work, the low value could be due to the abovementioned causes. The SRT was 10 d during the operation of the reactor and the salt concentration fluctuated between 5 – 13 g

NaCl/L. Although the salt concentration was lower than the previous works, it could also have provoked a gradual population shift. Moreover, the inoculum of the reactor came from a biological reactor of a fish cannery, adapted to even higher salinity, so the nitrifying bacteria might be different populations compared to an inoculum non-adapted to salinity. In addition, other factors could also affect the value of this kinetic parameter, like the complexity of the incoming industrial wastewater (Table 5.2, Chapter 5).

8.5.1. Validation of the model

After the calibration of the model with a salt concentration of 13 g NaCl/L, it was validated with a different influent composition and a salt concentration of 5 g NaCl/L. The calibrated apparent μ_{max} were used to calculate the value of μ_{max} of all the types of bacteria without salinity effect, and under the salinity conditions of the validation by Eq.8.4. The values of $K_{Inh,50}$ (biomass adapted to salinity) were taken from Table 8.2.

$$\mu_{Obs} = \mu_{max} \frac{K_{Inh,50}}{K_{Inh,50} + S_{Inh}} \qquad \text{(Eq.8.4)}$$

The results of the calculations show that heterotrophic bacteria were the least affected by the presence of salt. The maximum growth rate was reduced with 23 and 10 % under salinity conditions corresponding to calibration and validation, respectively. The value of μ_{max} of both AOB and NOB suffered higher reductions, especially with the salt concentration of 13 g NaCl/L (calibration), showing a higher sensitivity of nitrifying bacteria to the increase of salinity (Table 8.3).

Table 8.3: Values of μ_{max} of the bacteria populations under the salt concentrations used as input in the model.

		Calibration		**Validation**	
Salinity (g NaCl/L)	0	13		5	
	μ_{max} (d^{-1})	**μ_{max} (d^{-1})**	**μ_{max} reduction (%)***	**μ_{max} (d^{-1})**	**μ_{max} reduction (%)***
HB	7.76	6	23	6.97	10
AOB	0.27	0.18	34	0.22	17
NOB	0.16	0.10	37	0.13	19

*The reduction percentage was calculated as the difference between the value of μ_{max} without and with salinity, divided by the value of μ_{max} without salinity.

In the validation step, the results of the model were compared with an operational cycle from day 216. The COD consumption was accurately reproduced (Figure 8.6.a). However, the predicted ammonia oxidation was faster than the experimental data (Figure 8.6.b). The ammonia and nitrite concentration of the effluent were underestimated and overestimated, respectively, both in a 65 % (calculated as the difference between the experimental and the model value, divided by the experimental value). This could be due to the fact that the experimental cycle measurement was done in a moment when the reactor was not working in steady-state conditions. A few days before the cycle measurement (days 196 – 209), the washout of part of the biomass took place, associated

to the change of salinity (see details in Chapter 5). Although a stable effluent quality was achieved in these days, the biomass might have been still adapting to the new conditions of the reactor.

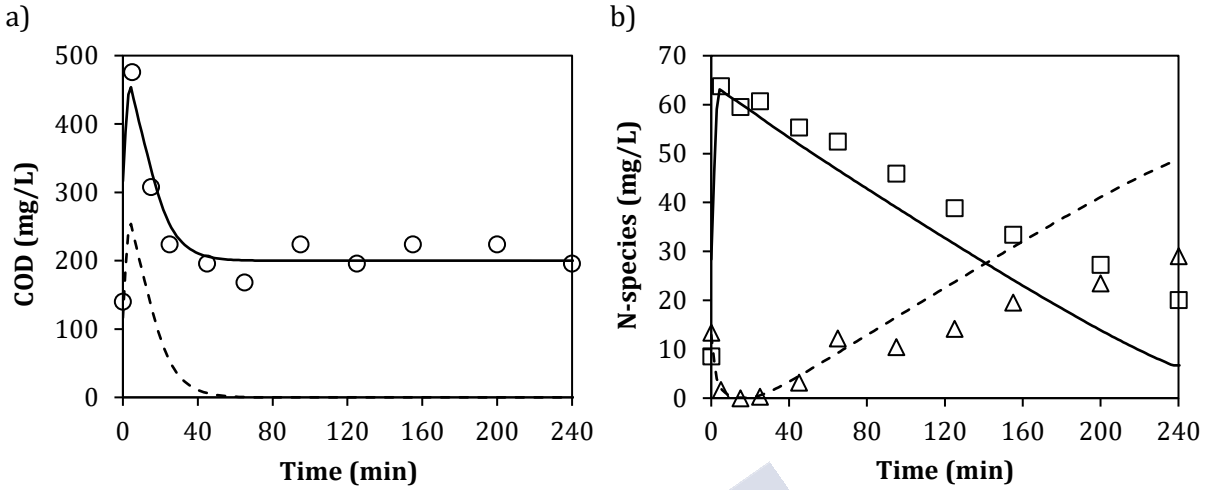

Figure 8.6: (a) S_{COD} (-) and S_S (- -) profile predicted with ASM3; and S_{COD} (○) profile from experimental data. (b) S_{NH} (-) and S_{NO2} (- -) profile predicted with ASM3; and S_{NH} (□) and S_{NO2} (△) profiles from experimental data. Cycle profiles corresponding to the results of the model validation.

In order to validate the model with experimental data from steady-state conditions, the effluent quality predicted by the model was also compared with the effluent quality measured experimentally during Stage IV before the washout of the biomass (Figure 8.7). The results indicated that, despite the different conversion rates of AOB, the model was able to predict the effluent concentrations of both organic matter and nitrogen compounds.

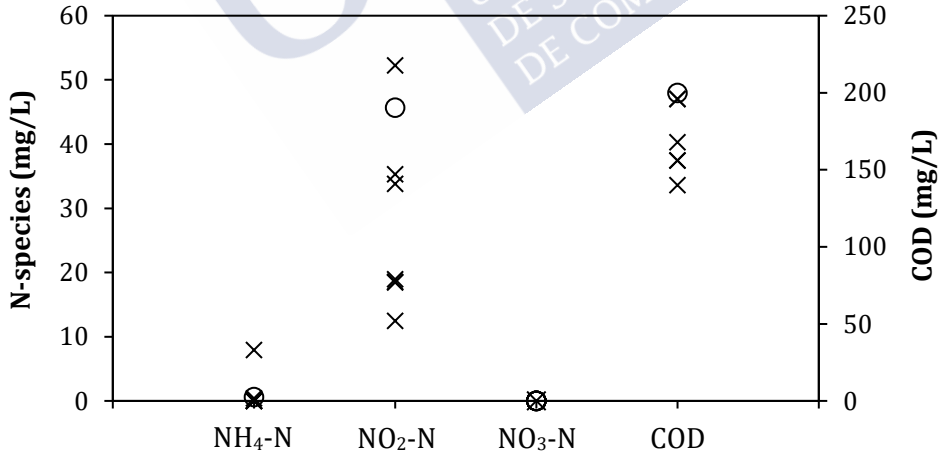

Figure 8.7: Comparison of the effluent quality from the experimental data (x) and predicted by the model (○).

The biological model considering the inhibition of salinity on the biological activity was calibrated with a representative cycle measurement from an operational stage of an AGS reactor with 13 g NaCl/L. In addition, it was validated with the effluent measurements of a different stage, with 5 g NaCl/L. However, the model has some shortcomings. It was observed experimentally that salt fluctuations not only affected the biological activity, but also the physical properties of the

biomass (see Chapter 5). In this model, only the effect of salinity on the bioconversion processes was considered. In addition, the salt concentrations used as input of the model were low-moderate, and the model should be tested with higher concentrations (20 – 40 g NaCl/L). Further research is needed to (1) test the biological model with higher salt concentrations to assess the impact of salinity on the biological activity and (2) study the feasibility of incorporating also the effect of salinity on the physical properties of the biomass.

8.6. CONCLUSIONS

To provide an accurate description of the biological processes occurring in an AGS reactor, two modifications were applied to the ASM3. These modifications consisted of: 1) the description of the COD removal as a simultaneous growth and storage process, and 2) the split of the nitrification process into two-steps.

The calibrated kinetic parameters of the heterotrophic bacteria were found to be similar to previous research works modelling AGS with ASM3. However, the maximum growth rates of AOB and NOB were found to be considerably lower. The cause of this discrepancy could be attributed to the complexity of the industrial wastewater, the presence of salt, or the high sludge retention time of the biomass.

The results of the validation demonstrated that the calibrated model was able to correctly predict the effluent composition of the AGS reactor for COD and nitrogen species.

The modifications applied to the model were proven to be successful in predicting the performance of an AGS reactor. However, further research is needed to overcome the shortcomings of the model. This model could be further used as a starting point for future research. For instance, the model could be applied in the design stage of future AGS reactors or for system optimisation and scenario analysis of existing reactors treating saline wastewater.

8.7. REFERENCES

Baeten, J.E., van Loosdrecht, M.C.M., Volcke, E.I.P., 2018. Modelling aerobic granular sludge reactors through apparent half-saturation coefficients. Water Res. https://doi.org/10.1016/j.watres.2018.09.025

Baeten, J.E., van Loosdrecht, M.C.M., Volcke, E.I.P., 2017. Improving the accuracy of granular sludge and biofilm reactor simulations in Aquasim through artificial diffusion. Biotechnol. Bioeng. https://doi.org/10.1002/bit.26323

Bassin, J.P., Pronk, M., Muyzer, G., Kleerebezem, R., Dezotti, M., van Loosdrecht, M.C.M., 2011. Effect of elevated salt concentrations on the aerobic granular sludge process: Linking microbial activity with microbial community structure. Appl. Environ. Microbiol. https://doi.org/10.1128/AEM.05016-11

Campo, R., Di Bella, G., 2019. Petrochemical slop wastewater treatment by means of aerobic granular sludge: effect of granulation process on bio-adsorption and hydrocarbons removal. Chem. Eng. J. https://doi.org/10.1016/j.cej.2019.122083

Carrera, J., Baeza, J.A., Vicent, T., Lafuente, J., 2003. Biological nitrogen removal of high-strength ammonium industrial wastewater with two-sludge system. Water Res. https://doi.org/10.1016/S0043-1354(03)00338-5

Chen, H., Chen, Q.Q., Jiang, X.Y., Hu, H.Y., Shi, M.L., Jin, R.C., 2016. Insight into the short- and long-term effects of Cu(II) on denitrifying biogranules. J. Hazard. Mater. https://doi.org/10.1016/j.jhazmat.2015.11.012

Chen, Q.Q., Xu, L.Z.J., Zhang, Z.Z., Sun, F.Q., Shi, Z.J., Huang, B.C., Fan, N.S., Jin, R.C., 2019. Insight into the short- and long-term effects of quinoline on anammox granules: Inhibition and acclimatization. Sci. Total Environ. https://doi.org/10.1016/j.scitotenv.2018.09.285

Chiellini, C., Munz, G., Petroni, G., Lubello, C., Mori, G., Verni, F., Vannini, C., 2013. Characterization and comparison of bacterial communities selected in conventional activated sludge and membrane bioreactor pilot plants: A focus on nitrospira and planctomycetes bacterial phyla. Curr. Microbiol. https://doi.org/10.1007/s00284-013-0333-6

Corsino, S.F., Capodici, M., Morici, C., Torregrossa, M., Viviani, G., 2016a. Simultaneous nitritation-denitritation for the treatment of high-strength nitrogen in hypersaline wastewater by aerobic granular sludge. Water Res. https://doi.org/10.1016/j.watres.2015.10.041

Corsino, S.F., Capodici, M., Morici, C., Torregrossa, M., Viviani, G., 2016b. Simultaneous nitritation-denitritation for the treatment of high-strength nitrogen in hypersaline wastewater by aerobic granular sludge. Water Res. 88, 329–336. https://doi.org/10.1016/j.watres.2015.10.041

Cui, Y.W., Zhang, H.Y., Ding, J.R., Peng, Y.Z., 2016. The effects of salinity on nitrification using halophilic nitrifiers in a Sequencing Batch Reactor treating hypersaline wastewater. Sci. Rep. https://doi.org/10.1038/srep24825

Dan, N.P., Visvanathan, C., Basu, B., 2003. Comparative evaluation of yeast and bacterial treatment of high salinity wastewater based on biokinetic coefficients. Bioresour. Technol. https://doi.org/10.1016/S0960-8524(02)00204-3

De Kreuk, M.K., Picioreanu, C., Hosseini, M., Xavier, J.B., Van Loosdrecht, M.C.M., 2007. Kinetic model of

a granular sludge SBR: Influences on nutrient removal. Biotechnol. Bioeng. https://doi.org/10.1002/bit.21196

Figueroa, M., Mosquera-Corral, A., Campos, J.L., Méndez, R., 2008. Treatment of saline wastewater in SBR aerobic granular reactors. Water Sci. Technol. https://doi.org/10.2166/wst.2008.406

Gao, D., Peng, Y., Wu, W.M., 2010. Kinetic model for biological nitrogen removal using shortcut nitrification-denitrification process in sequencing batch reactor. Environ. Sci. Technol. https://doi.org/10.1021/es100514x

Gonzalez-Silva, B.M., Jonassen, K.R., Bakke, I., Østgaard, K., Vadstein, O., 2016. Nitrification at different salinities: Biofilm community composition and physiological plasticity. Water Res. https://doi.org/10.1016/j.watres.2016.02.050

Hauduc, H., Rieger, L., Takács, I., Héduit, A., Vanrolleghem, P.A., Gillot, S., 2010. A systematic approach for model verification: Application on seven published activated sludge models. Water Sci. Technol. https://doi.org/10.2166/wst.2010.898

Henze, M., Gujer, W., Mino, T., Loosdrecht, M. van, 2000. Activated Sludge Models ASM1, ASM2, ASM2d and ASM3 IWA Scientific and Technical Report No.9, Journal of Chemical Information and Modeling. https://doi.org/10.1017/CBO9781107415324.004

Henze, M., van Loosdrecht, M.C.M., Ekama, G.A., Brdjanovic, D., 2008. Biological Wastewater Treatment: Principles, Modelling and Design. https://doi.org/10.2166/9781780401867

Isanta, E., Figueroa, M., Mosquera-Corral, A., Campos, L., Carrera, J., Pérez, J., 2013. A novel control strategy for enhancing biological N-removal in a granular sequencing batch reactor: A model-based study. Chem. Eng. J. https://doi.org/10.1016/j.cej.2013.07.118

Jiménez, E., Giménez, J.B., Seco, A., Ferrer, J., Serralta, J., 2012. Effect of pH, substrate and free nitrous acid concentrations on ammonium oxidation rate. Bioresour. Technol. https://doi.org/10.1016/j.biortech.2012.07.079

Kaelin, D., Manser, R., Rieger, L., Eugster, J., Rottermann, K., Siegrist, H., 2009. Extension of ASM3 for two-step nitrification and denitrification and its calibration and validation with batch tests and pilot scale data. Water Res. https://doi.org/10.1016/j.watres.2008.12.039

Krishna, C., Van Loosdrecht, M.C.M., 1999. Substrate flux into storage and growth in relation to activated sludge modeling. Water Res. https://doi.org/10.1016/S0043-1354(99)00031-7

Li, X., Luo, J., Guo, G., Mackey, H.R., Hao, T., Chen, G., 2017. Seawater-based wastewater accelerates development of aerobic granular sludge: A laboratory proof-of-concept. Water Res. https://doi.org/10.1016/j.watres.2017.03.002

Liu, S., Yang, F., Gong, Z., Su, Z., 2008. Assessment of the positive effect of salinity on the nitrogen removal performance and microbial composition during the start-up of CANON process. Appl. Microbiol. Biotechnol. https://doi.org/10.1007/s00253-008-1536-9

Moussa, M.S., Sumanasekera, D.U., Ibrahim, S.H., Lubberding, H.J., Hooijmans, C.M., Gijzen, H.J., Van Loosdrecht, M.C.M., 2006. Long term effects of salt on activity, population structure and floc characteristics in enriched bacterial cultures of nitrifiers. Water Res. https://doi.org/10.1016/j.watres.2006.01.029

Munz, G., Mori, G., Vannini, C., Lubello, C., 2010. Kinetic parameters and inhibition response of ammonia-and nitrite-oxidizing bacteria in membrane bioreactors and conventional activated sludge processes. Environ. Technol. https://doi.org/10.1080/09593331003793828

Ni, B.J., Yu, H.Q., Sun, Y.J., 2008. Modeling simultaneous autotrophic and heterotrophic growth in aerobic granules. Water Res. https://doi.org/10.1016/j.watres.2007.11.010

Pai, T.Y., Wang, S.C., Lo, H.M., Chiang, C.F., Liu, M.H., Chiou, R.J., Chen, W.Y., Hung, P.S., Liao, W.C., Leu, H.G., 2009. Novel modeling concept for evaluating the effects of cadmium and copper on heterotrophic growth and lysis rates in activated sludge process. J. Hazard. Mater. https://doi.org/10.1016/j.jhazmat.2008.11.009

Peng, S., Han, X., Song, F., Zhang, L., Wei, C., Lu, P., Zhang, D., 2018. Inhibition of benzene, toluene, phenol and benzoate in single and combination on Anammox activity: implication to the denitrification–Anammox synergy. Biodegradation. https://doi.org/10.1007/s10532-018-9853-x

Phanwilai, S., Piyavorasakul, S., Noophan, P. (Lek), Daniels, K.D., Snyder, S.A., 2020. Inhibition of anaerobic ammonium oxidation (anammox) bacteria by addition of high and low concentrations of chloramphenicol and comparison of attached- and suspended-growth. Chemosphere. https://doi.org/10.1016/j.chemosphere.2019.124570

Pronk, M., Bassin, J.P., De Kreuk, M.K., Kleerebezem, R., Van Loosdrecht, M.C.M., 2014. Evaluating the main and side effects of high salinity on aerobic granular sludge. Appl. Microbiol. Biotechnol. https://doi.org/10.1007/s00253-013-4912-z

Pronk, M., de Kreuk, M.K., de Bruin, B., Kamminga, P., Kleerebezem, R., van Loosdrecht, M.C.M., 2015. Full scale performance of the aerobic granular sludge process for sewage treatment. Water Res. 84, 207–217. https://doi.org/10.1016/j.watres.2015.07.011

Ramos, C., Fernández, I., Suárez-Ojeda, M.E., Carrera, J., 2015. Inhibition of the anammox activity by aromatic compounds. Chem. Eng. J. https://doi.org/10.1016/j.cej.2015.05.071

Reichert, P., 1998. Computer Program for the Identification and Simulation of Aquatic Systems (AQUASIM), Swiss Federal Institute for Environmental Science and Technology (EAWAG), 144-151

Song, Y.X., Chai, L.Y., Tang, C.J., Xiao, R., Li, B.R., Wu, D., Min, X.B., 2018. Influence of ZnO nanoparticles on anammox granules: The inhibition kinetics and mechanism analysis by batch assays. Biochem. Eng. J. https://doi.org/10.1016/j.bej.2018.02.006

Thwaites, B.J., Van Den Akker, B., Reeve, P.J., Short, M.D., Dinesh, N., Alvarez-Gaitan, J.P., Stuetz, R., 2018. Ecology and performance of aerobic granular sludge treating high-saline municipal wastewater. Water Sci. Technol. https://doi.org/10.2166/wst.2017.626

Torà, J.A., Lafuente, J., Baeza, J.A., Carrera, J., 2010. Combined effect of inorganic carbon limitation and inhibition by free ammonia and free nitrous acid on ammonia oxidizing bacteria. Bioresour. Technol. https://doi.org/10.1016/j.biortech.2010.03.005

Val Del Río, A., Figueroa, M., Mosquera-Corral, A., Campos, J.L., Méndez, R., 2013. Stability of aerobic granular biomass treating the effluent from a seafood industry. Int. J. Environ. Res. https://doi.org/10.22059/ijer.2013.606

van den Akker, B., Reid, K., Middlemiss, K., Krampe, J., 2015. Evaluation of granular sludge for

secondary treatment of saline municipal sewage. J. Environ. Manage. 157, 139–145. https://doi.org/10.1016/j.jenvman.2015.04.027

Vázquez-Padín, J.R., Mosquera-Corral, A., Campos, J.L., Méndez, R., Carrera, J., Pérez, J., 2010. Modelling aerobic granular SBR at variable COD/N ratios including accurate description of total solids concentration. Biochem. Eng. J. https://doi.org/10.1016/j.bej.2009.12.009

Wang, X., Yang, T., Lin, B., Tang, Y., 2017. Effects of salinity on the performance, microbial community, and functional proteins in an aerobic granular sludge system. Chemosphere. https://doi.org/10.1016/j.chemosphere.2017.06.047

Wang, Z., Gao, M., She, Z., Wang, S., Jin, C., Zhao, Y., Yang, S., Guo, L., 2015. Effects of salinity on performance, extracellular polymeric substances and microbial community of an aerobic granular sequencing batch reactor. Sep. Purif. Technol. https://doi.org/10.1016/j.seppur.2015.02.042

Wang, Z., van Loosdrecht, M.C.M., Saikaly, P.E., 2017. Gradual adaptation to salt and dissolved oxygen: Strategies to minimize adverse effect of salinity on aerobic granular sludge. Water Res. https://doi.org/10.1016/j.watres.2017.08.026

Wiesmann, U., 1994. Biological nitrogen removal from wastewater. Adv. Biochem. Eng. Biotechnol. https://doi.org/10.1007/bfb0008736

Zhao, J., Huang, J., Guan, M., Zhao, Y., Chen, G., Tian, X., 2016. Mathematical simulating the process of aerobic granular sludge treating high carbon and nitrogen concentration wastewater. Chem. Eng. J. https://doi.org/10.1016/j.cej.2016.07.098

Zhou, M., Gong, J., Yang, C., Pu, W., 2013. Simulation of the performance of aerobic granular sludge SBR using modified ASM3 model. Bioresour. Technol. https://doi.org/10.1016/j.biortech.2012.09.076

APPENDIX A: reference case

Data used for the calibration of the model.

Symbol	Definition	Value	Units	Reference
Input data				
$S_{NHx,in}$	Influent NH_x concentration	73	g N/m^3	Experimental data
$S_{S,in}$	Influent soluble readily biodegradable COD	440	g COD/m^3	Experimental data
$S_{I,in}$	Influent soluble inert COD	170	g COD/m^3	Experimental data
$X_{S,in}$	Influent particulate slowly biodegradable COD	83	g COD/m^3	Experimental data
$X_{I,in}$	Influent particulate inert COD	87	g COD/m^3	Experimental data
Granule characteristics				
ε_w	Granule porosity	0.8	-	De Kreuk et al. (2007)
R_{SS}	Surface mean diameter of granules at steady state	1.25	mm	Experimental data
ρ_{BM}	Density of biomass	1.13×10^6	g COD/m^3	Experimental data
ρ_{PHA}	Density of PHA	1×10^9	g COD/m^3	De Kreuk et al. (2007)
n_g	Number of granules	59593	-	Experimental data
ε_{PHA}	Initial concentration of PHA	0	-	Experimental data
ε_{OHO}	Initial concentration of OHO	0.19	-	Experimental data
ε_{AOB}	Initial concentration of AOB	0.01	-	Experimental data
ε_{NOB}	Initial concentration of NOB	0	-	Experimental data
Reactor and operational characteristics				
$V_{reactor}$	Total reactor volume	1.7	L	Experimental data
VER	Volume exchange ratio	50	%	Experimental data
t_{cycle}	Total operation time cycle	4	h	Experimental data
$t_{feeding}$	Time of feeding	5	min	Experimental data
$t_{settling}$	Time of settling	1	min	Experimental data
$t_{discharge}$	Time of discharge	7	min	Experimental data
T	Temperature	23	°C	Experimental data
S_{O2}	Oxygen concentration	8.6	g O_2/m^3	Experimental data
$VSS_{reactor}$	Sludge concentration in the reactor	5.9	kg VSS/m^3	Experimental data
$ISS_{reactor}/TSS_{reactor}$	Ash content of the reactor	0.16	kg ISS/kg TSS	Experimental data

Data used for the validation of the model.

Symbol	Definition	Value	Units	Reference
Input data				
$S_{NHx,in}$	Influent NH_x concentration	106	g N/m^3	Experimental data
$S_{S,in}$	Influent soluble readily biodegradable COD	700	g COD/m^3	Experimental data
$S_{I,in}$	Influent soluble inert COD*	200	g COD/m^3	Experimental data
$X_{S,in}$	Influent particulate slowly biodegradable COD	34	g COD/m^3	Experimental data
$X_{I,in}$	Influent particulate inert COD	36	g COD/m^3	Experimental data
Granule characteristics				
ε_w	Granule porosity	0.8	-	De Kreuk et al. (2007)
R_{SS}	Surface mean diameter of granules at steady state	1.1	mm	Experimental data
ρ_{BM}	Density of biomass	9.62×10^5	g COD/m^3	Experimental data
ρ_{PHA}	Density of PHA	1×10^9	g COD/m^3	De Kreuk et al. (2007)
n_g	Number of granules	89000	-	Experimental data
ε_{PHA}	Initial concentration of PHA	0	-	Experimental data
ε_{OHO}	Initial concentration of OHO	0.19	-	Experimental data
ε_{AOB}	Initial concentration of AOB	0.01	-	Experimental data
ε_{NOB}	Initial concentration of NOB	0	-	Experimental data
Reactor and operational characteristics				
$V_{reactor}$	Total reactor volume	1.7	L	Experimental data
VER	Volume exchange ratio	50	%	Experimental data
t_{cycle}	Total operation time cycle	4	h	Experimental data
$t_{feeding}$	Time of feeding	5	min	Experimental data
$t_{settling}$	Time of settling	1	min	Experimental data
$t_{discharge}$	Time of discharge	7	min	Experimental data
T	Temperature	23	°C	Experimental data
S_{O2}	Oxygen concentration	8.6	g O_2/m^3	Experimental data
$VSS_{reactor}$	Sludge concentration in the reactor	3.6	kg VSS/m^3	Experimental data
$ISS_{reactor}$/ $TSS_{reactor}$	Ash content of the reactor	0.2	kg ISS/kg TSS	Experimental data

APPENDIX B: bioconversion reactions

Hydrolysis	$k_h \left(\frac{X_S/X_{BH}}{K_X + (X_S/X_{BH})}\right) X_H$
Heterotrophic bacteria	
Aerobic storage of X_{STO}	$k_{STO} \left(\frac{S_S}{K_{SH} + S_S}\right)\left(\frac{S_O}{K_{OH} + S_O}\right) X_H$
Anoxic storage of X_{STO} (NO_2)	$k_{STO}\eta_g \left(\frac{K_{OH}}{K_{OH} + S_O}\right)\left(\frac{S_S}{K_{SH} + S_S}\right)\left(\frac{S_{NO_2}}{K_{NO2H} + S_{NO_2}}\right) X_H$
Anoxic storage of X_{STO} (NO_3)	$k_{STO}\eta_g \left(\frac{K_{OH}}{K_{OH} + S_O}\right)\left(\frac{S_S}{K_{SH} + S_S}\right)\left(\frac{S_{NO_3}}{K_{NO3H} + S_{NO_3}}\right) X_H$
Aerobic growth on S_S	$\mu_H \left(\frac{S_S}{K_{SH} + S_S}\right)\left(\frac{S_O}{K_{OH} + S_O}\right)\left(\frac{S_{NH}}{K_{NHH} + S_{NH}}\right) X_H$
Anoxic growth on S_S NO_2	$\mu_H\eta_g \left(\frac{K_{OH}}{K_{OH} + S_O}\right)\left(\frac{S_S}{K_{SH} + S_S}\right)\left(\frac{S_{NO_2}}{K_{NO2H} + S_{NO_2}}\right)\left(\frac{S_{NH}}{K_{NHH} + S_{NH}}\right) X_H$
Anoxic growth on S_S NO_3	$\mu_H\eta_g \left(\frac{K_{OH}}{K_{OH} + S_O}\right)\left(\frac{S_S}{K_{SH} + S_S}\right)\left(\frac{S_{NO_2}}{K_{NO3H} + S_{NO_2}}\right)\left(\frac{S_{NH}}{K_{NHH} + S_{NH}}\right) X_H$
Aerobic growth on X_{STO}	$\mu_H \left(\frac{S_O}{K_{OH} + S_O}\right)\left(\frac{S_{NH}}{K_{NHH} + S_{NH}}\right)\left(\frac{X_{STO}/X_{BH}}{K_{STO} + (X_{STO}/X_{BH})}\right) X_H$
Anoxic growth on X_{STO} (NO_2)	$\mu_H\eta_g \left(\frac{K_{OH}}{K_{OH} + S_O}\right)\left(\frac{S_{NO_2}}{K_{NO_2} + S_{NO_2}}\right)\left(\frac{S_{NH}}{K_{NHH} + S_{NH}}\right)\left(\frac{X_{STO}/X_{BH}}{K_{STO} + (X_{STO}/X_{BH})}\right) X_H$
Anoxic growth on X_{STO} (NO_3)	$\mu_H\eta_g \left(\frac{K_{OH}}{K_{OH} + S_O}\right)\left(\frac{S_{NO_3}}{K_{NO_3} + S_{NO_3}}\right)\left(\frac{S_{NH}}{K_{NHH} + S_{NH}}\right)\left(\frac{X_{STO}/X_{BH}}{K_{STO} + (X_{STO}/X_{BH})}\right) X_H$
Aerobic endogenous respiration	$b_H \left(\frac{S_O}{K_{OH} + S_O}\right) X_H$
Anoxic endogenous respiration (NO_2)	$b_H\eta_g \left(\frac{K_{OH}}{K_{OH} + S_O}\right)\left(\frac{S_{NO_2}}{K_{NO2N} + S_{NO_2}}\right) X_H$
Anoxic endogenous respiration (NO_3)	$b_H\eta_g \left(\frac{K_{OH}}{K_{OH} + S_O}\right)\left(\frac{S_{NO_3}}{K_{NO3N} + S_{NO_3}}\right) X_H$
Aerobic endogenous respiration of X_{STO}	$b_{STO} \left(\frac{S_O}{K_{OH} + S_O}\right) X_{STO}$
Anoxic endogenous respiration X_{STO} (NO_2)	$b_{STO}\eta_g \left(\frac{K_{OH}}{K_{OH} + S_O}\right)\left(\frac{S_{NO_2}}{K_{NO2N} + S_{NO_2}}\right) X_{STO}$
Anoxic endogenous respiration X_{STO} (NO_3)	$b_{STO}\eta_g \left(\frac{K_{OH}}{K_{OH} + S_O}\right)\left(\frac{S_{NO_3}}{K_{NO3N} + S_{NO_3}}\right) X_{STO}$

Ammonia oxidising bacteria (AOB)	
Aerobic growth AOB	$\mu_A \left(\frac{S_{NH}}{K_{NHA} + S_{NH}}\right)\left(\frac{S_O}{K_{OA} + S_O}\right) X_A$
Aerobic endogenous respiration	$b_A \left(\frac{S_O}{K_{OA} + S_O}\right) X_A$
Anoxic endogenous respiration (NO_2)	$b_A \eta_g \left(\frac{K_{OA}}{K_{OA} + S_O}\right)\left(\frac{S_{NO_2}}{K_{NO2A} + S_{NO_2}}\right) X_A$
Anoxic endogenous respiration (NO_3)	$b_A \eta_g \left(\frac{K_{OA}}{K_{OA} + S_O}\right)\left(\frac{S_{NO_3}}{K_{NO2A} + S_{NO_3}}\right) X_A$
Nitrite oxidising bacteria (NOB)	
Aerobic growth NOB	$\mu_N \left(\frac{S_{NO_2}}{K_{NO2N} + S_{NO_2}}\right)\left(\frac{S_O}{K_{ON} + S_O}\right) X_N$
Aerobic endogenous respiration	$b_N \left(\frac{S_O}{K_{ON} + S_O}\right) X_N$
Anoxic endogenous respiration (NO_2)	$b_N \eta_g \left(\frac{K_{ON}}{K_{ON} + S_O}\right)\left(\frac{S_{NO_2}}{K_{NO2N} + S_{NO_2}}\right) X_N$
Anoxic endogenous respiration (NO_3)	$b_N \eta_g \left(\frac{K_{ON}}{K_{ON} + S_O}\right)\left(\frac{S_{NO_3}}{K_{NO3N} + S_{NO_3}}\right) X_N$

APPENDIX C: Stoichiometric matrix

		S_{O2}	S_I	S_S	S_{NH}	S_{NO2}	S_{NO3}	X_I	X_S	X_H	X_{STO}	X_A	X_N
Heterotrophic bacteria													
1	Aerobic hydrolysis		f_{SI}	$1-f_{SI}$	$-i_{NSS}\cdot(1-f_{SI})-(f_{SI}\cdot i_{NSI})+i_{NXS}$				-1				
2	Aerobic storage of S_S	$-(1/Y_{STO}-1)$		$-1/Y_{STO}$							1		
3	Anoxic storage of S_S - NO_2			$-1/Y_{STO}$		$-(1/Y_{STO}-1)/1.71$					1		
4	Anoxic storage of S_S - NO_3			$-1/Y_{STO}$			$-(1/Y_{STO}-1)/2.86$				1		
5	Aerobic growth - Ss	$-(1/Y_H-1)$		$-1/Y_H$	$-i_{NXB}$					1			
6	Anoxic growth - NO_2			$-1/Y_H$	$-i_{NXB}$	$-(1/Y_H-1)/1.71$				1			
7	Anoxic growth - NO_3			$-1/Y_H$	$-i_{NXB}$		$-(1/Y_H-1)/2.86$			1			
8	Aerobic growth - X_{STO}	$-(1/Y_{HSTO}-1)$			$-i_{NXB}$					1	$-1/Y_{HSTO}$		
9	Anoxic growth - NO_2				$-i_{NXB}$	$-(1/Y_{HSTO}-1)/1.71$				1	$-1/Y_{HSTO}$		
10	Anoxic growth - NO_3				$-i_{NXB}$		$-(1/Y_{HSTO}-1)/2.86$			1	$-1/Y_{HSTO}$		
11	Aerobic respiration - Ss	$-(1-f_X)$			$i_{NXB}-i_{XI}\cdot f_X$			f_X		-1			
12	Anoxic endogenous respiration - NO_2				$i_{NXB}-i_{XI}\cdot f_X$	$-(1-f_X)/1.71$		f_X		-1			
13	Anoxic endogenous respiration - NO_3				$i_{NXB}-i_{XI}\cdot f_X$		$-(1-f_X)/2.86$	f_X		-1			

		S_{O2}	S_I	S_S	S_{NH}	S_{NO2}	S_{NO3}	X_I	X_S	X_H	X_{STO}	X_A	X_N
Heterotrophic bacteria													
14	Aerobic respiration - X_{STO}	-1									-1		
15	Anoxic respiration of X_{STO} - NO_2					-1/1.71					-1		
16	Anoxic respiration of X_{STO} - NO_3						-1/2.86				-1		
Ammonia Oxidising Bacteria													
17	Aerobic growth	$-(3.43-Y_A)/Y_A$			$-i_{XB}-1/Y_A$	$1/Y_A$						1	
18	Aerobic endogenous respiration	$-(1-f_X)$			$i_{NXB}-i_{XI}\cdot f_X$			f_X				-1	
19	Anoxic endogenous respiration - NO_2				$i_{NXB}-i_{XI}\cdot f_X$	$-(1-f_X)/1.71$		f_X				-1	
20	Anoxic endogenous respiration - NO_3				$i_{NXB}-i_{XI}\cdot f_X$		$-(1-f_X)/2.86$	f_X				-1	
Nitrite Oxidising Bacteria													
21	Aerobic growth	$-(1.14-Y_N)/Y_N$			$-i_{XB}$	$-1/Y_N$	$1/Y_N$						1
22	Aerobic endogenous respiration	$-(1-f_X)$			$i_{NXB}-i_{XI}\cdot f_X$			f_X					-1
23	Anoxic endogenous respiration - NO_2				$i_{NXB}-i_{XI}\cdot f_X$	$-(1-f_X)/1.71$		f_X					-1
24	Anoxic endogenous respiration - NO_3				$i_{NXB}-i_{XI}\cdot f_X$		$-(1-f_X)/2.86$	f_X					-1

APPENDIX D: kinetic and stoichiometric parameters

Kinetic parameters				
Symbol	**Definition**	**Value**	**Units**	**Reference**
μ_H*	Maximum specific growth rate for HB	2.46	d^{-1}	Henze et al. (2000)
μ_A*	Maximum specific growth rate for AOB	1.10	d^{-1}	Wiesmann (1994)
μ_N*	Maximum specific growth rate for NOB	1.28	d^{-1}	Wiesmann (1994)
μ_H	Maximum specific growth rate for HB	6	d^{-1}	Calibrated
μ_A	Maximum specific growth rate for AOB	0.18	d^{-1}	Calibrated
μ_N	Maximum specific growth rate for NOB	0.10	d^{-1}	Calibrated
b_H	Decay coefficient for HB	0.25	d^{-1}	Henze et al. (2000)
b_A	Decay coefficient for AOB	0.074	d^{-1}	Wiesmann (1994)
b_N	Decay coefficient for NOB	0.074	d^{-1}	Wiesmann (1994)
b_{STO}	Aerobic respiration rate of X_{STO}	0.25	d^{-1}	Henze et al. (2000)
K_{OH}	Oxygen half-saturation coefficient for HB	0.2	g $O_2 \cdot m^{-3}$	Henze et al. (2000)
K_{OA}	Oxygen half-saturation coefficient for AOB	0.3	g $O_2 \cdot m^{-3}$	Wiesmann (1994)
K_{ON}	Oxygen half-saturation coefficient for NOB	1.1	g $O_2 \cdot m^{-3}$	Wiesmann (1994)
K_S	Org. Mat. Half-saturation coefficient for HB	2	g COD$\cdot m^{-3}$	Henze et al. (2000)
K_{STO}	X_{STO} half-saturation coefficient for HB	1	g $COD_{STO}\cdot$(g $COD_{XH})^{-1}$	Henze et al. (2000)
K_{NO2}	NO_2 half-saturation coefficient for denitrifying HB	0.5	g NO_2-N$\cdot m^{-3}$	Vázquez-Padín et al. (2010)
K_{NO3}	NO_3 half-saturation coefficient for denitrifying HB	0.5	g NO_3-N$\cdot m^{-3}$	Vázquez-Padín et al. (2010)
K_{NH_A}	Ammonia half-saturation coefficient for AOB	5.71	g NH_4-N$\cdot m^{-3}$	Wiesmann (1994)
K_{NH_HB}	Ammonia half-saturation coefficient for HB	0.05	g NH_4-N$\cdot m^{-3}$	Hauduc et al. (2010)
K_{NO2N}	NO_2 half-saturation coefficient for NOB	0.001	kg NO_2-N$\cdot m^{-3}$	Vázquez-Padín et al. (2010)
k_{STO}*	Storage rate constant	6.16	g $COD_{Ss}\cdot$(g $COD_{XH})^{-1}\cdot d^{-1}$	Henze et al. (2000)
k_{STO}	Storage rate constant	8	g $COD_{Ss}\cdot$(g $COD_{XH})^{-1}\cdot d^{-1}$	Calibrated
η_g	Corrector factor for μ_H under anoxic conditions	0.6	-	Henze et al. (2000)
k_h	Maximum specific hydrolysis rate	3.69	g $COD_{sd}\cdot$(g COD_{cell}/day)$^{-1}$	Henze et al. (2000)
K_X	Half-saturation coef. For hydrolysis of slowly biod. Substrate	1	g $COD_{sd}\cdot$(g $COD_{cell})^{-1}$	Henze et al. (2000)
Y_H	Heterotrophic yield	0.57	kg COD$\cdot$kg COD	Vázquez-Padín et al. (2010)

*Default values used as a first step during the calibration of the model.

Stoichiometric parameters				
Symbol	**Definition**	**Value**	**Units**	**Reference**
Y_A	AOB yield	0.18	kg COD·kg COD	Vázquez-Padín et al. (2010)
Y_N	NOB yield	0.08	kg COD·kg COD	Vázquez-Padín et al. (2010)
Y_{STO}	Yield for storage substrate	0.8	kg COD·kg COD	Vázquez-Padín et al. (2010)
Y_{HSTO}	Heterotrophic yield from X_{STO}	0.68	kg COD·kg COD	Vázquez-Padín et al. (2010)
f_{SI}	Production of S_I in hydrolysis	0	kg COD·kg COD	Henze et al. (2000)
i_{NXB}	Mass of N per mass of COD in biomass	0.07	g N·(g COD)$^{-1}$	Henze et al. (2000)
i_{NSS}	N content of S_S	0.03	g N·(g COD)$^{-1}$	Henze et al. (2000)
i_{NSI}	N content of S_I	0.01	g N·(g COD)$^{-1}$	Henze et al. (2000)
i_{NXI}	N content of X_I	0.02	g N·(g COD)$^{-1}$	Henze et al. (2000)
i_{NXS}	N content of X_S	0.04	g N·(g COD)$^{-1}$	Henze et al. (2000)

All the kinetic parameters were corrected taking into account the operation temperature, as suggested by Hauduc et al., (2010), with Eq.8.D1.

$$k(T) = k(20°C) \cdot \theta_{pow}^{\,T-20} \qquad \text{(Eq.8.D1)}$$

Where k(T) is the kinetic parameter corrected to the working temperature, k(20°C) is the value of the kinetic parameter at 20 °C, T is the temperature (°C) and θ_{pow} is calculated from Eq. 8.D2:

$$\theta_{pow} = \left(\frac{k(T_1)}{k(T_2)}\right)^{1/(T_1-T_2)} \qquad \text{(Eq.8.D2)}$$

The values of k(T1) and k(T2) corresponded to the values of the kinetic parameters from ASM3 at 10 and 20 °C. Stoichiometric and kinetic parameters values are presented in Appendix D.

APPENDIX E: estimation of the inhibition constants

The half-inhibition constant was estimated by reading in the graphs the salt concentration corresponding to the 50 % decrease of the maximum activity.

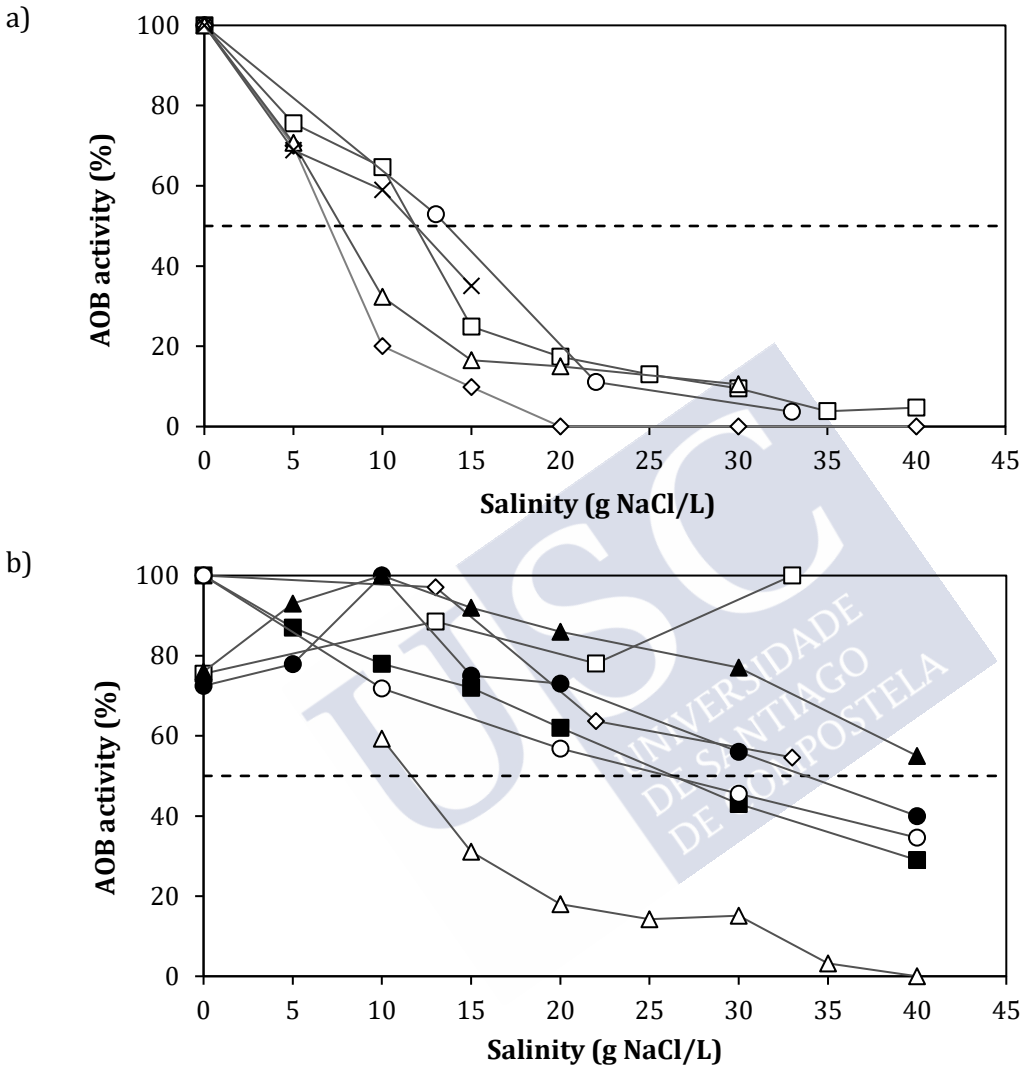

Figure E.1: (a) AOB activity with different salt concentrations of biomass non-adapted to salinity. Data from Moussa et al. (2006) (○), González-Silva et al. (2016) (□), Wang et al. (2017) (△), Bassin et al. (2012) (◇), Moussa et al. (2003) (x). (b) AOB activity with different salt concentrations of biomass adapted to salinity. Data from Wang et al. (2015) (○, gradually adapted to salt), González-Silva et al. (2016) (adapted to 33 (□) and 22 (◇) g/L), Moussa et al. (2006) (△, adapted to 10 g/L), Bassin et al. (2011) (adapted to 11 (■), 22 (●) and 33 (▲) g/L).

a)

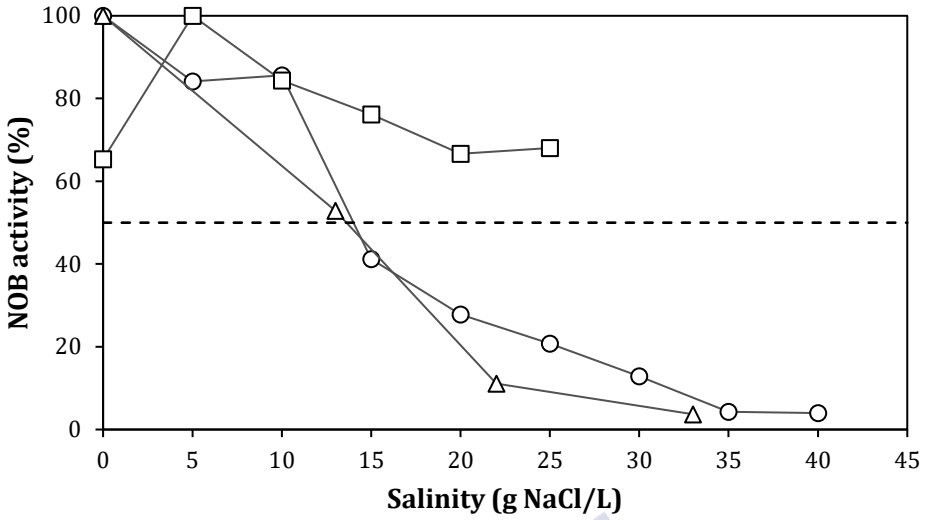

b)

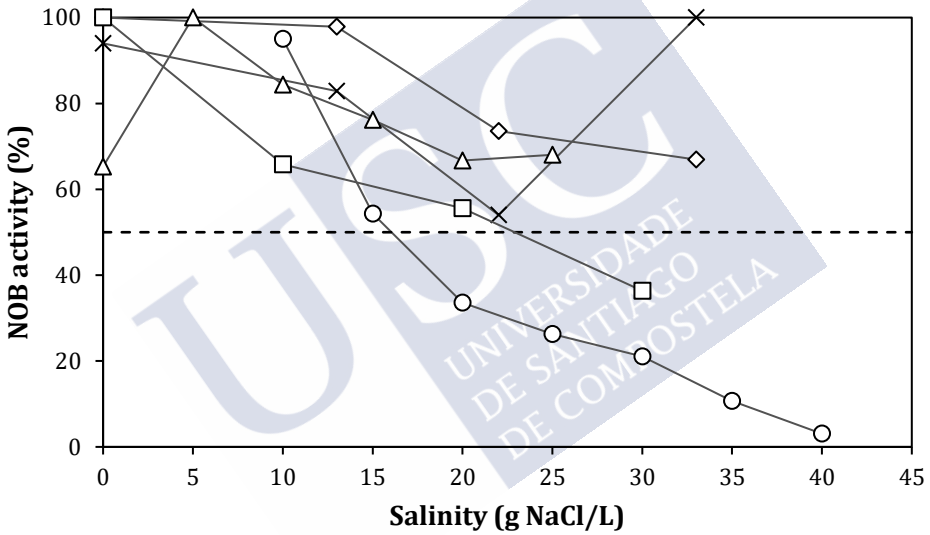

Figure E.2: (a) NOB activity with different salt concentrations of biomass non-adapted to salinity. Data from Moussa et al. (2006) (○), Wang et al. (2017) (□), González-Silva et al. (2016) (△). (b) NOB activity with different salt concentrations of biomass adapted to salinity. Data from Moussa et al. (2006) (○, adapted to 10 g/L), Wang et al. (2015) (□, gradually adapted), Wang et al. (2017) (△, gradually adapted), González-Silva et al. (2016) (adapted to 22 (◇) and 33 (x) g/L).

The inhibition constant of heterotrophic bacteria was determined based on specific values reported in literature (Wang et al., 2015) due to the lack of specific activity assays at different salt concentrations.

USC
UNIVERSIDADE
DE SANTIAGO
DE COMPOSTELA

General conclusions

The present thesis focuses on the optimisation of the aeration strategy and the scale up of the Aerobic Granular Sludge (AGS) technology for the treatment of fish-canning wastewater characterised by its large variable composition and salt concentration. The main conclusions of the chapters with experimental results within this thesis are detailed below:

Pulsed aeration strategy

In anaerobic-fed AGS reactors (**Chapter 3**), pulsed aeration (SGV of 3.6 cm/s) was found to be a better option to speed up the granulation process and achieve denser granules, compared to a continuous air supply with the same volume of air added per cycle (SGV of 1.2 cm/s). In addition, the pulsed regime favoured the faster development of PAOs and stimulated the presence of GAOs. The differences regarding the COD, N and P removal efficiencies at long-term operation between the pulsed and continuously aerated system were not significative. In both cases, the COD, N and P removal efficiencies were of 85, 95 and 30 %, respectively, treating OLRs of 0.8 kg COD/(m^3·d), NLRs of 0.1 kg N/(m^3·d) and PLRs of 0.3 g P/(m^3·d).

After a long-term storage of almost 2 years of the AGS reactors from the previous experiment, heterotrophic and AOB activities were recovered after 2 and 12 days of operation after both reactors re-start up. No significant differences were observed regarding the aeration regime during the reactivation process of aerobic granules. Nevertheless, neither PAO nor NOB activities restored at the end of the reactivation assay.

In fully aerobic AGS reactors (**Chapter 4**), the pulsed regime did not suppose a reduction of the granulation time compared to continuous aeration. However, it had a big impact at long-term operation. With continuous aeration, the overgrowth of filamentous bacteria occurred, due to the low applied OLR (lower than 2 kg COD/(m^3·d)) and SGV (1.2 cm/s). The pulsed aeration, with an SGV of 3.6 cm/s, avoided the growth of filamentous bacteria. Well-shaped granules with good settleability were produced and higher biomass concentrations were achieved. The removal efficiencies were almost the same with pulsed and continuous aeration, being of 90 and 65 % for COD and N, respectively.

The decrease of the airflow of the pulses (**Chapter 3**) reduced air requirements in the pulsed regime compared to the continuous aeration. The reactor with pulsed regime was operated satisfactorily with a supply of 0.73 $L_{air}/(L_{reactor}$·min). The continuous aerated reactor maintained its stability with a supply of 1 $L_{air}/(L_{reactor}$·min). However, the minimum SGV required to maintain

the stability of the reactor was higher in the pulsed regime system (1.2 cm/s) compared to the continuous aeration (0.7 cm/s), to guarantee the biomass suspension inside the reactor.

The biomass properties and reactor performance were maintained after increasing the non-aeration time of the pulses from 2 to 4 s (**Chapter 4**). Nevertheless, the increase of the non-aeration time to 6 s provoked the loss of stability of the system, due to the low concentrations of dissolved oxygen reached in the system (under 2 mg O_2/L), which provoked the loss of balance between feast and famine respective duration due to long feast phases.

The next step in the implementation of the pulsed aeration strategy could be to evaluate the combination of the airflow reduction (**Chapter 3**) and the decrease of air pulses frequency (**Chapter 4**). Then, this strategy could be tested using real sewage instead of synthetic.

Reactor configuration: fully aerobic vs anaerobic-fed reactor

The anaerobic-fed configuration enabled the maintenance of stable granular biomass with lower OLRs and SGVs, compared to the fully aerobic configuration. With the anaerobic-fed reactor, both in a continuous and pulsed regime, granules properties remained stable with SGVs of 0.7 and 1.2 cm/s, respectively, treating OLRs of 0.8 kg COD/(m^3·d). However, with the fully aerobic configuration (**Chapter 4**), a stable granular system was not achieved with an applied OLR of 2 kg COD/(m^3·d) and continuous aeration (SGV of 1.2 cm/s).

The comparison between the fully aerobic and the anaerobic-fed configuration treating fish-canning wastewater (**Chapter 5**) showed a shorter granulation period of 34 days in the anaerobic-fed reactor. However, the aerobic granules obtained with the fully aerobic configuration were more stable against the OLR and salinity fluctuations of the feeding (1.80 – 6.65 kg COD_S/(m^3·d) and 4.9 – 13.4 g NaCl/L, respectively), presented better settleability and larger average diameter.

Regarding the reactor performance, the soluble COD removal was slightly better in the anaerobic-fed reactor (80 – 90 %), but nitrogen removal was significantly better in the fully aerobic configuration (up to 80 %, compared to 40 % in the anaerobic-fed reactor). Since the anaerobic-fed reactor suffered more instability episodes due to the fluctuations of the feeding, the SRT was shorter, so that nitrifying bacteria were not developed.

In terms of AGS properties, an anaerobic feeding was not beneficial, however, it enabled the production of a better-quality effluent.

Fish-canning wastewater treatment: laboratory vs pilot scale

At laboratory scale (**Chapter 5**), there was no need of wastewater pre-treatment before being fed to the reactor, whereas at pilot scale (**Chapters 6, 7**) it was necessary to include pre-treatment units. A rotary drum was used to remove the solids present in the low-strength wastewater. The grease and solids of the high-strength stream were removed in a grease separator, with a minimum residence time of 2 h.

At laboratory scale, the influent composition was stable for a longer period of time compared to pilot scale. The collected batches of wastewater allowed the maintenance of the same feeding

composition during almost a month, whereas at pilot scale the feeding composition varied as the production of the factory did.

The operational strategy of the pilot-scale reactor was designed to cope with the fluctuations of the feeding and to avoid a complete stop of the reactor during the non-working days. To do that, the length of the cycles was modified depending on the duration of the stops. At laboratory-scale, the discontinuous wastewater production was not a problem.

At laboratory-scale (**Chapter 5**), the granulation process was completed after 90 days with a fully aerobic configuration. The obtained granules remained stable against the alternating OLRs and salinity concentrations of the fish-canning wastewater.

The system was able to remove the 75 – 85 % of the COD from the incoming wastewater, with applied OLRs of 1.8 – 6.6 kg COD/(m^3·d). From day 140 onwards, the SRT was long enough (above 6 days) to promote nitrification. This led to significantly larger N removal efficiencies (up to 80 %) compared to previous operational days.

At pilot-scale (**Chapter 7**), the biomass properties and performance of the reactor depended on the type of wastewater used as feeding.

When the pilot-scale reactor was fed with low-strength wastewater, the first granules were observed after 30 days, and biomass with good settleability was developed (SVI_5 of 30 – 40 mL/g TSS). However, the biomass growth was limited because of the low applied OLRs (0.5 – 2.0 kg COD_S/(m^3·d)). In addition, the nutrient deficiency of the wastewater (COD/N ratios of 100/0.5 – 100/0.2) provoked the overgrowth of filamentous bacteria.

High COD and N removal efficiencies of 60 – 80 and 70 – 80 %, respectively, were achieved treating low-strength wastewater. The nitrogen removal, only associated with biomass growth, was enough to reduce the nitrogen concentration below the discharge limit.

Although the treatment of the low-strength wastewater seemed difficult, a possible solution would be to mix this flow with another stream containing nitrogen, like the high-load stream.

The high-strength wastewater was more suitable to enhance the selection of granule-forming organisms. After approximately 30 days of operation, the first aggregates were observed, and the settleability of the biomass was improved (SVI_5 of 50 – 70 mL/g TSS). However, the time of operation (178 days) was not enough to complete the granulation process, presumably due to the complexity of the wastewater. Nevertheless, the overgrowth of filamentous bacteria did not occur.

The COD removal efficiencies were higher and more stable (80 – 90 %) compared to low-strength wastewater treatment. However, the nitrogen removal efficiencies were lower (30 – 40 %) due to the higher nitrogen concentrations of the feeding and the absence of nitrifying bacteria activity.

The reconfiguration of the operational cycles during non-working days did not have a short-term effect on the biological activity of the reactor. However, this, in addition to other factors like the composition fluctuations, the complexity and the salinity of the wastewater, presumably hindered the granulation process treating both low-strength and high-strength wastewater.

When treating low-strength wastewater, the effluent of the plant fulfilled part of the discharge requirements, except for COD, BOD_5 and greases concentrations, associated to the deficient operation of the pre-treatment units. When treating high-strength wastewater, the COD, BOD_5, nitrogen and phosphorus concentrations were over the discharge limits. Consequently, an additional treatment is needed previous to effluent discharge.

Influence of salinity on the reactor performance

The presence of salt and its fluctuations in concentration had an effect not only on the biological activities of the biomass, but also on the physical properties of the aggregates. Both the sudden increase and decrease of salinity provoked changes on the system.

The salinity of the wastewater (4.9 – 13.3 g NaCl/L) presumably caused the absence of NOB activity during the laboratory-scale operation (**Chapter 5**). The nitrogen removal pathway was nitritation – denitritation. FISH analysis performed to identify the main bacterial populations confirmed the absence of NOB and the presence of AOB in the granular sludge.

The highest Extracellular Polymeric Substances (EPS) production, the best physical properties and the highest biomass retention were achieved at the highest salinity tested in the reactor operated at laboratory scale (13.3 g NaCl/L) (**Chapter 5**).

The sudden change of salinity during non-steady-state conditions caused a rapid washout of biomass. However, when mature granules were present, the effects associated to salinity fluctuations were not immediate, and the biomass had a higher capacity to withstand the fluctuations.

The results of the model developed in **Chapter 8**, confirmed the detrimental effect of salinity on the activity of the nitrifying populations. The calibrated kinetic parameters of the heterotrophic bacteria were found to be similar to previous research works modelling AGS with ASM3. Thus, salinity did not have a big impact on heterotrophic activity. However, the maximum growth rates of AOB and NOB were found to be considerably lower. The cause of this discrepancy could be attributed mainly to the presence of salt. However, other factors, like the complexity of the wastewater could have hindered nitrifying activity as well.

Publications & Conferences

International Journal Publications

P. Carrera, A. Mosquera-Corral, R. Méndez, J.L. Campos, A. Val del Río (2019). Pulsed aeration enhances aerobic granular biomass properties. Biochemical Engineering Journal, 149: 107244. DOI: https://doi.org/10.1016/j.bej.2019.107244.

P. Carrera, R. Campo, R. Méndez, G. Di Bella, J.L. Campos, A. Mosquera-Corral, A. Val del Río (2019). Does the feeding strategy enhance the aerobic granular sludge stability treating saline effluents? Chemosphere, 226: 865-873. DOI: 10.1016/j.chemosphere.2019.03.127.

C. Cofré, J.L. Campos, D. Valenzuela, J.P. Pavissich, N. Camus, M. Belmonte, A. Pedrouso, **P. Carrera**, A. Mosquera-Corral, A. Val del Río (2018). Novel system configuration with activated sludge like-geometry to develop aerobic granular biomass under continuous flow. Bioresource Technology 267: 778-781. DOI: 10.1016/j.biortech.2018.07.146.

R. Campo, **P. Carrera-Fernández**, G. Di Bella, A. Mosquera-Corral, A. Val del Río (2017). Fish-canning wastewater treatment by means of aerobic granular sludge for C, N and P removal. In: Mannina G. (eds) Frontiers International Conference of Wastewater Treatment and Modelling. Springer, Cham, pp 530-535. DOI: 10.1007/978-3-319-58421-8_83.

Book Chapters

A. Val del Río, **P. Carrera-Fernández**, J.L. Campos Gómez, A. Mosquera-Corral (2017). Technologies for the Treatment and Recovery of Nutrients from Industrial Wastewater, chapter 2: Nutrients Pollution in Water Bodies: Related Legislation in Europe and the United States (pages 21-42 of 391). IGI Global. ISBN: ISBN13: 9781522510376 ISBN10: 1522510370.

Patents

P. Carrera, A. Val del Río, A. Mosquera-Corral, J.L. Campos, J.M. Lema. Método y Sistema para la eliminación de fósforo, carbono orgánico y nitrógeno mediante biomasa granular aerobia y aeración pulsante. Patent **ES 2 702 430 B2**. Date of publication: September 27th 2018.

Conferences

C. Cofré, J.L. Campos, D. Valenzuela, J.P. Pavissich, N. Camus, A. Pedrouso, **P. Carrera**, A. Val del Río, A. Mosquera-Corral. *Continuous flow aerobic granular sludge system as a post-treatment of effluents from industrial anaerobic digesters.* Poster. XII Latin American Workshop and Symposium on Anaerobic Digestion. Medellín (Colombia), October 21st 2018.

P. Carrera, A. Fra, A. Val del Río, J.L. Campos, R. Méndez, A. Mosquera-Corral. *Sistemas biológicos basados en biomasa granular aerobia para el tratamiento de aguas residuales procedentes de la industria conservera*. Poster + flash presentation. XXXV Jornadas Nacionales de Ingeniería Química. Salamanca (Spain), July 4 – 6th 2018.

A. Pichel, **P. Carrera**, S. Santorio, A. Val del Río, R. Méndez, A. Mosquera-Corral. *Los límites de la extracción de EPS en biopelículas para el tratamiento de aguas residuales*. Oral presentation. II Simposio de Investigación en Tecnologías Ambientales (Red REGATA-CRETUS). Santiago de Compostela (Spain), June 7th 2018.

P. Carrera, A. Val del Río, R. Méndez, A. Mosquera-Corral. *Sistemas de biomasa granular aerobia para o tratamento de augas residuais da industria conserveira*. Oral presentation. VI Encontro da Mocidade Investigadora. Santiago de Compostela (Spain), May 30th 2018.

P. Carrera, R. Campo, R. Méndez, A. Mosquera-Corral, A. Val del Río. *Features of systems based on aerobic granular sludge to treat saline wastewater*. Poster. IWA Biofilms: Granular Sludge Conference (GSC). Delft (The Netherlands), March 18 – 21st 2018.

N. Camus, J.P. Pavissich, J.L. Campos, C. Cofré, A. Pedrouso, **P. Carrera**, A. Val del Río, A. Mosquera-Corral. *Fractal dimension: A useful parameter for monitoring the stability of aerobic granular biomass*. Poster. IWA Biofilms: Granular Sludge Conference (GSC). Delft (The Netherlands), March 18 – 21st 2018.

C. Cofré, J.L. Campos, D. Valenzuela, J.P. Pavissich, N. Camus, A. Pedrouso, **P. Carrera**, A. Val del Río, A. Mosquera-Corral. *Development of aerobic granular biomass in a continuous flow system*. Poster. IWA Biofilms: Granular Sludge Conference (GSC). Delft (The Netherlands), March 18 – 21st 2018.

R. Campo, **P. Carrera-Fernández**, G. Di Bella, A. Mosquera-Corral, A. Val del Río. *Fish-canning wastewater treatment by means of aerobic granular sludge for C, N and P removal*. Oral presentation. Frontiers International Conference on Wastewater Treatment (FICWTM2017). Palermo (Italy), May 21st, 2017.

P. Carrera, A. Val del Río, I. Rodríguez-Verde, R. Méndez, A. Mosquera-Corral. *Operation of an aerobic granular reactor to treat industrial saline wastewater*. Oral presentation. 10th IWA International Conference on Biofilm Reactors. Dublin (Ireland), May 9 – 12th, 2017.

C. M. Castro-Barros, **P. Carrera**, A. Val del Río, J. Manzano, A. Mosquera-Corral, I. Rodriguez-Verde. *Aerobic pilot-scale biofilm-based technologies for the treatment of high strength saline wastewater*. Poster. 10th IWA International Conference on Biofilm Reactors. Dublin (Ireland), May 9 – 12th, 2017.

P. Carrera, A. Val del Río, R. Méndez, A. Mosquera-Corral. *Adjusting COD requirements for P removal in aerobic granular reactors.* Oral presentation*.* 3rd IWA Specialized International Conference: Ecotechnologies for Wastewater Treatment 2016 (ecoSTP16). Cambridge (United Kingdom), June 27 – 30th, 2016.

A. Val del Río, A. Pedrouso, **P. Carrera**, R. Méndez, A. Mosquera-Corral. *Aerobic granular biomass versatility applied for industrial wastewater treatment*. Poster. BIOFILMS7-Microbial Works of Art. Porto (Portugal), June 26 – 28th, 2016.